The Thesis Committee for Kelly David Thomson
Certifies that this is the approved version of the following thesis:

Detrital zircon (U-Th)/(Pb-He) geo- and thermo-chronometric constraints on provenance and foreland basin evolution of the Ainsa Basin, south-central Pyrenees, Spain

APPROVED BY
SUPERVISING COMMITTEE:

Supervisor:

Daniel F. Stockli

Brian K. Horton

Julian D. Clark

Detrital zircon (U-Th)/(Pb-He) geo- and thermo-chronometric constraints on provenance and foreland basin evolution of the Ainsa Basin, south-central Pyrenees, Spain

by

Kelly David Thomson, B.S.

Thesis

Presented to the Faculty of the Graduate School of

The University of Texas at Austin

in Partial Fulfillment

of the Requirements

for the Degree of

Master of Science in Geological Sciences

The University of Texas at Austin

August 2016

Acknowledgements

I would like to express my gratitude to my advisor, Dr. Daniel Stockli, for his guidance, advice, and contributions to this project. I would also like to thank my committee members Dr. Brian Horton and Dr. Julian Clark, and non-committee mentors Andrea Fildani and Mason Dykstra, their feedback and expertise have been invaluable to completing this project. I would like to thank the Jackson School of Geosciences, Statoil – Austin, and the Geologic Society of America for financial support of my field, analytical and tuition costs. I would like to thank lab managers Des Patterson, Lisa Stockli, Sol Cooperdock, Dan Arnost, and Yomayra Roman for assistance in mineral separation and data acquisition. I am also grateful for field assistance from Cai Puigdefàbregas, Margo Odlum, Louis Honegger, and Marta Roige. I would like to additionally thank Sebastian Castelltort and all participants of the 2014 ETH Sedimentology of the South Pyrenees field course, and the Hotel Apolo in Ainsa, Spain. I extend my gratitude to the entire Stockli research group, especially Spencer Seman, Renas Koshnaw, Edgardo Pujols, Doug Barber, Emily Cooperdock, Mike Prior, Adam Goldsmith and Cody Colleps, and fellow graduate student Tomas Capaldi, . Special thanks to Philip Guerrero for all that he does for the students and Geology Department. I would like to thank my parents David and DJ Thomson, Margie Thomson and Jane Edwards, and my sisters Katelyn and Krista for their support and encouragement. Lastly I would like to thank my partner Amy Atwater for her constant support and encouragement of my pursuit of a graduate degree in geology, and her invaluable help with mineral separation, fieldwork, and revision of this manuscript.

Abstract

Detrital zircon (U-Th)/(Pb-He) geo- and thermo-chronometric constraints on provenance and foreland basin evolution of the Ainsa Basin, south-central Pyrenees, Spain

Kelly David Thomson, M.S. Geo. Sci.

The University of Texas at Austin, 2016

Supervisor: Daniel F. Stockli

Synorogenic foreland basin fill of the south central Pyrenees preserves the eroded remnants of the early stages of Pyrenean fold-thrust belt evolution and topographic growth. Detailed isotopic provenance analysis allows for the reconstruction of sediment sources and boundary conditions of sediment routing systems. Detrital zircon (DZ) (U-Th)/(Pb-He) double-dating of foreland basin sediment is a powerful tool for sedimentary provenance analysis and constraining the exhumational history of mountain belts. This study integrates published structural, stratigraphic, and petrologic data, with new geochronometric and thermochronometric data in a four dimensional source-to-sink approach to decipher provenance and thermal evolution during Pyrenean orogenesis. The Ainsa Basin within the south Pyrenean foreland basin system contains the Hecho Group, a

succession of turbiditic channels and levees deposited in the transition zone between the fluvial-deltaic systems of the Tremp-Graus-Ager basin in the east to the submarine fan complex of the Jaca basin in the west.

This study presents 2175 new DZ U-Pb ages and 246 new DZ (U-Th)/(Pb-He) double-dated ages from 20 samples collected from the Eocene Hecho group turbidites and the overlying Sobrarbe-Escanilla fluvio-deltatic sandstone in the Ainsa Basin of the south central Pyrenees. These data along with previous DZ U-Pb studies indicate a progressive shift in sediment provenance during orogenesis. The basin was initially being fed by Cadomian/Caledonian plutonic and metamorphic rocks exposed in the eastern Pyrenees with minor sediment contribution from sources located to the south and south east of the basin. Progressive westward exhumation of the Pyrenean Axial Zone promoted a shift in the dominant sediment source to subsequently exhumed Variscan plutons and recycled Mesozoic deposits in the central Pyrenean Axial Zone. Based on DZ (U-Th)/He results, four main cooling events are identified: Pyrenean orogenesis (~56 Ma), initial inversion (~80 Ma), Cretaceous rifting (~100 Ma), and pre-Mesozoic cooling ages related to earlier tectonic phases. This study imposes new constraints on the paleogeographic evolution of the Pyrenees and illustrates that active contractional structures are the dominant control on sediment routing evolution by introducing new sources and controlling sediment pathways during orogenesis.

Table of Contents

List of Figures

INTRODUCTION

The evolution of sediment delivery networks within active fold-thrust belts and coupled foreland basin systems is tied to the evolution of structural deformation in the mountain belt due to the interplay between surface processes and tectonics in critically tapered fold-thrust wedges (Davis et al., 1983; Dahlen et al., 1984; Flemings and Jordan, 1990; Whipple, 2009). Sedimentary provenance analysis investigates ancient sediment delivery networks though detailed mineralogical analysis (Dickerson, 1988). Detrital geochronometry is a powerful tool for investigating sediment provenance and reconstructing the tectonic setting at the time of deposition (e.g., Fedo et al., 2003; Gehrels, 2014). Detrital thermochronolmetry of foreland basin sedimentary deposits allows for the reconstruction of the early tectonic history of orogenic evolution (Garver et al., 1999; Rahl et al., 2007). Combining these geochronometric and thermochronometric methodologies to a single grain creates a "double date", placing crystallization and cooling age constrains which serve as a proxy for the crystallization and thermotectonic history of the initial source rocks feeding the basin sediment. Large n high resolution double dating has become a powerful tool in reconstructing provenance evolution and tectonic history of foreland basin systems (Garver et al., 1999; Rahl et al., 2003.; Reiners et al., 2005; Carrapa et al., 2009; Carrapa, 2010; Saylor et al., 2012; Fosdick et al., 2015; Hart et al., 2016;). Detrital zircon (DZ) (U-Th)/(Pb-He) double dating is a particular useful geo- and thermochronometer given the high (>700°C) and low (180°C) temperature sensitivity

windows of the system (Reiners et al., 2005; Wolf and Stockli, 2010) and abundance of zircon as an accessory mineral phase in most crystalline and siliciclastic sedimentary rocks.

The Pyrenees mountain belt (Fig. 1) resulted from the inversion of a hyperextend continental margin during oblique convergence between the Iberian and Eurasian plates beginning in the late Cretaceous and extending through the Miocene (Vergés, 2002: Mouthereau et al., 2014). A deep narrow trough (foredeep) formed in the subsiding peripheral foreland basin on the southern side of the asymmetrically uplifting orogen and was initially delivered sediment from a sedimentary network flowing parallel (E to W) to the orogenic axis. Exhumation rates peaked in the Oligocene (Fitzgerald et al., 1999; Metcalf et al., 2009; Sinclair et al., 2005) and were contemporaneous with coarse clastic progradation into the foreland delivering sediment from fans and fluvial networks flowing perpendicular to the orogenic axis. This transition from axis parallel to axis transverse sediment transport occurred in the mid Eocene and is preserved in early foreland basin deposits (Whitchurch et al. 2011).

The Ainsa Basin (Fig. 2) evolved from a foredeep to piggyback basin in the south central Pyrenean fold-thrust belt and was a part of a continuous south Pyrenean foreland basin system during the Eocene (Puigdefàbregas et al., 1992; Bentham & Burbank, 1996) . Sediment was delivered to the Ainsa Basin via deeply incised submarine canyons within the shelf slope funneling sediment from the fluvial and shallow marine Tremp-Graus-Ager basins in the east (Lunsen, 1970; Mutti, 1977). The Tremp-Graus-Ager basins are located in the South Central Pyrenean Unit (SCPU) (Fig. 1), a large salient in the Pyrenean thrust front, and transported sediment from the emergent fold-thrust belt and basement uplifts in

the north and east to the Ainsa-Jaca Basin (Puigdefàbregas and Souquet, 1986). The slope-basin floor depozone deposits of Ainsa Basin represent an important sediment delivery zone which transported sediment to the western deep marine submarine fan and lobe complex in the Jaca basin (Mutti, 1977). The Ainsa Basin lays directly down dip from the paleo shelf-slope break. The location of the shelf-slope break is structurally controlled and focused above lateral ramp transfer structures connecting faults in the SCPU to the western Pyrenees (Lunsen, 1970). The structural control of the shelf slope break spatially restricted the shallow marine and coastal zones ability to store sediment and buffer variations in sediment supply (sensu Romans et al., 2015). Therefore, unbuffered sediment supply variations would be transferred into the deep marine environment and preserved in stratigraphy (Castelltort and Van Den Driessche, 2003). The highly variable climatic (Zachos et al., 2008) and eustatic (Kominz et al., 2008) regimes in the Eocene contemporaneous with the initiation of exhumation within the emergent Pyrenean fold-thrust belt and Axial Zone (Puigdefàbregas et al., 1992; Muñoz 1992) make the Ainsa Basin an ideal setting to investigate sedimentary dynamics such as sediment budgeting (Micheal et al., 2014), grain size fractionation (Allen et al., 2013; Parsons et al. 2014), and climatic cyclicity (Cantalejo and Pickering, 2015) in response to allogenic forcing.

Stratigraphic and facies models have utilized continuous outcrop exposures of the Ainsa Basin to link proximal and distal depositional zones and constrain the sedimentary provenance evolution with petrographic analysis (e.g. Mutti et al. 1985; Puigdefàbregas and Souquet, 1986; Mutti et al., 1988; Fontana et al., 1989; Bentham and Burbank, 1996; Remacha and Fernández 2003; Gupta and Pickering, 2008; Caja et al., 2010). Few studies

have been conducted to constrain the sediment provenance through detailed detrital geochronometry and thermochronometry (Gupta, 2008; Whitchurch et al. 2011; Filleadeau et al., 2012). Caja and others (2010) interpreted the upsection increase of lithics, feldspars, and angular clasts within the Hecho Group to reflect an unroofing pattern eroding though Mesozoic sediments before eroding Paleozoic basement within the growing Pyrenean hinterland. Whitchurch and others (2011) interpreted a DZ provenance shift from Cadomian (~600 Ma) to Variscan (~300 Ma) dominated spectra to reflect a major drainage reorganization from an axis parallel (axial) to an axis perpendicular (transverse) flowing sedimentary network. These competing models cannot be tested by DZ U-Pb analysis alone because of the similarities in U-Pb signatures of the eastern Pyrenean axial zone (Denèle et al., 2014) with the Mesozoic cover strata (Hart et al., 2016). A major shift in DZ (U-Th)/He age distributions is hypothesized for Mesozoic basin unroofing as erosion progressively removes sediment with inherited cooling ages before eroding deeper crustal levels with Pyrenean cooling ages, while an axial to transverse provenance shift will have a constant flux of Pyrenean cooled grains. However, DZ (U-Th)/He analysis alone is not enough to discriminate these models, because an major shift in DZ (U-Th)/He spectra could also reflect a provenance shift from non-Pyrenean sources with inherited cooling ages to recently exhumed Pyrenean cooled source regions. DZ (U-Th)/(Pb-He) double dating is the only way to discriminate these two competing models. A shift in the Pyrenean cooled U-Pb spectra is hypothesized for an axial to transverse provenance change, while an unchanging Pyrenean cooled U-Pb spectra is hypothesized for unroofing of Mesozoic basins. This approach utilizes the well-constrained stratigraphic and structural evolution of

south central Pyrenees with three dimensional basin boundary conditions elucidated from DZ U-Pb provenance analysis. The continuous exposure, biostratigraphic/ magnetostratigraphic depositional models (Puigdefàbregas and Souquet, 1986; Bentham and Burbank, 1996; Mochales et al., 2012; Scotchman et al., 2014; Mochales et al., 2016), and well-constrained structural evolution (Teixell, 1998; Fitzgerald et al., 1999; Sinclair et al., 2005; Metcalf et al., 2009; Erdos et al., 2014; Teixel et al. 2016) of the Ainsa Basin provide a unique setting to apply DZ double dating methodology in high resolution. Furthermore the crystallization and cooling age constrains of the crystalline basement exposed in the Axial Zone allow for a detailed sedimentary provenance analysis and reconstruction of sediment source regions throughout early orogenesis (Solé et al., 2003; Denèle et al., 2014; Hart et al., 2016; Martínez et al., 2016;). This study presents new DZ (U-Th)/Pb-He double dates from the Hecho group turbidites and the overlying Sobrarbe-Escanilla fluvio-deltatic sandstones from the Ainsa Basin within the South Central Pyrenees. This study approaches the problem of reconstructing sediment provenance from a four dimensional source to sink perspective, in which the entire sediment delivery network is considered from erosional sediment source regions, to fluvial and marine transfer zones, and deep marine terminal sinks (Allen, 2008). This approach seeks to investigate and constrain all potential allogenic forcing mechanisms (i.e. sea level, climate, and tectonics) and autogenic dynamics within sedimentary systems which produce the observed stratigraphic architecture preserved in the basin. These findings have direct implications for tectonic and paleogeographic reconstructions of early Pyrenean mountain building. Furthermore these detrital geo- and thermochronometric data have implications

for constraining chronostratigraphic models, investigate the thermotectonic evolution of the Pyrenees, and provide insights into the interactions of tectonics with dynamic sedimentary processes such as bypass, sediment staging, and recycling from source to sink.

The aim of this study is to constrain the sources of siliciclastic material being delivery to the Pyrenean foreland basin and to examine how the thermotectonic history of those respective source regions influenced the redistribution of sediment during mountain building. This study addresses competing models of provenance evolution proposed for the Ainsa Basin. These new DZ U-Pb and (U-Th)/He data and basin boundary constrains are utilized to compile a new paleogeographic model. Approaching the problem of sediment provenance from a four dimensional source to sink (Sømme et al., 2009; Allen et al., 2013) perspective this study integrates multidisciplinary research on basin deposition to constrain the South Central Pyrenees foreland basin evolution. This study has broader implications for interpretive studies of provenance signals, sediment bypass and recycling, interactions between axial and transverse drainage in basin systems around the world.

GEOLOGIC BACKGROUND

The Pyrenees Mountains are a 400 km east-west trending orogenic belt along the border of France and Spain and is the western most expression of the Alpine-Himalayan orogenic belt (Fig. 1). The Pyrenean orogeny resulted from the oblique convergence between the Iberian and the Eurasian plates and the partial subduction of the Iberian margin beneath Eurasia (Fig. 1) (Choukroune and ECORS Team, 1989; Muñoz et al., 1992; Vergés 2002; Vissers and Meijer, 2012). The Pyrenees are a double-vergent orogenic wedge that

can be divided into five distinct structural zones. North of the Pyrenees mountain belt lies the undeformed Aquitaine basin, a retro-wedge foreland basin (Fig. 1). South of the Aquitaine basin is the North Pyrenean Zone, the French retro-wedge fold-thrust belt, characterized by steeply dipping north vergent reverse faults exhuming Paleozoic basement and highly deformed Mesozoic strata. The retro-wedge fold-thrust belt is bound to the south by the North Pyrenean Fault separating the fold thrust belt from the Axial Zone (Ford et al., 2016). The Axial Zone is composed of Paleozoic crystalline basement structurally thickened by south vergent antiformally stacked thrust sheets (Muñoz et al., 1992). The Axial Zone is bound to the south by the South Pyrenean pro-wedge fold-thrust belt, characterized by low angle south vergent thrust faults translating Mesozoic and Cenozoic basin fill above a décollement of Triassic evaporates (Puigdefàbregas et al., 1992). The South Pyrenean fold thrust belt contains the foredeep and piggy back basin deposits discussed in this manuscript. The South Pyrenean fold-thrust belts ends in the External Sierras thrust fault where it is thrust over the Ebro peripheral foreland basin. The Ebro basin the flat lying undeformed region south of the Pyrenees extending from the south Pyrenean fold-thrust belt to the Catalan Coastal Ranges and Iberian Range (Fig. 5). Extensive field studies and seismic studies have established a well-constrained tectonic evolution for the Pyrenees orogen (Choukroune and the ECORS Team, 1989; Muñoz et al., 1992; Teixell, 1998; Beaumont et al., 2000; Teixell et al., 2016). Estimates of total shortening are 165 km across the ECORS profile in the central Pyrenees (Beaumont et al., 2000) and 90 km across the Anso-Arzacq profile in the western Pyrenees (Teixell, 1998) (Fig. 1). The style of deformation and tectonic evolution during Pyrenean convergence

was influenced by preexisting geometries established in early tectonic phases (Puigdefàbregas & Souquet, 1986; Beaumont et al. 2000; Teixell et al., 2016).

Tectonic Evolution of the Pyrenees

The Iberian plate amalgamated from island arc accretion in the Cadomian/ Pan African orogeny (550-650 Ma). Metamorphism and plutonium of the Caledonian orogeny (450-500 Ma) deformed and intruded the Proterozoic-Paleozoic basement (Dewey et al. 1973). During the Variscan orogeny (380-280 Ma) the Iberian microplate was sutured into the growing Pangea supercontinent as Laurentia, Gondwana and Baltica collided (Dewey et al., 1973). The Variscan orogeny was a period of widespread metamorphism and granitic plutonism across the Iberian Plate (Matte, 1986). Permian-Triassic extension promoted by orogenic collapse of the Variscan orogen lead to the break-up of Pangea and the establishment of the Tethyan seaway in the Mediterranean (Ziegler, 1999). Mid-Jurassic ocean spreading in the central Atlantic caused a sinistral transtensional system between Africa and Europe wrenching the Iberian Microplate opening oceanic pull apart basins alone the Pyrenean-Eurasian margin (Vissers and Meijer, 2012). The Iberian Microplate rotated 35° counter-clockwise (with respect to Eurasia) in response to sea floor spreading in the Bay of Biscay (Vissers and Meijer, 2012). The North Pyrenean fault zone accommodated transtensional displacement between the Iberian and Eurasian plates and generated oceanic pull-apart basins with subsidence peaking in the Albian-Aptian (Vergés et al., 2002; Hart et al., 2016; Teixell et al., 2016). Plate kinematic reorganization between the Atlantic, Eurasian, and African plates in the late Santonian lead to transpressional rift

inversion and the onset of the Pyrenean orogeny (e.g. Bosworth et al., 1999). Convergence was spatially diachronous and began with the inversion of hyperextended rift structures and overthrusting of Mesozoic synrift basin fill (Fig. 3). Basin inversion continued until the Paleocene when a change in the relative motions of Europe and Africa caused subdued convergence rates between Iberia and Eurasia resulting in a period of tectonic quiescence along the Pyrenean margin (Dewey et al., 1973; Rosenbaum et al., 2002). After the 10-15 Myr non-contractional phase (Rosenbaum et al., 2002) convergence resumed between Iberia and Eurasia in the early Eocene. Reactivated inverted faults and thin-skinned thrusting initiated (Teixell 1998; Beaumont et al., 2000; Teixell et al. 2016). Paleozoic basement thrust sheets (Nogueres, Orri and Rialp) were thrust and exhumed from north to south producing the antiformally stacked Axial Zone (Fig. 1)(Muñoz, 1992). Exhumation propagated diachronously from east to west during oblique convergence (Fitzgerald et al., 1999; Vergés, 2002). Crustal loading of the Iberian-Eurasian plate boundary resulted in flexural subsidence on the Iberian and Eurasian plates. Sediment eroding from the emerging orogen was deposited in a narrow underfilled foreland basin. Sediment routing systems evolved in response to fold-thrust belt and Axial Zone exhumation redistributing sediment into the foreland basin. Peak exhumation rates were reached in the Oligocene (Fitzgerald et al., 1999), contemporaneous with topographic damming of the western Pyrenees and establishment of an internally drained foreland basin (Costa et al., 2010). The increase topographic load caused the flexural profile to increase in wavelength expanding the zone of subsidence and quickly filled the basin with propagation of conglomeritic megafans far into the foreland (Fitzgerald et al., 1999; Metcalf et al., 2009). Internal

drainage of the Ebro Basin lasted until the Miocene when the Valencia trough rifted from the Catalan Coastal Range providing a basin outlet to the Mediterranean (Vergés 2002). Thick packages of conglomerate deposits in the Ebro Basin were incised and eroded as internal drainage ended (Beamud et al., 2011). The well constrained tectonic and structural history allow for detailed analysis of sedimentary and stratigraphic response to structural deformation at high temporal and spatial resolutions.

The Ainsa Basin

The Ainsa Basin is located along the western edge of the South Central Pyrenean Unit (SCPU), a large salient in the south Pyrenean fold-thrust belt (Muñoz et al., 2013) (Fig. 2). The Ainsa Basin was part of the greater south Pyrenean foreland basin, it represents a sediment transfer zone connecting the fluvial-deltaic systems of the Tremp-Graus-Ager piggy back basins located in the SCPU to the deep marine submarine fan system of the Jaca basin to the west (Mutti, 1977). The Ainsa Basin is defined as the Eocene basin fill located between the Boltaña and Mediano anticlines (Pudigdefabregas and Souquet, 1986), which grew syndepositionally as lateral ramp transfer structures between the SCPU and western Pyrenean thrusts. Syndepositional structural growth effected basin sedimentation and the stratigraphic evolution of the basin by guiding sediment routing systems through the Ainsa Basin.

Paleogene History of the Ainsa Basin

Paleocene

During the period of tectonic quiescence in the Paleocene (Rosenbaum et al. 2002) widespread non marine red bed deposition occurred (Tremp Fm/Garumnian Fm) throughout the southern Pyrenees (Puigdefàbregas and Souquet, 1986). Syndepositional growth structures of the Tremp Formation within the Ager and Tremp basins indicate the Montsec High formed a topographic barrier during Paleocene red bed deposition (Gomez-Graz et al., 2016). Limited basement involvement in thrusting resulted in slow tectonic subsidence during the Paleocene (Puigdefàbregas et al., 1992). The quiet tectonic activity during the Paleocene beveled topography leading to a major marine transgression and establishment of a carbonate platform across the southern Pyrenees.

Ypresian

A decrease in seafloor spreading in the northern mid Atlantic at ~55 Ma (Dewey et al., 1973) caused the relative motion between Europe and Africa to resume convergence. Rejuvenated fault activity along the Bóixols-Cotiella and Montsec-Peña Montañesa thrusts resulted in increased tectonic subsidence and provided sediment to the basin. Shallow marine carbonate deposits of the Alveolina limestone developed at the start of the Eocene and are attributed to a major transgression over the relatively flat lying Garumnian facies red beds (Pudigdefabregas and Souquet, 1986). The first Eocene siliciclastics, overlying the Alveolina limestone, are delivered to the basin in response to rapid foreland basin deepening from tectonic subsidence. The Roda sandstone deltaic complex of the Tremp-

Graus region grades into marine marls and turbidites of the Figols Formation in the Ainsa Basin (Pudigdefabregas and Souquet, 1986). By the late Ypresian, the San Esteban Alluvial Fan delivered sediment from the Nogueres thrust sheet into the basin (Pudigdefabregas et al., 1992). In the Ainsa-Jaca region deposition of the Hecho group began with the Fosado and Arro turbidite complexes and Torla submarine fan complexes to the west (Pudigdefabregas and Souquet, 1986; Mutti 1977). Sedimentation rates decreased from the early Ypresian (0.15 km/Myr) to the late Ypresian (~0.1 km/Myr) (Mochales et al., 2002). The Guara shallow marine carbonate platform developed along the southern margin of the Ainsa-Jaca basin and periodically failed along the northern platform shelf margin producing deposition of ~200m thick "megaturbidites" comprised mainly of blocks of carbonate (Séguret et al. 1984; Labaume et al. 1987). These megaturbidites are laterally extensive within the Jaca basin and are utilized as correlative intervals; eight units (MT1 - MT8) are recognized as marker beds pinning the ages of interbedded lobe complexes (Remacha et al., 2003).

Early Lutetian

Propagation of the thrust front and development of the Gavarnie-Serres Marginales thrust sheet (Fig. 1) changed the Ainsa Basin from a foredeep to a piggy-back basin (Pudigdefabregas et al., 1992; Teixell, 1998). Foredeep migration caused a decrease in sedimentation rate from 0.1-0.15 km/Myr to 0.07 km/Myr (Mochales et al. 2012). The Mediano, Olson, and Anisclo syndepositional fold-thrust structures became active, initiating parallel to the Gavarnie thrust front and were later rotated during differential

thrust displacement across the Ainsa Oblique Zone (Muñoz et al 2013). Exhumation and erosion was focused in the Nogueres thrust sheet with ~0.3 km/ Myr exhumation rates estimated for the Axial Zone (Fitzgerald et al 1999, Beamud et al. 2011). Caja and others (2010) described the source regions for sediments during the Lutetian, and hypothesize the large proportion of extrabasinal carbonate grains were derived from the erosion of carbonate units located along the Montsec thrust and from the Cretaceous carbonates on the Mediano Anticline.

Mid-Late Lutetian:

Deformation of the Boltaña anticline initiated during the middle Lutetian, forming as a fault propagation fold. The Boltaña anticline formed parallel to the Mediano anticline and was rotated clockwise during differential displacement of the SCPU and the western Pyrenees. The Boltaña and Mediano rotated 15° clockwise from the original orientation parallel to the frontal thrusts by 42 Ma (Beamud, 2013; Muñoz et al. 2013). These syndepositional structures created paleobathemetery which guided channelized turbidite channels through the Ainsa Basin. Duplexing of the Axial Zone antiformal stack by the Orri thrust sheet underthrusting the Nogueres thrust sheet increased basin subsidence (Vergés et al. 2002) and sedimentation rates within the Ainsa Basin to 0.3 km/Myr (Mochales et al 2012). Duplexing, internal deformation of the thrust sheets, and out of sequence reactivation of the Bóixols thrust during the mid-late Lutetian is proposed to be a phase of wedge reorganization to maintain a critical taper (Costa et al., 2010; Dahlen, 1990).

Bartonian/Priabonian:

The early Bartonian is characterized by pronounced changes in basin configuration (Nijman, 1989) most notably a southwest migration of the foredeep into the Ebro basin, passive translation of piggyback basins and initiation of internal drainage in the Ebro basin (Bentham et al., 1992; Costa et al., 2010). The Boltaña and Mediano anticlines had rotated 45° clockwise by 37 Ma since the mid Lutetian (42 Ma) caused by a differential displacement of 45 km between the SCPU and western Pyrenees (Beamud, 2013; Muñoz et al., 2013). Sedimentation rates in the Ainsa Basin decreased to 0.16 km/Myr (Mochales et al., 2012) while remaining at 0.25 km/Myr in the Jaca Basin to the west (Hogan & Burbank, 1996). The Ebro basin was isolated from the Atlantic Ocean by the Early Priabonian (~36 Ma) due to a eustatic sea-level fall and topographic growth in the western Pyrenees (Costa et al., 2010). Sedimentation rates increased in the Jaca basin to 0.63 km/Myr (Hogan and Burbank, 1996). The increased sedimentation rates in the Tremp-Graus region from 0.05 km/ Myr to 0.1 km/Myr (Beamud, 2013) was contemporaneous with paleocurrents changing from E-W to N-S directed transport and wide spread facies changes from fluvial-deltaic to conglomeratic facies in the Pyrenean foreland and wedge top basins. The cessation of sediment bypass to the Atlantic lead to basin backfilling of sediments onto the Pyrenean fold-thrust belt that adjusted the critical wedge to a subcritical state initiating enhanced exhumation within the Axial Zone through duplexing of the antiformal stack by the Rialp thrust sheet and backthrusting along the Morreres backthrust (Costa et al., 2010). Exhumation rates for the Axial Zone increased to 1-2 km/Myr (Fitzgerald et al. 1999; Metcalf et al., 2009; Beamud, 2013)

Stratigraphy of the Ainsa Basin

The Ainsa Basin contains a succession of turbiditic channel and levee deposits, deposited from the late Ypresian until the late Lutetian (Mutti, 1977; Pudigdefabregas and Souquet, 1986) (Fig. 4). Pickering and Bayliss (2009) recognized 7 turbiditic sand bodies separated by marine marls and slump deposits. The turbidite complexes making up the Hecho group are; Fosado-Los Molinos, Arro, Gerbe, Banaston, Ainsa, Morillo, and Guaso. In the Ainsa Basin region the turbidites are channelized with distinct erosive bases and are fed from incisional canyons cutting through the shelf and slope to the east (Clark and Pickering, 1996). To the west, across the Boltaña anticline in the Jaca basin, the turbidites thin and spread out unconfined across the basin floor creating extensive submarine fan complexes (Mutti 1977). Extensive studies have been conducted to discriminate tectonic from climatic or eustatic forcing of deep marine sedimentation within the Ainsa Basin (Fontana et al. 1989; Picking and Bayliss 2009; Caja et al., 2010; Cantalejo and Pickering 2014). The Hecho Group deep marine deposits are overlain by the Sobrarbe Deltaic complex which prograded into the basin from the south between the Mediano and Boltaña Anticlines (Pudigdefabregas and Souquet, 1986). This is overlain by the Escanilla fluvial system and marks the transition to widespread nonmarine deposition around the southern Pyrenean piggy back and foreland basins.

Provenance Studies in Ainsa

Many petrographic, geochemical, and stratigraphic studies have been conducted to address the sediment provenance of the Hecho Group turbidites (Fontana et al., 1989;

Gupta and Pickering 2008; Heard and Pickering, 2008; Mansurbeg et al., 2009; Caja et al., 2010; Roige et al., 2016). Caja and others (2010) show the Ainsa Basin was initially filled with quartz rich arenites (Figols Fm.), followed by calclithites and hybrid arenites as feldspars, lithic fragments, and carbonate grains increased from the uplifting Paleozoic basement and emerging fold-thrust structures. The source of the carbonate grains can be separated by grain types: extrabasinal carbonate grains were sourced primarily from Cretaceous and Paleocene carbonated eroding from the fold-thrust belt and intrabasinal carbonate grains were sourced from the Guara carbonate platform directly south of the basin. The source of the siliciclastic material is less constrained. Caja and others (2010) noted the siliciclastic component of the Hecho group evolved from quartz rich feldspar poor arenites to hybrid arenites with increasing components of feldspars, plutonic and metamorphic lithic fragments and more angular clasts. This was interpreted to reflect an initial source region of intensely weathered Paleozoic basement transitioning to less weathered Paleozoic basement sources as unroofing brought deeper structural levels to the surface. Previous detrital zircon studies of Filleaudeau and others (2012), Whitchurch and others (2011), and Gupta (2008) found that the distribution of zircon U-Pb ages evolved from spectra dominated by Cadomian (~600 Ma) and Caledonian (~450 Ma) age components in the late Cretaceous through the Paleocene to spectra dominated by Variscan grains (~300 Ma) by the late Eocene and Oligocene. This was interpreted to reflect a provenance change from an Eastern Pyrenean source to a Central Pyrenean source as the sediment delivery network evolved from an axis parallel flowing system to an axis perpendicular flowing. However, these studies used limited numbers of samples and grains

to describe the source of siliciclastic material over time (Whitchurch et al., 2011; Filleaudeau et al., 2012). This study will revisit this problem and methodology, applying higher temporal resolution and more extensive statistical treatment of sampling. Well-constrained source region characterization is imperative to reconstructing source provenance changes.

Source Region U-Pb Characterization

The first step in constraining sediment provenance evolution must be the characterization of the potential source regions and the age distributions of those sources. There are three potential source regions to consider in reconstructing detrital provenance; northern sources located within the Pyrenees, eastern sources of the Catalan Coastal Ranges, and southern sources of the Ebro massif and the Iberian ranges (Fig. 5). Western sources of sediment need not be considered as the western boundary of the Pyrenean fold-thrust belt and foreland basin was a deep ocean basin connected to the Atlantic in the early Paleogene.

Crystalline rocks of the Paleozoic basement within the Axial Zone of the Pyrenees have been dated using ^{40}Ar-^{39}Ar and U-Pb geochronology (Solé et al., 2003; Whitchurch et al., 2011 and refs within) (Fig. 5). The U-Pb ages for granitoid and metamorphic exposures are summarized in figure 5 and display distinct spatial trends. The Central Pyrenean Paleozoic basement hosts many granitoid intrusions ranging from granitic to granodiorite in composition (Denèle et al., 2014) with ages ranging from 280-330 Ma, and were emplaced during the Variscan Orogeny. The eastern Pyrenean Axial Zone contains

Cadomian (~600 Ma) and Caledonian (~450 Ma) metamorphics ranging in composition from ortho- to paragneisses in association with Variscan granitoids. These bodies were granitoids emplaced during the Caledonian and Cadomian orogenesis respectively and later experienced ductile deformation and metamorphism during the Variscan orogeny. Solé and others (2003) identified several bodies of Cretaceous alkaline magmatic bodies with ages ranging from 90-110 Ma in the eastern Pyrenees. Paleozoic and Mesozoic strata provided overburden above the Cadomian and Variscan basement rocks. Ordovician through Devonian metasediments are rich in detrital zircons dominated by a Cadomian component (520-700 Ma), minor components of Caledonian (420-520 Ma) and presence of all components >700 Ma (Hart et al., 2016; Margalef et al., 2016). Carboniferous strata of the Pyrenean Axial Zone mark an introduction of syndepositional volcanic zircons sourced from the Variscan arc (Martinez et al., 2015). Variscan grains (280-330 Ma) remain second to Cadomian grains in Carboniferous-Permian strata. Triassic deposits show a marked decrease in Variscan grains relative to Cadomian and Kibaran (900-1200 Ma) age components (Hart, 2015; Hart et al, 2016). Mesozoic cover rocks are mostly composed of carbonates (Lunsen, 1970; Mey et al., 1968, Pudigdefabregas et al., 1992) but have minor siliciclastic bodies. Filleaudeau and others (2012) found that Albian sandstones of the Turbon Formation were dominated by Variscan grains with a peak centered on 318 Ma, minor components of Caledonian and Paleoproterozoic (1500-2200 Ma) grains are present. Whitchurch and others (2011) found the Campanian-Maastrichtian Aren Formation to be rich in Cadomian grains with minor components of Variscan, Caledonian, Kibaran, and Neoproterozoic (700-900 Ma) grains. DZ distributions for the Paleocene Garumnian

formation of the Tremp basin contain a significant Variscan component followed by a minor Cadomian component and minor contribution from older components (Whitchurch et al., 2011; Filleaudeau et al. 2012).

The Catalan Coastal Ranges (CCR) are a potential source region and are mostly composed of ~300 Ma Variscan basement (Denèle et al 2014) with the aforementioned small Cretaceous magma bodies. Cretaceous alkaline magmatic bodies ranging in age from 60-80 Ma are observed in the northern CCR (Solé et al 2003). An important sedimentary unit of the CCR is the Carboniferous Culm Fm, this represents the forearc basin during the Variscan orogeny and has a large component of early Variscan volcanic zircon grains (Julivert et al. 1990; Delvolvé et al., 1998; Martinez et al., 2015). The Ebro Massif and Iberian Ranges are primarily composed of Variscan basement rocks with crystallization ages between 280 and 310 Ma (Martinez et al., 2015).

Source Region Exhumational History

Thermochronometric studies of the basement rocks of the Axial Zone reveal an extensive exhumational phase from 70-20 Ma (Morris et al., 1998; Fitzgerald et al., 1999; Sinclair et al., 2005; Metcalf et al., 2009; Beamud et al., 2011; Rahl et al. 2011; Rushlow et al., 2013; Erdos et al., 2014;). Bedrock zircon fission track, zircon (U-Th)/He, apatite fission track and apatite (U-Th)/He studies show several clear spatial trends in cooling ages of all thermochronometers; a decrease in ages from north to south (Sinclair et al., 2005) indicates a north to south propagation of exhumation, and a decrease in ages from east to west (Fitzgerald et al., 1999) indicates diachronous exhumation propagating from east to west. The early to mid Lutetian is a period of rapid east to west thrust propagation

(Mouthereau et al., 2014). The northern Pyrenean Axial Zone basement rocks have Paleocene cooling ages that may reflect cooling by crustal thickening caused by Iberian underplating of Eurasia and not necessarily exhumation related cooling (Vacherat et al., 2014). Low-temperature thermochronometers such as apatite fission track are not as useful for this study as mid temperature thermochrometers like zircon fission track or zircon (U-Th)/He, because the lower temperature sensitivity records post orogenic incision and cooling associated with to isostatic adjustments after the internally drained Ebro Basin found an outlet to the Mediterranean. This study seeks to use both DZ U-Pb and (U-Th)/He of the siliciclastic component of the Hecho Group turbidites to discriminate the sediment sources and exhumational history of early fold-thrust evolution during orogenesis.

METHODOLOGY

Field Methods and Sample Preparation

20 sandstone samples ranging in size from 2-5 kg were collected from representative outcrop exposures of each turbidite complex within the Ainsa Basin (Fig. 2, Appendix. A). Turbidite complexes were sampled from 10-50 cm thick beds from the Ta turbidite horizon (Shanmugam, 1997) to accurately represent the sediment flux associated with the turbidite deposit and minimize effects by hydrodynamic sorting (Malusà et al., 2015). Sample locations were recorded by Garmin® GPS. Zircon separates were isolated from the samples by standard mineral separation procedures; jaw and disc crushing, Gemini water table separation, Frantz® isodynamic magnetic separation, and heavy liquid separtation (bromoform, and MEI (methylene iodide)). Mineral separation and analysis

was carried out at the UTChron geo-/thermochronology laboratory of the Department of Geological Sciences at the University of Texas at Austin.

Zircon U-Pb Geochronology

Zircons were grain mounted onto double-sided adhesive on plastic pucks (2.54 cm in diameter). Grains were left unpolished as to allow for rim piercing method on a LA-ICP-MS (Campbell et al., 2005; Marsh and Stockli, 2015; Hart et al., 2016). Zircon U-Pb analysis was completed using a PhotonMachine Analyte G.2 excimer laser with a HeLex 238 sample cell attached to a Thermo Scietific Element2 Inductively Coupled Plasms-Mass Spectrometer for isotopic analysis. GJ1 was used as a primary standard (Jackson et al., 2004) three secondary standard (91500 (Wiedenbeck et al., 2004), Plesovice (Salama et al., 2008), Pak1 (in house standard)) were used to monitor data quality. At least 120 grains per sample were analysis for a 95% confidence of capturing every age component, which is at least 5% of the total population (Vermeesch, 2004). Laser pits 30 μm in diameter and ~15 μm in depth were ablated into the face of the zircon crystal orthogonal to the C axis of the crystal. Analysis of non-polished grains allows for depth profiling of the results with the ability to resolve multiple age zones within crystals resulting in both rim and core ages for a single zircon grain (Campbell et al., 2005; Marsh and Stockli, 2015; Hart et al., 2016) This method also allows the analysis to exclude zones of Pb loss or mineral inclusions ablated in the zircon from the age integration, which could otherwise skew results. Data were reduced and interpreted with the VizualAge™ data reduction scheme for the Iolite™ plug-in on Igor Pro™ software (Paton et al., 2011; Petrus and Kamber, 2012). No common

Pb correction was applied; ages are reported with two sigma absolute errors. Individual grains were excluded during data reduction if the grains were not zircon or there was evidence of errors in analysis. $^{206}Pb/^{238}U$ ages are reported for grains younger than 850 Ma, $^{207}Pb/^{206}Pb$ ages are reported for grains older than 850 Ma. Individual grain ages were excluded if there was a $^{206}Pb/^{238}U$ 2σ error greater than 10%, or $^{206}Pb/^{238}U$ and $^{207}Pb/^{235}U$ discordance greater than 10% for grains younger than 850 Ma or $^{206}Pb/^{238}U$ age and $^{206}Pb/^{207}Pb$ discordance greater than 20% for grains older than 850 Ma.

Zircon (U-Th)/He Thermochronology

Individual zircon grains were selected for double dating analysis based on the relative abundance of U-Pb age components and the criteria for (U-Th)/He analysis (non-fractured, inclusion free grains between 63 and 150 μm in width, with a length no more than three times the width) (Farley, 2002; Saylor et al., 2012; Hart, 2015). Grains were individually packed into platinum (Pt) foil packets. The packets were heated and degassed under ultra-high vacuum; total He concentration was measured on a quadrupole mass spectrometer. Completely degassed grains were removed from Pt packets and dissolved with a combination of Hf and HNO_3. Dissolved samples were analyzed on a Thermo Scientific Element2 Inductively Coupled Plasma-Mass Spectrometer for absolute U, Th, and Sm concentrations. Fish Canyon Tuff zircons were run with unknown grains to monitor data quality (Reiners et al., 2005). 8% standard error was applied to all measurements. Individual analysis were excluded if grains were partially or completely broken during unpacking from Pt packets, or if evidence for incomplete dissolution was present. Results

were filtered out for grains with effective U (eU) measurements greater than 650 ppm due to effects of high radiation damage on the crystallographic integrity of the zircon crystal and effects on He diffusion mechanisms (Guenthner et al., 2013).

RESULTS

U-Pb Results

Detrital zircon U-Pb results are summarized as density distributions (Fig. 6) (Vermeesch, 2012), and tabulated in appendix B. U-Pb ages are binned into groups reflecting the most significant components of the distribution and important crystalogenic phases in the Pyrenees and Alpine –Pyrenean region. The components are divided as follows: Cenozoic (0-66 Ma), Late Mesozoic (66-180 Ma), Permian-Triassic (180-280 Ma), late Variscan (280 -310 Ma), Early Variscan (310-330 Ma), Pre-Variscan (330-420 Ma), Caledonian (420-520 Ma), Cadomian-Pan African (520-700 Ma), Neoproterozoic (700-900 Ma), Kibaran (900 – 1200 Ma), Mesoproterozoic (1200 – 1500 Ma), Paleoproterozoic (1500 – 2200 Ma), Archean – Paleoproterozoic (2200 – 4600 Ma).

Fosado Turbidite System

Two samples of the Fosado turbidite complex were collected and analyzed. The results of each individual analysis yelled indistinguishable zircon U-Pb spectra and therefore the samples have been grouped in increase the statistical robustness of the dataset. Sample 1-Fosado was collected near the base of the Fosado turbidite complex, sample 14AB-F01 was collected near the village of Fosado and was located more central in the

turbidite complex. Analyses grouped from the two samples of the Fosado turbidites yielded 211 concordant grains. The most dominant component are Cadomian grains (26.1%, 55 grains), followed by Late Variscan grains (26.1%, 55 grains), Kibaran (11.4%, 24 grains), Early Variscan (10%, 21 grains), and Neoproterozoic grains (9%, 19 grains). The remaining 17.9% is distributed between the other components, with no components containing more than 7% of the population. The youngest grain in the Fosado samples is 234.5 Ma and the oldest grain is 2853 Ma. Rim and core age relationships are observed on 3.3% (seven grains) of the sampled grains. Three grains have Variscan rims on Cadomian/Pan African cores, one grain has a Caledonian rim on a Cadomian core, and three grains have Cadomian age rims on Proterozoic cores.

Arro Turbidite System

One sample, 2-Arro, was collected from the Arro turbidite complex. The sample was collected near the village of Arro along highway N-260. The sample yielded 125 concordant U-Pb ages. The most dominant component is Late Variscan grains (24%, 30 grains), followed by Early Variscan (22.4%, 28 grains), Cadomian (16.8%, 21 grains), Kibaran (9.6%, 12 grains), and Caledonian (8.8%, 11 grains). The remaining 18.4% is distributed between the remaining components with no component accounting for more than 5% of the population. The youngest grain is 276.2 Ma and the oldest grain is 2682 Ma. Rim and core relationships is observed on 6.4 % (eight grains) of the sampled grains. Five have Variscan rims on Caledonian (2 grains), Cadomian (two grains) and

Neoproterozoic cores (one grain), two grains have Caledonian rims on Cadomian and Neoproterozoic cores, and one grain has a Cadomian rim on a Kibaran core.

Gerbe Turbidite System

Three samples were collected from the Gerbe Turbidite complex. Samples 3-Gerbe and 14AB-G07 were collected from a road cut along highway N-260 and sample 15AB-150 was collected from a stratigraphically higher turbidite near the village of Gerbe. The U-Pb results for all three samples were statistically indistinguishable and grouped to yielded 346 concordant U-Pb ages. The most dominant component is Cadomian grains (30.6% 106 grains), followed by Kibaran (13% 45 grains), Late Variscan (12.1% 42 grains), Neoproterozoic (11% 38 grains), Caledonian (9% 31 grains), Archean-Paleoproterozoic (9% 31 grains), and Paleoportoerozoic (6.9% 24 grains). The remaining 8.4% is distributed among the other components with no component accounting for more that 5% of the population. The youngest grain is 256.1 Ma and the oldest grain is 2926 Ma. Rim and core relationships are observed on 0.58% (2 grains) of the sampled population. One grain has a Caledonian rim on a Neoproterozoic core, the other grain has a Cadomian rim on a Neoproterozoic core.

Banaston Turbidite System

Two samples were collected from the Banaston turbidite complex. Sample 15AB-118 was collected along a roadcut on highway N-260 west of the village of Boltaña and sample 15AB-352 was collected from the hill above the village of Banaston. The samples were statistically indistinguishable and grouped yielding 251 concordant grains. The most

dominant component is Late Variscan grains (35.9%, 90 grains), followed by Cadomian (15.5 %, 39 grains), Early Variscan (10.4%, 26 grains), Paleoproterozoic (8.4%, 21 grains) and Neoproterozoic (7.6%, 19 grains). The remaining 22.2%, is distributed among the other components with no components accounting for more than 6% of the population. The youngest grain is 215.1 Ma and the oldest grain is 3519 Ma. Rim and core relationships are not observed on any grains.

Ainsa Turbidite System

Ainsa I

Two samples were collected from the Ainsa I turbidite complex. Sample 4-Ainsa was collected south of the village of Ainsa at a quarry along highway A-138. Sample 14AB-A06 was collected north of the village of Ainsa along an outcrop exposed under a bridge on highway A-138. The samples yielded indistinguishable DZ spectra and were grouped resulting in 214 concordant ages. The most dominant component is Late Variscan grains (44.9%, 96 grains), followed by Early Variscan (11.7%, 25 grains), Cadomian (8.9%, 19 grains), pre-Variscan (7.9%, 17 grains), Archean-Paleoproterozoic (6.5%, 14 grains), and Permo-Triassic (6.1%, 13 grains). The remaining 14% is distributed between the other components with no component being more than 5% of the population. The youngest grain is 221.2 Ma and the oldest grain is 3380 Ma. Rim and core relationships are observed on 1.41% (three grains) of the sampled population. One grain has a Variscan rim on a Cadomian core, one grain has a Cadomian rim on a Neoproterozoic core, and the final grain has a Neoproterozoic rim on a Kibaran core.

Ainsa II

Two samples were collected from the Ainsa II turbidite complex. Samples 14AB-A05 and 14AB-A04 were collected along an outcrop north of the village of Ainsa on the Barranco Forcaz. Sample 15AB-A04 was collected near the base of the Ainsa II turbidite complex and sample 15AB-A05 was collected stratigraphically higher in the center of the turbidite package. The samples yielded statistically indistinguishable DZ spectra and were grouped into a single sample resulting in 216 ages. The most dominant component is Cadomian grains (20.8%, 45 grains), followed by Early Variscan (15.7%, 34 grains), Late Variscan (13%, 28 grains), pre-Variscan (12%, 26 grains), Caledonian (8.3%, 18 grains), Neoproterozoic (7.4%, 16 grains), Paleoproterozoic (6.9%, 15 grains), and Kibaran (6%, 13 griains). The remaining 9.9% is distributed between the other components with no component accounting for more than 5% of the population. The youngest grain is 240.7 Ma and the oldest grain is 3198 Ma. Rim and core relationships are not observed on any of the analyzed grains.

Morillo Turbidite System

Three samples were collected from the Morillo turbidite complex. Sample 14AB-M02 was collected along an outcrop exposure on a path along the south bank of the Rio Ara directly south of the village of Boltaña. Samples 6-Morillo was collected from an access road off A-2205 near Casa Pelal and Rio Ena, west of the village of Ainsa. 5-Morillo was collected from outcrops at Moprillo de Tou, South of Ainsaalong a creek exposure west of the village of Ainsa, downhill from road A-2205. The samples yielded statistically

indistinguishable DZ spectra and were grouped resulting in 350 concordant ages. The most dominant component is Late Variscan grains (41.4%, 145 grains), followed by Early Variscan (20.3%, 71 grains), Cadomian (10.6%, 37 grains), Paleoproterozoic (6%, 21 grains). The remaining 21.7% is distributed between the remaining components with no component accounting for more than 5% of the population. The Morillo sample has the first appearance of Mesozoic age component with one grain accounting for 0.3% of the population. The youngest grain is 93 Ma and the oldest grain is 3326 Ma. Rim and core relationships are observed on 1.43% (5 grains) of the sampled population. Two grains have Variscan rims on Early Variscan and Cadomian cores, two grains have Cadomian rims on Neoproterozoic and Kibaran cores, and one grain has a Mesoproterozoic rim on a Paleoproterozoic.

Guaso Turbidite System

Two samples were collected from the Guaso turbidite complex. Sample 7-Guaso was collected from a creek exposure west of the village of Ainsa and upstream from the 6-Morillo sample location. Sample 13-Guaso was collected from a roadcut along road A-2205 near the village of Guaso. The samples yielded indistinguishable DZ spectra and were grouped resulting in 249 ages. The most dominant component is Early Variscan grains (30.5%, 76 grains), followed by Late Variscan (18.1%, 45 grains), Cadomian (16.1%, 40 grains), Caledonian (12.4%, 31 grains), and Kibaran (7.6%, 19 grains). The remaining 15.3% is distributed among the other components with no component accounting for more than 5% of the population. The Guaso sample has the largest percentage of Mesozoic

(1.6%, 4 grains) and Cenozoic grains (0.8%, 2 grains) of all the samples. This is the only sample with grains from the Cenozoic component. The youngest grain is 45.11 Ma and the oldest grain is 2836 Ma. Rim and core relationships are observed on 7.63% (19 grains) of the sampled population. One grain has a Cenozoic rim on a Caledonian core, 16 grains have Variscan rims with Caledonian (five grains), and Cadomian (11 grains) cores. One grain has a Caledonian rim on a Cadomian core, and one grain has a Cadomian rim on a Kibaran core.

Sobrarbe Fluvio-Deltaic System

One sample was collected from the Sobrarbe delta. Sample 10-Sobrarbe was collected from a road outcrop near the village of Mondot. The sample yielded 122 concordant grains. The most dominant component is Late Variscan (63.1%, 77 grains), followed by Early Variscan (27%, 33 grains), and Kibaran (3.3%, 4 grains). The remaining 6.6% is distributed between the remaining components with no component accounting for more than 4% of the population. The youngest grain is 283.4 Ma and the oldest grain is 2885 Ma. Rim and core relationships are observed on 1.64% (two grains) of the sampled grains. One grain has a Variscan rim on a Caledonian core, and the other grain has a Cadomian rim on a Kibaran core.

Escanilla Fluvio-Deltaic System

Two samples were collected from the Escanilla fluvio-deltaic system. Sample 11-Escanilla was collected near the village of Olson ~100 m beneath the Olson member conglomerate of the Escanilla formation. Sample 12-Escanilla was collected near the

village of Olson and above the Olson member. The samples were grouped and resulted in 249 ages. The most dominant component is Late Variscan grains (28.9%, 72 grains), followed by Early Variscan (19.3%, 48 grains), Cadomian (18.5%, 46 grains), pre-Variscan (9.6%, 24 grains), and Paleoproterozoic (6.8%, 17 grains). The remaining 16.9% is distributed between the remaining components, with no component accounting for more than 4% of the population. The youngest grain is 282.8 Ma and the oldest grain is 3011 Ma. Rim and core relationships are observed on 6% (15 grains) of the sampled grains. Ten grains have Variscan rims on Caledonian (one grain), Cadomian (five grains), Neoproterozoic (one grain), Mesoproterozoic (one grain), and Archean-Paleoproterozoic (two grains) cores. Four grains have Cadomian rims on Cadomian (one grain), Neoproterozoic (one grain), Kibaran (one grain), and Paleoproterozoic (one grain) cores. The final zoned grain has a Paleoproterozoic rim on an Archean core.

Zircon (U-Th)/He Results

Detrital zircon (U-Th)/He results are summarized as density distributions (Fig. 7) (Vermeesch, 2012), and tabulated in appendix C. Double-dating age relationships are summarized in figure 8. (U-Th)/He ages are binned into groups reflecting the most significant components of the distribution and important cooling phases in Pyrenean thermotectonic history. The bins are divided as follows: Pyrenean compression (30-70 Ma), initial basin inversion centered in the Santonian (70-90 Ma), Cretaceous rifting (90-140 Ma), early rift phases and plutonic cooling (140-300 Ma) and inherited cooling events (>300 Ma).

Fosado Turbidite system

One sample, 1-Fosado was selected as a representative sample for (U-Th)/(Pb-He) double dating. 24 Of the 25 grains were yield useable (U-Th)/He ages. The most dominant component are Pyrenean cooled grains (54.2%, 13 grains), followed by grains cooled during Cretaceous rifting (25%, 6 grains), initial basin inversion (16.7%, 4 grains), and early rifting/plutonic cooling (4.1%, 1 grain). The youngest cooling age is 38.13 Ma and the oldest cooling age is 167.69 Ma.

Arro Turbidite system

Of the 25 grains selected from the 2-Arro sample 24 yielded usable (U-Th)/He ages. The most dominant component are grains cooled during Cretaceous rifting (37.5%, 9 grains), followed by early rifting/plutonic cooling (27.2%, 7 grains), initial basin inversion (16.7%, 4 grains), and Pyrenean orogenic cooling (16.7%, 4 grains). The youngest cooling age is 56.64 Ma the oldest cooling age is 219.26 Ma.

Gerbe Turbidite System

Sample 14AB-G07 was selected from the three Gerbe samples ran for DZ U-Pb distributions for (U-Th)/(Pb-He) double dating. Analysis yielded 25 usable (U-Th)/He ages. The most dominant component are grains cooled during Pyrenean orogenesis (56%, 14 grains), followed by grains cooled during initial basin inversion (24%, 6 grains), Cretaceous rifting (8%, 2 grains), early rifting/plutonic cooling (8%, 2 grains), and inherited cooling ages (4%, 1 grain). The youngest grain has a cooling age of 38.75 Ma and the oldest grain has a cooling age of 301.77 Ma.

Banaston Turbidite System

Sample 15AB-118 was selected of the two Banaston samples ran for DZ U-Pb distribution for (U-Th)/(Pb-He) double dating. From the 25 grains selected 24 yielded useable ages. The most dominant component are grains cooled during early rifting/ plutonic cooling (50%, 12 grains), followed by grains cooled during Pyrenean Orogenesis (20.8%, 5 grains), initial basin inversion (16.7%, 4 grains), and Cretaceous rifting (12.5%, 3 grains). The youngest cooling age is 54.30 Ma and the oldest cooling age is 268.29 Ma.

Ainsa Turbidite System

Ainsa I

Sample 4-Ainsa was selected from the two Ainsa I samples ran for DZ U-Pb distributions. Analysis yielded 24 useable grains of the 25 picked for (U-Th)/He analysis. The most dominant component is Cretaceous rifting (33.3%, 8 grains), followed by Pyrenean orogenic cooling (25%, 6 grains), cooling from early rifting and plutonic cooling (25%, 6 grains), and initial basin inversion derived cooling (16.7% 4 grains). The youngest cooling age is 42.34 Ma and the oldest cooling age is 255.94 Ma.

Ainsa II

Sample 14AB-A05 was selected from the two Ainsa II samples ran for DZ U-Pb. From the 25 grains picked for double dating 22 grains yielded useable (U-Th)/He ages. The most dominant component is Pyrenean cooling (27.3%, 6 grains); in equal proportion is the initial inversion cooling component (27.3%, 6 grains). These are followed in relative

proportion by both grains cooled during Cretaceous rifting and early rifting/plutonic cooling both in equal proportion each accounting for 22.7% (5 grains) of the sample respectively. The youngest cooling age is 49.95 Ma and the oldest cooling age is 274.28 Ma

Morillo Turbidite System

Sample 14AB-M02 was selected from the three Morillo samples collected for double dating. From the 25 grains picked for (U-Th)/He analysis 24 yielded usable ages. The most dominant component of the detrital cooling distribution is Pyrenean orogenic cooling (50%, 12 grains), this is followed in relative proportion by the component cooled during early rifting and plutonic cooling (20.8%, 5 grains), Cretaceous rifting (16.7%, 4 grains), and initial basin inversion (12.5%, 3 grains). The youngest cooling age is 44.03 Ma and the oldest cooling age is 268.03 Ma.

Guaso Turbidite System

Sample 7-Guaso was selected from the two Guaso sampled collected for double dating. Of the 25 grains picked for double dating 24 grains yielded usable (U-Th)/He ages. The most dominant cooling component from the sample is Pyrenean orogenic cooling (40.9%, 9 grains), this is followed in relative abundances by both early rifting/plutonic cooling and initial basin inversion cooling in equal proportion accounting for 22.7% (5 grains) of the cooling distribution. The remaining 13.9% (3 grains) have cooling ages greater than 300 Ma reflecting inherited cooling ages. The youngest cooling age is 46.76 Ma while the oldest cooling age is 398.42 Ma.

Sobrarbe Fluvio-Deltaic System

Sample 10-Sobrabre yielded 25 usable (U-Th)/He ages. The most dominant cooling component are grains cooled during Pyrenean orogenesis (60.0%, 15 grains), followed by grains cooled during Cretaceous rifting (28%, 7 grains) and the remaining 12% is accounted for by grains cooled during initial basin inversion. The youngest cooling age is 45.74 Ma and the oldest cooling age is 128.88 Ma.

Escanilla Fluvio-deltaic system

Sample 12- Escanilla was selected for double dating from the two Escanilla samples collected. (U-Th)/He analysis yielded 23 useable cooling ages from the 25 grains picked. The most dominant component is Pyrenean cooling (65.2%, 15 grains), followed in relative abundance by grains cooled during initial basin inversion (17.4%, 4 grains), Cretaceous rifting (13%, 3 grains), and the remaining 4.3% (1 grain) has a cooling age reflecting early rifting. The youngest cooling age is 45.38 Ma and the oldest cooling age is 193.88 Ma.

DISCUSSION

DZ U-Pb Overall Trends

The overall patterns in DZ U-Pb data from the lower to upper Hecho Group can be summarized as follows, the DZ U-Pb data from the basal Fosado turbidites to the Escanilla fluvial deposits show a gradual increase in the Late Variscan component and a decrease in the Cadomian component and components >700 Ma (Fig. 9). These results are consistent with previous DZ studies (Whitchurch et al., 2011; Filleaueau et al., 2012) which interpreted the transition from Cadomian to Variscan dominated DZ components to reflect

a progressive switch from an axial drainage network, tapping Cadomian and Caledonian crystalline rocks of the eastern Pyrenees, to a transverse drainage network, tapping Variscan plutons of the central Pyrenees. This switch in source region has been suggested to be coeval with the initiation of exhumation along thrusts in the central and western Pyrenees, and the initiation of antiformal stacking within the Pyrenean Axial Zone (Teixell, 1998; Beaumont et al., 2000; Whitchurch et al., 2011). The Cadomian/Pan African DZ U-Pb signature has been identified as a signature of an eastern Pyrenean source due to the presences of Cadomian orthogneiss bodies in the exposed basement of the eastern Pyrenean Axial Zone (Gupta, 2008; Whitchurch et al., 2011; Filleaudeau et al., 2012). However, these studies failed to recognize the possible ambiguity in the source of Cadomian zircons which may also be derived from recycling of Mesozoic and Paleozoic sedimentary and metasedimentary units. Recent DZ studies of Paleozoic metasediments (Hart et al., 2016; Margalef et al., 2016) reveal a DZ U-Pb distribution similar to that observed in the crystalline basement of the Eastern Pyrenees. These new constraints on source region evolution must be considered in four dimensional paleogeographic reconstructions to discriminate whether the apparent change in signatures are due to a provenance shift from an eastern to a central Pyrenean source, attributed to a progressive unroofing of Paleozoic-Mesozoic sediments before eroding deeper structural levels containing the Variscan plutons, or contributions from the eastern and southern sources of the Ebro Massif, Iberian Range or Catalan Coastal Ranges. Caja and others (2010) observed a progressive shift in the petrography of the Hecho Group from quartz-rich feldspar-poor arenites, which initially filled the basin, towards an increase in feldspar and lithic grains in conjunction with an

increase in plutonic and metamorphic rock fragments up section. This was interpreted to reflect a progressive unroofing signature of the Pyrenean thrust sheets eroding through sedimentary and metamorphic cover rocks exposing Variscan basement (Caja et al., 2010). An exclusively transverse unroofing model for the Pyrenees would first erode Mesozoic and Paleozoic cover rocks before taping deeper structural levels and eroding Variscan plutons, eventually leading to the erosional unroofing of Cadomian metamorphic rocks intruded by Variscan plutons. In this hypothesis the DZ signatures would evolve from Cadomian dominated signatures from basin recycling to Variscan dominated and back to Cadomian dominated. However, new data from this study are not consistent with a simple two dimensional unroofing model and therefore a temporally variable three dimensional model must be invoked to describe the observed trends.

Cretaceous Volcanic Zircons

The small component of Cretaceous aged zircons within the Guaso (four zircons, 1.6%) and Morillo (one zircon, 0.3%) samples have been identified as volcanic zircon grains characterized by the identical U-Pb and (U-Th)/He ages (Fig. 8). Gupta (2008) found one Cretaceous zircon within the Banaston turbidites. In terms of the source, the zircons are speculated to have originated from either the Sant Feliu de Buxalleu, S' Agaro, or Aiguablava Cretaceous alkaline magmatic bodies located in the Catalan Coastal Ranges (CCR) (Solé et al 2003). Two hypotheses about the paleodrainage networks can be drawn from the presence of these Cretaceous volcanic zircons. First, the extensive catchment area delivering sediment to the Ainsa Basin extended to the CCR and taped erosional source

regions within the CCR. In this case the presence of multiple turbidites containing these grains indicates long lived fluvial connectivity to the CCR. Alternatively, these zircons may be derived from Mesozoic or early Cenozoic sediments from Pyrenean post rift and early foreland basin fill that were recycled into the Eocene fluvial network bringing sediment to the basin. In this hypothesis long lived fluvial connectivity to the CCR to the rest of the basin is not necessary to explain the presence of the Cretaceous aged DZs. In either hypothesis the relative volumetric contribution from the CCR appears to be small when compared to the Pyrenean sediment contribution, but these grains provide an important indicator of the CCR source region.

DZ (U-Th)/He Trends

DZ (U-Th)/He data reveal an overall increase in the Pyrenean cooling age component (70-20 Ma) and decrease in early rifting and plutonic cooling age components (140-300 Ma) (Fig. 11). The component of Cretaceous rifting (90-140 Ma) decreases slightly from ~35% at the base of the section to ~15% at the top. The inversion component (70-90 Ma) shows little up section variation, remaining at ~18% throughout the section. Zircons with inherited cooling ages (>300 Ma) are only present in two samples, the Gerbe and the Guaso turbidites. The constant component of Pyrenean cooled zircons indicates a continual flux of sediment sourced from tectonically exhumed source regions within the emergent fold-thrust belt and basement thrust sheets. The decrease of the Cretaceous and inversion cooled zircons are interpreted as the unroofing and recycling of Mesozoic basins sediments. The constant component of zircons with early rift and inherited cooling ages

are interpreted as sediment input from sources outside the Pyrenees or Mesozoic basin fill which was not buried to depths deep enough to reset the zircon (U-Th)/He thermochronometers. The youngest component of DZ (U-Th)/He ages decreases upsection and falls within 0-10 Myr of the depositional age (Fig. 10). However, the oldest single zircon cooling age and oldest cooling component increases in age up section (Fig. 10). This trend in the old DZ (U-Th)He age component is opposite of expected trends for a classic unroofing sequence, where it is expected that all cooling ages will get younger as unroofing taps deeper structural levels. Two hypothesis can be invoked to describe this trend, a provenance shift in the non-Pyrenean source region taping catchments with progressively older cooling histories, or a "double-unroofing" sequence in which the sediments are unroofed from shallow sedimentary basins containing unreset zircons resulting in an inversion of the up section unroofing signature in the original sedimentary basin. One powerful application of the double-dating technique is the ability to elucidate the thermal history of specific U-Pb components and their change through time. Lag-time analysis, defined as the difference between cooling and depositional age, is another powerful tool for estimating rates of exhumation and tectonic dynamics of exhumation and erosion (Garver et al., 1999; Saylor et al. 2012; Hart, 2015).

Short Lag-Time Zircon (U-Th)/He Ages

The component of zircons with short lag-times (lag-time = cooling age – depositional age, Garver et al., 1999) show clear trends with respect to stratigraphy (Figs. 9,11). Zircons with a lag-time < 20 Myr are interpreted to represent the flux of tectonically

exhumed material shead off of the emergent Pyrenean thrust sheets. A lag-time of 5-10 Myr is observed for youngest three cooled zircons in each sample. Beginning with the Arro turbidite complex the shortened lag-time component varies between 10 Myr and 0 Myr up section. A clear upsection pattern is seen for the different U-Pb components with lag-times < 20 Myr (Fig.9, 11). The component of short lag-time zircons with Late Variscan crystallization ages increases and the component of short lag-time Cadomian zircons decreases upsection. All short lag-time zircons with U-Pb ages > 700 Ma decrease up section, while there is a minor increase in the short lag-time Early Variscan zircons. Summing the Late Variscan and Cadomian components approximates the relative amount of material derived from the crystalline basement thrust sheets of the emergent Pyrenean Axial Zone (Fig. 11). The sum of these two components reveal a relatively constant sediment flux derived from the emergent Pyrenees.

The compensatory relationship between Cadomian and Late Variscan components indicates a westward propagation of progressive deformation and decreasing input from Cadomian sources in the eastern Pyrenees, compensated by greater input from Variscan plutonic sources in the central Pyrenees through time (Fig. 11). Thus, it is inferred that the relatively constant sediment flux derived from the emergent Pyrenees orogen experiences a progressive provenance shift in response to the westward propagating thrust deformation, and fold-thrust structures propagating into the foreland (Fitzgerald et al., 1999; Mouthereau et al., 2014). This is consistent with bedrock thermochronologic studies showing exhumation propagating from east to west in the Eocene (Fitzgerald et al., 1999; Verges et al., 2002) and interpretations of Whitchurch and others (2011) that the sediment delivery

network evolved from axial drainage taping sources in the eastern Pyrenean thrust sheets to a transverse drainage taping the central Pyrenean thrust sheets. The decrease in all short lag zircons with U-Pb ages >700 Ma indicates the cessation of Paleozoic metasediment unroofing as erosion reached deeper structural levels.

Chronostratigraphic Implications

Recent biostratigraphic and magnetostratigraphic studies have refined the depositional age models for the Ainsa Basin stratigraphy (Payros et al., 2009; Mochales et al., 2012; Scotchman et al., 2014; Mochales et al., 2016) (Fig. 12). All lag-time calculations for this study use the Scotchman and others (2014) depositional age model for the middle and upper Hecho Group and the Mochales and others (2012) age model for the lower two turbidite complexes. The average of the youngest three cooling ages obtained in this study reveal a constant 5-10 Myr lag-time for the youngest cooled component. The Fosado is the only sample where the cooling ages are younger than depositional ages. This may be caused by partial resting during post depositional burial and the proximity of the Fosado turbidites to imbricate thrust splays of the Peña Montañesa thrust (Fig. 2). However, no other samples show evidence of partial resetting of zircon grains.

Long Lag-Time Zircon (U-Th)/He Ages

Grains with a lag-time >20 Myr are interpreted to be derived from shallow positions in Pyrenean thrust sheets, or from the Iberian Ranges and CCR. Upsection trends in U-Pb components of long lag-time zircons are less obvious than those for short lag-time grains. Four major positive peaks are observed across the stratigraphy: long lag-time Cadomian

and pre Variscan zircons in Gerbe, long lag-time Late Variscan zircons in Ainsa I, early Variscan in Morillo, and long lag-time late Variscan zircons in the Sobrarbe. These grains are interpreted to be derived from sources exhumed prior to Pyrenean compression or were located in pre-compressional sediments above the zircon partial retention zone. Two options exist for the source of these long lag-time zircons, they are derived from exhumed basement outside the Pyrenees in the CCR, Ebro Massif, and/or Iberian Range exhumed in earlier events, or they are derived from recycling of Paleozoic-Mesozoic sediments that were not reset during their burial history.

Paleogeographic Evolution

The double dated zircon thermochronometric and geochronometric data place new spatial and temporal constraints on Pyrenean foreland basin evolution. A new paleogeographic model is established in the Ainsa Basin area by incorporating new constrains with previous paleogeographic, and tectonic models (Nijman 1998; Dreyer et al 1999; Whitchurch et al., 2011) and recent paleomagnetic restorations (Muñoz et al., 2013). Figure 13 displays three reconstructions of the paleogeographic evolution for the late Ypresian, Lutetian, and Bartonian. This overview paleogeographic model sheds light on the siliciclastic sediment sources and explains the major trends of these new detrital geo- and thermochronometric data.

Ainsa Basin Sedimentation rates ranged from 0.1-0.15 km/Myr during the late Ypresian as the Bóixols – Cotiella thrust sheet accommodated the greatest amount of shortening (Mochales et al., 2002; Beamud, 2013). Siliciclastic sediment feeding the

Fosado and Arro turbidites was primarily sourced from thrust sheet exhumed Cadomian-aged basement and Paleozoic metasedimentary rocks in the eastern Pyrenees, with minor sediment contributions from the Ebro Massif and CCR creating the observed long lag-time Variscan zircon population, interpreted to be sourced from intensely weathered Paleozoic plutons to the south and southeast of Ainsa Basin. Shortening along the Nogueres thrust sheet led to recycling of Mesozoic rift units supplying sediment to Ainsa Basin through the San Esteban Fan. The majority of sediment was routed parallel to the thrust fronts through the Ager and Tremp-Graus basins prior to significant foreland propagation along the Montsec thrust (Fig 13.A).

Thrust propagation and the development of the Gavarnie-Serres Marginales thrust sheet reorganized the Ainsa Basin from a foredeep to a piggyback depocenter by the late Lutetian. The Montsec thrust propagated ~42 km relative to its position in the late Ypresian (Muñoz et al., 2013). This promoted the Tremp-Graus Basin as the preferred sediment delivery pathway, and isolated the Tremp-Graus Basin from the eastern Ripoll Basin as a result of topographic damming along the Segre oblique ramp fault zone (Vergés and Muñoz, 1990). Siliciclastic sediment feeding the Ainsa, Morillo, and Guaso turbidite systems was primarily sourced from the Variscan plutons within the Paleozoic basement of the Nogueres thrust sheet. Recycling of Cretaceous basin fill along the frontal Montsec and Bóixols thrusts and possibly input the Ebro Massif and CCR introduced the long lag-time component and Cretaceous volcanic grains into the basin (Fig. 13.B).

Non-marine deposition of the Sobrarbe and Escanilla Formations represents a progradational depositional entering Ainsa Basin between the Boltaña and Mediano

anticlines. Sedimentation rates increase to 0.25 km/Myr in response to Ebro basin closure towards the Atlantic Ocean (Costa et al., 2010; Mochales et al., 2012). Siliciclastic sediment was primarily sourced from the Nogueres thrust sheet and routed into the Tremp-Graus basin through the Sis and Grup paleovalleys (Armitage et al., 2015). This progradation of coarse clastic material into the deep marine was contemporaneous with Ebro basin closure (Costa et al., 2010) and enhanced exhumation within the Axial Zone by antiformal stacking (Texiell., 1998; Beaumont et al., 2000; Beamud, 2013; Teixell et al., 2016) (Fig 13.C).

Oscillatory Nature of Detrital Zircon U-Pb and (U-Th)/He Signals

Although the major provenance trends are clear there exists an unexpected oscillation in U-Pb and (U-Th)/He age component signals (Figs. 9,11). The proportion of DZ U-Pb components alternates upsection with some components increasing and decreasing by 10-20% of the population in stratigraphically adjacent samples. Similar oscillations are observed in the DZ (U-Th)/He components. These signals are not an artifact of the inherent variability of small sample size, because the observed alternation is present in both the (U-Th)/He signal and the large n U-Pb signal. This oscillation can be potentially attributed to multiple mechanisms, including locally-derived variations in fold-thrust exhumation focusing erosion along the front of active thrusts, cyclicity in foredeep location (Nijman, 1998), or location switching of the subsidence focus within the foredeep-piggy-back basins establishing preferred sediment delivery pathways. Nijman (1998) observed a cyclical shift in basin axis (zone of maximum subsidence) location alternating between

northern and southern locations within the Tremp-Graus and Ager basins from the early Eocene into the Bartonian. The basin axis alternated at least four times from a northern location in the Tremp-Graus basin close to the alluvial fans and basement involved thrusts to a southern location in the Ager Basin on the southern limb of the Montsec thrust. The oscillatory shifts of basin axis may be attributed to periods of critical wedge reorganization from a subcritically to a critically tapered orogenic wedge (Davis et al., 1988; Dahlen, 1990).This shift in basin axis location alternated the dominant fluvial transport location from the Tremp-Graus basin to the Ager basin. The Ager basin received sediment sourced from the Eastern Pyrenees, CCR and southern source regions (Ebro Massif and Iberian Range) while the Tremp basin received more sediment from the central Pyrenean region. During basin axis oscillation it is hypothesized the DZ U-Pb distribution will have more eastern Pyrenean Cadomian grains when the basin axis is in the south and more central Pyrenean Variscan grains when the basin axis is in the north. The largest southward movement of the basin axis into the Ager basin occurred during the early Lutetian and corresponds temporally to the deposition of the Gerbe channel (Nijman, 1998). The Gerbe channel has the strongest proportion of Caledonian, Cadomian and older components relative to the Variscan components hypothetically indicating higher sediment flux from the Ager basin relative to the sediment flux from the Tremp-Graus basin. The basin axis rapidly migrated north to its initial position in the Tremp-Graus basin by the time of Banaston turbidite deposition in the early-mid Lutetian. This northward migration of basin axis hypothetically delivered a higher sediment flux from the Tremp-Graus basin (Nijman,

1998). The Variscan dominated DZ U-Pb signature of the Banaston turbidites reflects enhanced sediment supply from the Tremp-Graus basin.

In addition to local tectonic variability, global or regional forcing mechanisms should also be considered. Eustatic driven variability has been proposed as an important mechanism in establishing the sedimentary architecture (Huyghe et al., 2009; Honegger, 2015). Climatic variability driven by regional climate evolution and orbital forcing has also been employed as a principal forcing mechanism and may also produce variability in DZ signatures (Cantalejo and Pickering 2014). An important concept to consider given the strong dependence of stratigraphic architecture on eustacy is sea level control on catchment area. During periods of sealevel highstand and flooding of the axial trough the catchment area is reduced and sediment is only sourced locally, additionally the effects of regional base level rise cause the deltaic and fluvial depozones to become aggradational and accumulate sediments. The DZ U-Pb and (U-Th)/He signals will have fewer components and shorter lag-times as small restricted catchments in the thrust sheet deliver sediments directly into the depositional sink. After sea level reaches its maximum flooding level, the sea level falls triggering the catchment to expand reaching a greater variety of source regions. During sea level fall the fluvial and deltaic depozones become incisional reworking and recycling of deposits laid down during highstand deposition. The DZ U-Pb and (U-Th)/He signals during sea level fall will have more components from a greater variety of sources and longer lag times from longer sediment transport and reworking of the fluvio-deltaic plan. During lowstand period the base level fall allows for a large integrated drainage taping many sources, with net bypass or incisional recycling in the

transfer zone. DZ U-Pb and (U-Th)/He signals delivered during a sealevel lowstand will be more mixed with a greater variety of components. Climatically controlled sediment supply variations may produce the observed oscillations as well. During arid periods fluvial networks have less of a carrying capacity, sediment is staged within the transfer zone and ephemeral streams cease to contribute sediment. The DZ U-Pb and (U-Th)/He signals in an arid climatic regime will reflect sourced tapped by only the largest streams. During humid periods the increased precipitation rates increase the fluvial carrying capacity of streams and rivers, increasing the sediment flux and "flushing" of sediment stored in ephemeral catchments. For the particular case of the Eocene south Pyrenean foreland basins it is likely an interplay between these various forcing mechanisms which lead to the depositional stacking pattern.

Implications for 4D Sediment Dispersal in Early Fold-Thrust Belts

DZ (U-Th)/(Pb-He) double-dating offers a robust and powerful approach that can be applied to numerous early foreland basin models. A four dimensional source-to-sink approach is necessary for evaluating sedimentary provenance in narrow deep early foreland basins with a significant axis parallel flow. The interplay between the emergent fold and thrust structures, orogenic growth in the hinterland thrust sheets, and eustatic and climatic variability all play major roles in the evolution of sediment redistribution networks. The first order control on basin sedimentation is from tectonic growth of the fold-thrust belt and hinterland structures in response to major tectonic pulses at 1s-10s Myr timescales. Climatically induced variability in water discharge and geochemical weathering

environments can lead to major variations in sediment flux, particularly in systems with long transfer zones and potential for biologically enhanced temporary storage (Johnsson et al., 1991; Romans et al., 2015). Climatic cycles are driven by orbital cyclicity and changes in global atmospheric and oceanic circulation patterns which produce cycles within 40-100 Kyr timescales. Eustatic variability has the greatest potential for modulating the stratigraphic architecture within marine basins. Eustatic cycles have shorter wavelengths c than climatic cycles or tectonic pulse cycles. Furthermore, Eustacy effects sedimentation at the depositional sink without being propagated through a transfer zone which may buffer or mask the signal of environmental forcing.

CONCLUSIONS

DZ (U-Th)/(Pb-He) double-dating analysis reveals a complex provenance evolution for the Eocene Ainsa Basin. Sediment was initially sourced from Cadomian thrust sheets in the eastern Pyrenees, intensely weathered Variscan basement in the Ebro Massif, Iberian Range, and Catalan Coastal Ranges, and unroofed Paleozoic and Mesozoic strata in the Pyrenean fold-thrust belt. An upsection decrease in eastern Pyrenean Cadomian thrust sheet material compensated by an increase in central Pyrenean Variscan thrust sheets reflects the westward propagating deformation front. Sediment sourced from all regions was routed into the Ainsa Basin through the Tremp-Graus basins and Ager basins.

Cretaceous volcanic zircons in the Guaso, Morillo and Banaston (Gupta, 2008) indicate either a long lived fluvial connectivity to the Catalan Coastal Range and the

Eastern Pyrenees, or recycling of early foreland basin/syn- and postrift deposits which were connected to the Catalan Coastal ranges at time of deposition. The majority of siliciclastic sediment was derived from the emergent Pyrenean orogen during the Eocene based on the constant component of Pyrenean cooling ages, although basin recycling, unroofing contributed sediment throughout the Eocene.

The oscillatory nature of both the U-Pb and (U-Th)/He signals over time may be forced by local or regional tectonic forcing, pulses of thrust activity along the Bóixols and Montsec Thrusts modified the subsidence profile and drove spatial switching of the zone of maximum subsidence within the fluvial transfer zone. These subsidence pulses set up a period of oscillation between preferred sediment transports paths switching between the Ager and Tremp-Graus basins. Alternatively the DZ U-Pb and (U-Th)/He signal oscillation may be driven by global forcing mechanisms such as eustatic or climatic variability or orbital forcing. Oscillatory pulses in the preferred sediment transport path controlled the source of sediment entering the Ainsa Basin, although sea level modulated the flux of sediment entering the basin and ultimately control the stratigraphic architecture. The interactions between tectonic growth of the fold thrust belt and hinterland, with eustatic and climatic forcing controls the stratigraphic evolution of foreland basins. A four dimensional source-to-sink approach is necessary to evaluate basin provenance evolution.

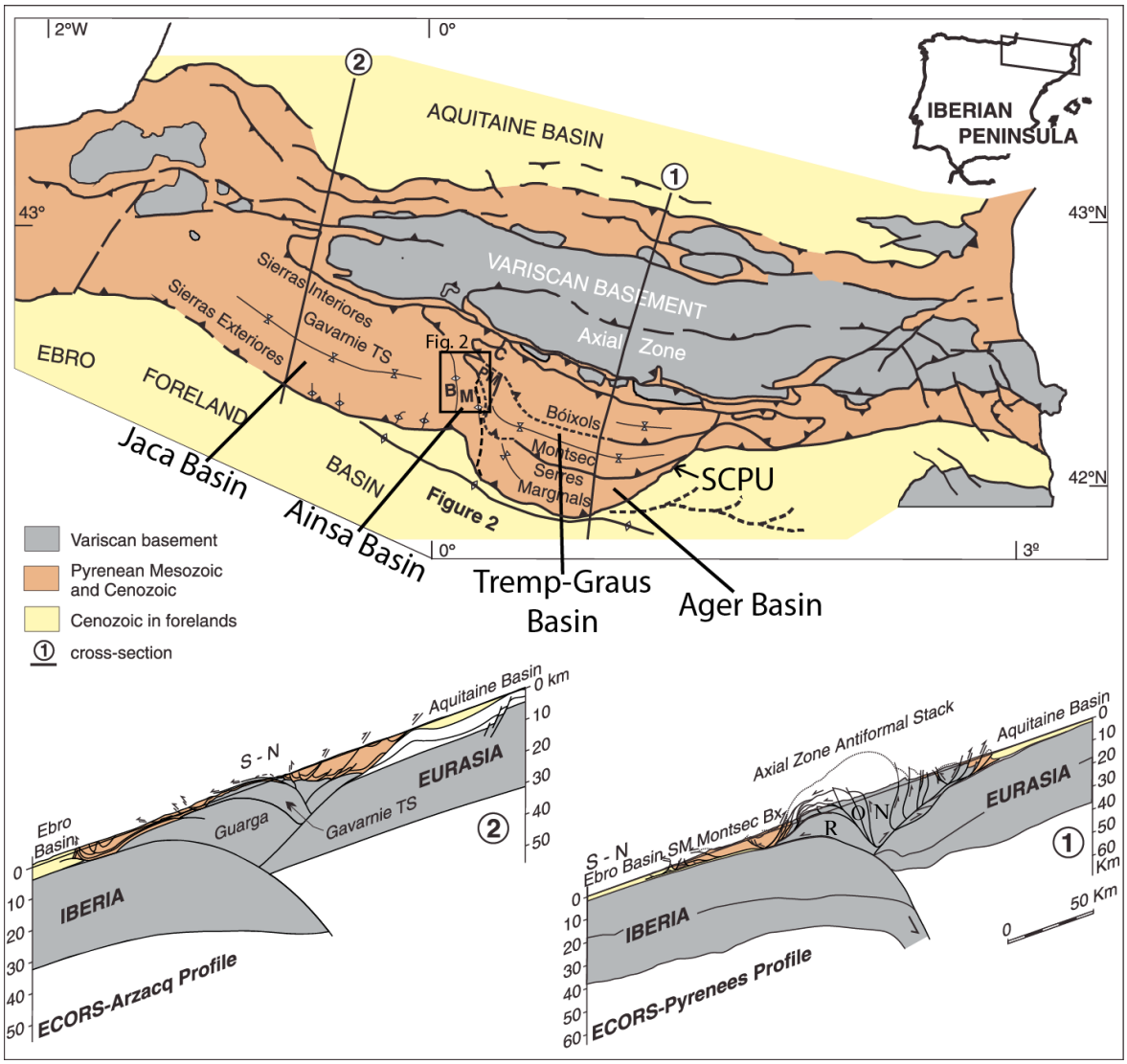

Figure 1: Map of the Pyrenees. Major structural and basin features annotated. Abbreviations: South Central Pyrenean Unit (SCPU), Boltaña anticline (B), Mediano anticline (M), Cotiella (C), Peña Montañesa (PM), Bóixols (Bx), Serres Marginals (SM), Rialp (R), Orri (O), Nogueres (N). Modified from Muñoz and others (2013), ECORS cross sections from Muñoz (1992), and Arzacq cross section from Teixell (1998).

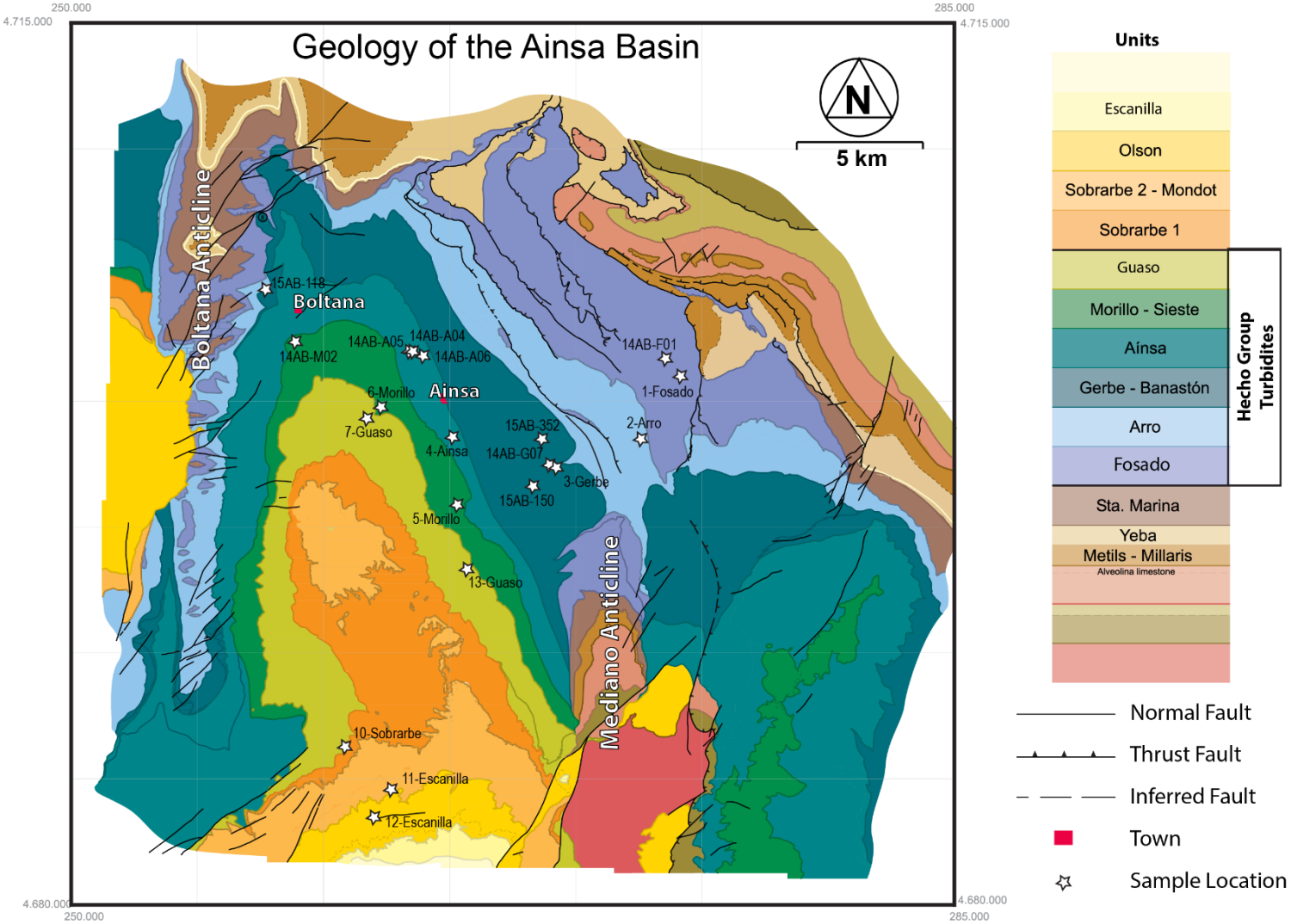

Figure 2. Geologic map of the Ainsa Basin (Puigdefàbregas, 2016) Sample locations denoted by stars.

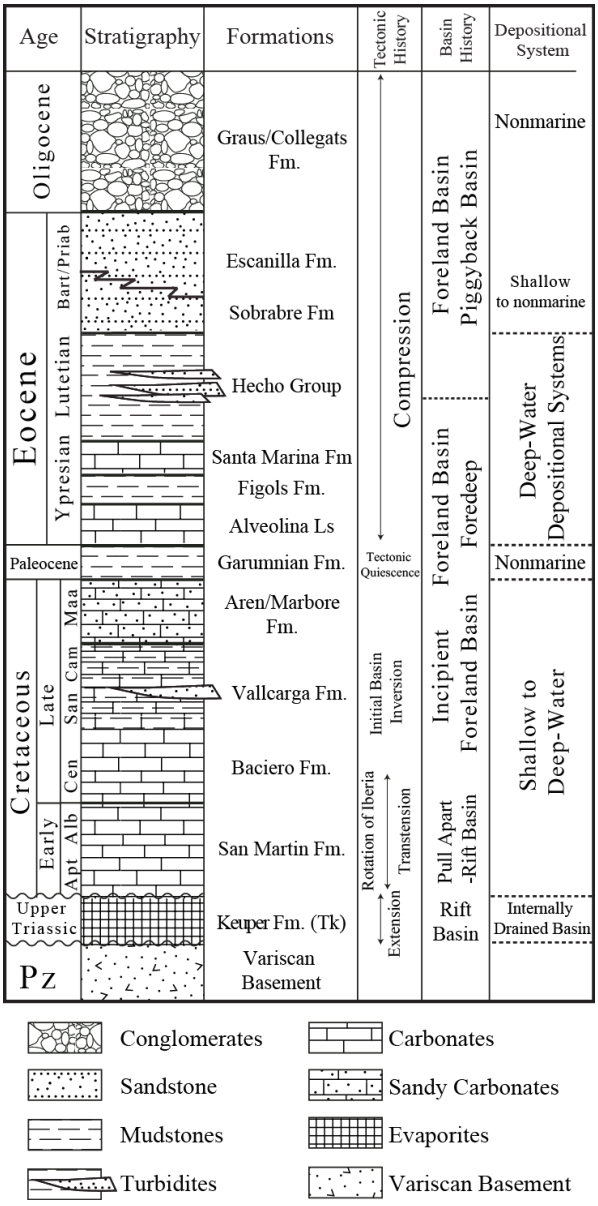

Figure 3. Stratigraphic Overview of the Ainsa Basin. Major formations, tectonic, basin history, and depositional system evolution synthesized. Vertical axis not to scale.

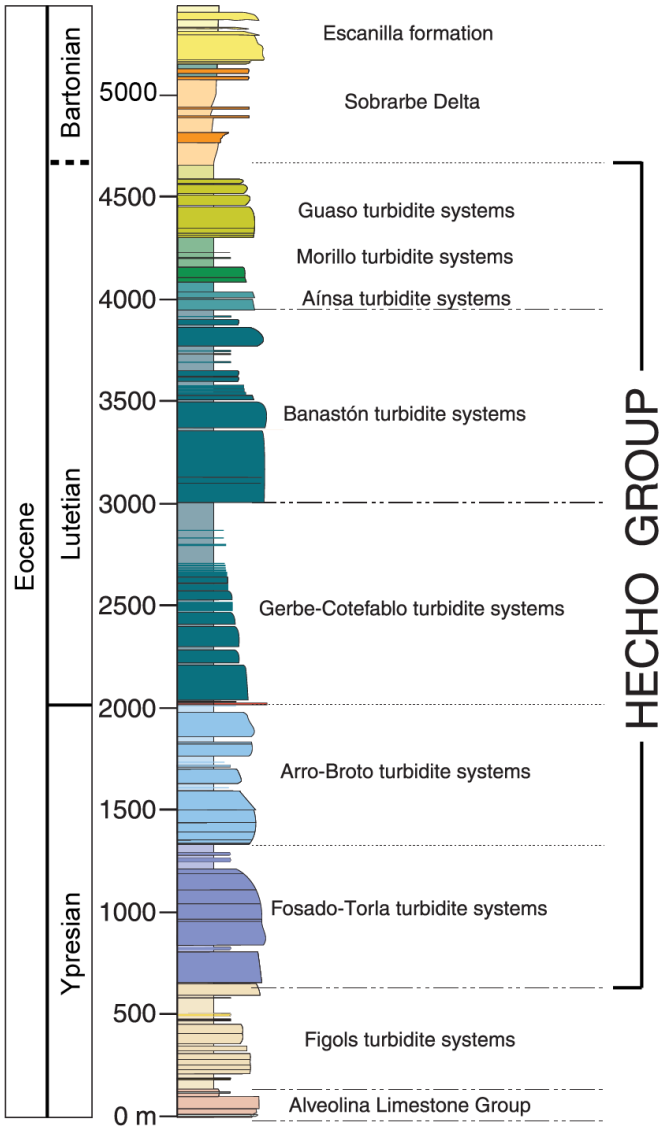

Figure 4. Stratigraphy of the Eocene Ainsa Basin, modified from Caja et al., (2010). Colors correspond to map units on figure 2.

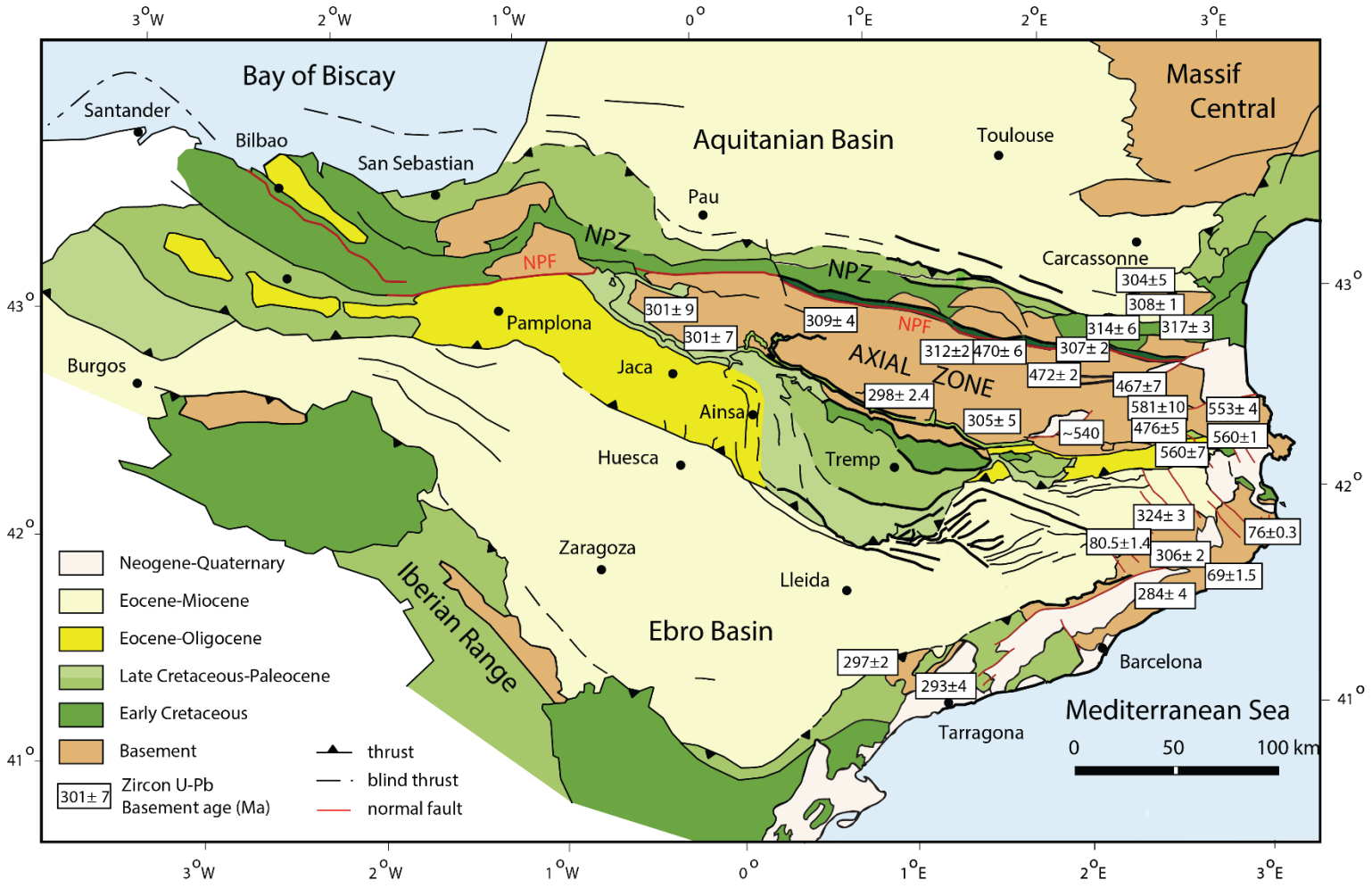

Figure 5. Geologic map with source area zircon U-Pb ages. Modified from Vissers and Meijer (2012) after Vergés (1995). U-Pb ages from Solé et al. (2002), Denèle et al. (2014), Martinez et al. (2015), Whitchurch et al (2011) and references within.

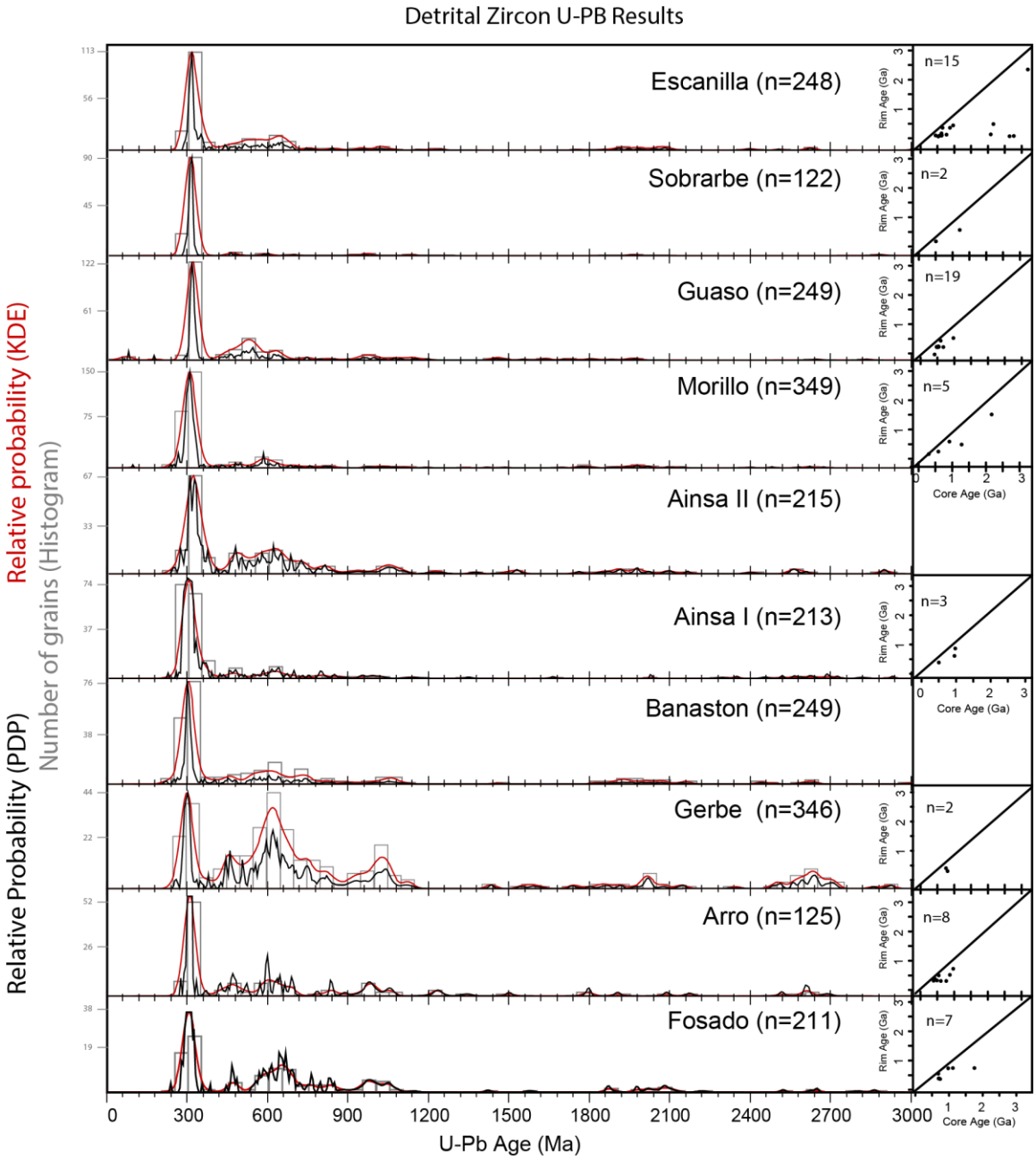

Figure 6. Detrital zircon U-Pb results displayed as kernel density estimators (KDE), probability density plots (PDP), and histograms (Vermeesch, 2012). Nonadaptive KDE bandwidth of 20 Ma, histogram bin width of 50 Ma. Rim age vs. core age scatterplots for each sample with rim and core grains present.

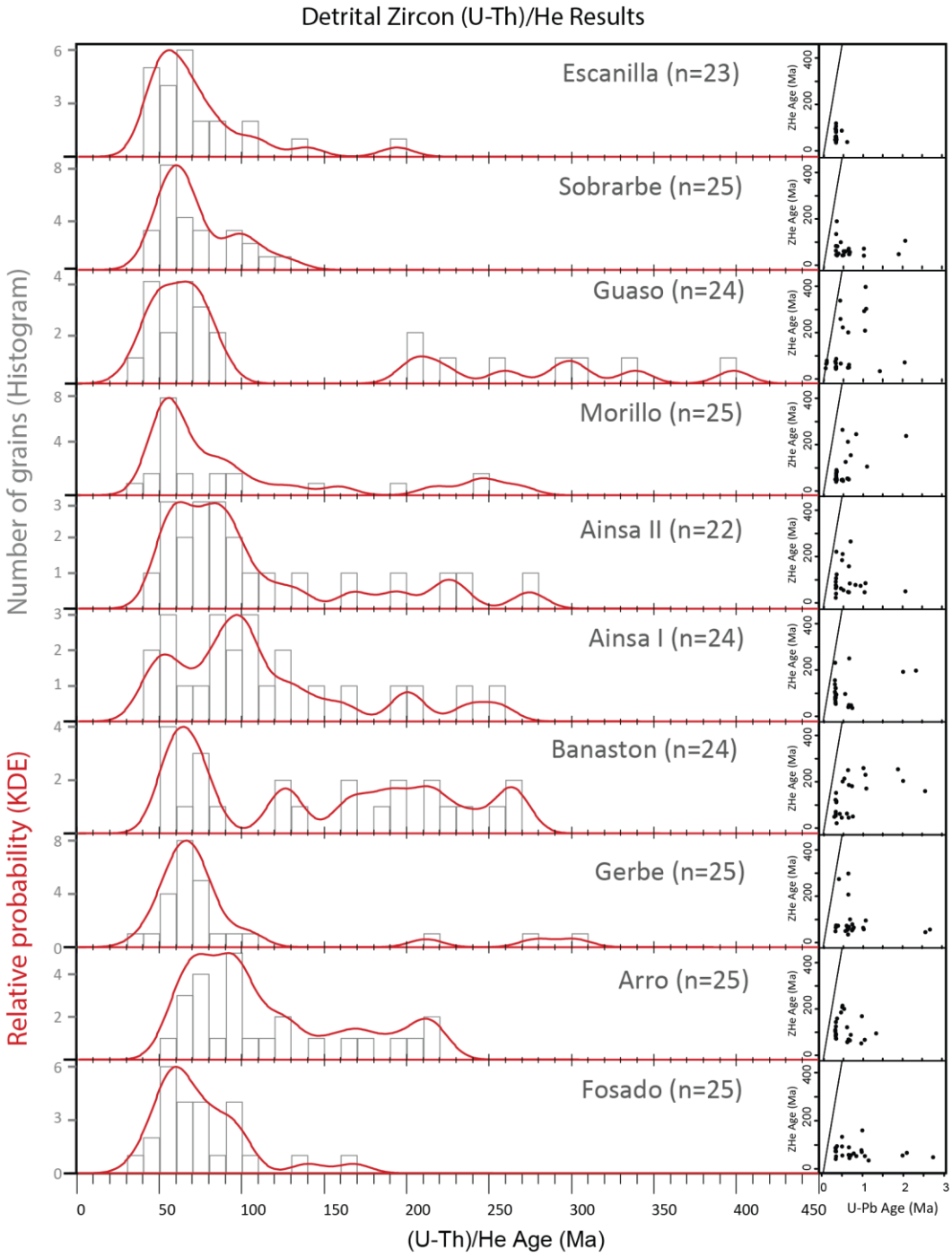

Figure 7. Detrital zircon (U-Th)/He results displayed as kernel density estimators (KDE), and histograms (Vermeesch, 2012). Nonadaptive KDE bandwidth of 10 Ma, histogram bin width of 10 Ma. (U-Th)/He age vs. U-Pb age scatterplots for each sample.

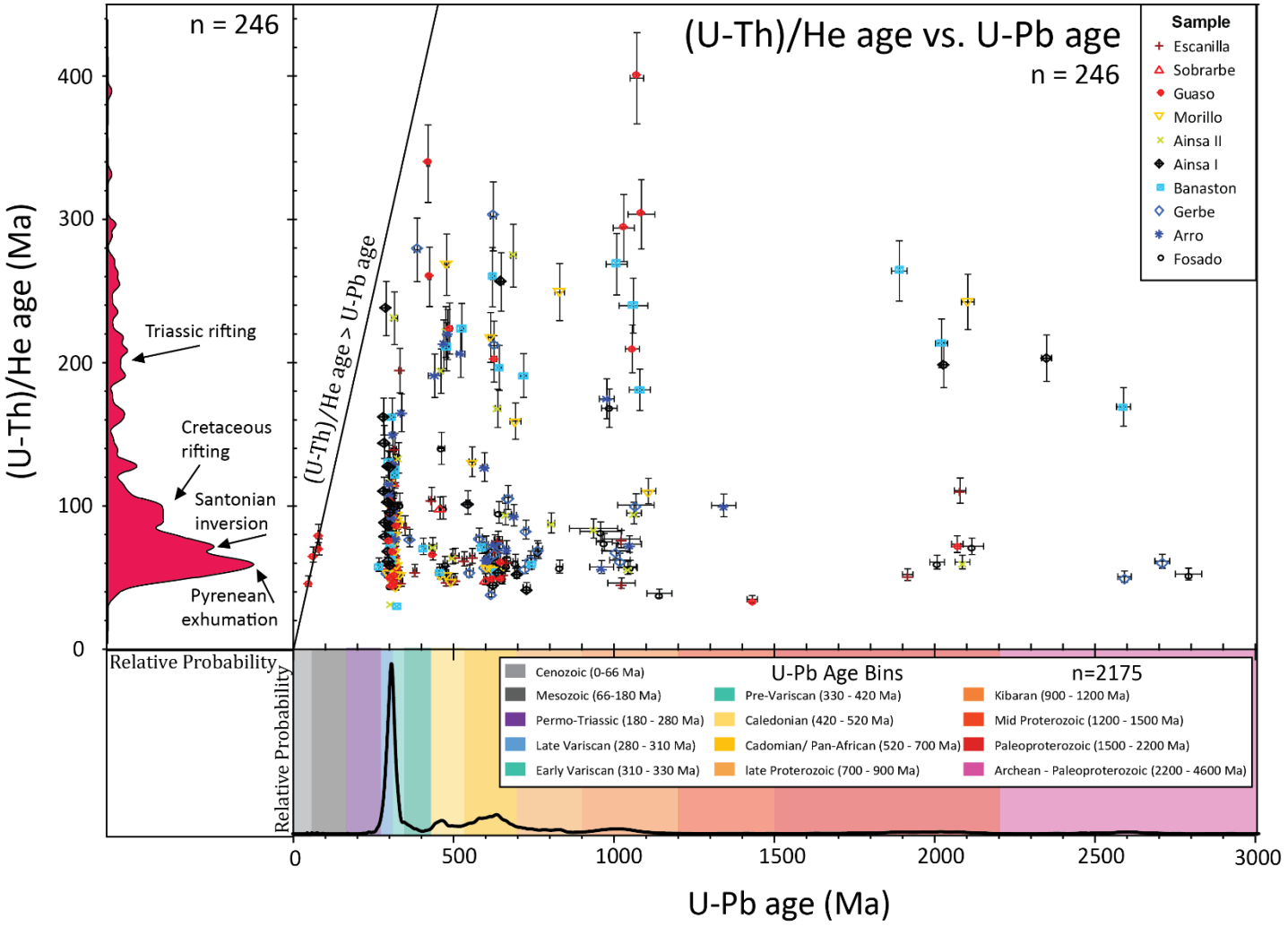

Figure 8. (U-Th)/He age vs U-Pb age

Figure 8. (U-Th)/He age vs U-Pb age. Scatterplot of (U-Th)/He age vs U-Pb age for double-dated grains, error bars represent 2σ errors. PDP of all U-Pb ages in this study (n = 2175) with color coated age components. Annotated KDE of all (U-Th)/He ages in this study (n = 246).

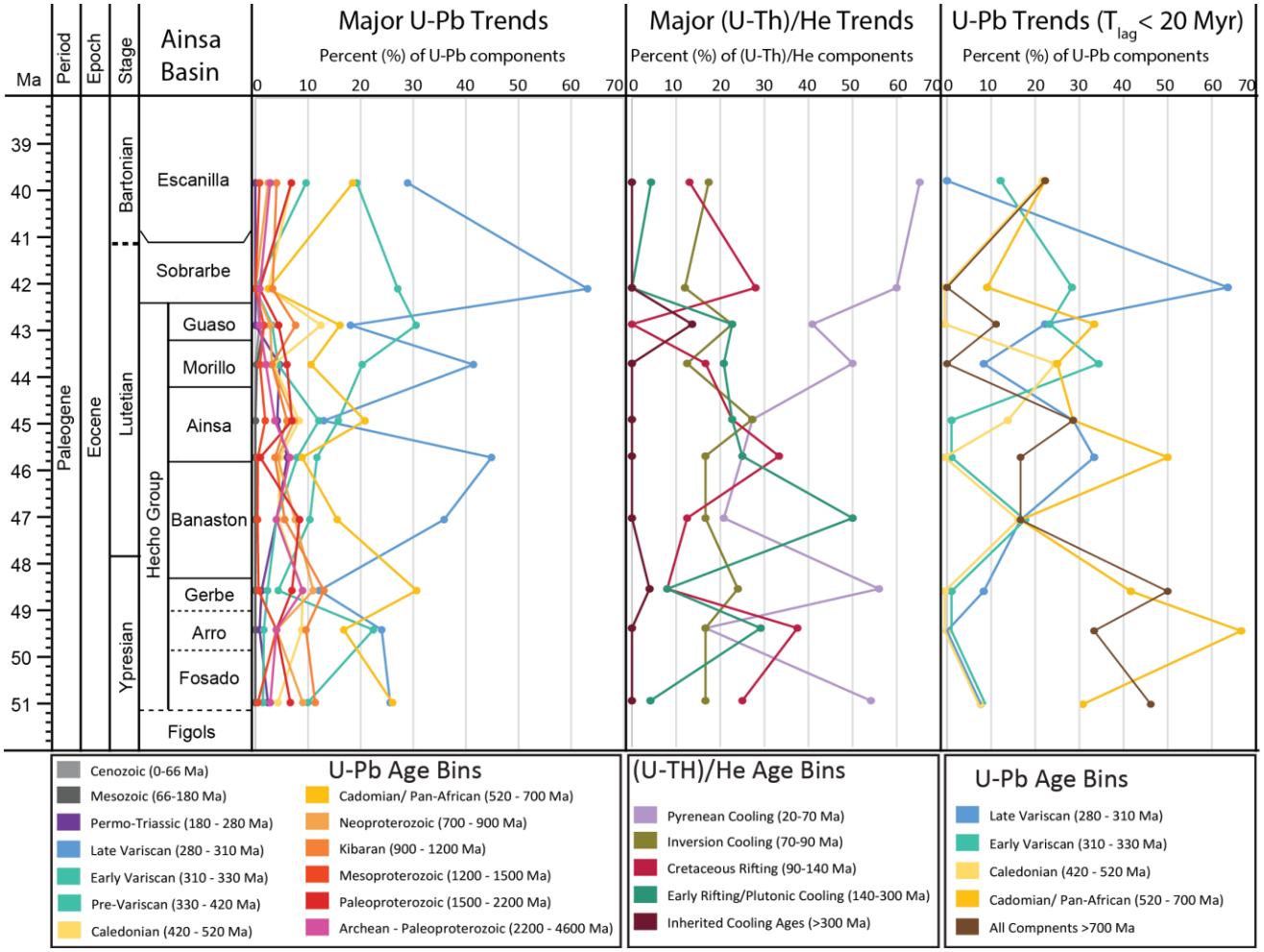

Figure 9. Stratigraphic Trends of U-Pb and (U-Th)/He results.

Figure 9. Stratigraphic Trends of U-Pb and (U-Th)/He results. Upsection changes in DZ U-Pb components indicate an increase in late and early Variscan grains in conjuncture with a decrease in Cadomian, Caledonian, and all components >700 Ma. Upsection changes in DZ (U-Th)/He components indicate an increase in Pyrenean cooled grains and a decrease in all other cooling components. Upsection U-Pb trends of grains with a lag-time <20 Myr indicates a compensatory relationship between Late Variscan and Cadomian components, with Late Variscan grains increasing as Cadomian grains decrease with respect to stratigraphy.

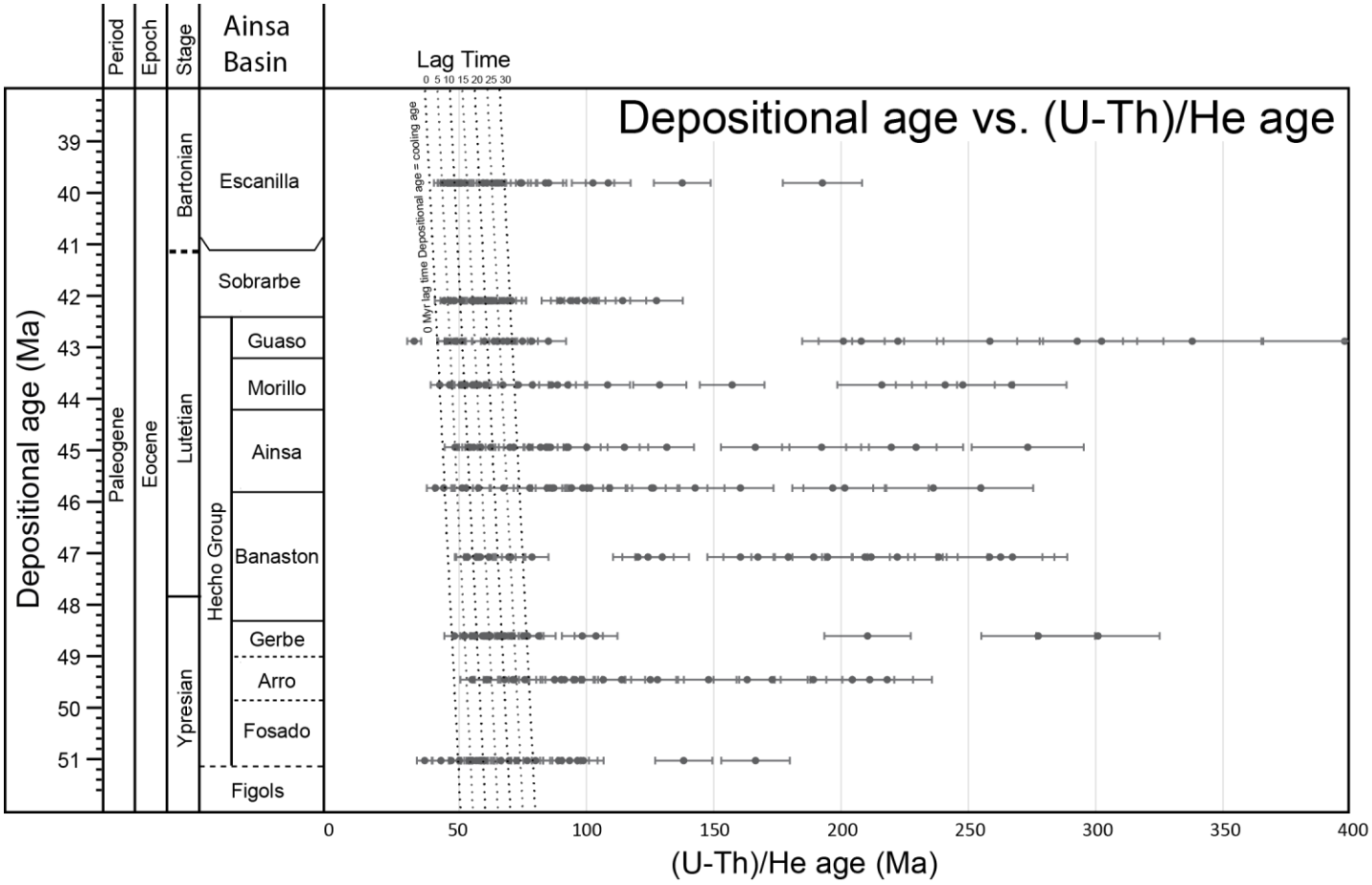

Figure 10. Lag-time plot. Depositional age vs. zircon (U-Th)/He age. 5-10 Myr lag-time throughout section. Oldest component of (U-Th)/He distribution getting older upsection.

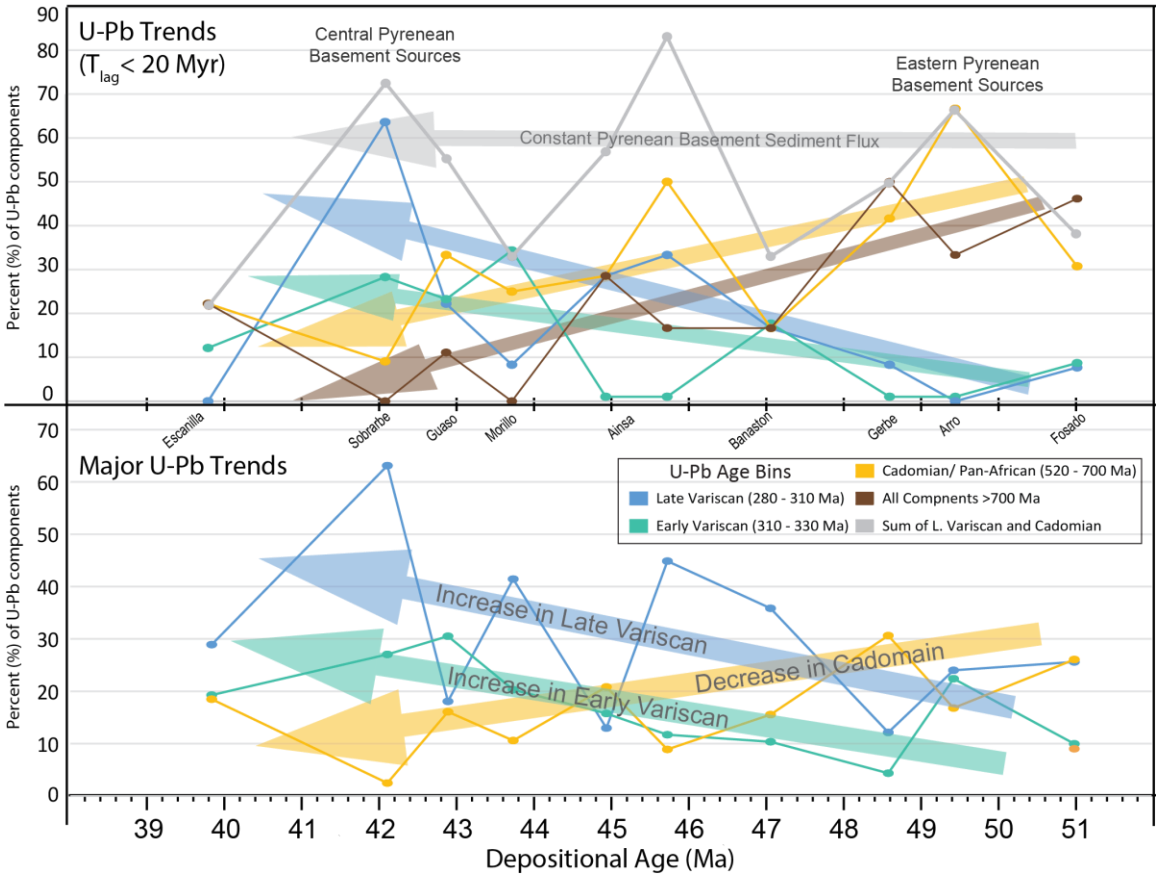

Figure 11. Stratigraphic evolution of U-Pb components. Upsection trends observed in all U-Pb data of the Ainsa Basin indicates an increase in Early and Late Variscan components and a decrease in Cadomian components. Upsections trends of U-Pb data with short lag-times reveal a compensatory relationship between the Cadomian and >700 Ma components with the early and late Variscan Components. These short lag-time components can be summed to approximate the constant flux of deeply exhumed material derived from basement thrust sheets.

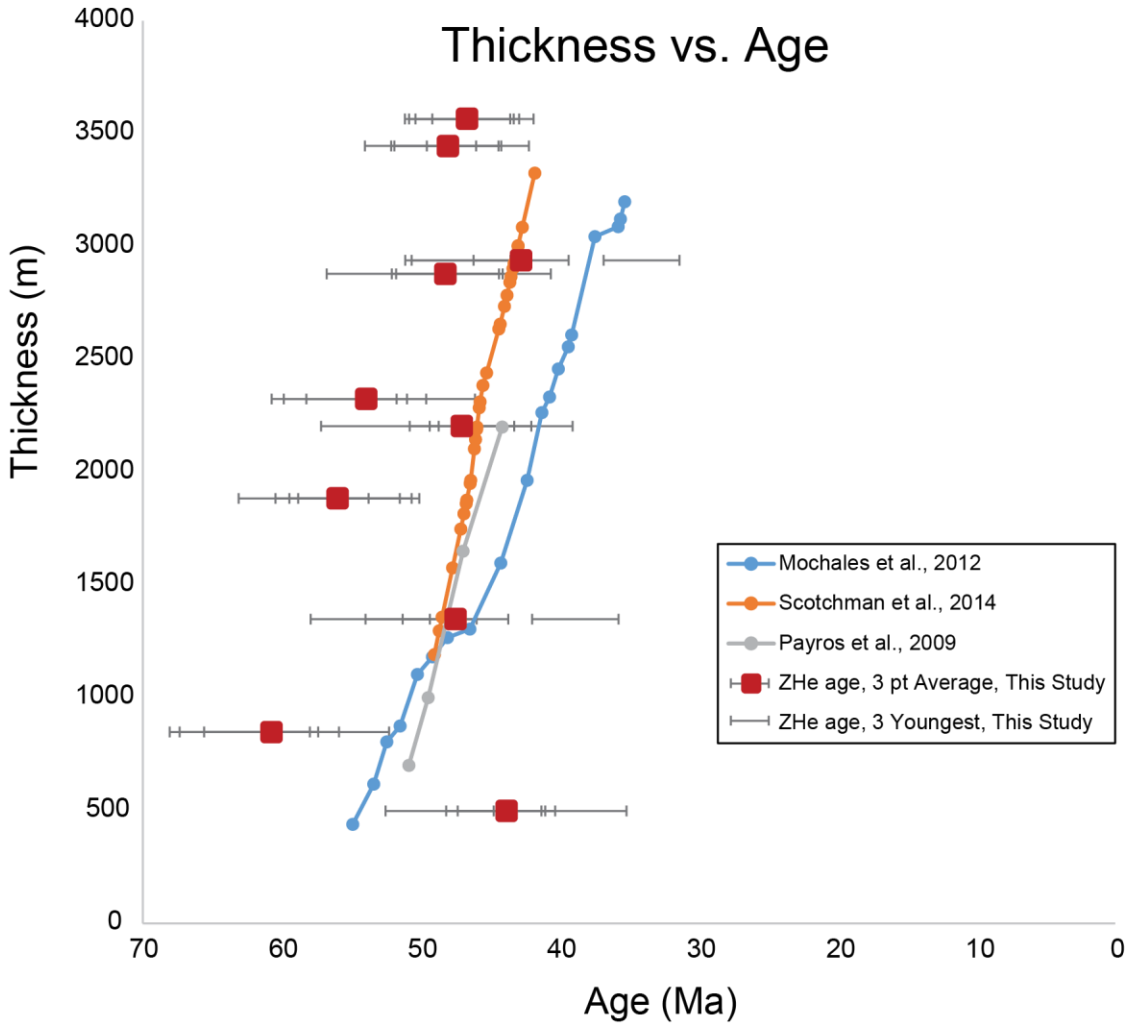

Figure 12. Chronostratigraphic thickness vs. depositional age models. Magnetostratigraphy from Payros et al. (2009) and Mochales et al. (2012), biostratigraphic age model from Scotchman et al. (2014). Mean ages of three youngest cooling ages in red, three youngest individual ages as 2σ error bars.

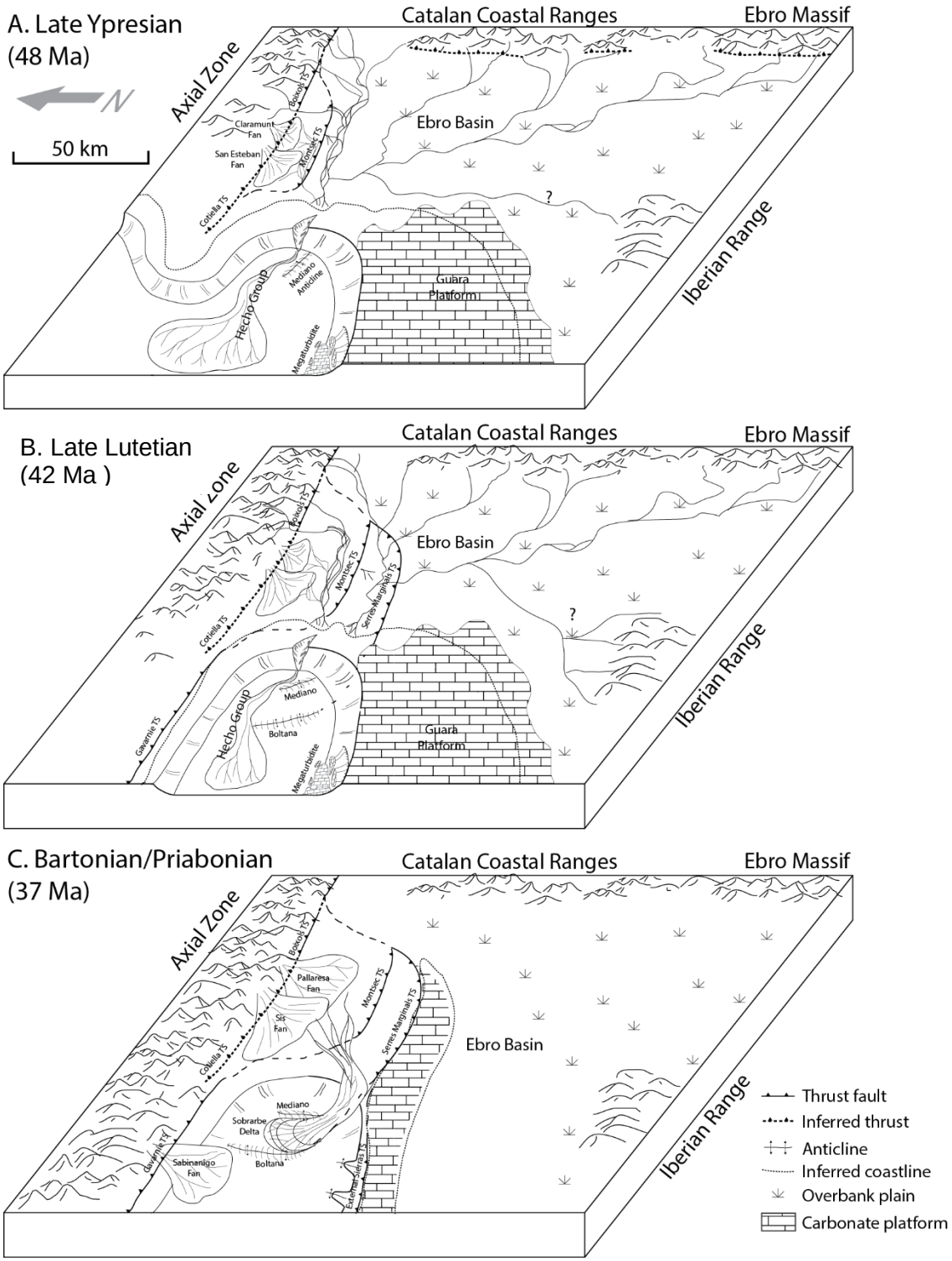

Figure 13. Paleogeographic reconstruction.

Figure 13. Paleogeographic reconstruction. Three paleogeographic reconstructions of the south Pyrenean foreland basin during the Eocene indicating all potential source regions and sediment delivery paths through the fold-thrust belt. Restorations for Late Ypresian (A, 48Ma), Lutetian (B, 42 Ma), Bartonian/Priabonian (C, 37 Ma).

Appendices

APPENDIX A: SAMPLE LOCATIONS

Sample ID	System	Long	Lat
11-Escanilla	Escanilla	0.122617	42.278474
12-Escanilla	Escanilla	0.116455	42.267407
10-Sobrarbe	Sobrarbe	0.101188	42.29224
7-Guaso	Guaso	0.106831	42.409038
13-Guaso	Guaso	0.156971	42.358007
5-Morillo	Morillo	0.151209	42.379942
6-Morillo	Morillo	0.11229	42.414713
14AB-M02	Morillo	0.070680631	42.43641008
14AB-M03	Morillo	0.071343137	42.43661828
14AB-A04	Ainsa II	0.127640001	42.43358999
14AB-A05	Ainsa II	0.12742	42.43343056
4-Ainsa	Ainsa I	0.14801	42.404218
14AB-A06	Ainsa I	0.1314	42.43364
15AB-352	Banaston	0.190405	42.404645
15AB-118	Banaston	0.05471	42.45504
3-Gerbe	Gerbe	0.197896	42.39448
14AB-G07	Gerbe	0.197719998	42.39455
2-Arro	Arro	0.238684	42.406398
1-Fosado	Fosado	0.256078	42.428614
14AB-F01	Fosado	0.248433333	42.43456667

APPENDIX B: DETRITAL ZIRCON U-PB GEOCHRONOLOGY RESULTS

Sample Name _Grain #	[U] ppm	U/Th	207/235	2σ error	206/238	2σ error	RHO	207/235 Age (Ma)	2σ error	206/238 Age (Ma)	2σ error	207/206 Age (Ma)	2σ error	Best age (Ma)	2σ error	% Discordance	Rim /Core
12_Escanilla_1	350	1.54	0.35850	0.00500	0.04939	0.00056	0.30868	311.0	3.7	310.7	3.4	313	34	310.7	3.4	0.10	
12_Escanilla_2	246	1.87	0.92400	0.01100	0.10840	0.00120	0.50702	664.2	5.8	663.6	7.2	671	23	663.6	7.2	0.09	
12_Escanilla_3	199.6	1.90	0.35780	0.00680	0.04886	0.00075	0.35500	310.3	5.1	307.5	4.6	326	44	307.5	4.6	0.90	
12_Escanilla_4	78	0.82	1.26200	0.02500	0.13740	0.00280	0.63703	829.0	11.0	830.0	16.0	825	35	830.0	16.0	0.12	
12_Escanilla_5	32.1	0.63	1.76200	0.03000	0.17360	0.00300	0.33982	1030.0	11.0	1031.0	16.0	1022	43	1022.0	43.0	0.88	
12_Escanilla_6	47.4	1.08	0.73300	0.02100	0.09020	0.00180	0.19571	559.0	12.0	557.0	11.0	627	60	557.0	11.0	0.36	
12_Escanilla_7	99.2	2.66	0.92600	0.01400	0.10630	0.00120	0.32040	665.0	7.3	651.3	6.9	708	32	651.3	6.9	2.06	
12_Escanilla_8	89.3	0.55	0.82800	0.01200	0.09880	0.00100	0.16468	611.9	6.5	607.3	6.1	614	33	607.3	6.1	0.75	
12_Escanilla_9	400	1.81	0.94900	0.01400	0.11070	0.00210	0.78077	677.4	7.4	677.0	12.0	680	24	677.0	12.0	0.06	
12_Escanilla_10	125	1.52	1.10600	0.02200	0.12350	0.00210	0.42586	756.0	10.0	751.0	12.0	788	46	751.0	12.0	0.66	
12_Escanilla_11	108.9	0.55	0.99500	0.01800	0.11300	0.00170	0.36711	702.0	8.9	690.0	10.0	740	39	690.0	10.0	1.71	
12_Escanilla_12	386	5.21	0.87390	0.00790	0.10316	0.00094	0.37510	638.1	4.4	632.9	5.5	666	22	632.9	5.5	0.81	
12_Escanilla_13	391	1.80	0.38520	0.00730	0.05028	0.00079	0.51569	330.6	5.4	316.2	4.9	450	36	316.2	4.9	4.36	
12_Escanilla_14	235	1.93	0.39120	0.00890	0.05245	0.00067	0.24647	335.1	6.5	329.6	4.1	350	59	329.6	4.1	1.64	
12_Escanilla_15	232	1.51	0.37280	0.00960	0.05009	0.00066	0.33044	321.2	7.1	315.1	4.1	368	53	315.1	4.1	1.90	
12_Escanilla_16	89.2	0.51	2.12200	0.02300	0.19420	0.00260	0.52482	1155.4	7.5	1144.0	14.0	1160	24	1160.0	24.0	1.38	
12_Escanilla_18	62.6	1.76	10.97000	0.13000	0.45220	0.00500	0.68269	2521.0	11.0	2405.0	22.0	2631	14	2631.0	14.0	8.59	
12_Escanilla_19	90	1.02	1.72100	0.04300	0.17170	0.00370	0.39013	1015.0	16.0	1021.0	20.0	1021	59	1021.0	59.0	0.00	
12_Escanilla_20	357	1.93	0.35780	0.00600	0.04902	0.00069	0.58369	310.3	4.5	308.5	4.2	319	31	308.5	4.2	0.58	
12_Escanilla_21	203	1.89	0.37030	0.00610	0.05037	0.00068	0.41364	319.7	4.5	316.8	4.2	331	42	316.8	4.2	0.91	
12_Escanilla_22	473	2.37	8.41000	0.13000	0.39500	0.00710	0.89349	2275.0	14.0	2145.0	33.0	2389	14	2389.0	14.0	10.21	
12_Escanilla_23	244	9.97	0.60100	0.01200	0.07650	0.00140	0.03709	477.2	7.7	475.0	8.4	477	43	475.0	8.4	0.46	
12_Escanilla_24	99	1.26	0.87600	0.02100	0.10360	0.00210	0.38780	639.0	11.0	637.0	13.0	629	46	637.0	13.0	0.31	

Sample Name _Grain #	[U] ppm	U/Th	207/235	2σ error	206/238	2σ error	RHO	207/235 Age (Ma)	2σ error	206/238 Age (Ma)	2σ error	207/206 Age (Ma)	2σ error	Best age (Ma)	2σ error	% Discordance	Rim /Core
12_Escanilla_25	17.6	33.60	6.39000	0.15000	0.37060	0.00840	0.62538	2029.0	21.0	2031.0	39.0	2032	36	2032.0	36.0	0.05	
12_Escanilla_26	258	1.79	0.46140	0.00730	0.06189	0.00089	0.37564	385.0	5.1	387.1	5.4	370	42	387.1	5.4	0.55	
12_Escanilla_27	216	1.13	0.85500	0.03100	0.09297	0.00091	0.27919	625.0	16.0	573.0	5.4	803	64	573.0	5.4	8.32	
12_Escanilla_28	40.9	0.76	5.85000	0.08200	0.34830	0.00400	0.43585	1956.0	12.0	1926.0	19.0	1991	24	1991.0	24.0	3.26	
12_Escanilla_29	104.9	1.46	4.30000	0.13000	0.26340	0.00700	0.70042	1697.0	22.0	1506.0	36.0	1947	39	1947.0	39.0	22.65	
12_Escanilla_30	178	1.81	0.58200	0.01000	0.07380	0.00110	0.40417	466.0	6.6	459.2	6.8	499	36	459.2	6.8	1.46	
12_Escanilla_31	356.4	6.23	0.38860	0.00930	0.05200	0.00110	0.57749	334.0	6.6	326.6	6.8	395	42	326.6	6.8	2.22	
12_Escanilla_32	185	2.27	0.35490	0.00760	0.04910	0.00099	0.33125	308.1	5.7	308.9	6.1	312	54	308.9	6.1	0.26	
12_Escanilla_33	213	0.84	0.69000	0.01500	0.08450	0.00230	0.60399	532.3	9.2	523.0	13.0	549	53	523.0	13.0	1.75	
12_Escanilla_34	235.5	3.96	0.87200	0.03300	0.10370	0.00370	0.42404	636.0	18.0	636.0	22.0	639	86	636.0	22.0	0.00	Rim
12_Escanilla_34	275.8	3.43	1.46800	0.03600	0.15100	0.00430	0.82318	916.0	15.0	906.0	24.0	954	30	954.0	30.0	5.03	Core
12_Escanilla_35	152	1.94	0.34780	0.00780	0.04717	0.00093	0.46494	302.7	5.9	297.1	5.7	345	53	297.1	5.7	1.85	
12_Escanilla_36	145.6	1.96	0.67500	0.01400	0.08280	0.00120	0.50663	523.1	8.2	512.7	7.1	574	35	512.7	7.1	1.99	
12_Escanilla_37	154.5	1.74	0.39800	0.00680	0.05433	0.00078	0.36396	340.0	5.0	341.0	4.8	349	41	341.0	4.8	0.29	
12_Escanilla_38	269	1.56	0.44920	0.00620	0.06020	0.00092	0.33297	376.6	4.4	376.8	5.6	361	39	376.8	5.6	0.05	
12_Escanilla_39	134.4	0.88	0.44520	0.00760	0.05935	0.00079	0.41696	373.6	5.3	371.6	4.8	404	36	371.6	4.8	0.54	
12_Escanilla_40	64.6	0.73	0.72100	0.02100	0.08800	0.00130	0.32794	550.0	12.0	543.7	7.5	589	59	543.7	7.5	1.15	
12_Escanilla_41	133.9	0.88	1.73900	0.01900	0.17270	0.00180	0.44093	1022.7	7.1	1027.0	10.0	1017	25	1017.0	25.0	0.98	
12_Escanilla_42	877	104.00	0.41300	0.01300	0.05590	0.00150	0.71368	354.0	10.0	350.7	9.4	380	55	350.7	9.4	0.93	Rim
12_Escanilla_42	108.9	0.61	5.76000	0.13000	0.34300	0.00770	0.13707	1940.0	20.0	1901.0	37.0	1987	60	1987.0	60.0	4.33	Core
12_Escanilla_44	229	0.82	0.39480	0.00620	0.05329	0.00070	0.48324	337.7	4.5	334.7	4.3	341	35	334.7	4.3	0.89	
12_Escanilla_45	321	0.74	0.40710	0.00460	0.05525	0.00055	0.38202	346.6	3.3	346.7	3.3	342	27	346.7	3.3	0.03	
12_Escanilla_46	680	15.20	8.53000	0.19000	0.39830	0.00800	0.78952	2288.0	20.0	2161.0	37.0	2409	22	2409.0	22.0	10.29	Rim
12_Escanilla_46	207.8	1.12	18.77000	0.56000	0.61100	0.02000	0.89026	3029.0	28.0	3074.0	78.0	3011	21	3011.0	21.0	2.09	Core
12_Escanilla_47	130.2	1.05	5.52100	0.07200	0.34260	0.00470	0.78304	1903.0	11.0	1903.0	21.0	1915	16	1915.0	16.0	0.63	

Sample Name _Grain #	[U] ppm	U/Th	207/235	2σ error	206/238	2σ error	RHO	207/235 Age (Ma)	2σ error	206/238 Age (Ma)	2σ error	207/206 Age (Ma)	2σ error	Best age (Ma)	2σ error	% Discordance	Rim /Core
12_Escanilla_48	468	2.18	0.37370	0.00600	0.05046	0.00065	0.40980	322.2	4.4	317.3	4.0	343	31	317.3	4.0	1.52	
12_Escanilla_49	146	1.68	0.35900	0.00750	0.04896	0.00066	0.41618	311.2	5.6	308.1	4.1	345	44	308.1	4.1	1.00	
12_Escanilla_50	255.6	1.73	11.62000	0.19000	0.47510	0.00620	0.60637	2573.0	15.0	2505.0	27.0	2623	23	2623.0	23.0	4.50	
12_Escanilla_51	360	1.82	0.35050	0.00640	0.04733	0.00072	0.40524	304.9	4.8	298.1	4.4	354	42	298.1	4.4	2.23	
12_Escanilla_52	610	2.16	0.39700	0.01900	0.05500	0.00290	0.88773	344.0	16.0	345.0	18.0	339	55	345.0	18.0	0.29	Rim
12_Escanilla_52	617	0.97	1.14200	0.01900	0.12620	0.00240	0.65308	773.3	9.2	766.0	14.0	787	31	766.0	14.0	0.94	Core
12_Escanilla_53	241	1.62	0.40250	0.00560	0.05459	0.00059	0.32617	343.8	3.9	342.6	3.6	341	31	342.6	3.6	0.35	
12_Escanilla_54	39.1	0.99	1.60200	0.03700	0.16330	0.00240	0.35374	971.0	14.0	976.0	13.0	944	43	944.0	43.0	3.39	
12_Escanilla_55	166	1.64	0.35720	0.00760	0.04868	0.00064	0.18407	310.5	5.8	306.4	4.0	324	54	306.4	4.0	1.32	
12_Escanilla_56	517	0.68	0.39670	0.00670	0.05389	0.00083	0.57144	339.0	4.9	338.3	5.1	353	34	338.3	5.1	0.21	
12_Escanilla_57	349	1.61	0.77500	0.01000	0.09370	0.00170	0.51391	582.5	6.0	577.1	9.9	605	33	577.1	9.9	0.93	
12_Escanilla_58	399	26.30	0.46400	0.02400	0.06180	0.00300	0.64681	387.0	16.0	386.0	18.0	355	91	386.0	18.0	0.26	Rim
12_Escanilla_58	47.2	1.28	0.86000	0.02200	0.10220	0.00180	0.20727	629.0	12.0	627.0	11.0	609	63	627.0	11.0	0.32	Core
12_Escanilla_59	32	1.32	0.65200	0.02100	0.08110	0.00210	0.31333	509.0	13.0	503.0	12.0	516	83	503.0	12.0	1.18	
12_Escanilla_60	290	0.43	6.19700	0.06100	0.35430	0.00440	0.66107	2003.5	8.5	1954.0	21.0	2043	18	2043.0	18.0	4.36	
12_Escanilla_61	17.73	0.45	0.72100	0.03200	0.08770	0.00230	0.04468	549.0	19.0	542.0	13.0	540	100	542.0	13.0	1.28	
12_Escanilla_62	314	7.80	0.95300	0.04100	0.11110	0.00570	0.60109	679.0	21.0	679.0	33.0	684	90	679.0	33.0	0.00	Rim
12_Escanilla_62	79.1	2.45	5.83000	0.12000	0.33070	0.00600	0.46106	1950.0	18.0	1842.0	29.0	2057	34	2057.0	34.0	10.45	Core
12_Escanilla_63	126.8	0.74	7.02500	0.06800	0.38990	0.00460	0.65039	2117.1	8.6	2122.0	21.0	2111	16	2111.0	16.0	0.52	
12_Escanilla_64	86.5	1.01	1.30100	0.01700	0.13890	0.00140	0.19543	845.8	7.3	838.3	7.7	848	28	838.3	7.7	0.89	
12_Escanilla_65	196	1.43	0.36670	0.00950	0.05033	0.00073	0.11359	316.7	7.1	316.5	4.5	303	57	316.5	4.5	0.06	
12_Escanilla_66	579	0.90	0.40220	0.00500	0.05470	0.00064	0.42528	343.8	3.8	343.3	3.9	349	29	343.3	3.9	0.15	
12_Escanilla_67	380	1.84	0.37100	0.00680	0.05018	0.00066	0.20227	320.2	5.0	315.6	4.0	374	50	315.6	4.0	1.44	
12_Escanilla_68	143.6	0.56	0.94400	0.01100	0.10988	0.00094	0.21081	674.5	5.5	672.0	5.4	681	32	672.0	5.4	0.37	
12_Escanilla_69	222	2.00	0.38320	0.00730	0.05261	0.00071	0.26193	329.1	5.3	330.5	4.3	318	45	330.5	4.3	0.43	

Sample Name _Grain #	[U] ppm	U/Th	207/235	2σ error	206/238	2σ error	RHO	207/235 Age (Ma)	2σ error	206/238 Age (Ma)	2σ error	207/206 Age (Ma)	2σ error	Best age (Ma)	2σ error	% Discordance	Rim /Core
12_Escanilla_70	136.7	1.64	0.37280	0.00780	0.04891	0.00083	0.19148	321.6	5.8	307.8	5.1	426	59	307.8	5.1	4.29	
12_Escanilla_71	214	2.07	0.35090	0.00680	0.04914	0.00059	0.34224	305.1	5.1	309.2	3.6	257	44	309.2	3.6	1.34	
12_Escanilla_72	335	3.45	5.00800	0.05200	0.31370	0.00340	0.65377	1820.2	8.7	1759.0	17.0	1898	17	1898.0	17.0	7.32	
12_Escanilla_73	158	1.78	0.80800	0.00920	0.09770	0.00100	0.25392	602.4	5.2	600.9	6.0	591	28	600.9	6.0	0.25	
12_Escanilla_74	117.2	1.27	0.88800	0.01800	0.10580	0.00140	0.29537	644.5	9.6	647.9	8.1	630	38	647.9	8.1	0.53	
12_Escanilla_75	282	3.67	0.61090	0.00960	0.07900	0.00083	0.37638	483.9	6.0	490.1	5.0	462	35	490.1	5.0	1.28	
12_Escanilla_76	272	0.77	0.38430	0.00610	0.05216	0.00062	0.45192	330.6	4.4	327.7	3.8	347	31	327.7	3.8	0.88	
12_Escanilla_77	47.5	2.92	0.76100	0.05000	0.09120	0.00290	0.15411	572.0	28.0	563.0	17.0	580	140	563.0	17.0	1.57	Rim
12_Escanilla_77	116.4	1.68	1.32100	0.03200	0.14180	0.00240	0.39788	858.0	13.0	855.0	13.0	865	38	865.0	38.0	1.16	Core
12_Escanilla_78	196.9	1.47	0.35380	0.00610	0.04892	0.00062	0.32655	307.4	4.6	307.8	3.8	273	39	307.8	3.8	0.13	
12_Escanilla_79	272	1.44	0.35770	0.00630	0.04906	0.00069	0.29353	310.3	4.7	308.7	4.3	315	45	308.7	4.3	0.52	
12_Escanilla_80	127	1.04	0.36850	0.00900	0.05025	0.00099	0.07031	318.1	6.7	316.0	6.1	290	64	316.0	6.1	0.66	
12_Escanilla_81	286.8	1.58	0.64320	0.00780	0.08112	0.00091	0.53765	504.1	4.8	502.7	5.4	500	27	502.7	5.4	0.28	
12_Escanilla_82	142	1.47	0.88300	0.01200	0.10500	0.00120	0.24718	643.8	6.5	643.7	6.9	626	33	643.7	6.9	0.02	
12_Escanilla_83	193.6	2.58	1.08500	0.01400	0.12150	0.00110	0.37612	747.1	6.4	739.4	6.5	758	27	739.4	6.5	1.03	
12_Escanilla_84	33	1.54	0.92700	0.03000	0.10830	0.00210	0.26293	667.0	16.0	663.0	12.0	666	71	663.0	12.0	0.60	
12_Escanilla_85	354.8	58.20	0.39800	0.01100	0.05310	0.00150	0.26391	339.7	8.2	333.5	9.0	411	72	333.5	9.0	1.83	Rim
12_Escanilla_85	344	0.43	0.87200	0.01700	0.10380	0.00220	0.33520	636.3	9.3	637.0	13.0	644	53	637.0	13.0	0.11	Core
12_Escanilla_86	207	1.55	0.38510	0.00800	0.05132	0.00075	0.39097	331.5	6.1	322.6	4.6	349	45	322.6	4.6	2.68	
12_Escanilla_87	435	2.43	0.37040	0.00770	0.05110	0.00100	0.10198	319.8	5.7	321.1	6.3	295	59	321.1	6.3	0.41	Rim
12_Escanilla_87	219.5	5.37	0.58500	0.01200	0.07612	0.00097	0.29720	467.5	7.5	472.9	5.8	465	41	472.9	5.8	1.16	Core
12_Escanilla_88	341	3.55	0.59500	0.01100	0.07540	0.00130	0.54766	475.0	7.2	468.3	7.8	509	38	468.3	7.8	1.41	
12_Escanilla_89	340	1.72	0.33870	0.00500	0.04718	0.00056	0.18656	296.1	3.8	297.1	3.5	277	40	297.1	3.5	0.34	
12_Escanilla_90	70.4	0.44	0.67200	0.01400	0.08410	0.00140	0.33876	522.4	8.4	520.2	8.2	522	53	520.2	8.2	0.42	
12_Escanilla_91	195.4	1.97	0.43350	0.00820	0.05632	0.00079	0.48890	365.4	5.8	353.2	4.8	457	42	353.2	4.8	3.34	

Sample Name _Grain #	[U] ppm	U/Th	207/235	2σ error	206/238	2σ error	RHO	207/235 Age (Ma)	2σ error	206/238 Age (Ma)	2σ error	207/206 Age (Ma)	2σ error	Best age (Ma)	2σ error	% Discordance	Rim /Core
12_Escanilla_93	37.7	0.67	1.76600	0.03400	0.17140	0.00300	0.43755	1036.0	13.0	1020.0	17.0	1066	42	1066.0	42.0	4.32	
12_Escanilla_94	352	1.62	0.38460	0.00550	0.05171	0.00059	0.31098	330.2	4.0	325.0	3.6	339	37	325.0	3.6	1.57	
12_Escanilla_95	332	0.98	5.86400	0.04500	0.35600	0.00240	0.58468	1956.8	6.9	1963.0	11.0	1945	12	1945.0	12.0	0.93	
12_Escanilla_96	91.3	1.58	0.82700	0.01400	0.09850	0.00110	0.19882	611.1	7.6	605.3	6.7	631	42	605.3	6.7	0.95	
12_Escanilla_97	320	1.01	0.40660	0.00580	0.05387	0.00057	0.42095	346.3	4.2	338.2	3.5	376	29	338.2	3.5	2.34	
12_Escanilla_98	127	1.39	0.35610	0.00750	0.04855	0.00073	0.30753	309.0	5.7	305.6	4.5	330	49	305.6	4.5	1.10	
12_Escanilla_99	80.3	1.88	6.95300	0.09300	0.38880	0.00520	0.72172	2105.0	12.0	2116.0	24.0	2086	17	2086.0	17.0	1.44	
12_Escanilla_100	331	1.58	0.36350	0.00710	0.04900	0.00066	0.41227	314.7	5.3	308.9	4.2	334	49	308.9	4.2	1.84	
12_Escanilla_101	77.3	0.85	6.81200	0.08100	0.37890	0.00450	0.55947	2086.0	11.0	2071.0	21.0	2079	18	2079.0	18.0	0.38	
12_Escanilla_102	724	4.67	0.92790	0.00800	0.10720	0.00110	0.59538	666.4	4.2	656.4	6.4	680	18	656.4	6.4	1.50	
12_Escanilla_103	217	2.81	0.85800	0.01000	0.10100	0.00120	0.41286	629.6	5.6	620.0	7.3	635	29	620.0	7.3	1.52	
12_Escanilla_104	183.2	0.83	0.80900	0.01700	0.09360	0.00200	0.45918	601.3	9.3	577.0	12.0	665	49	577.0	12.0	4.04	
12_Escanilla_105	143.9	0.90	0.42260	0.00830	0.05630	0.00072	0.30008	358.4	6.0	353.1	4.4	381	42	353.1	4.4	1.48	
12_Escanilla_106	234	2.43	0.35420	0.00670	0.04933	0.00069	0.50511	308.3	4.9	310.4	4.2	289	36	310.4	4.2	0.68	
12_Escanilla_107	339	1.00	0.43330	0.00740	0.05710	0.00074	0.49138	366.0	5.1	358.0	4.5	361	37	358.0	4.5	2.19	
12_Escanilla_108	150.2	1.01	2.43300	0.04500	0.21440	0.00340	0.73978	1254.0	14.0	1252.0	18.0	1247	24	1247.0	24.0	0.40	
12_Escanilla_109	40.8	1.26	0.66900	0.01700	0.08280	0.00150	0.01472	520.2	9.9	512.5	8.9	525	71	512.5	8.9	1.48	
12_Escanilla_110	34.6	0.19	0.53900	0.02000	0.06890	0.00150	0.05462	437.0	13.0	429.4	9.3	417	87	429.4	9.3	1.74	
12_Escanilla_111	598	2.25	0.36150	0.00890	0.04940	0.00140	0.63984	313.2	6.6	312.4	8.1	333	50	312.4	8.1	0.26	Rim
12_Escanilla_111	277	0.56	0.78600	0.02300	0.09340	0.00220	0.35725	588.0	13.0	575.0	13.0	596	63	575.0	13.0	2.21	Core
12_Escanilla_112	166.5	0.79	0.85100	0.01300	0.10062	0.00095	0.47750	624.9	6.9	618.0	5.6	656	25	618.0	5.6	1.10	
12_Escanilla_113	302	2.50	0.54500	0.01000	0.07002	0.00097	0.36966	441.3	6.9	436.2	5.8	457	37	436.2	5.8	1.16	
12_Escanilla_114	84.3	2.67	0.70000	0.01600	0.08600	0.00120	0.08450	539.7	9.6	531.6	7.4	541	58	531.6	7.4	1.50	
12_Escanilla_115	176.2	1.00	0.39640	0.00770	0.05334	0.00065	0.12784	338.7	5.6	335.0	4.0	371	46	335.0	4.0	1.09	
12_Escanilla_116	299	1.48	0.35600	0.00590	0.04976	0.00068	0.48694	309.1	4.4	313.0	4.2	271	33	313.0	4.2	1.26	

Sample Name _Grain #	[U] ppm	U/Th	207/235	2σ error	206/238	2σ error	RHO	207/235 Age (Ma)	2σ error	206/238 Age (Ma)	2σ error	207/206 Age (Ma)	2σ error	Best age (Ma)	2σ error	% Discordance	Rim /Core
12_Escanilla_117	46.2	0.78	1.69700	0.03700	0.16860	0.00360	0.43340	1008.0	14.0	1004.0	20.0	996	38	996.0	38.0	0.80	
12_Escanilla_118	82.6	1.43	0.69400	0.01100	0.08210	0.00150	0.01608	535.9	6.6	508.3	8.8	669	50	508.3	8.8	5.15	
12_Escanilla_119	130.6	1.11	0.36520	0.00700	0.04731	0.00072	0.26261	316.7	5.4	298.0	4.4	409	44	298.0	4.4	5.90	
12_Escanilla_120	94	1.40	0.73100	0.01300	0.09020	0.00140	0.38674	556.6	7.6	556.4	8.0	537	41	556.4	8.0	0.04	
11_Escanilla_1	185.2	1.46	0.35990	0.00690	0.04911	0.00075	0.33759	311.9	5.2	309.0	4.6	345	51	309.0	4.6	0.93	
11_Escanilla_2	232	1.55	0.35560	0.00840	0.04893	0.00085	0.63653	309.3	6.2	307.9	5.2	298	39	307.9	5.2	0.45	
11_Escanilla_3	212	1.90	0.36270	0.00650	0.04981	0.00059	0.37039	314.6	4.7	313.3	3.6	308	42	313.3	3.6	0.41	
11_Escanilla_4	280	2.21	0.36400	0.00700	0.04965	0.00051	0.51271	315.6	5.1	312.4	3.1	320	35	312.4	3.1	1.01	
11_Escanilla_5	540	179.00	0.33600	0.01200	0.04710	0.00130	0.73485	293.8	8.8	296.8	7.8	275	84	296.8	7.8	1.02	Rim
11_Escanilla_5	601.7	3.07	9.53000	0.15000	0.42360	0.00760	0.85431	2390.0	14.0	2276.0	35.0	2508	12	2508.0	12.0	9.25	Core
11_Escanilla_6	195	1.42	0.35480	0.00610	0.04902	0.00063	0.27974	308.8	4.7	308.5	3.9	343	40	308.5	3.9	0.10	
11_Escanilla_7	149.8	1.64	0.35490	0.00810	0.04797	0.00071	0.09386	308.0	6.1	302.0	4.4	304	57	302.0	4.4	1.95	
11_Escanilla_8	189	1.61	0.35110	0.00670	0.04819	0.00063	0.10286	305.3	5.0	303.4	3.9	299	45	303.4	3.9	0.62	
11_Escanilla_9	561	2.13	0.36260	0.00380	0.04956	0.00056	0.34748	314.1	2.8	311.8	3.4	338	30	311.8	3.4	0.73	
11_Escanilla_10	186	1.72	0.34820	0.00820	0.04698	0.00078	0.35777	303.0	6.2	295.9	4.8	340	51	295.9	4.8	2.34	
11_Escanilla_11	197	1.45	0.36370	0.00780	0.05035	0.00083	0.55782	314.6	5.8	316.6	5.1	312	42	316.6	5.1	0.64	
11_Escanilla_12	314	3.90	0.36900	0.01600	0.05120	0.00150	0.52480	319.0	12.0	322.1	9.4	312	93	322.1	9.4	0.97	
11_Escanilla_13	139.7	2.18	0.34740	0.00770	0.04721	0.00065	0.22930	302.4	5.8	297.9	3.9	349	57	297.9	3.9	1.49	
11_Escanilla_14	252	1.54	0.35950	0.00690	0.04964	0.00066	0.40599	311.6	5.1	312.3	4.0	300	44	312.3	4.0	0.22	
11_Escanilla_15	437	2.31	0.37040	0.00720	0.04817	0.00087	0.58579	319.8	5.3	303.2	5.3	421	42	303.2	5.3	5.19	
11_Escanilla_16	133	2.14	0.35470	0.00690	0.04902	0.00064	0.29101	308.6	5.1	308.5	3.9	307	42	308.5	3.9	0.03	
11_Escanilla_17	268	6.04	0.42000	0.01400	0.05530	0.00130	0.49453	355.9	9.9	346.8	8.1	413	67	346.8	8.1	2.56	
11_Escanilla_18	176	1.96	0.35690	0.00860	0.04927	0.00073	0.34904	309.6	6.4	310.0	4.5	305	49	310.0	4.5	0.13	
11_Escanilla_19	164	1.69	0.35350	0.00780	0.04989	0.00074	0.27636	307.8	5.9	313.8	4.6	238	49	313.8	4.6	1.95	
11_Escanilla_20	376	2.61	0.34400	0.01100	0.04770	0.00150	0.58590	299.7	8.1	300.2	9.4	280	64	300.2	9.4	0.17	

Sample Name _Grain #	[U] ppm	U/Th	207/235	2σ error	206/238	2σ error	RHO	207/235 Age (Ma)	2σ error	206/238 Age (Ma)	2σ error	207/206 Age (Ma)	2σ error	Best age (Ma)	2σ error	% Discordance	Rim /Core
11_Escanilla_21	460	6.10	0.37610	0.00820	0.05170	0.00100	0.58134	324.6	5.9	324.8	6.3	326	41	324.8	6.3	0.06	
11_Escanilla_22	541	1.22	0.40870	0.00550	0.05547	0.00060	0.42687	347.8	4.0	348.0	3.7	355	28	348.0	3.7	0.06	
11_Escanilla_23	251	1.58	0.35420	0.00830	0.04910	0.00110	0.37425	308.6	6.4	308.7	6.5	300	53	308.7	6.5	0.03	
11_Escanilla_24	253	2.76	0.54310	0.00900	0.06972	0.00098	0.49894	440.2	5.9	434.4	5.9	464	35	434.4	5.9	1.32	
11_Escanilla_25	184	1.44	0.36040	0.00710	0.04916	0.00067	0.11576	312.9	5.4	309.3	4.1	329	54	309.3	4.1	1.15	
11_Escanilla_26	254	2.94	0.34610	0.00540	0.04748	0.00056	0.21044	301.6	4.1	299.0	3.4	318	37	299.0	3.4	0.86	
11_Escanilla_27	890	1.10	0.41250	0.00590	0.05568	0.00083	0.83696	351.2	4.4	349.2	5.1	365	26	349.2	5.1	0.57	
11_Escanilla_28	130	1.09	4.40500	0.09300	0.27930	0.00630	0.74265	1715.0	17.0	1587.0	32.0	1849	27	1849.0	27.0	14.17	
11_Escanilla_29	180.4	1.20	0.33380	0.00690	0.04674	0.00067	0.33069	292.2	5.3	294.5	4.1	262	45	294.5	4.1	0.79	
11_Escanilla_30	867	1.27	0.41590	0.00690	0.05590	0.00093	0.77324	352.9	5.0	350.6	5.7	355	25	350.6	5.7	0.65	
11_Escanilla_31	186.1	1.27	0.34780	0.00660	0.04777	0.00069	0.13410	303.6	5.1	300.8	4.2	318	48	300.8	4.2	0.92	
11_Escanilla_32	274	2.81	0.35580	0.00780	0.04861	0.00072	0.07736	308.8	5.8	306.0	4.4	322	42	306.0	4.4	0.91	
11_Escanilla_33	148.1	1.87	0.34680	0.00610	0.04585	0.00057	0.03991	302.8	4.5	289.0	3.5	410	52	289.0	3.5	4.56	
11_Escanilla_34	156	1.77	0.35130	0.00670	0.04892	0.00071	0.19601	305.5	5.0	307.9	4.4	276	51	307.9	4.4	0.79	
11_Escanilla_35	275	2.54	0.35450	0.00750	0.04836	0.00086	0.47652	307.9	5.6	304.4	5.3	280	46	304.4	5.3	1.14	
11_Escanilla_36	58.2	1.31	0.56100	0.01500	0.07400	0.00110	0.08401	451.8	9.9	460.3	6.6	425	72	460.3	6.6	1.88	
11_Escanilla_37	252	2.92	0.36610	0.00680	0.05089	0.00058	0.38329	316.5	5.0	320.0	3.5	292	43	320.0	3.5	1.11	
11_Escanilla_38	169	1.61	0.37030	0.00760	0.05061	0.00060	0.21530	319.6	5.6	318.2	3.7	347	47	318.2	3.7	0.44	
11_Escanilla_39	197	1.68	0.36790	0.00670	0.04980	0.00068	0.33136	317.9	5.0	313.3	4.2	345	40	313.3	4.2	1.45	
11_Escanilla_40	283	1.57	0.35970	0.00590	0.04990	0.00054	0.24137	311.8	4.4	313.9	3.3	294	39	313.9	3.3	0.67	
11_Escanilla_41	202	2.05	0.35550	0.00560	0.04888	0.00063	0.25996	309.9	4.2	307.6	3.9	321	41	307.6	3.9	0.74	
11_Escanilla_42	48.8	0.57	0.73400	0.01500	0.08960	0.00180	0.10164	560.0	8.4	553.0	11.0	607	66	553.0	11.0	1.25	
11_Escanilla_43	173	1.78	0.35710	0.00610	0.04894	0.00052	0.20597	309.9	4.6	308.0	3.2	319	44	308.0	3.2	0.61	
11_Escanilla_44	402	1.75	0.37790	0.00670	0.05119	0.00071	0.48631	325.3	4.9	321.8	4.3	345	36	321.8	4.3	1.08	
11_Escanilla_45	115	2.06	0.65400	0.03000	0.08290	0.00270	0.27960	511.0	18.0	513.0	16.0	509	83	513.0	16.0	0.39	

Sample Name _Grain #	[U] ppm	U/Th	207/235	2σ error	206/238	2σ error	RHO	207/235 Age (Ma)	2σ error	206/238 Age (Ma)	2σ error	207/206 Age (Ma)	2σ error	Best age (Ma)	2σ error	% Discordance	Rim /Core
11_Escanilla_46	503	2.60	1.36200	0.03200	0.14210	0.00480	0.73249	872.0	14.0	857.0	27.0	939	50	939.0	50.0	8.73	
11_Escanilla_47	71.7	2.13	2.26700	0.05600	0.20420	0.00430	0.65647	1203.0	18.0	1197.0	23.0	1213	38	1213.0	38.0	1.32	
11_Escanilla_48	247	2.03	0.35030	0.00510	0.04847	0.00059	0.27492	304.8	3.9	305.1	3.6	290	42	305.1	3.6	0.10	
11_Escanilla_49	310	1.70	0.37430	0.00630	0.05151	0.00077	0.60515	322.6	4.6	323.7	4.7	343	37	323.7	4.7	0.34	
11_Escanilla_50	121	2.00	0.85000	0.01400	0.10030	0.00110	0.30039	624.0	7.8	616.1	6.2	649	34	616.1	6.2	1.27	
11_Escanilla_51	221	2.65	0.35010	0.00760	0.04765	0.00071	0.31216	304.6	5.7	300.0	4.3	358	55	300.0	4.3	1.51	
11_Escanilla_52	941	33.20	0.32910	0.00800	0.04510	0.00100	0.61932	288.8	6.1	284.6	6.3	325	54	284.6	6.3	1.45	Rim
11_Escanilla_52	90.5	2.47	0.70700	0.02100	0.08790	0.00200	0.10107	542.0	13.0	543.0	12.0	543	83	543.0	12.0	0.18	Core
11_Escanilla_53	97	1.47	0.36300	0.01300	0.04960	0.00110	0.00447	314.3	9.9	311.7	6.6	276	87	311.7	6.6	0.83	
11_Escanilla_54	186.9	1.28	0.32740	0.00570	0.04566	0.00061	0.22427	287.4	4.4	287.8	3.8	281	44	287.8	3.8	0.14	
11_Escanilla_55	580	3.26	0.32460	0.00440	0.04485	0.00047	0.47936	285.8	3.5	282.8	2.9	310	29	282.8	2.9	1.05	
11_Escanilla_56	1080	3.10	0.35650	0.00870	0.05020	0.00110	0.44295	309.5	6.5	315.7	6.5	278	53	315.7	6.5	2.00	Rim
11_Escanilla_56	238	2.06	0.86200	0.02000	0.10210	0.00210	0.52207	631.0	11.0	627.0	12.0	652	51	627.0	12.0	0.63	Core
11_Escanilla_57	232	1.37	0.34510	0.00530	0.04784	0.00049	0.29904	300.8	4.0	301.3	3.0	291	35	301.3	3.0	0.17	
11_Escanilla_58	191.8	1.62	0.34510	0.00710	0.04672	0.00087	0.36551	300.8	5.4	294.3	5.4	309	43	294.3	5.4	2.16	
11_Escanilla_59	85.6	0.77	5.52600	0.05100	0.34310	0.00270	0.61991	1904.1	7.9	1901.0	13.0	1906	15	1906.0	15.0	0.26	
11_Escanilla_60	526	1.56	0.36280	0.00580	0.04990	0.00054	0.26880	314.1	4.3	313.9	3.3	322	30	313.9	3.3	0.06	
11_Escanilla_61	237	11.69	0.69600	0.02300	0.08580	0.00330	0.67735	535.0	14.0	530.0	20.0	554	66	530.0	20.0	0.93	
11_Escanilla_62	176.4	1.31	0.34380	0.00620	0.04787	0.00042	0.04608	301.0	4.5	301.4	2.6	298	45	301.4	2.6	0.13	
11_Escanilla_63	167	2.12	0.35080	0.00660	0.04969	0.00064	0.27177	305.1	5.0	312.6	4.0	256	49	312.6	4.0	2.46	
11_Escanilla_64	242	2.50	0.35500	0.01000	0.04696	0.00057	0.14498	307.6	7.7	295.8	3.5	368	59	295.8	3.5	3.84	
11_Escanilla_65	345	1.79	0.38190	0.00750	0.05190	0.00120	0.64579	328.3	5.5	326.3	7.2	335	39	326.3	7.2	0.61	
11_Escanilla_66	183	1.37	0.34470	0.00670	0.04844	0.00060	0.15456	301.1	4.9	304.9	3.7	257	47	304.9	3.7	1.26	

Sample Name _Grain #	[U] ppm	U/Th	207/235	2σ error	206/238	2σ error	RHO	207/235 Age (Ma)	2σ error	206/238 Age (Ma)	2σ error	207/206 Age (Ma)	2σ error	Best age (Ma)	2σ error	% Discordance	Rim /Core
11_Escanilla_67	237	2.37	0.36430	0.00720	0.04985	0.00074	0.33649	315.2	5.4	313.6	4.5	313	44	313.6	4.5	0.51	
11_Escanilla_68	95	1.47	6.79400	0.08800	0.37980	0.00530	0.68161	2087.0	11.0	2075.0	25.0	2075	19	2075.0	19.0	0.00	
11_Escanilla_69	415	3.24	0.35260	0.00650	0.04870	0.00081	0.60367	307.1	4.8	306.5	5.0	304	34	306.5	5.0	0.20	
11_Escanilla_70	680	3.09	0.34770	0.00580	0.04855	0.00071	0.56490	302.8	4.3	305.6	4.4	299	29	305.6	4.4	0.92	
11_Escanilla_71	109.7	0.96	1.71900	0.02100	0.16900	0.00190	0.41089	1016.4	8.1	1006.0	10.0	1028	29	1028.0	29.0	2.14	
11_Escanilla_72	346	2.81	0.34710	0.00740	0.04722	0.00089	0.59495	302.4	5.5	297.4	5.5	334	43	297.4	5.5	1.65	
11_Escanilla_73	476	2.85	0.88720	0.00800	0.10604	0.00084	0.40722	645.3	4.4	649.7	4.9	623	20	649.7	4.9	0.68	
11_Escanilla_74	550	2.21	0.37140	0.00610	0.05082	0.00080	0.62218	321.1	4.6	319.5	4.9	325	34	319.5	4.9	0.50	
11_Escanilla_75	211.6	1.38	0.36150	0.00830	0.04925	0.00057	0.30991	313.0	6.2	309.9	3.5	358	53	309.9	3.5	0.99	
11_Escanilla_76	288	10.80	0.73300	0.02000	0.09180	0.00220	0.57908	558.0	12.0	566.0	13.0	532	49	566.0	13.0	1.43	Rim
11_Escanilla_76	220.4	4.68	0.92900	0.02300	0.10740	0.00230	0.70611	666.0	12.0	658.0	14.0	718	35	658.0	14.0	1.20	Core
11_Escanilla_77	230	2.20	0.35700	0.00620	0.04953	0.00061	0.23882	309.8	4.6	311.6	3.7	310	43	311.6	3.7	0.58	
11_Escanilla_78	218	1.39	0.35670	0.00740	0.04921	0.00066	0.40151	310.9	5.5	309.6	4.1	325	44	309.6	4.1	0.42	
11_Escanilla_79	189	1.69	0.36480	0.00640	0.04976	0.00054	0.38643	315.6	4.8	313.0	3.3	335	38	313.0	3.3	0.82	
11_Escanilla_80	44.6	0.72	4.58400	0.06900	0.30960	0.00440	0.57804	1747.0	13.0	1738.0	22.0	1750	25	1750.0	25.0	0.69	
11_Escanilla_81	142	2.17	0.35850	0.00830	0.04971	0.00065	0.34268	310.7	6.2	312.7	4.0	281	50	312.7	4.0	0.64	
11_Escanilla_82	274	1.83	0.87600	0.01100	0.10500	0.00110	0.52330	638.6	5.7	643.7	6.7	630	28	643.7	6.7	0.80	
11_Escanilla_83	190	1.92	0.36130	0.00720	0.04922	0.00061	0.44580	312.9	5.4	309.7	3.7	297	41	309.7	3.7	1.02	
11_Escanilla_84	185	1.74	0.34920	0.00650	0.04736	0.00071	0.30925	303.9	4.9	298.3	4.4	310	44	298.3	4.4	1.84	
11_Escanilla_86	278	1.71	0.49300	0.02500	0.05022	0.00081	0.54955	405.0	16.0	315.9	5.0	896	78	DISC	DISC	22.00	
11_Escanilla_87	498	157.60	0.33800	0.01400	0.04890	0.00120	0.24521	296.0	11.0	307.5	7.5	225	98	307.5	7.5	3.89	Rim
11_Escanilla_87	346	1.47	9.46000	0.17000	0.39070	0.00730	0.86974	2382.0	16.0	2125.0	34.0	2620	15	2620.0	15.0	18.89	Core
11_Escanilla_88	147	2.70	0.34470	0.00700	0.04851	0.00080	0.47621	300.4	5.3	305.9	4.8	253	43	305.9	4.8	1.83	
11_Escanilla_89	762	4.72	0.36000	0.00560	0.04862	0.00059	0.76977	312.0	4.2	306.0	3.6	351	27	306.0	3.6	1.92	
11_Escanilla_90	394	1.50	0.96100	0.01000	0.11240	0.00110	0.47089	684.4	5.1	686.3	6.6	671	24	686.3	6.6	0.28	

Sample Name _Grain #	[U] ppm	U/Th	207/235	2σ error	206/238	2σ error	RHO	207/235 Age (Ma)	2σ error	206/238 Age (Ma)	2σ error	207/206 Age (Ma)	2σ error	Best age (Ma)	2σ error	% Discordance	Rim /Core
11_Escanilla_91	390	1.45	0.35920	0.00540	0.04938	0.00064	0.37754	311.5	4.0	310.7	3.9	326	36	310.7	3.9	0.26	
11_Escanilla_92	192	1.85	0.36000	0.00710	0.04888	0.00075	0.39074	311.9	5.3	307.6	4.6	365	44	307.6	4.6	1.38	
11_Escanilla_93	472	0.87	0.85300	0.01100	0.10290	0.00110	0.33256	625.9	6.1	631.1	6.1	598	28	631.1	6.1	0.83	
11_Escanilla_94	103.9	1.60	5.95300	0.07900	0.35470	0.00450	0.64456	1968.0	12.0	1956.0	21.0	1983	18	1983.0	18.0	1.36	
11_Escanilla_95	455	1.63	0.34880	0.00540	0.04805	0.00055	0.44339	303.7	4.1	302.5	3.4	295	32	302.5	3.4	0.40	
11_Escanilla_96	234	2.58	0.38820	0.00670	0.05248	0.00054	0.30016	333.6	5.1	329.7	3.3	371	41	329.7	3.3	1.17	
11_Escanilla_97	212	1.62	0.34190	0.00600	0.04701	0.00065	0.36542	299.0	4.6	296.1	4.0	323	42	296.1	4.0	0.97	
11_Escanilla_98	302	1.59	0.35720	0.00590	0.04781	0.00059	0.33600	310.5	4.3	301.0	3.6	362	37	301.0	3.6	3.06	
11_Escanilla_99	136	1.21	0.40970	0.00780	0.05483	0.00065	0.22430	349.0	5.5	344.1	4.0	360	43	344.1	4.0	1.40	
11_Escanilla_100	245.2	1.34	0.34310	0.00600	0.04690	0.00059	0.28252	299.3	4.6	295.5	3.6	307	40	295.5	3.6	1.27	
11_Escanilla_101	598	3.74	0.33710	0.00720	0.04535	0.00086	0.67403	294.7	5.4	285.9	5.3	336	37	285.9	5.3	2.99	
11_Escanilla_102	305	2.00	0.35190	0.00730	0.04889	0.00084	0.43363	307.2	5.5	307.7	5.2	301	47	307.7	5.2	0.16	
11_Escanilla_103	35.14	0.73	0.78600	0.02200	0.09630	0.00170	0.18165	587.0	13.0	592.0	10.0	591	69	592.0	10.0	0.85	
11_Escanilla_104	113	1.01	0.79600	0.01500	0.09480	0.00130	0.31633	595.1	8.3	583.9	7.5	610	40	583.9	7.5	1.88	
11_Escanilla_105	122.4	1.73	0.35930	0.00770	0.04951	0.00073	0.48221	311.4	5.8	311.5	4.5	310	42	311.5	4.5	0.03	
11_Escanilla_106	165	1.76	0.37260	0.00810	0.05037	0.00076	0.16012	321.3	6.0	316.8	4.7	398	52	316.8	4.7	1.40	
11_Escanilla_107	630	3.90	0.35210	0.00640	0.04827	0.00074	0.71320	306.0	4.8	303.8	4.5	311	29	303.8	4.5	0.72	
11_Escanilla_108	232	2.73	0.36000	0.01500	0.04869	0.00057	0.03278	306.9	5.4	306.5	3.5	304	44	306.5	3.5	0.13	
11_Escanilla_109	121.8	2.03	0.55000	0.00930	0.07065	0.00078	0.26421	444.7	6.1	440.0	4.7	468	38	440.0	4.7	1.06	
11_Escanilla_110	203	1.61	0.34750	0.00600	0.04755	0.00063	0.29334	302.7	4.5	299.5	3.9	317	44	299.5	3.9	1.06	
11_Escanilla_111	194	1.52	0.35460	0.00760	0.04855	0.00069	0.39522	307.8	5.7	305.6	4.3	329	44	305.6	4.3	0.71	
11_Escanilla_112	174	1.46	0.35300	0.00810	0.04848	0.00063	0.50439	308.2	6.1	305.1	3.9	347	44	305.1	3.9	1.01	
11_Escanilla_113	82.6	1.00	0.62100	0.01200	0.07850	0.00110	0.34767	489.7	7.6	486.8	6.8	486	40	486.8	6.8	0.59	
11_Escanilla_114	540	2.19	0.36740	0.00600	0.04996	0.00073	0.50956	317.6	4.5	314.3	4.5	359	32	314.3	4.5	1.04	
11_Escanilla_115	380	1.40	0.34960	0.00560	0.04739	0.00053	0.53022	304.3	4.3	298.5	3.2	352	31	298.5	3.2	1.91	

Sample Name _Grain #	[U] ppm	U/Th	207/235	2σ error	206/238	2σ error	RHO	207/235 Age (Ma)	2σ error	206/238 Age (Ma)	2σ error	207/206 Age (Ma)	2σ error	Best age (Ma)	2σ error	% Discordance	Rim /Core
11_Escanilla_116	760	2.86	0.37000	0.01100	0.05020	0.00150	0.53239	319.4	8.4	315.5	9.2	352	50	315.5	9.2	1.22	
11_Escanilla_117	241	17.10	0.80200	0.02200	0.09630	0.00300	0.79694	598.0	13.0	593.0	18.0	626	51	593.0	18.0	0.84	
11_Escanilla_119	471	1.90	0.34880	0.00710	0.04769	0.00082	0.37714	304.4	5.1	300.3	5.0	326	40	300.3	5.0	1.35	
11_Escanilla_120	132.9	1.54	0.35270	0.00930	0.04971	0.00084	0.33070	307.2	7.1	312.7	5.1	282	58	312.7	5.1	1.79	
10_Sobrarbe_1	208.00000	1.90900	0.35960	0.00670	0.0	0.0	0.5	312.4	5	307	5.5	344.0	43.0	307	5.5	1.73	
10_Sobrarbe_2	224.00000	1.69600	0.35940	0.00680	0.1	0.0	0.2	311.5	5	316	3.8	271.0	44.0	316.4	3.8	1.57	
10_Sobrarbe_3	681.00000	1.53900	0.35830	0.00730	0.0	0.0	0.3	310.8	6	307	4.7	350.0	45.0	306.5	4.7	1.38	
10_Sobrarbe_4	429.00000	1.45500	0.35980	0.00590	0.0	0.0	0.6	311.9	4	311	4.2	301.0	29.0	311	4.2	0.29	
10_Sobrarbe_5	293.00000	1.42500	0.33960	0.00560	0.0	0.0	0.5	297.3	4	295	3.9	332.0	39.0	294.5	3.9	0.94	
10_Sobrarbe_6	491.00000	1.46800	0.36760	0.00580	0.0	0.0	0.4	317.7	4	313	3.9	344.0	38.0	312.6	3.9	1.61	
10_Sobrarbe_7	276.00000	1.69100	0.37140	0.00870	0.1	0.0	0.4	320.3	6	318	5.3	322.0	42.0	317.7	5.3	0.81	
10_Sobrarbe_8	588.00000	1.41500	0.35230	0.00730	0.0	0.0	0.6	306.9	6	308	6.2	271.0	46.0	307.6	6.2	0.23	
10_Sobrarbe_9	185.00000	1.60800	0.36300	0.00760	0.0	0.0	0.3	314.2	6	309	4.7	346.0	44.0	309.1	4.7	1.62	
10_Sobrarbe_10	414.00000	10.23000	0.38000	0.02600	0.1	0.0	0.8	326.0	19	330	16.0	230.0	74.0	330	16	1.23	Rim
10_Sobrarbe_10	130.20000	1.01100	0.61200	0.02900	0.1	0.0	0.5	484.0	18	474	18.0	566.0	73.0	474	18	2.07	Core
10_Sobrarbe_11	322.00000	2.75200	0.35750	0.00690	0.0	0.0	0.4	311.0	5	307	3.7	338.0	41.0	307.1	3.7	1.25	
10_Sobrarbe_12	263.00000	1.72400	0.34120	0.00810	0.0	0.0	0.6	297.7	6	301	5.8	281.0	45.0	300.9	5.8	1.07	
10_Sobrarbe_13	208.00000	1.34800	0.34920	0.00570	0.0	0.0	0.4	304.0	4	300	4.0	328.0	39.0	300	4	1.32	
10_Sobrarbe_14	806.00000	2.47000	0.35590	0.00860	0.0	0.0	0.5	310.4	7	306	8.5	344.0	58.0	306.1	8.5	1.39	
10_Sobrarbe_15	432.00000	2.09800	0.35700	0.01300	0.0	0.0	0.8	309.0	10	306	13.0	356.0	59.0	306	13	0.97	
10_Sobrarbe_16	1000.00000	3.08000	0.35200	0.01000	0.0	0.0	0.9	308.2	9	304	6.7	322.0	43.0	303.8	6.7	1.43	
10_Sobrarbe_17	271.00000	2.04800	0.34660	0.00610	0.0	0.0	0.3	302.0	5	304	3.9	287.0	40.0	303.7	3.9	0.56	
10_Sobrarbe_18	281.00000	1.33500	0.35420	0.00580	0.0	0.0	0.4	307.7	4	308	3.5	282.0	36.0	308	3.5	0.10	
10_Sobrarbe_19	167.00000	2.12800	0.36300	0.01000	0.0	0.0	0.3	313.9	8	308	7.4	335.0	77.0	307.8	7.4	1.94	
10_Sobrarbe_20	182.20000	0.88800	1.36000	0.06100	0.1	0.0	0.7	871.0	26	852	23.0	915.0	64.0	915	64	6.89	

Sample Name _Grain #	[U] ppm	U/Th	207/235	2σ error	206/238	2σ error	RHO	207/235 Age (Ma)	2σ error	206/238 Age (Ma)	2σ error	207/206 Age (Ma)	2σ error	Best age (Ma)	2σ error	% Discordance	Rim /Core
10_Sobrarbe_21	315.00000	1.38000	0.35940	0.00720	0.0	0.0	0.4	311.6	5	307	5.8	338.0	45.0	307.2	5.8	1.41	
10_Sobrarbe_22	491.00000	2.50000	0.37460	0.00720	0.1	0.0	0.6	322.7	5	320	5.1	343.0	36.0	319.9	5.1	0.87	
10_Sobrarbe_23	80.10000	1.08600	1.58300	0.03600	0.2	0.0	0.1	963.0	14	963	15.0	969.0	56.0	969	56	0.62	Rim
10_Sobrarbe_23	103.90000	1.05700	1.48800	0.04300	0.2	0.0	0.2	925.0	17	910	13.0	970.0	56.0	970	56	6.19	Core
10_Sobrarbe_24	256.00000	1.55300	0.36080	0.00880	0.0	0.0	0.3	312.4	7	307	5.1	333.0	54.0	306.5	5.1	1.89	
10_Sobrarbe_25	246.00000	1.64100	0.34060	0.00640	0.0	0.0	0.6	297.4	5	295	5.0	295.0	42.0	295.1	5	0.77	
10_Sobrarbe_26	319.00000	1.78700	0.33480	0.00610	0.0	0.0	0.0	293.0	5	290	4.3	296.0	44.0	290.2	4.3	0.96	
10_Sobrarbe_27	377.00000	1.67200	0.34980	0.00640	0.0	0.0	0.4	304.3	5	296	4.2	316.0	40.0	296.2	4.2	2.66	
10_Sobrarbe_28	287.00000	2.16200	0.35640	0.00730	0.0	0.0	0.5	309.2	5	302	3.6	348.0	41.0	302.3	3.6	2.23	
10_Sobrarbe_29	408.00000	1.43400	0.35130	0.00820	0.0	0.0	0.6	305.4	6	306	5.9	266.0	42.0	306	5.9	0.20	
10_Sobrarbe_30	290.00000	3.15000	0.37200	0.01000	0.0	0.0	0.7	320.6	8	304	9.5	414.0	53.0	304.4	9.5	5.05	
10_Sobrarbe_31	622.00000	2.89000	0.34140	0.00610	0.0	0.0	0.5	298.1	5	295	4.2	349.0	43.0	294.8	4.2	1.11	
10_Sobrarbe_32	191.50000	2.74000	0.34220	0.00890	0.0	0.0	0.4	298.4	7	300	3.8	277.0	48.0	299.7	3.8	0.44	
10_Sobrarbe_33	733.00000	3.90000	0.34290	0.00490	0.0	0.0	0.5	299.2	4	297	3.7	301.0	25.0	296.5	3.7	0.90	
10_Sobrarbe_34	359.00000	8.67000	0.60000	0.02000	0.1	0.0	0.6	477.0	13	460	11.0	549.0	49.0	460	11	3.56	
10_Sobrarbe_35	500.00000	1.63000	0.37690	0.00830	0.1	0.0	0.5	324.5	6	326	6.7	326.0	52.0	325.7	6.7	0.37	
10_Sobrarbe_36	453.00000	1.78000	0.34610	0.00610	0.0	0.0	0.4	301.7	5	302	5.4	279.0	43.0	302.3	5.4	0.20	
10_Sobrarbe_37	184.80000	2.30000	0.37600	0.00760	0.0	0.0	0.3	323.9	6	312	4.8	390.0	49.0	312.1	4.8	3.64	
10_Sobrarbe_38	215.00000	3.37000	0.36620	0.00930	0.0	0.0	0.5	316.6	7	309	4.7	351.0	48.0	308.6	4.7	2.53	
10_Sobrarbe_39	197.00000	2.01900	0.33200	0.01300	0.0	0.0	0.0	291.0	10	283	4.5	373.0	95.0	283.4	4.5	2.61	
10_Sobrarbe_40	258.00000	1.60500	0.35810	0.00730	0.0	0.0	0.2	310.6	6	305	3.3	345.0	42.0	304.6	3.3	1.93	
10_Sobrarbe_41	228.00000	1.85100	0.33660	0.00620	0.0	0.0	0.5	295.7	5	292	4.3	300.0	38.0	291.8	4.3	1.32	
10_Sobrarbe_42	358.00000	2.00000	0.34700	0.00540	0.0	0.0	0.4	302.3	4	299	3.6	332.0	38.0	299.2	3.6	1.03	
10_Sobrarbe_43	590.00000	3.59000	0.37350	0.00650	0.0	0.0	0.0	322.9	5	314	5.2	400.0	47.0	313.8	5.2	2.82	
10_Sobrarbe_44	362.00000	1.46700	0.35780	0.00570	0.0	0.0	0.2	310.4	4	310	3.2	299.0	38.0	309.9	3.2	0.16	

Sample Name _Grain #	[U] ppm	U/Th	207/235	2σ error	206/238	2σ error	RHO	207/235 Age (Ma)	2σ error	206/238 Age (Ma)	2σ error	207/206 Age (Ma)	2σ error	Best age (Ma)	2σ error	% Discordance	Rim /Core
10_Sobrarbe_45	245.00000	1.41200	0.36160	0.00810	0.0	0.0	0.4	313.1	6	308	4.1	317.0	49.0	307.8	4.1	1.69	
10_Sobrarbe_46	368.00000	1.85200	0.36320	0.00630	0.0	0.0	0.4	314.4	5	310	5.3	336.0	44.0	310.1	5.3	1.37	
10_Sobrarbe_47	551.00000	3.92000	0.56840	0.00460	0.1	0.0	0.3	456.9	3	456	2.8	451.0	19.0	455.7	2.8	0.26	
10_Sobrarbe_48	284.00000	2.20500	0.35710	0.00910	0.0	0.0	0.4	309.8	7	304	5.2	328.0	55.0	303.8	5.2	1.94	
10_Sobrarbe_49	285.00000	1.50900	0.35770	0.00540	0.0	0.0	0.3	310.3	4	308	3.7	306.0	33.0	308.1	3.7	0.71	
10_Sobrarbe_50	508.00000	2.85000	0.35160	0.00780	0.0	0.0	0.6	306.8	6	303	7.3	325.0	51.0	303.2	7.3	1.17	
10_Sobrarbe_51	850.00000	1.73800	0.36520	0.00730	0.0	0.0	0.5	315.8	5	314	4.2	315.0	35.0	313.8	4.2	0.63	
10_Sobrarbe_52	328.00000	2.86000	0.35730	0.00870	0.0	0.0	0.5	309.8	7	309	7.6	304.0	53.0	308.5	7.6	0.42	
10_Sobrarbe_53	304.0000	1.57200	0.34360	0.005	0.04749	0.00052	0.39188	299.8	4	299	3.2	312.0	31.0	299.1	3.2	0.23	
10_Sobrarbe_54	910.0000	5.40000	0.35220	0.007	0.0481	0.0013	0.62857	306.2	5	303	8.0	346.0	46.0	302.9	8	1.08	
10_Sobrarbe_55	680.0000	3.08000	0.35920	0.005	0.0491	0.00057	0.4716	311.5	4	309	3.5	325.0	25.0	309	3.5	0.80	
10_Sobrarbe_56	697.0000	1.82600	0.32490	0.007	0.0452	0.001	0.74506	285.5	6	285	6.4	301.0	47.0	285	6.4	0.18	
10_Sobrarbe_57	300.0000	1.47900	0.35250	0.005	0.04801	0.00043	0.45484	306.4	4	302	2.6	338.0	32.0	302.3	2.6	1.34	
10_Sobrarbe_58	701.0000	2.29000	0.33020	0.006	0.04551	0.00082	0.70915	289.5	5	287	5.0	302.0	34.0	286.9	5	0.90	
10_Sobrarbe_59	289.0000	1.17100	0.32850	0.005	0.04546	0.00056	0.1375	288.3	4	287	3.4	282.0	43.0	286.5	3.4	0.62	
10_Sobrarbe_60	186.0000	5.63000	14.25000	0.200	0.4999	0.0077	0.82419	2767	13	2612	33.0	2885.0	14.0	2885	14	9.46	
10_Sobrarbe_61	387.0000	1.35100	0.34290	0.005	0.04715	0.00052	0.35085	299.7	4	297	3.2	319.0	35.0	297	3.2	0.90	
10_Sobrarbe_62	870.0000	2.18000	0.36090	0.006	0.04918	0.00055	0.5034	312.7	5	310	3.4	343.0	31.0	309.5	3.4	1.02	
10_Sobrarbe_63	194.0000	1.68500	0.35470	0.009	0.0487	0.001	0.51966	308.9	7	307	6.2	299.0	44.0	306.8	6.2	0.68	
10_Sobrarbe_64	534.0000	3.40000	0.35790	0.006	0.04943	0.00081	0.66535	311	5	311	4.9	323.0	29.0	311	4.9	0.00	
10_Sobrarbe_65	213.0000	1.71000	0.35860	0.008	0.04859	0.0008	0.39437	310.8	6	306	4.9	327.0	50.0	305.8	4.9	1.61	
10_Sobrarbe_66	572.0000	13.78000	0.80410	0.007	0.09704	0.0008	0.60259	599	4	597	4.7	594.0	18.0	597	4.7	0.33	
10_Sobrarbe_67	205.0000	1.94700	0.34360	0.007	0.04813	0.00073	0.49162	299.7	5	303	4.5	269.0	44.0	303	4.5	1.10	
10_Sobrarbe_68	324.0000	1.45600	0.35280	0.006	0.04959	0.00057	0.28382	306.7	4	312	3.5	277.0	41.0	312	3.5	1.73	
10_Sobrarbe_69	453.0000	1.88700	0.36600	0.005	0.05034	0.00059	0.38664	316.5	4	317	3.6	321.0	33.0	316.6	3.6	0.03	

Sample Name _Grain #	[U] ppm	U/Th	207/235	2σ error	206/238	2σ error	RHO	207/235 Age (Ma)	2σ error	206/238 Age (Ma)	2σ error	207/206 Age (Ma)	2σ error	Best age (Ma)	2σ error	% Discordance	Rim /Core
10_Sobrarbe_70	149.1000	1.71100	0.34900	0.008	0.04951	0.0007	0.10361	303.7	6	312	4.3	267.0	53.0	311.5	4.3	2.57	
10_Sobrarbe_71	332.0000	3.11000	0.36260	0.007	0.04979	0.00068	0.40467	314.6	5	313	4.2	311.0	41.0	313.2	4.2	0.45	
10_Sobrarbe_72	451.0000	1.81000	0.35910	0.005	0.04952	0.00051	0.30183	311.4	4	312	3.2	311.0	32.0	311.5	3.2	0.03	
10_Sobrarbe_73	2326.0000	#######	0.34280	0.004	0.04718	0.0005	0.68864	299.3	3	297	3.1	326.0	19.0	297.2	3.1	0.70	
10_Sobrarbe_74	160.0000	1.71200	0.35230	0.008	0.04832	0.00069	0.26714	306.1	6	304	4.2	317.0	47.0	304.1	4.2	0.65	
10_Sobrarbe_75	138.0000	1.77000	0.34970	0.009	0.04924	0.00083	0.40601	304	7	310	5.1	252.0	51.0	309.8	5.1	1.91	
10_Sobrarbe_76	383.0000	3.51000	0.35760	0.006	0.04932	0.00064	0.41054	310.8	4	310	3.9	301.0	36.0	310.3	3.9	0.16	
10_Sobrarbe_77	185.0000	1.46400	0.35380	0.007	0.04927	0.00061	0.25549	307.3	5	310	3.7	305.0	43.0	310	3.7	0.88	
10_Sobrarbe_78	168.0000	1.81100	0.36860	0.008	0.04998	0.00068	0.13249	319.1	6	314	4.1	354.0	54.0	314.4	4.1	1.47	
10_Sobrarbe_79	390.0000	1.54300	0.35810	0.006	0.04881	0.00067	0.58742	310.6	5	307	4.1	320.0	34.0	307.2	4.1	1.09	
10_Sobrarbe_80	238.0000	1.77600	0.36450	0.007	0.05028	0.00065	0.40768	315.3	5	316	4.0	311.0	42.0	316.2	4	0.29	
10_Sobrarbe_81	393.0000	1.42700	0.36180	0.006	0.05011	0.00078	0.43487	313.4	5	315	4.8	304.0	37.0	315.2	4.8	0.57	
10_Sobrarbe_82	114.5000	1.70900	0.78700	0.014	0.0948	0.0013	0.22982	590.2	8	584	7.7	598.0	46.0	583.6	7.7	1.12	
10_Sobrarbe_83	311.0000	1.43200	0.35640	0.005	0.04946	0.00052	0.4993	310	4	311	3.2	303.0	32.0	311.2	3.2	0.39	
10_Sobrarbe_84	510.0000	2.86000	0.97500	0.038	0.1134	0.0024	0.51965	691	20	693	14.0	684.0	72.0	693	14	0.29	Rim
10_Sobrarbe_84	80.2000	1.56600	2.09800	0.037	0.1978	0.0025	0.27392	1148	12	1163	13.0	1130.0	42.0	1130	42	2.92	Core
10_Sobrarbe_85	710.0000	4.68000	0.35930	0.005	0.04925	0.00054	0.26989	311.5	4	310	3.3	310.0	34.0	309.9	3.3	0.51	
10_Sobrarbe_86	393.0000	0.95700	0.36030	0.007	0.04879	0.00081	0.48059	312.8	5	307	5.0	341.0	44.0	307	5	1.85	
10_Sobrarbe_87	496.0000	1.60000	0.36670	0.008	0.0489	0.0012	0.56955	317.1	6	308	7.6	389.0	46.0	307.8	7.6	2.93	
10_Sobrarbe_88	320.0000	3.23000	0.37100	0.010	0.0507	0.001	0.45653	320	8	319	6.3	315.0	59.0	318.8	6.3	0.37	
10_Sobrarbe_89	260.0000	1.43200	0.36350	0.006	0.05001	0.00048	0.11734	314.6	5	315	2.9	302.0	39.0	314.6	2.9	0.00	
10_Sobrarbe_90	185.0000	1.71400	0.35850	0.005	0.0489	0.00078	0.28478	311	4	308	4.8	328.0	41.0	307.8	4.8	1.03	
10_Sobrarbe_91	130.2000	1.80000	0.38300	0.012	0.04775	0.00094	0.2975	328.5	9	301	5.8	557.0	70.0	300.7	5.8	8.46	
10_Sobrarbe_92	338.0000	1.67500	0.35310	0.006	0.04942	0.00051	0.11598	306.9	4	311	3.2	310.0	41.0	310.9	3.2	1.30	
10_Sobrarbe_93	165.1000	1.70200	0.38100	0.015	0.0511	0.0012	0.61104	329	10	321	7.2	411.0	67.0	321.2	7.2	2.37	

Sample Name _Grain #	[U] ppm	U/Th	207/235	2σ error	206/238	2σ error	RHO	207/235 Age (Ma)	2σ error	206/238 Age (Ma)	2σ error	207/206 Age (Ma)	2σ error	Best age (Ma)	2σ error	% Discordance	Rim /Core
10_Sobrarbe_94	252.0000	1.74600	0.34970	0.007	0.04853	0.00071	0.32022	304.3	6	306	4.4	279.0	47.0	305.5	4.4	0.39	
10_Sobrarbe_95	337.0000	2.88000	0.37250	0.010	0.0514	0.0013	0.73502	321.9	7	323	7.7	320.0	37.0	323.2	7.7	0.40	
10_Sobrarbe_96	97.1000	1.82000	0.33600	0.015	0.047	0.0012	0.27496	294	12	296	7.5	290.0	100.0	296.2	7.5	0.75	
10_Sobrarbe_97	640.0000	2.13000	0.35130	0.006	0.04856	0.00077	0.51966	305.5	4	306	4.7	325.0	38.0	305.6	4.7	0.03	
10_Sobrarbe_98	1540.0000	12.00000	0.34740	0.004	0.04734	0.00067	0.4988	302.7	3	298	4.1	342.0	26.0	298.1	4.1	1.52	
10_Sobrarbe_99	337.0000	2.06400	0.36010	0.006	0.04874	0.0007	0.38519	312.2	5	307	4.3	377.0	37.0	306.8	4.3	1.73	
10_Sobrarbe_100	508.0000	3.09000	0.35720	0.005	0.04865	0.00057	0.35979	311	4	306	3.5	333.0	36.0	306.2	3.5	1.54	
10_Sobrarbe_101	250.0000	1.66500	0.34960	0.006	0.04847	0.00056	0.32032	304.2	5	305	3.4	292.0	40.0	305.1	3.4	0.30	
10_Sobrarbe_103	246.0000	1.46200	0.34080	0.007	0.04774	0.00079	0.3632	298.2	5	301	4.9	279.0	45.0	300.6	4.9	0.80	
10_Sobrarbe_104	255.0000	1.39300	0.35150	0.006	0.04916	0.0005	0.31025	306.3	5	309	3.1	280.0	42.0	309.4	3.1	1.01	
10_Sobrarbe_105	313.0000	1.44800	0.35560	0.006	0.04893	0.00063	0.06085	308.7	5	308	3.9	293.0	38.0	307.9	3.9	0.26	
10_Sobrarbe_106	533.0000	2.31000	0.35860	0.005	0.04891	0.00069	0.37823	311	4	308	4.2	355.0	39.0	307.8	4.2	1.03	
10_Sobrarbe_107	244.0000	1.49500	0.34590	0.009	0.04794	0.00085	0.03775	301.2	6	302	5.2	296.0	52.0	301.8	5.2	0.20	
10_Sobrarbe_108	294.0000	1.92400	0.36500	0.007	0.04957	0.00056	0.20819	315.7	5	312	3.4	320.0	44.0	311.9	3.4	1.20	
10_Sobrarbe_109	282.0000	2.53400	0.35330	0.007	0.04884	0.0006	0.43915	307	5	307	3.7	329.0	39.0	307.4	3.7	0.13	
10_Sobrarbe_110	168.4000	1.70900	0.33990	0.007	0.04685	0.00067	0.33947	296.8	5	296	4.1	304.0	48.0	295.6	4.1	0.40	
10_Sobrarbe_111	36.5000	0.46300	6.11000	0.130	0.367	0.0091	0.63826	1990	19	2013	43.0	1964.0	33.0	1964	33	2.49	
10_Sobrarbe_112	211.0000	3.01000	0.36620	0.009	0.05019	0.00068	0.41112	317.2	6	316	4.2	329.0	48.0	315.7	4.2	0.47	
10_Sobrarbe_113	156.7000	1.98000	0.35620	0.007	0.04906	0.0007	0.13214	309.1	5	309	4.3	303.0	51.0	308.7	4.3	0.13	
10_Sobrarbe_114	266.0000	1.51500	0.33780	0.008	0.04592	0.00087	0.43497	297	6	289	5.4	326.0	58.0	289.4	5.4	2.56	
10_Sobrarbe_115	195.0000	1.93100	0.35870	0.007	0.04945	0.00054	0.20695	311	5	312	3.2	309.0	43.0	311.6	3.2	0.19	
10_Sobrarbe_116	154.7000	1.60400	0.35260	0.008	0.04769	0.00077	0.10935	306.5	6	300	4.7	306.0	68.0	300.3	4.7	2.02	
10_Sobrarbe_117	389.0000	2.34000	0.37140	0.005	0.0519	0.00051	0.24745	320.6	4	326	3.1	288.0	32.0	326.1	3.1	1.72	
10_Sobrarbe_118	487.0000	1.86000	0.37300	0.011	0.0518	0.0013	0.43612	321.6	9	325	7.7	283.0	54.0	325.4	7.7	1.18	
10_Sobrarbe_119	324.0000	1.37800	0.34780	0.005	0.04815	0.00042	0.18437	303	4	303	2.6	290.0	37.0	303.1	2.6	0.03	

Sample Name _Grain #	[U] ppm	U/Th	207/235	2σ error	206/238	2σ error	RHO	207/235 Age (Ma)	2σ error	206/238 Age (Ma)	2σ error	207/206 Age (Ma)	2σ error	Best age (Ma)	2σ error	% Discordance	Rim /Core
10_Sobrarbe_120	194.6000	2.98300	0.35900	0.011	0.0503	0.0014	0.40334	311.6	8	316	8.4	231.0	95.0	316.4	8.4	1.54	
13Guaso_1	1170	30.00	0.3512	0.0052	0.04898	0.00075	0.489	305.5	3.9	308.2	4.6	294	35	308.2	4.6	0.88	Rim
13Guaso_1	46.6	1.12	0.6310	0.0160	0.08190	0.00190	0.032	496.4	9.9	507	11	463	87	507.0	11.0	2.14	Core
13Guaso_2	327	5.03	0.8520	0.0110	0.10100	0.00110	0.497	625.3	5.9	620.3	6.6	642	26	620.3	6.6	0.80	
13Guaso_3	62.7	0.52	13.4500	0.1200	0.48760	0.00500	0.569	2710.9	8.4	2560	22	2836	15	2836.0	15.0	9.73	
13Guaso_4	393	1.33	0.3509	0.0043	0.04909	0.00058	0.366	305.3	3.2	308.9	3.6	279	32	308.9	3.6	1.18	
13Guaso_5	301	1.20	0.3503	0.0055	0.04922	0.00066	0.092	305.3	4.1	309.7	4	295	47	309.7	4.0	1.44	
13Guaso_6	280	1.91	0.3584	0.0058	0.04879	0.00071	0.440	310.9	4.3	307	4.3	326	34	307.0	4.3	1.25	
13Guaso_7	168	4.89	0.5788	0.0088	0.07430	0.00110	0.308	463.4	5.7	462	6.8	482	40	462.0	6.8	0.30	
13Guaso_8	513	1.59	0.3614	0.0039	0.04963	0.00066	0.443	313.2	2.9	312.2	4.1	316	28	312.2	4.1	0.32	
13Guaso_9	241	1.20	0.3598	0.0058	0.04982	0.00066	0.254	311.9	4.3	313.4	4.1	314	40	313.4	4.1	0.48	
13Guaso_10	301	1.65	0.3562	0.0054	0.04898	0.00058	0.354	309.2	4	308.2	3.5	295	39	308.2	3.5	0.32	
13Guaso_11	362	1.50	0.3848	0.0068	0.05171	0.00073	0.205	330.4	5	325	4.5	361	42	325.0	4.5	1.63	
13Guaso_12	434	0.48	0.6780	0.0130	0.08070	0.00160	0.772	524.9	7.9	500	9.6	634	30	500.0	9.6	4.74	
13Guaso_13	328	1.33	0.3471	0.0056	0.04855	0.00065	0.271	302.3	4.2	305.6	4	283	44	305.6	4.0	1.09	
13Guaso_14	264.1	1.35	0.5330	0.0100	0.06891	0.00096	0.534	435.6	6.9	429.6	5.8	452	36	429.6	5.8	1.38	
13Guaso_15	817	11.38	0.3518	0.0059	0.04904	0.00065	0.264	306	4.4	308.6	4	300	41	308.6	4.0	0.85	Rim
13Guaso_15	124	1.27	0.6330	0.0120	0.08100	0.00200	0.184	498.1	7.4	502	12	463	63	502.0	12.0	0.78	Core
13Guaso_16	89.7	0.90	0.8750	0.0200	0.10110	0.00190	0.324	638	11	621	11	688	50	621.0	11.0	2.66	
13Guaso_17	143.5	1.24	0.3509	0.0087	0.04704	0.00061	0.149	305.1	6.6	296.3	3.8	372	58	296.3	3.8	2.88	
13Guaso_18	191	3.58	0.6400	0.0120	0.07900	0.00160	0.456	501.9	7.6	489.9	9.6	547	51	489.9	9.6	2.39	
13Guaso_19	385	1.83	0.3598	0.0061	0.04951	0.00054	0.498	311.8	4.5	311.5	3.3	312	35	311.5	3.3	0.10	
13Guaso_20	317	1.19	0.3542	0.0067	0.04852	0.00065	0.365	307.7	5.1	305.4	4	336	39	305.4	4.0	0.75	
13Guaso_21	619	1.58	0.3660	0.0056	0.04945	0.00071	0.243	317.2	4.3	311.1	4.3	353	39	311.1	4.3	1.92	
13Guaso_22	783	17.50	0.3559	0.0055	0.04888	0.00090	0.637	309.1	4.2	307.6	5.5	315	36	307.6	5.5	0.49	

Sample Name _Grain #	[U] ppm	U/Th	207/235	2σ error	206/238	2σ error	RHO	207/235 Age (Ma)	2σ error	206/238 Age (Ma)	2σ error	207/206 Age (Ma)	2σ error	Best age (Ma)	2σ error	% Discordance	Rim /Core
13Guaso_23	744	12.53	0.3451	0.0056	0.04869	0.00077	0.254	301.9	4.5	306.4	4.7	271	47	306.4	4.7	1.49	
13Guaso_24	868	11.11	0.3500	0.0110	0.04827	0.00096	0.747	304.8	8.4	303.9	5.9	313	62	303.9	5.9	0.30	Rim
13Guaso_24	120	0.94	0.6440	0.0160	0.07990	0.00220	0.469	504.3	9.6	496	13	527	60	496.0	13.0	1.65	Core
13Guaso_25	757	8.02	0.3605	0.0042	0.04965	0.00062	0.344	312.5	3.1	312.4	3.8	302	30	312.4	3.8	0.03	Rim
13Guaso_25	261	0.70	0.6680	0.0190	0.08360	0.00240	0.579	519	11	518	14	535	60	518.0	14.0	0.19	Core
13Guaso_26	282	3.71	0.3911	0.0093	0.05320	0.00100	0.458	336.1	6.5	334.1	6.4	360	48	334.1	6.4	0.60	
13Guaso_27	314	1.46	0.3630	0.0057	0.05008	0.00063	0.452	314.4	4.3	315	3.9	307	40	315.0	3.9	0.19	
13Guaso_28	575	9.70	0.3710	0.0130	0.05170	0.00200	0.526	320.2	9.4	325	12	282	85	325.0	12.0	1.50	Rim
13Guaso_28	182.9	0.91	0.6930	0.0140	0.08740	0.00130	0.428	534	8.1	540.3	7.5	478	36	540.3	7.5	1.18	Core
13Guaso_29	614	2.02	0.7972	0.0095	0.08980	0.00120	0.490	596.3	5.7	554.2	7.3	765	36	554.2	7.3	7.06	
13Guaso_30	293	1.04	1.6860	0.0220	0.16780	0.00240	0.703	1002.6	8.2	1000	13	1003	22	1003.0	22.0	0.30	
13Guaso_31	1130	14.19	0.3521	0.0078	0.04920	0.00120	0.695	306.2	5.9	309.6	7.3	299	39	309.6	7.3	1.11	Rim
13Guaso_31	109.9	1.01	0.6910	0.0170	0.08550	0.00150	0.347	535	11	528.8	9.1	551	61	528.8	9.1	1.16	Core
13Guaso_32	135.9	1.03	0.6890	0.0130	0.08710	0.00140	0.503	532.9	7.4	538.1	8.2	519	36	538.1	8.2	0.98	
13Guaso_33	504	2.18	0.3639	0.0054	0.04955	0.00071	0.259	315	4	311.7	4.4	325	39	311.7	4.4	1.05	
13Guaso_34	938	13.12	0.3900	0.0150	0.05260	0.00210	0.715	334	11	331	13	393	68	331.0	13.0	0.90	
13Guaso_35	7.6	0.45	1.8570	0.0730	0.17310	0.00590	0.163	1070	26	1028	32	1131	95	1131.0	95.0	9.11	
13Guaso_36	434	3.02	1.0870	0.0240	0.12210	0.00250	0.774	746	12	743	15	742	33	743.0	15.0	0.40	
13Guaso_37	358	0.49	0.7570	0.0140	0.09280	0.00200	0.784	571.7	8.4	572	12	557	32	572.0	12.0	0.05	
13Guaso_38	81.4	1.59	1.8920	0.0300	0.17890	0.00240	0.392	1077	11	1061	13	1112	32	1112.0	32.0	4.59	
13Guaso_39	506	1.02	0.3539	0.0053	0.04891	0.00069	0.602	307.5	4	308.4	4.4	297	30	308.4	4.4	0.29	
13Guaso_40	69.6	0.98	0.6860	0.0160	0.08450	0.00150	0.407	529.7	9.6	522.7	8.8	545	50	522.7	8.8	1.32	
13Guaso_42	155.1	1.54	0.3527	0.0076	0.04819	0.00077	0.312	306.4	5.7	303.4	4.7	309	51	303.4	4.7	0.98	
13Guaso_43	383	1.35	0.3814	0.0062	0.05086	0.00059	0.011	327.8	4.6	319.8	3.6	405	47	319.8	3.6	2.44	

Sample Name _Grain #	[U] ppm	U/Th	207/235	2σ error	206/238	2σ error	RHO	207/235 Age (Ma)	2σ error	206/238 Age (Ma)	2σ error	207/206 Age (Ma)	2σ error	Best age (Ma)	2σ error	% Discordance	Rim /Core
13Guaso_44	356.5	2.16	0.3605	0.0071	0.04943	0.00088	0.311	312.3	5.3	311	5.4	331	52	311.0	5.4	0.42	
13Guaso_45	147	1.40	0.3513	0.0078	0.04862	0.00085	0.292	306.2	5.7	306	5.2	284	55	306.0	5.2	0.07	
13Guaso_46	321.4	1.33	0.3654	0.0080	0.04891	0.00064	0.281	316	6	307.8	3.9	365	51	307.8	3.9	2.59	
13Guaso_47	648	1.88	0.3925	0.0093	0.05250	0.00150	0.572	336	6.8	329.8	9.5	359	59	329.8	9.5	1.85	
13Guaso_48	1080	2.08	0.3699	0.0034	0.05050	0.00049	0.509	319.5	2.5	317.6	3	334	21	317.6	3.0	0.59	
13Guaso_49	247	1.93	0.3621	0.0057	0.05008	0.00052	0.323	313.6	4.3	315	3.2	306	40	315.0	3.2	0.45	
13Guaso_50	533	2.02	0.3692	0.0045	0.05037	0.00066	0.421	319	3.3	316.7	4	325	30	316.7	4.0	0.72	
13Guaso_51	228.7	1.11	0.6772	0.0085	0.08362	0.00093	0.396	525.5	5.2	517.7	5.5	567	29	517.7	5.5	1.48	
13Guaso_52	678	2.42	0.3724	0.0048	0.05095	0.00045	0.383	321.3	3.5	320.4	2.8	312	26	320.4	2.8	0.28	
13Guaso_53	794	12.70	0.3533	0.0087	0.05040	0.00100	0.578	307.1	6.5	316.7	6.2	208	56	316.7	6.2	3.13	Rim
13Guaso_53	103.8	1.35	0.6980	0.0120	0.08830	0.00120	0.175	537.3	7	545.4	7.1	513	44	545.4	7.1	1.51	Core
13Guaso_54	242	0.53	1.7180	0.0250	0.17210	0.00220	0.623	1014.7	9.2	1023	12	1000	24	1000.0	24.0	2.30	
13Guaso_55	75.4	1.63	0.6200	0.0120	0.07830	0.00130	0.115	490.1	7.5	485.6	7.7	489	56	485.6	7.7	0.92	
13Guaso_56	268	5.71	0.6250	0.0120	0.08060	0.00150	0.560	492.6	7.3	499.5	8.8	454	38	499.5	8.8	1.40	
13Guaso_57	70.5	1.10	12.3800	0.1700	0.50170	0.00730	0.709	2632	13	2620	31	2649	17	2649.0	17.0	1.09	
13Guaso_58	234	1.03	0.3550	0.0059	0.04856	0.00061	0.376	308.3	4.4	305.7	3.7	309	40	305.7	3.7	0.84	
13Guaso_59	468	1.55	0.3567	0.0044	0.04924	0.00061	0.440	310.1	3.4	309.8	3.7	309	32	309.8	3.7	0.10	
13Guaso_60	278	1.37	0.3713	0.0067	0.05119	0.00075	0.358	320.4	4.9	321.8	4.6	317	40	321.8	4.6	0.44	
13Guaso_61	318	1.77	0.3719	0.0071	0.05037	0.00084	0.421	320.8	5.2	316.8	5.1	334	41	316.8	5.1	1.25	
13Guaso_62	1216	13.34	0.3573	0.0087	0.04880	0.00100	0.570	310.1	6.5	306.9	6.4	331	49	306.9	6.4	1.03	Rim
13Guaso_62	231.7	0.92	0.6920	0.0120	0.08790	0.00150	0.141	535.1	6.8	543.1	9	515	51	543.1	9.0	1.50	Core
13Guaso_63	161.8	0.94	0.6790	0.0130	0.08570	0.00130	0.059	525.7	7.8	529.7	7.8	531	56	529.7	7.8	0.76	
13Guaso_64	703	8.90	0.3543	0.0080	0.04936	0.00088	0.774	307.8	6	310.5	5.4	293	34	310.5	5.4	0.88	
13Guaso_65	1110	1.88	0.3702	0.0046	0.05048	0.00052	0.451	319.7	3.4	317.5	3.2	346	28	317.5	3.2	0.69	
13Guaso_67	261.1	0.87	0.7130	0.0130	0.09000	0.00130	0.259	546.3	7.7	555.4	7.4	519	40	555.4	7.4	1.67	

Sample Name _Grain #	[U] ppm	U/Th	207/235	2σ error	206/238	2σ error	RHO	207/235 Age (Ma)	2σ error	206/238 Age (Ma)	2σ error	207/206 Age (Ma)	2σ error	Best age (Ma)	2σ error	% Discordance	Rim /Core
13Guaso_68	466	1.14	0.3650	0.0056	0.05029	0.00076	0.464	315.7	4.2	316.3	4.7	301	34	316.3	4.7	0.19	
13Guaso_71	215	1.91	0.3710	0.0081	0.05122	0.00089	0.346	320	6	321.9	5.4	289	52	321.9	5.4	0.59	
13Guaso_72	778	11.43	0.3544	0.0059	0.04953	0.00083	0.807	308	4.4	311.6	5.1	292	36	311.6	5.1	1.17	Rim
13Guaso_72	52.6	1.05	0.6630	0.0180	0.08210	0.00190	0.119	516	11	509	12	549	82	509.0	12.0	1.36	Core
13Guaso_73	810	12.77	0.3640	0.0140	0.05000	0.00100	0.543	315	10	314.4	6.1	298	75	314.4	6.1	0.19	Rim
13Guaso_73	54.9	1.36	0.6910	0.0220	0.08800	0.00220	0.117	532	13	543	13	449	81	543.0	13.0	2.07	Core
13Guaso_74	725	13.61	0.3611	0.0055	0.05002	0.00066	0.457	312.9	4.1	314.6	4	301	37	314.6	4.0	0.54	Rim
13Guaso_74	50.5	1.03	0.6870	0.0540	0.08980	0.00380	0.621	529	33	554	22	490	140	554.0	22.0	4.73	Core
13Guaso_76	612	1.03	0.3659	0.0044	0.05067	0.00063	0.523	316.5	3.3	318.6	3.9	293	30	318.6	3.9	0.66	
13Guaso_77	186	1.22	0.3690	0.0110	0.04964	0.00095	0.103	318.6	8.2	312.3	5.8	312	77	312.3	5.8	1.98	
13Guaso_78	653	14.86	0.3673	0.0068	0.04850	0.00071	0.388	317.5	5	305.3	4.3	414	36	305.3	4.3	3.84	
13Guaso_79	256	1.08	0.6877	0.0096	0.08670	0.00130	0.455	531.2	5.8	536.2	7.6	497	34	536.2	7.6	0.94	
13Guaso_80	756	2.19	0.3871	0.0053	0.05261	0.00070	0.426	332.1	3.9	330.5	4.3	353	32	330.5	4.3	0.48	
13Guaso_81	185	7.02	0.5779	0.0091	0.07395	0.00088	0.517	464.2	5.9	459.9	5.3	494	33	459.9	5.3	0.93	
13Guaso_82	515.6	1.50	0.3666	0.0058	0.05060	0.00074	0.545	317.5	4.4	318.2	4.5	287	33	318.2	4.5	0.22	
13Guaso_83	409	1.61	0.4097	0.0088	0.05080	0.00110	0.483	348.4	6.3	319.1	6.6	554	48	319.1	6.6	8.41	
13Guaso_84	207	0.91	0.3704	0.0072	0.05183	0.00079	0.242	320.4	5.2	325.7	4.9	286	47	325.7	4.9	1.65	
13Guaso_85	1116	12.28	0.3633	0.0085	0.05110	0.00130	0.605	314.5	6.3	321	8	263	52	321.0	8.0	2.07	Rim
13Guaso_85	226	0.96	0.6980	0.0160	0.08780	0.00180	0.363	537	9.3	542	11	522	52	542.0	11.0	0.93	Core
13Guaso_86	1013	14.53	0.3694	0.0096	0.05118	0.00074	0.186	319.1	7.1	321.8	4.5	291	52	321.8	4.5	0.85	Rim
13Guaso_86	88.1	0.93	0.6920	0.0120	0.08760	0.00130	0.096	533.9	7.3	541.2	7.7	533	52	541.2	7.7	1.37	Core
13Guaso_87	625	1.28	0.3556	0.0044	0.04905	0.00059	0.634	308.8	3.3	308.7	3.7	308	27	308.7	3.7	0.03	
13Guaso_88	302	1.94	0.3872	0.0092	0.05198	0.00099	0.483	332	6.8	327.6	6.3	343	53	327.6	6.3	1.33	
13Guaso_89	505	8.29	0.3782	0.0064	0.05143	0.00084	0.488	325.5	4.8	323.3	5.1	357	36	323.3	5.1	0.68	
13Guaso_90	343	1.71	0.3750	0.0060	0.05295	0.00065	0.441	323.2	4.5	332.6	4	266	37	332.6	4.0	2.91	

Sample Name _Grain #	[U] ppm	U/Th	207/235	2σ error	206/238	2σ error	RHO	207/235 Age (Ma)	2σ error	206/238 Age (Ma)	2σ error	207/206 Age (Ma)	2σ error	Best age (Ma)	2σ error	% Discordance	Rim /Core
13Guaso_91	350	1.25	0.3620	0.0092	0.05020	0.00120	0.606	313.4	6.9	315.8	7.4	287	47	315.8	7.4	0.77	
13Guaso_92	362	1.32	0.3737	0.0075	0.05137	0.00076	0.475	322.1	5.5	322.9	4.7	333	41	322.9	4.7	0.25	
13Guaso_93	1151	12.22	0.3526	0.0096	0.04910	0.00130	0.757	308.1	6.8	308.7	7.7	299	39	308.7	7.7	0.19	Rim
13Guaso_93	215	1.04	0.6690	0.0140	0.08510	0.00170	0.452	519.5	8.8	526	10	503	44	526.0	10.0	1.25	Core
13Guaso_94	183.6	0.99	0.6920	0.0130	0.08650	0.00120	0.266	534.8	7.7	534.6	6.9	545	42	534.6	6.9	0.04	
13Guaso_95	523	1.99	0.3631	0.0095	0.05040	0.00140	0.647	314.8	7	316.8	8.4	293	47	316.8	8.4	0.64	
13Guaso_96	43	1.01	0.6800	0.0220	0.08590	0.00180	0.002	526	13	531	11	504	82	531.0	11.0	0.95	
13Guaso_97	409	1.53	0.3551	0.0071	0.04895	0.00086	0.456	308.3	5.3	308	5.3	287	46	308.0	5.3	0.10	
13Guaso_98	371	1.26	0.3628	0.0059	0.05001	0.00064	0.005	314.2	4.4	314.6	3.9	306	45	314.6	3.9	0.13	
13Guaso_99	778	10.76	0.3632	0.0065	0.05010	0.00082	0.524	314.4	4.9	315.1	5	326	35	315.1	5.0	0.22	
13Guaso_100	231.8	1.22	0.6500	0.0130	0.08270	0.00180	0.645	509.2	7.8	512	11	496	41	512.0	11.0	0.55	
13Guaso_101	655	1.49	0.3782	0.0055	0.05253	0.00093	0.524	325.5	4.1	330	5.7	305	34	330.0	5.7	1.38	
13Guaso_103	419	1.58	0.3872	0.0071	0.05193	0.00080	0.408	332.1	5.2	326.4	4.9	355	43	326.4	4.9	1.72	
13Guaso_104	192.3	1.50	0.5620	0.0150	0.07210	0.00170	0.419	452.8	9.5	449	10	451	67	449.0	10.0	0.84	
13Guaso_105	385	1.22	0.3775	0.0046	0.05107	0.00052	0.255	325.1	3.4	321.1	3.2	357	29	321.1	3.2	1.23	
13Guaso_106	652	1.71	0.3708	0.0065	0.05113	0.00089	0.693	320.1	4.8	321.4	5.5	305	32	321.4	5.5	0.41	
13Guaso_107	318.5	1.51	3.9280	0.0970	0.28290	0.00980	0.678	1618	20	1602	49	1634	42	1634.0	42.0	1.96	
13Guaso_108	591	1.22	0.3567	0.0051	0.04970	0.00071	0.594	310.1	3.8	312.7	4.3	301	28	312.7	4.3	0.84	
13Guaso_109	376	2.04	0.3990	0.0069	0.05373	0.00076	0.469	342	4.8	337.3	4.7	344	36	337.3	4.7	1.37	
13Guaso_110	448	1.41	0.3764	0.0049	0.05201	0.00057	0.264	324.3	3.6	326.8	3.5	298	36	326.8	3.5	0.77	
13Guaso_111	746	1.49	0.3701	0.0047	0.05050	0.00083	0.450	319.6	3.5	317.6	5.1	316	38	317.6	5.1	0.63	
13Guaso_112	1137	1.00	0.3651	0.0052	0.05032	0.00073	0.703	316.4	3.9	317.1	4.6	312	26	317.1	4.6	0.22	
13Guaso_113	384	1.49	0.3788	0.0061	0.05270	0.00072	0.407	326.5	4.4	331	4.4	315	34	331.0	4.4	1.38	
13Guaso_114	943	12.05	0.3613	0.0070	0.04960	0.00110	0.328	313.1	5.2	311.9	7	333	58	311.9	7.0	0.38	Rim
13Guaso_114	252.6	0.86	0.6890	0.0120	0.08730	0.00130	0.507	532	7	540.8	8.2	496	36	540.8	8.2	1.65	Core

Sample Name _Grain #	[U] ppm	U/Th	207/235	2σ error	206/238	2σ error	RHO	207/235 Age (Ma)	2σ error	206/238 Age (Ma)	2σ error	207/206 Age (Ma)	2σ error	Best age (Ma)	2σ error	% Discordance	Rim /Core
13Guaso_115	69.1	1.02	0.6840	0.0150	0.08420	0.00130	0.247	528.6	8.9	521	7.8	534	48	521.0	7.8	1.44	
13Guaso_116	428	1.93	0.3641	0.0047	0.05065	0.00047	0.292	315.2	3.5	318.5	2.9	287	30	318.5	2.9	1.05	
13Guaso_117	284	1.61	0.3740	0.0100	0.05090	0.00110	0.562	322.3	7.6	320.1	6.5	359	55	320.1	6.5	0.68	
13Guaso_118	164	1.39	0.3660	0.0093	0.05020	0.00082	0.378	316.3	6.9	315.7	5	314	49	315.7	5.0	0.19	
13Guaso_119	474	1.19	0.3763	0.0054	0.05131	0.00070	0.348	324.7	4.1	322.6	4.3	339	39	322.6	4.3	0.65	
13Guaso_120	456	7.40	0.6024	0.0072	0.07692	0.00097	0.425	479.1	4.4	477.6	5.8	462	30	477.6	5.8	0.31	
7_Guaso_1	493	1.79	0.3632	0.0055	0.05028	0.00067	0.485	314.9	4	316.2	4.1	318	30	316.2	4.1	0.41	
7_Guaso_2	213.9	1.36	0.3521	0.0063	0.04906	0.00051	0.256	306.1	4.7	308.7	3.2	278	38	308.7	3.2	0.85	
7_Guaso_3	142.4	2.20	0.6341	0.0091	0.08110	0.00120	0.354	499.1	5.8	502.5	6.9	493	36	502.5	6.9	0.68	
7_Guaso_4	55.8	2.35	2.0720	0.0270	0.19420	0.00270	0.422	1138.7	8.8	1144	15	1117	31	1117.0	31.0	2.42	
7_Guaso_5	124.6	0.64	6.3750	0.0640	0.35910	0.00520	0.690	2028.2	8.8	1980	24	2070	18	2070.0	18.0	4.35	
7_Guaso_6	415	0.99	0.0444	0.0014	0.00702	0.00014	0.426	44.1	1.4	45.11	0.87	72	56	45.1	0.9	2.29	
7_Guaso_7	431	1.96	0.8980	0.0190	0.10530	0.00190	0.616	653	10	645	11	665	39	645.0	11.0	1.23	
7_Guaso_8	45.8	1.16	0.9370	0.0220	0.10760	0.00160	0.115	670	11	658.5	9.2	699	59	658.5	9.2	1.72	
7_Guaso_10	416	1.11	4.5880	0.0620	0.28810	0.00370	0.851	1746	11	1632	19	1882	17	1882.0	17.0	13.28	
7_Guaso_11	1050	7.20	0.3873	0.0050	0.05241	0.00065	0.488	332.3	3.6	329.9	4.1	340	29	329.9	4.1	0.72	
7_Guaso_12	429.3	20.20	3.4400	0.0410	0.25090	0.00290	0.667	1512.9	9.4	1443	15	1617	16	1617.0	16.0	10.76	
7_Guaso_13	491	1.33	0.3568	0.0048	0.04853	0.00053	0.473	309.7	3.6	305.5	3.2	336	27	305.5	3.2	1.36	
7_Guaso_14	42.67	0.30	1.5590	0.0390	0.15580	0.00260	0.081	953	15	933	14	996	57	996.0	57.0	6.33	
7_Guaso_15	397	1.80	0.3589	0.0062	0.04928	0.00074	0.648	311.2	4.7	310.1	4.5	304	33	310.1	4.5	0.35	
7_Guaso_16	105.1	1.09	4.4050	0.0510	0.30240	0.00330	0.718	1713.8	9.4	1703	17	1722	15	1722.0	15.0	1.10	
7_Guaso_17	180.2	1.04	0.8860	0.0180	0.10340	0.00130	0.316	645.6	9	634.2	7.6	687	46	634.2	7.6	1.77	
7_Guaso_18	420	2.42	0.3586	0.0058	0.04890	0.00078	0.610	311.1	4.3	307.8	4.8	338	35	307.8	4.8	1.06	
7_Guaso_19	99	2.07	1.5650	0.0220	0.15910	0.00210	0.443	955.6	8.6	951	12	977	32	977.0	32.0	2.66	
7_Guaso_20	7.72	1.07	1.5950	0.0650	0.15930	0.00540	0.322	971	27	952	30	1015	99	1015.0	99.0	6.21	

Sample Name _Grain #	[U] ppm	U/Th	207/235	2σ error	206/238	2σ error	RHO	207/235 Age (Ma)	2σ error	206/238 Age (Ma)	2σ error	207/206 Age (Ma)	2σ error	Best age (Ma)	2σ error	% Discordance	Rim /Core
7_Guaso_21	77.3	1.02	1.6810	0.0340	0.16120	0.00210	0.369	1000	13	963	12	1087	37	1087.0	37.0	11.41	
7_Guaso_22	339	0.94	0.1826	0.0033	0.02689	0.00033	0.033	170.2	2.9	171.1	2.1	171	45	171.1	2.1	0.53	
7_Guaso_23	543	1.26	1.3060	0.0370	0.13590	0.00570	0.722	848	16	821	32	932	54	821.0	32.0	3.18	
7_Guaso_24	465	2.38	5.7360	0.0730	0.32550	0.00480	0.888	1936	11	1816	23	2073	12	2073.0	12.0	12.40	
7_Guaso_25	157.8	0.95	0.8700	0.0200	0.10300	0.00160	0.677	632.9	9.9	631.7	9.6	664	31	631.7	9.6	0.19	
7_Guaso_26	96.3	0.93	3.9400	0.1200	0.25210	0.00670	0.923	1619	25	1449	34	1850	36	1850.0	36.0	21.68	
7_Guaso_27	83	0.67	0.0855	0.0067	0.01219	0.00048	0.059	83.1	6.2	78.1	3.1	250	170	78.1	3.1	6.02	
7_Guaso_28	448	6.50	0.6310	0.0110	0.08120	0.00180	0.633	496.5	7	503	11	482	39	503.0	11.0	1.31	Rim
7_Guaso_28	85.7	1.15	0.7910	0.0260	0.09840	0.00240	0.255	591	15	605	14	553	78	605.0	14.0	2.37	Core
7_Guaso_29	265	1.38	4.0800	0.0610	0.27200	0.00340	0.735	1650	12	1551	17	1792	15	1792.0	15.0	13.45	
7_Guaso_30	352	7.80	1.8860	0.0260	0.18070	0.00210	0.546	1075.7	9	1071	12	1096	21	1096.0	21.0	2.28	
7_Guaso_31	482	1.76	0.3593	0.0045	0.04896	0.00058	0.405	311.6	3.3	308.1	3.6	355	29	308.1	3.6	1.12	
7_Guaso_33	92.9	0.94	0.5510	0.0130	0.07150	0.00120	0.351	446.3	8.6	445.2	7.5	437	49	445.2	7.5	0.25	
7_Guaso_34	220	1.64	0.3655	0.0074	0.04958	0.00077	0.555	316.2	5.5	311.9	4.7	365	39	311.9	4.7	1.36	
7_Guaso_35	271.9	1.84	0.7268	0.0081	0.08947	0.00077	0.428	554.5	4.8	552.4	4.6	572	24	552.4	4.6	0.38	
7_Guaso_36	23.95	1.11	1.7380	0.0390	0.17390	0.00320	0.302	1023	15	1033	18	1020	45	1020.0	45.0	1.27	
7_Guaso_37	340.9	1.35	0.3590	0.0100	0.04883	0.00074	0.166	311.1	7.5	307.3	4.6	301	67	307.3	4.6	1.22	
7_Guaso_38	288	11.50	0.5679	0.0084	0.07410	0.00088	0.372	456.4	5.5	461.5	5.4	424	32	461.5	5.4	1.12	
7_Guaso_39	106.4	1.60	2.1530	0.0290	0.19610	0.00320	0.557	1165.5	9.1	1154	17	1191	31	1191.0	31.0	3.11	
7_Guaso_40	187	0.50	0.5630	0.0088	0.07276	0.00076	0.216	453.1	5.7	452.8	4.6	457	34	452.8	4.6	0.07	
7_Guaso_41	55.8	0.76	5.0660	0.0650	0.32130	0.00450	0.661	1831	11	1795	22	1868	20	1868.0	20.0	3.91	
7_Guaso_42	558	1.70	0.3644	0.0045	0.05122	0.00053	0.362	315.4	3.4	322	3.2	270	29	322.0	3.2	2.09	
7_Guaso_43	235	1.38	0.3599	0.0076	0.04893	0.00050	0.347	311.8	5.6	307.9	3.1	318	44	307.9	3.1	1.25	
7_Guaso_44	128.7	1.06	3.1700	0.0360	0.25330	0.00280	0.623	1449.1	8.7	1457	14	1430	16	1430.0	16.0	1.89	
7_Guaso_45	334	1.45	0.3683	0.0052	0.05066	0.00058	0.280	318.3	3.9	318.5	3.5	308	30	318.5	3.5	0.06	

Sample Name _Grain #	[U] ppm	U/Th	207/235	2σ error	206/238	2σ error	RHO	207/235 Age (Ma)	2σ error	206/238 Age (Ma)	2σ error	207/206 Age (Ma)	2σ error	Best age (Ma)	2σ error	% Discordance	Rim /Core
7_Guaso_46	37.3	0.80	0.8900	0.0230	0.10420	0.00180	0.065	648	12	639	10	642	72	639.0	10.0	1.39	
7_Guaso_47	359	1.39	0.3601	0.0064	0.04901	0.00063	0.535	312.1	4.8	308.4	3.9	335	37	308.4	3.9	1.19	
7_Guaso_48	86.2	2.10	1.0930	0.0270	0.12130	0.00300	0.587	749	13	738	17	791	44	738.0	17.0	1.47	
7_Guaso_49	878	24.20	0.8660	0.0130	0.10150	0.00150	0.785	632.9	7.1	624.2	8.4	663	20	624.2	8.4	1.37	
7_Guaso_50	520	1.62	0.3678	0.0071	0.04946	0.00085	0.654	317.8	5.3	311.1	5.2	333	34	311.1	5.2	2.11	
7_Guaso_51	163	1.41	0.3674	0.0070	0.04979	0.00063	0.279	317.5	5.2	313.2	3.9	303	45	313.2	3.9	1.35	
7_Guaso_52	186	1.56	3.3410	0.0330	0.25870	0.00250	0.545	1490.3	7.7	1483	13	1498	19	1498.0	19.0	1.00	
7_Guaso_53	58.3	1.14	0.8850	0.0230	0.10310	0.00220	0.317	643	12	632	13	634	62	632.0	13.0	1.71	
7_Guaso_54	32.5	0.59	1.8960	0.0410	0.17970	0.00260	0.313	1081	15	1065	14	1084	42	1084.0	42.0	1.75	
7_Guaso_55	46.81	1.27	1.6970	0.0450	0.16630	0.00270	0.417	1008	17	992	15	1038	51	1038.0	51.0	4.43	
7_Guaso_56	586	1.74	0.3575	0.0067	0.04756	0.00062	0.564	310.1	5	299.5	3.8	398	35	299.5	3.8	3.42	
7_Guaso_57	495	1.53	0.3533	0.0046	0.04883	0.00069	0.489	307.1	3.4	307.3	4.2	307	27	307.3	4.2	0.07	
7_Guaso_58	134.3	0.98	1.9260	0.0190	0.18440	0.00180	0.424	1089.8	6.5	1092.4	9.5	1070	21	1070.0	21.0	2.09	
7_Guaso_59	101.4	0.91	1.3990	0.0320	0.14000	0.00260	0.491	888	14	844	14	997	47	844.0	14.0	4.95	
7_Guaso_60	267	1.75	0.7750	0.0200	0.09320	0.00240	0.692	582	12	575	14	583	34	575.0	14.0	1.20	
7_Guaso_61	267	2.04	0.8865	0.0090	0.10520	0.00120	0.332	644.9	4.7	644.6	6.8	648	28	644.6	6.8	0.05	
7_Guaso_62	408	1.38	0.3578	0.0045	0.04982	0.00056	0.358	310.5	3.4	313.4	3.5	282	34	313.4	3.5	0.93	
7_Guaso_63	371	8.17	0.5734	0.0066	0.07402	0.00081	0.630	460	4.3	460.3	4.8	454	23	460.3	4.8	0.07	
7_Guaso_64	484	1.77	0.3790	0.0066	0.05154	0.00081	0.707	326.7	4.8	323.9	4.9	332	28	323.9	4.9	0.86	
7_Guaso_65	128	1.92	0.7690	0.0220	0.09280	0.00170	0.616	578	13	572	10	618	47	572.0	10.0	1.04	
7_Guaso_66	525	1.41	0.3626	0.0045	0.04975	0.00049	0.347	314.1	3.3	313	3	328	27	313.0	3.0	0.35	
7_Guaso_68	84.4	0.83	5.8690	0.0670	0.35180	0.00420	0.680	1959	10	1943	20	1962	17	1962.0	17.0	0.97	
7_Guaso_69	316	1.46	0.5234	0.0072	0.06776	0.00084	0.212	427.3	4.8	422.6	5	450	38	422.6	5.0	1.10	
7_Guaso_70	506	6.04	0.8520	0.0150	0.09400	0.00140	0.478	625.3	8.4	579	8.3	794	35	579.0	8.3	7.40	
7_Guaso_71	238	1.45	0.3587	0.0083	0.04968	0.00075	0.454	310.8	6.2	312.5	4.6	276	48	312.5	4.6	0.55	

Sample Name _Grain #	[U] ppm	U/Th	207/235	2σ error	206/238	2σ error	RHO	207/235 Age (Ma)	2σ error	206/238 Age (Ma)	2σ error	207/206 Age (Ma)	2σ error	Best age (Ma)	2σ error	% Discordance	Rim /Core
7_Guaso_72	98.2	0.42	0.8340	0.0150	0.10046	0.00090	0.371	615.1	8.3	617.1	5.3	602	37	617.1	5.3	0.33	
7_Guaso_73	75.9	1.17	1.0630	0.0160	0.12210	0.00140	0.168	736.8	7.9	742.6	8	734	40	742.6	8.0	0.79	
7_Guaso_74	275.4	1.37	0.3610	0.0056	0.04904	0.00055	0.018	312.9	4.2	308.6	3.4	342	46	308.6	3.4	1.37	
7_Guaso_75	481	1.46	0.3628	0.0053	0.05010	0.00048	0.469	314.1	4	315.1	2.9	303	28	315.1	2.9	0.32	
7_Guaso_76	395	1.83	0.3516	0.0060	0.04901	0.00055	0.332	305.8	4.5	308.4	3.4	288	37	308.4	3.4	0.85	
7_Guaso_77	465	1.42	0.3565	0.0054	0.04865	0.00043	0.134	309.4	4	306.2	2.6	324	38	306.2	2.6	1.03	
7_Guaso_78	417	2.23	0.3484	0.0052	0.04788	0.00072	0.702	303.4	3.9	301.5	4.4	328	28	301.5	4.4	0.63	
7_Guaso_79	414	1.90	0.3798	0.0049	0.05218	0.00039	0.120	326.8	3.6	327.9	2.4	324	30	327.9	2.4	0.34	
7_Guaso_80	818	52.10	0.4041	0.0071	0.05495	0.00090	0.715	344.5	5.1	345.9	5.8	338	32	345.9	5.8	0.41	
7_Guaso_81	980	3.37	0.7990	0.0330	0.09590	0.00340	0.740	596	18	590	20	672	61	590.0	20.0	1.01	Rim
7_Guaso_81	43.9	0.61	1.5490	0.0340	0.15900	0.00240	0.349	949	13	953	14	958	50	958.0	50.0	0.52	Core
7_Guaso_82	162	1.72	0.3622	0.0065	0.04945	0.00078	0.285	314.3	5	311.1	4.8	339	46	311.1	4.8	1.02	
7_Guaso_83	585	1.93	0.3572	0.0060	0.04953	0.00057	0.329	310	4.5	311.6	3.5	319	41	311.6	3.5	0.52	
7_Guaso_84	166.9	1.16	0.0805	0.0039	0.01193	0.00032	0.152	79	3.6	76.4	2	169	99	76.4	2.0	3.29	
7_Guaso_85	651	1.36	0.4584	0.0073	0.06179	0.00088	0.578	383	5.1	386.5	5.4	352	29	386.5	5.4	0.91	
7_Guaso_86	80.5	0.38	0.8010	0.0220	0.09610	0.00170	0.466	597	12	591.4	9.8	649	52	591.4	9.8	0.94	
7_Guaso_87	234	1.46	0.3625	0.0074	0.05054	0.00075	0.431	313.8	5.5	318.4	4.7	286	44	318.4	4.7	1.47	
7_Guaso_88	644	1.78	0.3785	0.0070	0.05115	0.00064	0.305	325.8	5.2	321.6	3.9	369	46	321.6	3.9	1.29	
7_Guaso_89	138	0.60	0.9320	0.0320	0.09670	0.00150	0.584	667	17	594.8	8.6	930	56	DISC	DISC	10.82	
7_Guaso_90	656	1.53	0.6007	0.0059	0.07592	0.00077	0.606	478	3.6	471.7	4.6	511	19	471.7	4.6	1.32	
7_Guaso_91	120	0.68	5.3700	0.0590	0.33880	0.00440	0.697	1881.3	9.8	1881	21	1890	19	1890.0	19.0	0.48	
7_Guaso_92	31.28	1.56	0.8530	0.0310	0.09980	0.00210	0.085	624	17	613	13	689	90	613.0	13.0	1.76	
7_Guaso_93	82.7	0.60	1.1790	0.0190	0.13030	0.00210	0.431	789.9	8.9	790	12	818	35	790.0	12.0	0.01	
7_Guaso_94	264.5	1.27	0.3553	0.0067	0.04871	0.00065	0.251	308.5	5	306.6	4	302	45	306.6	4.0	0.62	
7_Guaso_95	121.6	2.04	0.6120	0.0160	0.07710	0.00130	0.334	484.1	9.9	478.4	8	518	56	478.4	8.0	1.18	

Sample Name _Grain #	[U] ppm	U/Th	207/235	2σ error	206/238	2σ error	RHO	207/235 Age (Ma)	2σ error	206/238 Age (Ma)	2σ error	207/206 Age (Ma)	2σ error	Best age (Ma)	2σ error	% Discordance	Rim /Core
7_Guaso_96	474	1.54	0.3335	0.0060	0.04582	0.00072	0.329	292.1	4.6	288.8	4.4	318	47	288.8	4.4	1.13	
7_Guaso_97	977	3.78	0.0614	0.0013	0.00930	0.00014	0.376	60.5	1.2	59.69	0.92	74	46	59.7	0.9	1.34	
7_Guaso_98	136.5	1.01	1.6750	0.0240	0.16580	0.00210	0.365	999.9	9.2	989	12	1029	33	1029.0	33.0	3.89	
7_Guaso_99	703	262.00	0.3830	0.0130	0.04890	0.00150	0.503	329	9.9	307.7	9.3	539	72	307.7	9.3	6.47	Rim
7_Guaso_99	105.5	1.48	0.9780	0.0410	0.11200	0.00330	0.679	691	21	684	19	732	64	684.0	19.0	1.01	Core
7_Guaso_100	980	1.64	0.3472	0.0041	0.04775	0.00060	0.502	302.9	3	300.7	3.7	334	25	300.7	3.7	0.73	
7_Guaso_101	364	1.18	5.0560	0.0640	0.30920	0.00380	0.838	1828	11	1736	19	1932	11	1932.0	11.0	10.14	
7_Guaso_102	518	1.81	0.3689	0.0055	0.05053	0.00045	0.027	318.7	4	317.7	2.7	311	34	317.7	2.7	0.31	
7_Guaso_103	137	1.14	0.6760	0.0130	0.08340	0.00120	0.263	524.2	7.6	516.5	7.1	547	46	516.5	7.1	1.47	
7_Guaso_104	177.1	0.67	0.5415	0.0096	0.06962	0.00088	0.083	439.1	6.3	433.9	5.3	436	48	433.9	5.3	1.18	
7_Guaso_105	286	1.75	0.3462	0.0069	0.04691	0.00077	0.134	301.6	5.2	295.5	4.7	335	49	295.5	4.7	2.02	
7_Guaso_106	1135	5.96	0.0735	0.0031	0.01049	0.00032	0.465	72	2.9	67.3	2.1	172	81	67.3	2.1	6.53	Rim
7_Guaso_106	231.8	1.55	0.5880	0.0210	0.07070	0.00220	0.797	469	13	440	13	598	66	440.0	13.0	6.18	Core
7_Guaso_107	153	2.57	1.6760	0.0230	0.16250	0.00170	0.512	998.8	8.6	970.5	9.5	1056	22	1056.0	22.0	8.10	
7_Guaso_108	603	1.82	0.3584	0.0047	0.04949	0.00061	0.488	311.3	3.5	311.4	3.7	304	30	311.4	3.7	0.03	
7_Guaso_109	219	1.86	2.2400	0.0330	0.20370	0.00220	0.510	1195	11	1195	12	1199	26	1199.0	26.0	0.33	
7_Guaso_110	209	1.40	0.3289	0.0058	0.04518	0.00059	0.401	288.6	4.4	284.9	3.7	313	39	284.9	3.7	1.28	
7_Guaso_111	640	1.93	0.3792	0.0059	0.05079	0.00083	0.578	326.3	4.3	319.3	5.1	367	37	319.3	5.1	2.15	
7_Guaso_112	464	189.00	0.3397	0.0071	0.04749	0.00082	0.679	296.8	5.3	299.1	5	289	35	299.1	5.0	0.77	
7_Guaso_113	385	1.48	0.3630	0.0065	0.04857	0.00064	0.547	314.3	4.9	305.7	3.9	350	36	305.7	3.9	2.74	
7_Guaso_114	324	1.69	0.6625	0.0086	0.08250	0.00110	0.364	516	5.3	511	6.8	524	33	511.0	6.8	0.97	
7_Guaso_115	315	2.10	0.5139	0.0080	0.06703	0.00076	0.306	421.5	5.2	418.2	4.6	440	37	418.2	4.6	0.78	
7_Guaso_116	423	1.47	0.3779	0.0048	0.05125	0.00052	0.215	325.4	3.5	322.2	3.2	348	34	322.2	3.2	0.98	
7_Guaso_117	630	3.19	0.3622	0.0057	0.04993	0.00065	0.508	313.7	4.3	314.1	4	320	31	314.1	4.0	0.13	
7_Guaso_118	214	3.67	6.1650	0.0480	0.35660	0.00230	0.346	2000.3	6.9	1966	11	2041	14	2041.0	14.0	3.67	

Sample Name _Grain #	[U] ppm	U/Th	207/235	2σ error	206/238	2σ error	RHO	207/235 Age (Ma)	2σ error	206/238 Age (Ma)	2σ error	207/206 Age (Ma)	2σ error	Best age (Ma)	2σ error	% Discordance	Rim /Core
7_Guaso_119	202	1.61	1.4860	0.0150	0.14920	0.00150	0.267	924.2	6.4	896.5	8.5	973	27	973.0	27.0	7.86	
7_Guaso_120	98.5	1.12	0.6240	0.0110	0.07820	0.00130	0.262	492	7	485.4	7.5	534	44	485.4	7.5	1.34	
14AB-M02_1	117.9	1.55	0.4020	0.0110	0.05553	0.00095	0.162	343.2	7.8	348.3	5.8	319	66	348.3	5.8	1.49	
14AB-M02_2	420	3.03	0.2710	0.0160	0.03690	0.00220	0.931	244	13	233	14	375	44	233.0	14.0	4.51	
14AB-M02_3	150.1	1.93	0.3680	0.0093	0.04961	0.00077	0.504	317.7	6.9	312.1	4.7	354	52	312.1	4.7	1.76	
14AB-M02_4	243.1	4.40	0.8820	0.0200	0.10470	0.00290	0.600	641	11	641	17	648	46	641.0	17.0	0.00	
14AB-M02_5	418	2.43	0.3841	0.0076	0.05140	0.00084	0.487	329.8	5.6	323.1	5.2	405	36	323.1	5.2	2.03	
14AB-M02_6	278	2.28	0.3149	0.0096	0.04420	0.00120	0.689	277.5	7.4	278.6	7.1	298	50	278.6	7.1	0.40	
14AB-M02_7	30.7	1.20	2.1850	0.0980	0.18190	0.00600	0.633	1189	32	1077	33	1337	67	1337.0	67.0	19.45	
14AB-M02_8	332	1.85	0.3731	0.0057	0.05232	0.00056	0.542	321.8	4.2	329.2	3.4	284	34	329.2	3.4	2.30	
14AB-M02_9	387.3	2.62	0.3596	0.0051	0.05010	0.00074	0.431	311.8	3.8	315.1	4.5	318	39	315.1	4.5	1.06	
14AB-M02_10	648	2.09	0.3594	0.0058	0.04818	0.00073	0.526	312.2	4.4	303.3	4.5	372	31	303.3	4.5	2.85	
14AB-M02_11	168.8	3.69	1.3150	0.0280	0.13740	0.00270	0.558	853	12	829	15	913	44	829.0	15.0	2.81	
14AB-M02_12	358	2.07	0.3586	0.0060	0.04979	0.00060	0.107	311	4.5	313.2	3.7	293	44	313.2	3.7	0.71	
14AB-M02_13	193.2	1.99	0.3703	0.0069	0.05131	0.00049	0.165	321	5.3	322.5	3	303	45	322.5	3.0	0.47	
14AB-M02_14	559	2.65	0.3751	0.0054	0.05074	0.00051	0.481	323.3	4	319.1	3.1	361	30	319.1	3.1	1.30	
14AB-M02_15	99.1	1.04	0.9410	0.0210	0.11070	0.00240	0.404	672	11	677	14	659	61	677.0	14.0	0.74	
14AB-M02_16	645	1.56	0.3847	0.0069	0.05233	0.00077	0.669	330.3	5.1	328.8	4.7	340	31	328.8	4.7	0.45	
14AB-M02_17	192	1.93	0.3824	0.0068	0.05199	0.00073	0.264	328.6	5	327.3	4.4	350	44	327.3	4.4	0.40	
14AB-M02_18	627	2.54	0.3669	0.0042	0.05001	0.00038	0.194	317.7	3.1	314.6	2.3	334	26	314.6	2.3	0.98	
14AB-M02_19	415	1.98	0.3814	0.0050	0.05224	0.00061	0.289	328.5	3.6	328.3	3.7	324	37	328.3	3.7	0.06	
14AB-M02_20	612	3.66	0.3505	0.0066	0.04649	0.00086	0.411	304.9	5	292.9	5.3	397	36	292.9	5.3	3.94	
14AB-M02_21	390	2.19	0.3533	0.0045	0.04786	0.00066	0.442	307.1	3.4	301.3	4.1	316	35	301.3	4.1	1.89	
14AB-M02_22	169.4	7.93	0.6231	0.0099	0.07670	0.00110	0.291	491.5	6.2	476.3	6.4	534	38	476.3	6.4	3.09	

Sample Name _Grain #	[U] ppm	U/Th	207/235	2σ error	206/238	2σ error	RHO	207/235 Age (Ma)	2σ error	206/238 Age (Ma)	2σ error	207/206 Age (Ma)	2σ error	Best age (Ma)	2σ error	% Discordance	Rim /Core
14AB-M02_23	191	2.49	0.3685	0.0074	0.05105	0.00079	0.293	319.2	5.7	320.9	4.8	314	48	320.9	4.8	0.53	
14AB-M02_24	261	2.23	0.3614	0.0066	0.04933	0.00059	0.093	313.6	4.8	310.4	3.7	320	44	310.4	3.7	1.02	
14AB-M02_25	176	1.20	0.6180	0.0110	0.07923	0.00083	0.074	488.3	6.7	491.5	4.9	482	39	491.5	4.9	0.66	
14AB-M02_26	376	2.03	0.3868	0.0070	0.05277	0.00072	0.374	331.8	5.1	331.5	4.4	307	36	331.5	4.4	0.09	
14AB-M02_27	14.42	1.40	1.8870	0.0630	0.17580	0.00460	0.303	1073	22	1043	25	1117	74	1117.0	74.0	6.62	
14AB-M02_28	530	2.71	0.4046	0.0092	0.05252	0.00081	0.411	344.6	6.6	329.9	4.9	423	44	329.9	4.9	4.27	
14AB-M02_29	201	2.20	0.3597	0.0061	0.04969	0.00056	0.223	311.8	4.6	312.6	3.5	281	43	312.6	3.5	0.26	
14AB-M02_30	445	1.74	0.3565	0.0059	0.04935	0.00066	0.391	309.4	4.4	310.5	4.1	291	40	310.5	4.1	0.36	
14AB-M02_31	211	2.03	0.3548	0.0082	0.04829	0.00088	0.367	308.1	6.1	304	5.4	343	54	304.0	5.4	1.33	
14AB-M02_32	715	24.20	0.4390	0.0110	0.05358	0.00097	0.361	368.8	7.6	336.4	5.9	545	61	336.4	5.9	8.79	
14AB-M02_33	152.8	2.18	0.4201	0.0082	0.05707	0.00079	0.195	355.8	5.9	357.8	4.8	338	48	357.8	4.8	0.56	
14AB-M02_34	423	3.81	0.3884	0.0068	0.05259	0.00084	0.417	332.9	5	330.4	5.1	348	41	330.4	5.1	0.75	
14AB-M02_35	635	2.84	0.3760	0.0054	0.05182	0.00072	0.424	323.9	4	325.6	4.4	275	35	325.6	4.4	0.52	
14AB-M02_36	411	2.34	0.3744	0.0067	0.04936	0.00054	0.391	322.7	4.9	310.6	3.3	388	44	310.6	3.3	3.75	
14AB-M02_37	199	1.83	0.6500	0.0200	0.07670	0.00220	0.783	508	12	476	13	672	53	476.0	13.0	6.30	
14AB-M02_38	316	2.06	0.3673	0.0075	0.04818	0.00073	0.125	317.4	5.6	303.3	4.5	389	56	303.3	4.5	4.44	
14AB-M02_39	314	2.09	0.3464	0.0078	0.04751	0.00056	0.345	301.7	5.8	299.2	3.4	320	52	299.2	3.4	0.83	
14AB-M02_40	57.5	1.11	1.1130	0.0300	0.12350	0.00240	0.277	760	14	750	14	770	57	750.0	14.0	1.32	
14AB-M02_41	214	2.05	0.3675	0.0078	0.04991	0.00058	0.074	318.2	5.7	313.9	3.5	329	52	313.9	3.5	1.35	
14AB-M02_42	324	2.56	0.3776	0.0074	0.05225	0.00078	0.463	325.8	5.3	328.3	4.8	304	41	328.3	4.8	0.77	
14AB-M02_43	951	2.30	0.3847	0.0058	0.05325	0.00072	0.614	330.3	4.3	334.4	4.4	283	32	334.4	4.4	1.24	
14AB-M02_44	88.4	1.67	7.1400	0.1200	0.33370	0.00480	0.754	2130	15	1856	23	2394	18	2394.0	18.0	22.47	
14AB-M02_45	332	1.84	0.3736	0.0075	0.05159	0.00072	0.396	322.7	5.6	324.3	4.4	278	43	324.3	4.4	0.50	
14AB-M02_46	221	7.36	0.6737	0.0084	0.08429	0.00074	0.348	522.7	5.1	521.6	4.4	511	28	521.6	4.4	0.21	
14AB-M02_47	560	2.24	0.3627	0.0044	0.05015	0.00052	0.280	314.2	3.2	315.4	3.2	288	31	315.4	3.2	0.38	

Sample Name _Grain #	[U] ppm	U/Th	207/235	2σ error	206/238	2σ error	RHO	207/235 Age (Ma)	2σ error	206/238 Age (Ma)	2σ error	207/206 Age (Ma)	2σ error	Best age (Ma)	2σ error	% Discordance	Rim /Core
14AB-M02_48	291	1.68	0.3545	0.0068	0.04899	0.00074	0.308	308.7	5.3	308.3	4.6	304	49	308.3	4.6	0.13	
14AB-M02_49	270	1.89	0.7550	0.0120	0.09220	0.00140	0.631	571	6.7	568.5	8.4	552	29	568.5	8.4	0.44	
14AB-M02_50	116.8	2.20	4.7890	0.0520	0.32140	0.00400	0.516	1782.3	9.1	1796	19	1758	21	1758.0	21.0	2.16	
14AB-M02_51	518	2.23	0.3731	0.0074	0.05114	0.00067	0.045	321.7	5.5	321.5	4.1	302	42	321.5	4.1	0.06	
14AB-M02_52	474	2.12	0.3647	0.0039	0.04983	0.00043	0.287	315.6	2.9	313.4	2.7	315	26	313.4	2.7	0.70	
14AB-M02_54	493	1.73	0.3658	0.0045	0.04970	0.00053	0.309	316.5	3.4	312.7	3.3	343	31	312.7	3.3	1.20	
14AB-M02_55	204	2.87	0.3555	0.0066	0.04831	0.00054	0.079	308.6	4.9	304.1	3.3	314	48	304.1	3.3	1.46	
14AB-M02_56	142	1.74	6.7600	0.1100	0.40200	0.00700	0.806	2079	15	2182	31	1972	19	1972.0	19.0	10.65	
14AB-M02_57	232	1.97	0.3736	0.0072	0.05112	0.00058	0.000	323.4	5.3	321.4	3.5	322	51	321.4	3.5	0.62	
14AB-M02_58	741	2.49	0.3536	0.0068	0.04840	0.00110	0.599	307.2	5.1	305.3	6.8	326	48	305.3	6.8	0.62	
14AB-M02_59	286	3.54	0.3718	0.0055	0.05122	0.00068	0.302	321.4	3.9	322	4.2	313	38	322.0	4.2	0.19	
14AB-M02_60	330	13.30	0.9370	0.0210	0.10930	0.00280	0.667	672	11	669	16	672	43	669.0	16.0	0.45	Rim
14AB-M02_60	56.5	1.85	1.6920	0.0750	0.18470	0.00560	0.094	1011	30	1092	30	850	110	850.0	110.0	8.01	Core
14AB-M02_61	795	1.81	0.3677	0.0047	0.05025	0.00059	0.569	317.8	3.5	316	3.6	341	25	316.0	3.6	0.57	
14AB-M02_62	330	1.69	1.8750	0.0220	0.18350	0.00220	0.548	1071.7	7.8	1086	12	1065	25	1065.0	25.0	1.97	
14AB-M02_63	114.3	2.07	0.3720	0.0100	0.05077	0.00076	0.255	321.3	7.6	319.2	4.7	347	61	319.2	4.7	0.65	
14AB-M02_64	155.6	2.26	0.3689	0.0076	0.05131	0.00073	0.292	318.6	5.6	322.5	4.4	312	47	322.5	4.4	1.22	
14AB-M02_65	279	2.31	0.3622	0.0065	0.04922	0.00057	0.206	313.6	4.9	309.7	3.5	356	45	309.7	3.5	1.24	
14AB-M02_66	255	2.43	0.3680	0.0065	0.05131	0.00057	0.285	318	4.8	322.5	3.5	317	38	322.5	3.5	1.42	
14AB-M02_67	246.7	9.43	0.7290	0.0120	0.09220	0.00110	0.588	555.8	7.1	568.8	6.6	520	35	568.8	6.6	2.34	
14AB-M02_68	599	70.00	0.3570	0.0110	0.04980	0.00150	0.857	309.5	8.5	313.4	9.2	325	39	313.4	9.2	1.26	
14AB-M02_69	339	0.82	0.7549	0.0098	0.09413	0.00090	0.469	570.7	5.7	579.9	5.3	550	26	579.9	5.3	1.61	
14AB-M02_70	630	8.71	0.3410	0.0140	0.04560	0.00140	0.804	297	11	287.4	8.8	446	50	287.4	8.8	3.23	
14AB-M02_71	328	3.29	0.3364	0.0077	0.04438	0.00089	0.745	294.2	5.9	279.9	5.5	441	51	279.9	5.5	4.86	
14AB-M02_72	413	2.17	0.3921	0.0059	0.05338	0.00056	0.277	335.7	4.3	335.2	3.4	391	36	335.2	3.4	0.15	

Sample Name _Grain #	[U] ppm	U/Th	207/235	2σ error	206/238	2σ error	RHO	207/235 Age (Ma)	2σ error	206/238 Age (Ma)	2σ error	207/206 Age (Ma)	2σ error	Best age (Ma)	2σ error	% Discordance	Rim /Core
14AB-M02_73	484	2.79	0.3635	0.0052	0.05006	0.00060	0.450	314.7	3.9	314.9	3.7	347	32	314.9	3.7	0.06	
14AB-M02_74	233	1.61	0.3750	0.0077	0.05151	0.00054	0.411	324.8	5.7	323.8	3.3	367	43	323.8	3.3	0.31	
14AB-M02_75	167.1	2.11	0.3700	0.0110	0.05231	0.00073	0.096	319.1	7.8	328.7	4.5	271	64	328.7	4.5	3.01	
14AB-M02_76	604	2.10	0.3681	0.0043	0.05108	0.00046	0.211	318.2	3.2	321.1	2.8	350	30	321.1	2.8	0.91	
14AB-M02_77	123.6	0.92	6.6100	0.1000	0.37090	0.00510	0.709	2059	14	2033	24	2103	20	2103.0	20.0	3.33	
14AB-M02_78	160.3	1.11	0.8060	0.0140	0.09990	0.00110	0.282	599.6	7.6	613.5	6.3	593	40	613.5	6.3	2.32	
14AB-M02_79	77	0.87	4.4760	0.0880	0.30670	0.00530	0.713	1725	16	1724	26	1767	25	1767.0	25.0	2.43	
14AB-M02_80	230	1.87	0.3685	0.0068	0.05020	0.00056	0.214	318.3	5.1	315.8	3.4	380	44	315.8	3.4	0.79	
14AB-M02_81	102	1.55	4.0300	0.2000	0.26790	0.00890	0.921	1644	39	1544	48	1795	34	1795.0	34.0	13.98	
14AB-M02_82	192.9	1.86	0.3659	0.0082	0.05198	0.00068	0.156	316.3	6.1	326.6	4.2	264	55	326.6	4.2	3.26	
14AB-M02_83	208	3.74	0.5650	0.0100	0.07350	0.00110	0.361	454	6.8	457.4	6.4	447	43	457.4	6.4	0.75	
14AB-M02_84	296.1	9.21	0.8417	0.0088	0.10220	0.00110	0.315	620.5	5	627.3	6.2	625	25	627.3	6.2	1.10	
14AB-M02_85	102.1	1.85	1.7710	0.0310	0.17440	0.00260	0.310	1035	11	1036	14	1028	41	1028.0	41.0	0.78	
14AB-M02_86	143.4	0.60	5.5890	0.0680	0.35560	0.00450	0.481	1914	10	1961	22	1873	23	1873.0	23.0	4.70	
14AB-M02_87	246	2.02	7.7300	0.1300	0.41910	0.00750	0.808	2198	15	2255	34	2140	19	2140.0	19.0	5.37	
14AB-M02_88	19	1.21	1.0050	0.0370	0.11280	0.00290	0.224	708	19	691	17	746	84	691.0	17.0	2.40	
14AB-M02_89	28.9	1.68	1.0050	0.0470	0.11580	0.00290	0.027	710	22	706	17	720	100	706.0	17.0	0.56	
14AB-M02_90	124	0.89	0.7280	0.0170	0.09020	0.00170	0.394	555.9	9.8	556	10	559	48	556.0	10.0	0.02	
14AB-M02_91	122.5	1.68	1.3560	0.0190	0.14630	0.00220	0.433	870.9	8.4	880	12	828	33	828.0	12.0	1.04	
14AB-M02_92	457	1.69	0.3714	0.0064	0.05033	0.00059	0.061	320.5	4.7	317	3.5	328	41	317.0	3.5	1.09	
14AB-M02_93	232	5.27	0.6010	0.0079	0.07679	0.00082	0.098	477.6	5	476.9	4.9	469	37	476.9	4.9	0.15	
14AB-M02_94	296	2.18	0.3655	0.0064	0.04985	0.00067	0.429	316.7	4.7	313.6	4.1	296	36	313.6	4.1	0.98	
14AB-M02_95	330	2.22	0.3597	0.0066	0.04714	0.00066	0.328	311.8	4.9	296.9	4	408	40	296.9	4.0	4.78	
14AB-M02_96	450	1.89	0.3598	0.0054	0.04939	0.00049	0.281	312.4	4	310.8	3	314	36	310.8	3.0	0.51	
14AB-M02_97	496.7	2.64	0.3685	0.0057	0.05033	0.00062	0.330	318.4	4.2	316.5	3.8	318	35	316.5	3.8	0.60	

Sample Name _Grain #	[U] ppm	U/Th	207/235	2σ error	206/238	2σ error	RHO	207/235 Age (Ma)	2σ error	206/238 Age (Ma)	2σ error	207/206 Age (Ma)	2σ error	Best age (Ma)	2σ error	% Discordance	Rim /Core
14AB-M02_98	512	4.24	0.3874	0.0054	0.05309	0.00074	0.544	332.3	4	333.4	4.5	312	32	333.4	4.5	0.33	
14AB-M02_99	226	2.24	0.3728	0.0066	0.05103	0.00062	0.359	321.5	4.9	320.8	3.8	329	39	320.8	3.8	0.22	
14AB-M02_100	338	5.58	0.6179	0.0095	0.07920	0.00110	0.451	488.3	5.9	491	6.3	497	30	491.0	6.3	0.55	
14AB-M02_101	23.51	1.11	6.0200	0.1200	0.36480	0.00750	0.311	1976	18	2003	36	1960	40	1960.0	40.0	2.19	
14AB-M02_102	119	1.24	0.4458	0.0093	0.06064	0.00080	0.001	373.9	6.5	379.5	4.8	322	56	379.5	4.8	1.50	
14AB-M02_103	233.1	1.93	3.4680	0.0500	0.24080	0.00320	0.572	1519	11	1390	16	1689	23	1689.0	23.0	17.70	
14AB-M02_104	390	2.02	0.3765	0.0067	0.05125	0.00062	0.256	324.3	4.9	322.2	3.8	326	40	322.2	3.8	0.65	
14AB-M02_105	488	121.00	0.4164	0.0063	0.05565	0.00061	0.616	353.2	4.5	349.1	3.7	364	28	349.1	3.7	1.16	
14AB-M02_106	428	1.81	0.3665	0.0066	0.05066	0.00075	0.256	316.9	4.9	318.6	4.6	301	41	318.6	4.6	0.54	
14AB-M02_107	179.8	1.19	5.2420	0.0810	0.31160	0.00450	0.712	1859	13	1748	22	1983	22	1983.0	22.0	11.85	
14AB-M02_108	290.8	0.47	0.8227	0.0094	0.10080	0.00130	0.406	609.3	5.3	619.2	7.8	568	28	619.2	7.8	1.62	
14AB-M02_109	394	1.86	0.3613	0.0063	0.05018	0.00067	0.427	313.6	4.6	315.6	4.1	322	35	315.6	4.1	0.64	
14AB-M02_110	163.5	2.07	0.7640	0.0130	0.09442	0.00099	0.398	575.6	7.3	581.6	5.9	555	37	581.6	5.9	1.04	
14AB-M02_111	378.2	2.78	1.9760	0.0300	0.18870	0.00220	0.623	1107	10	1114	12	1106	23	1106.0	23.0	0.72	
14AB-M02_112	381	1.88	0.3685	0.0062	0.05233	0.00071	0.439	318.3	4.6	328.8	4.3	260	33	328.8	4.3	3.30	
14AB-M02_113	342.5	1.69	1.7250	0.0300	0.17060	0.00310	0.719	1017	11	1015	17	1027	25	1027.0	25.0	1.17	
14AB-M02_114	379.5	2.90	0.3685	0.0075	0.05070	0.00110	0.345	319	5.5	318.9	7	332	58	318.9	7.0	0.03	
14AB-M02_115	783	2.00	0.3702	0.0053	0.05043	0.00062	0.525	319.7	3.9	317.2	3.8	311	30	317.2	3.8	0.78	
14AB-M02_116	147.7	2.13	0.3736	0.0073	0.05170	0.00071	0.086	322	5.4	324.9	4.4	288	55	324.9	4.4	0.90	
14AB-M02_117	334	1.67	0.8160	0.0210	0.09640	0.00130	0.471	605	12	593.3	7.7	600	45	593.3	7.7	1.93	
14AB-M02_118	1480	1.78	0.3798	0.0046	0.05232	0.00056	0.650	326.8	3.4	328.7	3.4	322	21	328.7	3.4	0.58	
14AB-M02_119	333	143.00	0.3860	0.0110	0.05120	0.00120	0.605	330.8	7.9	322.1	7.3	385	52	322.1	7.3	2.63	
14AB-M02_120	258.1	1.92	11.8400	0.2600	0.48370	0.00970	0.877	2590	21	2542	42	2614	16	2614.0	16.0	2.75	
14AB-M02_121	392	44.56	0.8075	0.0072	0.09782	0.00065	0.271	600.9	4.1	601.6	3.8	588	23	601.6	3.8	0.12	
6-Morillo_1	511	3.16	0.3069	0.0075	0.04140	0.00090	0.891	271.4	5.7	261.5	5.6	348	32	261.5	5.6	3.65	

Sample Name _Grain #	[U] ppm	U/Th	207/235	2σ error	206/238	2σ error	RHO	207/235 Age (Ma)	2σ error	206/238 Age (Ma)	2σ error	207/206 Age (Ma)	2σ error	Best age (Ma)	2σ error	% Discordance	Rim /Core
6-Morillo_2	672	1.45	0.3362	0.0046	0.04676	0.00059	0.631	294.2	3.5	294.6	3.6	278	28	294.6	3.6	0.14	
6-Morillo_3	378	1.74	0.3412	0.0061	0.04588	0.00066	0.568	298.5	4.5	289.1	4.1	365	34	289.1	4.1	3.15	
6-Morillo_4	549	3.21	0.3448	0.0080	0.04595	0.00097	0.514	300.5	6	289.6	6	353	48	289.6	6.0	3.63	
6-Morillo_5	258	2.10	0.3246	0.0063	0.04204	0.00066	0.573	285.3	4.9	265.4	4.1	452	37	265.4	4.1	6.98	
6-Morillo_6	598	1.98	0.3193	0.0068	0.04263	0.00085	0.746	281.1	5.2	269.1	5.2	406	32	269.1	5.2	4.27	
6-Morillo_7	131.2	1.66	0.3550	0.0087	0.04831	0.00054	0.230	308.1	6.5	304.1	3.3	311	58	304.1	3.3	1.30	
6-Morillo_8	740	6.70	0.8680	0.0150	0.10210	0.00200	0.935	634	8.3	626	11	656	19	626.0	11.0	1.26	
6-Morillo_9	350	3.55	0.8340	0.0130	0.09820	0.00110	0.640	615.3	7.2	604.1	6.7	640	25	604.1	6.7	1.82	
6-Morillo_10	26.4	0.42	4.4800	0.1400	0.27780	0.00610	0.282	1724	25	1580	31	1920	59	1920.0	59.0	17.71	
6-Morillo_11	258	1.40	0.3278	0.0060	0.04598	0.00065	0.558	288.2	4.5	289.8	4	285	37	289.8	4.0	0.56	
6-Morillo_12	449	1.52	0.3412	0.0044	0.04571	0.00056	0.071	297.9	3.4	288.1	3.4	364	41	288.1	3.4	3.29	
6-Morillo_13	183.8	0.86	0.5600	0.0110	0.06970	0.00130	0.526	451.2	7.1	434	7.7	534	40	434.0	7.7	3.81	
6-Morillo_14	693	2.14	0.3503	0.0052	0.04783	0.00082	0.627	304.8	3.9	301.1	5.1	321	32	301.1	5.1	1.21	
6-Morillo_15	191.9	0.95	0.7760	0.0110	0.09460	0.00100	0.573	582.8	6.5	582.4	5.9	568	30	582.4	5.9	0.07	
6-Morillo_16	1562	12.75	0.3799	0.0050	0.04566	0.00073	0.062	326.9	3.7	287.8	4.5	597	46	DISC	DISC	11.96	
6-Morillo_17	244	1.02	0.0981	0.0045	0.01453	0.00044	0.095	94.9	4.1	93	2.8	150	110	93.0	2.8	2.00	
6-Morillo_18	182	0.86	0.7460	0.0130	0.08860	0.00150	0.271	565.4	7.4	547.3	8.6	624	41	547.3	8.6	3.20	
6-Morillo_19	353	1.25	0.5460	0.0110	0.06850	0.00110	0.715	441.9	7.4	427.7	6.8	520	26	427.7	6.8	3.21	
6-Morillo_20	416	1.59	0.3323	0.0063	0.04454	0.00073	0.503	291.8	4.7	280.9	4.5	360	37	280.9	4.5	3.74	
6-Morillo_21	930	1.84	0.2963	0.0065	0.03951	0.00078	0.889	263.3	5.1	249.7	4.8	380	29	249.7	4.8	5.17	
6-Morillo_22	548	16.20	0.4920	0.0160	0.06400	0.00170	0.913	406	11	400	11	430	26	400.0	11.0	1.48	
6-Morillo_23	57.9	1.83	0.3900	0.0150	0.04665	0.00099	0.066	333	11	293.9	6.1	576	89	DISC	DISC	11.74	
6-Morillo_24	295.9	1.29	9.5900	0.1100	0.40230	0.00510	0.920	2397	10	2179	23	2574	9	2574.2	8.9	15.35	
6-Morillo_25	394	1.51	0.3559	0.0055	0.04864	0.00053	0.072	309.1	4.1	306.2	3.2	310	43	306.2	3.2	0.94	
6-Morillo_26	334	1.86	0.3394	0.0058	0.04710	0.00068	0.573	296.6	4.4	296.7	4.2	307	33	296.7	4.2	0.03	

Sample Name _Grain #	[U] ppm	U/Th	207/235	2σ error	206/238	2σ error	RHO	207/235 Age (Ma)	2σ error	206/238 Age (Ma)	2σ error	207/206 Age (Ma)	2σ error	Best age (Ma)	2σ error	% Discordance	Rim /Core
6-Morillo_27	420	2.81	0.3011	0.0052	0.04190	0.00073	0.503	267.1	4.1	264.6	4.5	307	39	264.6	4.5	0.94	
6-Morillo_28	198	1.78	1.0960	0.0230	0.11810	0.00200	0.762	750	11	720	12	879	24	720.0	12.0	4.00	
6-Morillo_29	1510	5.34	0.2880	0.0100	0.03770	0.00150	0.889	256.2	8	238.6	9.3	405	36	238.6	9.3	6.87	
6-Morillo_31	218	1.97	0.3621	0.0071	0.04920	0.00063	0.199	313.5	5.3	309.6	3.9	335	48	309.6	3.9	1.24	
6-Morillo_32	417	1.49	0.4210	0.0053	0.05668	0.00061	0.274	356.6	3.8	355.4	3.7	348	31	355.4	3.7	0.34	
6-Morillo_33	355	2.11	0.3329	0.0056	0.04612	0.00057	0.478	291.6	4.3	290.6	3.5	307	36	290.6	3.5	0.34	
6-Morillo_34	388	1.55	0.3619	0.0052	0.04980	0.00049	0.365	313.5	3.9	313.3	3	329	33	313.3	3.0	0.06	
6-Morillo_35	245.1	1.97	0.8331	0.0099	0.09893	0.00097	0.448	615	5.5	608.1	5.7	655	24	608.1	5.7	1.12	
6-Morillo_36	313.5	1.09	0.5120	0.0095	0.06460	0.00120	0.683	419.4	6.4	403.2	7	528	33	403.2	7.0	3.86	
6-Morillo_37	704	4.89	0.3080	0.0053	0.04173	0.00070	0.726	272.5	4.1	263.5	4.3	341	29	263.5	4.3	3.30	
6-Morillo_38	408	2.59	0.3307	0.0052	0.04535	0.00056	0.443	289.9	4	285.9	3.5	330	37	285.9	3.5	1.38	
6-Morillo_39	178.3	1.80	0.3460	0.0065	0.04768	0.00060	0.100	302.1	4.9	300.3	3.7	307	51	300.3	3.7	0.60	
6-Morillo_40	102.5	1.05	0.7960	0.0160	0.09770	0.00160	0.297	595.2	9.1	600.9	9.6	582	51	600.9	9.6	0.96	
6-Morillo_41	400	1.71	0.3149	0.0071	0.04196	0.00057	0.310	278.6	5.7	265	3.6	408	52	265.0	3.6	4.88	
6-Morillo_42	797	2.72	0.2800	0.0052	0.03684	0.00083	0.749	250.5	4.2	233.2	5.2	400	33	233.2	5.2	6.91	
6-Morillo_43	828	10.25	0.3600	0.0082	0.04810	0.00110	0.881	312.7	6.2	302.9	7	402	25	302.9	7.0	3.13	
6-Morillo_44	130.7	1.28	0.3491	0.0077	0.04666	0.00058	0.165	305.1	5.8	294	3.6	380	49	294.0	3.6	3.64	
6-Morillo_45	303	1.55	0.3392	0.0052	0.04700	0.00064	0.446	296.4	3.9	296	4	292	36	296.0	4.0	0.13	
6-Morillo_46	471	2.30	0.3591	0.0060	0.04965	0.00076	0.615	311.3	4.5	312.4	4.7	327	29	312.4	4.7	0.35	
6-Morillo_47	299	1.71	0.3387	0.0049	0.04688	0.00070	0.462	296.6	3.8	295.3	4.3	336	33	295.3	4.3	0.44	
6-Morillo_48	142.9	5.67	0.7470	0.0110	0.09081	0.00089	0.343	566.1	6.5	560.3	5.3	610	31	560.3	5.3	1.02	
6-Morillo_49	127.8	1.20	4.9190	0.0450	0.29540	0.00310	0.705	1805	7.7	1668	15	1968	14	1968.0	14.0	15.24	
6-Morillo_50	239.6	1.68	5.8520	0.0400	0.34320	0.00240	0.690	1953.8	5.9	1902	11	2011	10	2011.0	10.0	5.42	
6-Morillo_51	361	1.15	0.3416	0.0052	0.04806	0.00055	0.448	298.2	3.9	302.6	3.4	270	35	302.6	3.4	1.48	
6-Morillo_52	139	0.95	1.2510	0.0180	0.13430	0.00150	0.213	825.2	7.9	812.1	8.3	878	30	812.1	8.3	1.59	

Sample Name _Grain #	[U] ppm	U/Th	207/235	2σ error	206/238	2σ error	RHO	207/235 Age (Ma)	2σ error	206/238 Age (Ma)	2σ error	207/206 Age (Ma)	2σ error	Best age (Ma)	2σ error	% Discordance	Rim /Core
6-Morillo_53	297	2.13	0.3382	0.0056	0.04603	0.00052	0.366	296.2	4.3	290.1	3.2	341	40	290.1	3.2	2.06	
6-Morillo_54	448	2.52	0.3454	0.0059	0.04631	0.00053	0.412	301.1	4.5	291.8	3.3	346	38	291.8	3.3	3.09	
6-Morillo_55	368	1.52	0.3429	0.0055	0.04729	0.00058	0.482	299.7	4.1	297.9	3.6	346	33	297.9	3.6	0.60	
6-Morillo_56	196	2.02	0.3458	0.0069	0.04815	0.00073	0.273	301.3	5.2	303.1	4.5	286	45	303.1	4.5	0.60	
6-Morillo_57	435	2.19	0.3530	0.0053	0.04859	0.00055	0.409	306.8	3.9	305.8	3.4	332	30	305.8	3.4	0.33	
6-Morillo_58	51.6	1.39	0.7860	0.0200	0.09360	0.00220	0.031	590	12	577	13	646	71	577.0	13.0	2.20	
6-Morillo_59	463	2.07	0.3539	0.0055	0.04727	0.00052	0.341	307.5	4.1	297.7	3.2	379	33	297.7	3.2	3.19	
6-Morillo_60	572	1.57	0.3731	0.0045	0.05048	0.00051	0.621	321.8	3.4	317.4	3.1	347	25	317.4	3.1	1.37	
6-Morillo_61	629	2.25	0.3649	0.0045	0.04913	0.00046	0.571	315.7	3.4	309.2	2.9	369	24	309.2	2.9	2.06	
6-Morillo_62	204.6	0.94	1.2600	0.0250	0.13270	0.00190	0.684	827	11	803	11	884	27	803.0	11.0	2.90	
6-Morillo_63	109.7	1.95	0.3270	0.0100	0.04661	0.00089	0.335	287	7.9	293.7	5.5	250	66	293.7	5.5	2.33	
6-Morillo_64	188.9	1.69	0.3392	0.0064	0.04654	0.00055	0.308	297.6	4.9	293.2	3.4	313	42	293.2	3.4	1.48	
6-Morillo_65	213	1.56	0.3425	0.0064	0.04715	0.00058	0.222	298.9	4.8	297	3.6	295	40	297.0	3.6	0.64	
6-Morillo_66	452	2.41	0.3372	0.0048	0.04690	0.00051	0.443	294.9	3.6	295.5	3.2	309	30	295.5	3.2	0.20	
6-Morillo_67	247	3.06	1.2420	0.0300	0.12770	0.00380	0.868	819	14	774	22	905	38	774.0	22.0	5.49	
6-Morillo_68	426	1.56	0.3588	0.0057	0.04891	0.00057	0.587	311.8	4.4	307.8	3.5	327	36	307.8	3.5	1.28	
6-Morillo_69	219.7	0.99	0.9780	0.0130	0.11130	0.00110	0.538	692.2	6.6	680.1	6.4	722	26	680.1	6.4	1.75	
6-Morillo_70	440	1.59	0.3393	0.0069	0.04614	0.00080	0.722	296.4	5.2	290.7	5	330	34	290.7	5.0	1.92	
6-Morillo_71	168	1.72	0.4290	0.0120	0.04557	0.00075	0.504	362	8.3	287.2	4.6	853	51	DISC	DISC	20.66	
6-Morillo_72	305	2.42	0.3101	0.0055	0.03923	0.00062	0.524	274.7	4.4	248	3.8	493	37	248.0	3.8	9.72	
6-Morillo_73	531	2.48	0.3441	0.0064	0.04611	0.00078	0.703	300.1	4.8	290.6	4.8	377	36	290.6	4.8	3.17	
6-Morillo_74	2220	2.58	0.2238	0.0046	0.02867	0.00060	0.555	204.9	3.8	182.2	3.7	474	39	DISC	DISC	11.08	
6-Morillo_75	357	2.01	0.3504	0.0083	0.04804	0.00096	0.605	304.7	6.2	302.4	5.9	291	44	302.4	5.9	0.75	
6-Morillo_76	423	2.53	0.3501	0.0078	0.04710	0.00130	0.694	305.3	6	296.6	7.9	368	50	296.6	7.9	2.85	
6-Morillo_77	1030	1.95	0.3500	0.0057	0.04799	0.00088	0.816	304.6	4.3	302.2	5.4	314	25	302.2	5.4	0.79	

Sample Name _Grain #	[U] ppm	U/Th	207/235	2σ error	206/238	2σ error	RHO	207/235 Age (Ma)	2σ error	206/238 Age (Ma)	2σ error	207/206 Age (Ma)	2σ error	Best age (Ma)	2σ error	% Discordance	Rim /Core
6-Morillo_78	314	3.53	0.3576	0.0051	0.04923	0.00047	0.445	310.3	3.8	310.2	2.8	325	33	310.2	2.8	0.03	
6-Morillo_79	389	1.52	0.3512	0.0053	0.04772	0.00043	0.233	305.5	4	300.5	2.7	324	33	300.5	2.7	1.64	
6-Morillo_80	21.67	0.94	1.6050	0.0370	0.16050	0.00250	0.238	976	14	959	14	999	50	999.0	50.0	4.00	
6-Morillo_81	539.8	2.27	0.3399	0.0043	0.04668	0.00041	0.332	297.5	3.3	294.1	2.5	301	31	294.1	2.5	1.14	
6-Morillo_82	640	1.42	0.3430	0.0041	0.04748	0.00052	0.405	299.4	3.1	299	3.2	298	29	299.0	3.2	0.13	
6-Morillo_83	191	1.58	0.3347	0.0065	0.04506	0.00054	0.180	292.9	5	284.1	3.4	360	46	284.1	3.4	3.00	
6-Morillo_84	448	2.65	0.3387	0.0080	0.04580	0.00085	0.833	295.9	6.1	288.6	5.2	364	30	288.6	5.2	2.47	
6-Morillo_85	287	2.16	0.3435	0.0064	0.04726	0.00064	0.409	299.6	4.8	297.6	4	292	39	297.6	4.0	0.67	
6-Morillo_86	92.9	0.98	0.7700	0.0140	0.09210	0.00110	0.280	579	8	567.9	6.6	627	41	567.9	6.6	1.92	
6-Morillo_87	171.4	1.58	0.3638	0.0074	0.04913	0.00065	0.062	314.8	5.5	309.2	4	325	53	309.2	4.0	1.78	
6-Morillo_88	360	1.40	0.3463	0.0053	0.04773	0.00051	0.178	301.9	4	300.6	3.1	312	41	300.6	3.1	0.43	
6-Morillo_89	475	2.12	0.7492	0.0089	0.08881	0.00087	0.551	567.5	5.2	548.5	5.1	626	22	548.5	5.1	3.35	
6-Morillo_90	345	1.90	0.3608	0.0061	0.04851	0.00050	0.269	312.7	4.5	305.3	3	364	40	305.3	3.0	2.37	
6-Morillo_91	285	2.42	0.3476	0.0076	0.04810	0.00100	0.397	302.6	5.7	302.7	6.2	277	54	302.7	6.2	0.03	
6-Morillo_92	326	2.10	0.3308	0.0064	0.04597	0.00054	0.408	290.7	4.8	289.7	3.3	291	42	289.7	3.3	0.34	
6-Morillo_93	261	20.20	0.3838	0.0058	0.05127	0.00059	0.055	329.7	4.3	322.3	3.6	374	44	322.3	3.6	2.24	
6-Morillo_94	218	0.87	0.7880	0.0100	0.09490	0.00100	0.593	589.7	5.9	584.5	6.1	613	28	584.5	6.1	0.88	
6-Morillo_95	247	1.74	4.0600	0.1500	0.26500	0.01100	0.784	1640	30	1511	57	1799	50	1799.0	50.0	16.01	
6-Morillo_96	318	2.23	0.3366	0.0066	0.04469	0.00062	0.371	294.4	5	281.8	3.8	382	41	281.8	3.8	4.28	
6-Morillo_97	225	1.44	0.3618	0.0051	0.04965	0.00050	0.201	314	3.9	312.4	3.1	319	38	312.4	3.1	0.51	
6-Morillo_98	234	2.53	0.3635	0.0073	0.04817	0.00047	0.416	314.5	5.4	303.3	2.9	409	39	303.3	2.9	3.56	
6-Morillo_99	249	1.34	0.3428	0.0059	0.04707	0.00055	0.387	299.1	4.5	296.5	3.4	308	39	296.5	3.4	0.87	
6-Morillo_100	298	1.67	0.3674	0.0062	0.05027	0.00061	0.513	317.5	4.6	316.2	3.7	332	31	316.2	3.7	0.41	
6-Morillo_101	132.8	1.29	0.8690	0.0120	0.10288	0.00090	0.284	635.5	6.3	631.2	5.3	651	30	631.2	5.3	0.68	
6-Morillo_102	768	2.05	0.3589	0.0041	0.04821	0.00051	0.494	311.3	3	303.5	3.1	371	25	303.5	3.1	2.51	

Sample Name _Grain #	[U] ppm	U/Th	207/235	2σ error	206/238	2σ error	RHO	207/235 Age (Ma)	2σ error	206/238 Age (Ma)	2σ error	207/206 Age (Ma)	2σ error	Best age (Ma)	2σ error	% Discordance	Rim /Core
6-Morillo_103	46.7	0.34	4.6190	0.0870	0.30880	0.00520	0.283	1752	16	1734	26	1761	37	1761.0	37.0	1.53	
6-Morillo_105	257	2.86	0.3469	0.0059	0.04789	0.00052	0.195	302.2	4.4	301.5	3.2	306	42	301.5	3.2	0.23	
6-Morillo_106	414	1.71	0.3384	0.0054	0.04643	0.00059	0.556	296.3	4.1	292.5	3.6	319	31	292.5	3.6	1.28	
6-Morillo_107	284	2.62	0.3393	0.0053	0.04694	0.00045	0.217	296.5	4	295.7	2.8	288	37	295.7	2.8	0.27	
6-Morillo_108	259	6.43	0.6134	0.0097	0.07717	0.00087	0.606	486.7	5.8	479.2	5.2	518	26	479.2	5.2	1.54	
6-Morillo_109	949	13.00	0.8020	0.0160	0.09360	0.00140	0.794	597.5	8.7	576.8	8	649	25	576.8	8.0	3.46	Rim
6-Morillo_109	125.7	1.06	2.1590	0.0360	0.19560	0.00360	0.723	1167	12	1152	19	1188	26	1188.0	26.0	3.03	Core
6-Morillo_110	338	1.81	0.3540	0.0046	0.04906	0.00045	0.258	308.1	3.3	308.8	2.8	298	32	308.8	2.8	0.23	
6-Morillo_111	159	1.38	0.3506	0.0058	0.04829	0.00042	0.007	305	4.4	304	2.6	318	43	304.0	2.6	0.33	
6-Morillo_112	197	1.64	0.3558	0.0067	0.04840	0.00048	0.303	308.8	5	304.7	3	334	40	304.7	3.0	1.33	
6-Morillo_113	181	1.49	0.3392	0.0055	0.04678	0.00052	0.231	296.9	4.1	294.7	3.2	310	39	294.7	3.2	0.74	
6-Morillo_114	200	1.55	0.3602	0.0050	0.04825	0.00050	0.013	312.3	3.7	303.7	3.1	368	39	303.7	3.1	2.75	
6-Morillo_115	510	1.69	0.3609	0.0041	0.04976	0.00041	0.337	312.8	3.1	313.1	2.5	304	24	313.1	2.5	0.10	
6-Morillo_116	245	1.90	0.3480	0.0052	0.04881	0.00049	0.132	303.1	3.9	307.2	3	268	34	307.2	3.0	1.35	
6-Morillo_117	188	0.86	0.7800	0.0110	0.09442	0.00096	0.556	585.2	6.1	581.6	5.6	594	29	581.6	5.6	0.62	
6-Morillo_118	949	1.50	0.3909	0.0038	0.05316	0.00052	0.675	335	2.8	333.9	3.2	354	16	333.9	3.2	0.33	
6-Morillo_119	326	1.71	0.5228	0.0063	0.06786	0.00073	0.516	427.4	4.3	423.2	4.4	463	22	423.2	4.4	0.98	
6-Morillo_120	170	1.82	0.3567	0.0068	0.04911	0.00064	0.311	309.5	5.1	309	3.9	322	42	309.0	3.9	0.16	
5-Morillo_1	347	2.55	0.3494	0.0050	0.04717	0.00043	0.346	304.1	3.7	297.1	2.7	356	32	297.1	2.7	2.30	
5-Morillo_2	82.7	1.51	0.3811	0.0078	0.05329	0.00082	0.236	328.2	5.6	334.7	5	300	50	334.7	5.0	1.98	
5-Morillo_3	191	2.30	0.3637	0.0070	0.05043	0.00046	0.148	314.7	5.2	317.1	2.8	308	43	317.1	2.8	0.76	
5-Morillo_4	931	8.20	0.3538	0.0034	0.04828	0.00043	0.396	307.5	2.5	304.3	2.6	335	23	304.3	2.6	1.04	
5-Morillo_5	210	1.43	1.4720	0.0150	0.15100	0.00190	0.505	919.7	6.5	907	10	969	22	969.0	22.0	6.40	
5-Morillo_6	185	1.44	12.0300	0.1100	0.49700	0.00530	0.820	2607.2	8.1	2603	22	2612	11	2612.0	11.0	0.34	

Sample Name _Grain #	[U] ppm	U/Th	207/235	2σ error	206/238	2σ error	RHO	207/235 Age (Ma)	2σ error	206/238 Age (Ma)	2σ error	207/206 Age (Ma)	2σ error	Best age (Ma)	2σ error	% Discordance	Rim /Core
5-Morillo_7	241	1.83	0.3343	0.0055	0.04656	0.00047	0.419	292.6	4.2	293.4	2.9	299	33	293.4	2.9	0.27	
5-Morillo_8	374	2.18	0.3457	0.0049	0.04725	0.00051	0.172	301.3	3.7	297.6	3.2	312	36	297.6	3.2	1.23	
5-Morillo_9	340	1.65	0.3559	0.0054	0.04940	0.00068	0.337	309	4	311.3	4.2	306	33	311.3	4.2	0.74	
5-Morillo_10	670	1.33	0.3480	0.0040	0.04844	0.00079	0.680	303.2	3	304.9	4.8	259	35	304.9	4.8	0.56	
5-Morillo_11	245.1	1.18	1.0920	0.0120	0.12400	0.00110	0.487	749.1	6.1	753.5	6.5	730	21	753.5	6.5	0.59	
5-Morillo_12	674	84.60	3.2080	0.0280	0.25150	0.00350	0.703	1458.8	6.7	1446	18	1480	17	1480.0	17.0	2.30	Rim
5-Morillo_12	359.9	2.06	6.1040	0.0810	0.36200	0.00420	0.597	1991	12	1991	20	2002	15	2002.0	15.0	0.55	Core
5-Morillo_13	456	2.00	0.8849	0.0088	0.10380	0.00089	0.449	643.4	4.8	636.6	5.2	682	23	636.6	5.2	1.06	
5-Morillo_14	287	2.98	0.7920	0.0100	0.09413	0.00097	0.535	592	5.9	579.9	5.7	651	23	579.9	5.7	2.04	
5-Morillo_15	289	1.43	0.3553	0.0062	0.04833	0.00060	0.488	308.5	4.6	304.2	3.7	334	34	304.2	3.7	1.39	
5-Morillo_16	222	2.00	5.9930	0.0510	0.34900	0.00300	0.420	1974.6	7.4	1930	14	2021	18	2021.0	18.0	4.50	
5-Morillo_17	287	1.69	0.3683	0.0071	0.04923	0.00066	0.009	318.3	5.3	309.8	4.1	401	47	309.8	4.1	2.67	
5-Morillo_18	217	2.39	0.3495	0.0054	0.04787	0.00050	0.261	304.2	4.1	301.4	3	316	40	301.4	3.0	0.92	
5-Morillo_19	498	1.37	0.3655	0.0047	0.04920	0.00047	0.185	316.2	3.5	309.6	2.9	369	35	309.6	2.9	2.09	
5-Morillo_20	523	2.37	0.3420	0.0100	0.04820	0.00140	0.469	298.4	7.7	303.3	8.6	265	76	303.3	8.6	1.64	Rim
5-Morillo_20	274.3	5.43	0.7060	0.0100	0.08660	0.00100	0.314	543.1	5.9	535.6	6	586	31	535.6	6.0	1.38	Core
5-Morillo_24	340	2.96	0.3641	0.0062	0.05022	0.00072	0.642	315.1	4.6	315.9	4.4	298	28	315.9	4.4	0.25	
5-Morillo_21	406	1.34	0.3381	0.0044	0.04649	0.00043	0.322	295.6	3.3	292.9	2.7	326	29	292.9	2.7	0.91	
5-Morillo_22	533	1.38	0.3414	0.0042	0.04673	0.00049	0.663	298.2	3.2	294.4	3	324	24	294.4	3.0	1.27	
5-Morillo_23	214	1.45	0.3572	0.0063	0.04878	0.00049	0.330	311	4.7	307	3	358	36	307.0	3.0	1.29	
5-Morillo_25	538	1.44	0.3467	0.0039	0.04754	0.00048	0.367	302.1	2.9	299.4	2.9	333	27	299.4	2.9	0.89	
5-Morillo_26	535	1.35	0.3425	0.0045	0.04698	0.00046	0.036	298.9	3.4	295.9	2.9	319	26	295.9	2.9	1.00	
5-Morillo_27	293	1.19	0.3491	0.0055	0.04840	0.00060	0.172	303.9	4.1	304.7	3.7	291	37	304.7	3.7	0.26	
5-Morillo_29	458	1.52	0.3480	0.0052	0.04800	0.00051	0.385	303.1	3.9	302.2	3.1	315	32	302.2	3.1	0.30	
5-Morillo_30	323	1.38	0.3408	0.0048	0.04669	0.00043	0.396	297.6	3.7	294.1	2.6	332	31	294.1	2.6	1.18	

Sample Name _Grain #	[U] ppm	U/Th	207/235	2σ error	206/238	2σ error	RHO	207/235 Age (Ma)	2σ error	206/238 Age (Ma)	2σ error	207/206 Age (Ma)	2σ error	Best age (Ma)	2σ error	% Discordance	Rim /Core
5-Morillo_31	80.7	1.19	5.5210	0.0530	0.34470	0.00380	0.536	1904.3	8.4	1909	18	1896	17	1896.0	17.0	0.69	
5-Morillo_32	430.3	108.70	0.3457	0.0072	0.04725	0.00090	0.272	301.4	5.4	297.6	5.5	274	41	297.6	5.5	1.26	
5-Morillo_33	257	0.54	0.8157	0.0091	0.09620	0.00110	0.329	605.4	5.1	592.1	6.3	656	27	592.1	6.3	2.20	
5-Morillo_35	333	2.16	0.3336	0.0059	0.04596	0.00058	0.462	293.2	4.5	289.7	3.6	312	38	289.7	3.6	1.19	
5-Morillo_36	243	1.94	0.3392	0.0062	0.04742	0.00062	0.374	297	4.6	298.7	3.8	278	40	298.7	3.8	0.57	
5-Morillo_37	217	1.47	0.3318	0.0058	0.04612	0.00054	0.352	290.8	4.4	290.6	3.3	291	41	290.6	3.3	0.07	
5-Morillo_38	336.9	1.33	0.3631	0.0067	0.04919	0.00059	0.471	314.4	5	309.5	3.6	353	38	309.5	3.6	1.56	
5-Morillo_39	557	1.76	0.3396	0.0039	0.04667	0.00035	0.340	296.8	2.9	294	2.1	309	26	294.0	2.1	0.94	
5-Morillo_40	369	3.09	0.3577	0.0060	0.04836	0.00066	0.220	311.2	4.6	304.4	4	347	42	304.4	4.0	2.19	
5-Morillo_41	242	1.82	0.3330	0.0060	0.04660	0.00053	0.293	291.7	4.5	293.6	3.3	281	43	293.6	3.3	0.65	
5-Morillo_42	475	2.46	0.6225	0.0074	0.07901	0.00074	0.480	491.2	4.6	490.2	4.4	502	23	490.2	4.4	0.20	
5-Morillo_43	482	2.95	0.3410	0.0130	0.04510	0.00190	0.530	297.6	9.5	284	12	415	91	284.0	12.0	4.57	
5-Morillo_45	220	0.67	12.1220	0.0810	0.48640	0.00450	0.657	2613.5	6.2	2555	20	2664	10	2664.0	10.0	4.09	
5-Morillo_46	177.3	1.42	0.3244	0.0060	0.04530	0.00051	0.344	285.1	4.6	285.6	3.1	287	43	285.6	3.1	0.18	
5-Morillo_47	292	2.09	0.3583	0.0061	0.04916	0.00059	0.165	310.8	4.6	309.3	3.6	325	43	309.3	3.6	0.48	
5-Morillo_48	188	2.33	0.3583	0.0072	0.04919	0.00057	0.231	310.7	5.4	309.6	3.5	324	44	309.6	3.5	0.35	
5-Morillo_49	160	1.24	0.3417	0.0062	0.04727	0.00050	0.128	298.3	4.7	297.7	3.1	291	42	297.7	3.1	0.20	
5-Morillo_50	361	1.88	0.3492	0.0089	0.04570	0.00110	0.616	304.6	6.8	288	6.6	438	49	288.0	6.6	5.45	
5-Morillo_51	263	1.66	0.3295	0.0054	0.04486	0.00055	0.442	289.1	4.1	282.9	3.4	331	37	282.9	3.4	2.14	
5-Morillo_52	604	1.80	0.3312	0.0058	0.04568	0.00055	0.507	290.4	4.4	287.9	3.4	303	35	287.9	3.4	0.86	
5-Morillo_53	69	0.91	0.7940	0.0160	0.09440	0.00100	0.138	593.8	8.8	581.4	6.1	631	47	581.4	6.1	2.09	
5-Morillo_54	470	2.55	0.3504	0.0066	0.04760	0.00063	0.601	304.8	5	299.8	3.9	334	33	299.8	3.9	1.64	
5-Morillo_55	680	2.82	0.3222	0.0043	0.04293	0.00045	0.455	283.5	3.3	271	2.8	369	28	271.0	2.8	4.41	
5-Morillo_56	319	1.28	0.3335	0.0045	0.04590	0.00052	0.224	292.2	3.4	289.3	3.2	316	39	289.3	3.2	0.99	
5-Morillo_57	127.3	1.82	0.3484	0.0074	0.04718	0.00059	0.167	303.3	5.6	297.1	3.6	358	50	297.1	3.6	2.04	

Sample Name _Grain #	[U] ppm	U/Th	207/235	2σ error	206/238	2σ error	RHO	207/235 Age (Ma)	2σ error	206/238 Age (Ma)	2σ error	207/206 Age (Ma)	2σ error	Best age (Ma)	2σ error	% Discordance	Rim /Core
5-Morillo_59	1380	3.57	0.3608	0.0060	0.04699	0.00091	0.655	312.7	4.5	296	5.6	444	35	296.0	5.6	5.34	
5-Morillo_60	314	1.34	0.3410	0.0048	0.04632	0.00060	0.389	297.8	3.6	291.9	3.7	342	34	291.9	3.7	1.98	
5-Morillo_61	284	1.81	0.3443	0.0056	0.04724	0.00050	0.330	300.2	4.2	297.6	3.1	331	33	297.6	3.1	0.87	
5-Morillo_62	491	3.89	0.3565	0.0054	0.04705	0.00054	0.506	309.4	4	296.4	3.3	418	28	296.4	3.3	4.20	
5-Morillo_63	1433	6.91	0.2273	0.0042	0.02298	0.00049	0.843	207.9	3.5	146.5	3.1	983	23	DISC	DISC	29.53	
5-Morillo_64	466	1.75	0.3619	0.0044	0.04847	0.00033	0.335	313.5	3.3	305.1	2.1	386	26	305.1	2.1	2.68	
5-Morillo_65	271	80.60	0.3561	0.0091	0.04738	0.00084	0.159	309.1	6.8	298.4	5.2	359	73	298.4	5.2	3.46	
5-Morillo_66	354	1.32	0.3439	0.0038	0.04776	0.00043	0.211	300	2.8	300.8	2.6	307	29	300.8	2.6	0.27	
5-Morillo_67	47.3	0.48	0.7750	0.0190	0.09440	0.00120	0.044	583	11	581.7	6.9	571	58	581.7	6.9	0.22	
5-Morillo_68	184	1.93	0.3651	0.0058	0.05010	0.00070	0.116	316.4	4.4	315.1	4.3	333	46	315.1	4.3	0.41	
5-Morillo_69	652	2.22	0.3835	0.0048	0.05177	0.00060	0.101	329.6	3.5	325.3	3.7	347	33	325.3	3.7	1.30	
5-Morillo_70	125.8	2.13	0.3604	0.0065	0.04863	0.00068	0.225	312.3	4.8	306	4.2	351	47	306.0	4.2	2.02	
5-Morillo_71	238	1.92	0.3869	0.0061	0.05008	0.00061	0.199	331.9	4.5	315	3.7	463	39	315.0	3.7	5.09	
5-Morillo_72	332	1.63	0.3310	0.0043	0.04563	0.00046	0.283	290.3	3.3	287.6	2.8	299	34	287.6	2.8	0.93	
5-Morillo_73	883	4.92	0.3397	0.0064	0.04605	0.00059	0.673	297.5	4.8	290.2	3.6	374	28	290.2	3.6	2.45	
5-Morillo_74	109.4	1.23	1.7800	0.0260	0.17220	0.00180	0.188	1037.3	9.7	1024.2	9.9	1071	30	1071.0	30.0	4.37	
5-Morillo_75	418.8	2.15	0.3439	0.0059	0.04766	0.00056	0.299	300	4.4	300.1	3.4	315	41	300.1	3.4	0.03	
5-Morillo_76	218	1.72	0.3452	0.0059	0.04727	0.00052	0.134	301	4.5	297.7	3.2	339	45	297.7	3.2	1.10	
5-Morillo_77	488	1.68	0.3515	0.0050	0.04862	0.00050	0.439	305.7	3.8	306	3.1	313	31	306.0	3.1	0.10	
5-Morillo_78	306	1.79	0.3593	0.0059	0.04865	0.00047	0.298	311.5	4.4	306.2	2.9	323	36	306.2	2.9	1.70	
5-Morillo_79	165.1	1.50	1.4980	0.0220	0.15310	0.00200	0.633	929.2	8.9	918	11	965	24	965.0	24.0	4.87	
5-Morillo_80	455	124.00	0.3520	0.0066	0.04786	0.00057	0.470	306.1	5	301.4	3.5	334	39	301.4	3.5	1.54	
5-Morillo_81	511	2.01	0.3410	0.0045	0.04699	0.00055	0.440	297.8	3.4	296	3.4	310	29	296.0	3.4	0.60	
5-Morillo_82	213	1.84	0.3434	0.0059	0.04697	0.00058	0.324	300.7	4.5	295.9	3.6	353	38	295.9	3.6	1.60	
5-Morillo_83	415	1.57	0.3789	0.0068	0.04950	0.00066	0.634	326	5	311.4	4.1	421	30	311.4	4.1	4.48	

Sample Name _Grain #	[U] ppm	U/Th	207/235	2σ error	206/238	2σ error	RHO	207/235 Age (Ma)	2σ error	206/238 Age (Ma)	2σ error	207/206 Age (Ma)	2σ error	Best age (Ma)	2σ error	% Discordance	Rim /Core
5-Morillo_84	24.7	1.04	1.5830	0.0360	0.15820	0.00240	0.338	966	14	946	13	1021	48	1021.0	48.0	7.35	
5-Morillo_85	266	2.39	0.3631	0.0058	0.04952	0.00057	0.296	314.3	4.3	311.6	3.5	329	40	311.6	3.5	0.86	
5-Morillo_86	402	1.39	0.3495	0.0040	0.04882	0.00041	0.108	304.3	3	307.3	2.5	280	32	307.3	2.5	0.99	
5-Morillo_87	254	1.75	0.3420	0.0089	0.04465	0.00091	0.252	299.9	7.1	281.6	5.6	454	67	281.6	5.6	6.10	
5-Morillo_88	60.7	2.95	0.9070	0.0160	0.10330	0.00150	0.276	654.7	8.3	633.7	9	739	42	633.7	9.0	3.21	
5-Morillo_89	175	2.91	0.3561	0.0064	0.04856	0.00049	0.134	309.1	4.8	305.7	3	332	42	305.7	3.0	1.10	
5-Morillo_90	684	1.46	0.3542	0.0058	0.04783	0.00068	0.676	308.3	4.2	301.2	4.2	360	26	301.2	4.2	2.30	
5-Morillo_91	482	2.01	0.3584	0.0044	0.04898	0.00045	0.472	310.9	3.3	308.3	2.8	333	26	308.3	2.8	0.84	
5-Morillo_92	90.8	1.53	5.1190	0.0540	0.31570	0.00280	0.556	1841.2	8.9	1768	14	1932	16	1932.0	16.0	8.49	
5-Morillo_93	603	1.97	0.3467	0.0044	0.04590	0.00058	0.402	302.1	3.3	289.3	3.6	395	31	289.3	3.6	4.24	
5-Morillo_94	172	1.11	24.8600	0.1900	0.65860	0.00670	0.700	3302.7	7.4	3266	27	3326	12	3326.0	12.0	1.80	
5-Morillo_95	566	1.69	0.3407	0.0045	0.04576	0.00044	0.305	297.6	3.4	288.4	2.7	374	31	288.4	2.7	3.09	
5-Morillo_96	429	2.28	0.3341	0.0050	0.04197	0.00044	0.249	292.6	3.8	265	2.7	519	39	265.0	2.7	9.43	
5-Morillo_98	460	1.14	0.3610	0.0110	0.04818	0.00067	0.150	312.6	8.3	303.4	4.1	337	55	303.4	4.1	2.94	
5-Morillo_100	197	2.02	0.3781	0.0072	0.04943	0.00057	0.330	325.4	5.3	311	3.5	435	42	311.0	3.5	4.43	
5-Morillo_101	496	1.45	0.3427	0.0044	0.04722	0.00039	0.240	299.1	3.3	297.4	2.4	314	29	297.4	2.4	0.57	
5-Morillo_102	456	3.96	0.3565	0.0048	0.04857	0.00041	0.244	310	3.5	305.7	2.5	330	33	305.7	2.5	1.39	
5-Morillo_103	374	1.35	0.3424	0.0057	0.04733	0.00051	0.377	298.8	4.3	298.1	3.2	305	34	298.1	3.2	0.23	
5-Morillo_104	425	1.70	0.3552	0.0048	0.04910	0.00048	0.289	308.5	3.6	309	2.9	324	31	309.0	2.9	0.16	
5-Morillo_105	130.5	2.13	0.3518	0.0065	0.04864	0.00059	0.184	305.9	4.9	306.2	3.7	321	49	306.2	3.7	0.10	
5-Morillo_106	351	1.68	0.3610	0.0040	0.04803	0.00035	0.060	312.9	3	302.4	2.2	399	32	302.4	2.2	3.36	
5-Morillo_107	407	1.69	0.3720	0.0049	0.05108	0.00051	0.205	321	3.6	321.1	3.1	327	33	321.1	3.1	0.03	
5-Morillo_108	259	1.85	6.4910	0.0410	0.36560	0.00250	0.637	2044.4	5.6	2008	12	2082	10	2082.0	10.0	3.55	
5-Morillo_109	439	1.12	7.9750	0.0670	0.35870	0.00380	0.818	2228.9	7.8	1976	18	2472	10	2471.9	9.9	20.06	
5-Morillo_110	206	1.09	0.3499	0.0056	0.04712	0.00057	0.257	304.5	4.2	296.8	3.5	364	39	296.8	3.5	2.53	

Sample Name _Grain #	[U] ppm	U/Th	207/235	2σ error	206/238	2σ error	RHO	207/235 Age (Ma)	2σ error	206/238 Age (Ma)	2σ error	207/206 Age (Ma)	2σ error	Best age (Ma)	2σ error	% Discordance	Rim /Core
5-Morillo_111	59.1	3.40	1.0210	0.0170	0.11480	0.00130	0.256	714.9	8.9	701.8	7.9	744	36	701.8	7.9	1.83	
5-Morillo_112	158	0.97	2.7610	0.0250	0.22420	0.00160	0.498	1345.4	6.7	1304.1	8.2	1413	16	1413.0	16.0	7.71	
5-Morillo_114	242	2.02	0.3471	0.0063	0.04786	0.00082	0.441	302.3	4.8	301.3	5	281	45	301.3	5.0	0.33	
5-Morillo_115	348	1.58	0.3624	0.0045	0.04970	0.00046	0.370	313.9	3.3	312.7	2.8	337	28	312.7	2.8	0.38	
5-Morillo_116	463	1.91	0.3687	0.0067	0.04887	0.00084	0.036	318.7	5	307.6	5.2	376	64	307.6	5.2	3.48	
5-Morillo_117	24.7	0.45	5.2570	0.0830	0.31520	0.00440	0.553	1862	14	1765	21	1956	27	1956.0	27.0	9.76	
5-Morillo_118	408	1.86	0.7180	0.0120	0.08020	0.00140	0.679	550.2	7	497.2	8.2	783	30	497.2	8.2	9.63	
5-Morillo_119	234	1.42	0.3466	0.0056	0.04816	0.00044	0.224	302	4.2	303.2	2.7	295	37	303.2	2.7	0.40	
14AB-A04_1	218	2.05	0.3290	0.0130	0.04660	0.00170	0.469	288.3	9.9	293	10	269	87	293.0	10.0	1.63	
14AB-A04_2	399	2.35	0.2743	0.0092	0.03228	0.00093	0.706	245.8	7.3	204.8	5.8	683	56	DISC	DISC	16.68	
14AB-A04_3	1430	4.55	0.2590	0.0086	0.03100	0.00110	0.818	233.5	7	196.6	7.1	614	44	DISC	DISC	15.80	
14AB-A04_4	89.4	2.16	0.3360	0.0150	0.04390	0.00180	0.251	296	11	277	11	430	120	277.0	11.0	6.42	
14AB-A04_5	132	25.60	0.4090	0.0130	0.05470	0.00150	0.521	347.6	9.2	343.3	8.9	360	64	343.3	8.9	1.24	
14AB-A04_6	353	1.88	0.3920	0.0110	0.05250	0.00110	0.647	336.5	7.7	329.9	6.7	369	44	329.9	6.7	1.96	
14AB-A04_7	181	1.56	0.3940	0.0120	0.05390	0.00100	0.357	338.1	9.3	338.2	6.3	336	73	338.2	6.3	0.03	
14AB-A04_8	236	2.52	12.8500	0.2500	0.54200	0.00880	0.627	2666	18	2790	37	2571	25	2571.0	25.0	8.52	
14AB-A04_9	159	2.39	0.3767	0.0097	0.05120	0.00120	0.482	325.2	7.3	321.6	7.5	344	57	321.6	7.5	1.11	
14AB-A04_10	139	2.36	0.3779	0.0078	0.05208	0.00083	0.124	325.2	5.7	327.2	5.1	303	51	327.2	5.1	0.62	
14AB-A04_11	880	11.22	0.4070	0.0160	0.04134	0.00087	0.562	346	12	261.1	5.4	946	57	DISC	DISC	24.54	
14AB-A04_12	363	142.00	0.3543	0.0076	0.04805	0.00083	0.316	307.7	5.7	302.5	5.1	345	53	302.5	5.1	1.69	
14AB-A04_13	115.7	1.73	3.8790	0.0580	0.29530	0.00430	0.642	1608	12	1674	22	1530	23	1530.0	23.0	9.41	
14AB-A04_14	148	0.95	1.9370	0.0530	0.18370	0.00480	0.669	1091	18	1086	26	1092	43	1092.0	43.0	0.55	
14AB-A04_15	619	3.15	0.3222	0.0056	0.04332	0.00084	0.781	283.5	4.3	273.3	5.2	342	27	273.3	5.2	3.60	
14AB-A04_16	367	3.41	0.3727	0.0063	0.05154	0.00086	0.396	321.5	4.7	324	5.3	301	41	324.0	5.3	0.78	
14AB-A04_18	565	193.00	0.4040	0.0110	0.05530	0.00180	0.746	344.1	7.6	347	11	340	47	347.0	11.0	0.84	Rim

Sample Name _Grain #	[U] ppm	U/Th	207/235	2σ error	206/238	2σ error	RHO	207/235 Age (Ma)	2σ error	206/238 Age (Ma)	2σ error	207/206 Age (Ma)	2σ error	Best age (Ma)	2σ error	% Discordance	Rim /Core
14AB-A04_18	104.4	0.93	0.8190	0.0330	0.09880	0.00280	0.486	606	18	607	16	608	81	607.0	16.0	0.17	Core
14AB-A04_19	118	1.11	7.5400	0.1000	0.43920	0.00660	0.711	2176	12	2351	29	2020	19	2020.0	19.0	16.39	
14AB-A04_20	279	3.13	0.5980	0.0140	0.07540	0.00180	0.857	475.4	8.7	469	11	505	52	469.0	11.0	1.35	Rim
14AB-A04_20	172	0.59	1.0660	0.0270	0.12040	0.00230	0.637	736	13	733	13	755	43	733.0	13.0	0.41	Core
14AB-A04_21	205	5.54	0.2810	0.0120	0.03800	0.00130	0.685	252.4	9.6	240.7	8.4	379	67	240.7	8.4	4.64	
14AB-A04_22	181.4	0.50	0.8530	0.0140	0.10110	0.00130	0.431	625.5	7.6	621	7.6	640	35	621.0	7.6	0.72	
14AB-A04_23	39.1	0.93	1.9950	0.0550	0.19460	0.00530	0.606	1119	19	1145	29	1049	50	1049.0	50.0	9.15	
14AB-A04_24	412	171.00	0.3900	0.0110	0.05400	0.00150	0.669	334.2	8	339.2	9	250	51	339.2	9.0	1.50	
14AB-A04_25	345	2.64	0.3707	0.0080	0.05133	0.00095	0.531	319.8	5.9	322.6	5.8	292	42	322.6	5.8	0.88	
14AB-A04_26	194.6	2.23	0.3541	0.0066	0.04756	0.00069	0.233	308.4	5.1	299.5	4.2	363	52	299.5	4.2	2.89	
14AB-A04_27	298	5.25	0.6060	0.0140	0.07570	0.00140	0.635	480.3	8.7	470.4	8.4	530	40	470.4	8.4	2.06	
14AB-A04_28	315	4.47	1.4330	0.0400	0.13400	0.00380	0.837	901	17	811	22	1157	28	811.0	22.0	9.99	
14AB-A04_29	264	3.91	0.7437	0.0095	0.09080	0.00110	0.435	564.3	5.5	560.1	6.7	576	33	560.1	6.7	0.74	
14AB-A04_30	325	5.40	0.3065	0.0079	0.04200	0.00110	0.507	271.1	6.1	264.9	6.9	322	59	264.9	6.9	2.29	
14AB-A04_31	492	1.89	0.3726	0.0071	0.05093	0.00095	0.638	321.3	5.3	320.2	5.8	327	36	320.2	5.8	0.34	
14AB-A04_32	75.4	1.25	0.9150	0.0250	0.10550	0.00230	0.330	658	13	646	13	717	60	646.0	13.0	1.82	
14AB-A04_33	31	2.39	0.8980	0.0400	0.10620	0.00350	0.072	649	21	650	20	620	120	650.0	20.0	0.15	
14AB-A04_34	760	54.30	0.4242	0.0071	0.05894	0.00096	0.687	358.9	5.1	369.1	5.8	306	33	369.1	5.8	2.84	
14AB-A04_35	22.4	3.84	8.1100	0.2400	0.37700	0.01300	0.727	2242	27	2059	60	2401	45	2401.0	45.0	14.24	
14AB-A04_36	427	10.95	0.3150	0.0150	0.03650	0.00180	0.823	277	11	231	11	729	63	DISC	DISC	16.61	
14AB-A04_37	669	50.00	0.3812	0.0097	0.05160	0.00140	0.773	328.3	7	324.3	8.5	347	37	324.3	8.5	1.22	
14AB-A04_38	876	100.00	0.4020	0.0110	0.05620	0.00150	0.876	342.5	7.8	352.4	9	268	30	352.4	9.0	2.89	
14AB-A04_39	54.9	1.00	1.0270	0.0280	0.11890	0.00240	0.219	717	14	727	13	707	60	727.0	13.0	1.39	
14AB-A04_40	88.2	1.83	0.3430	0.0180	0.04390	0.00160	0.363	301	14	276.6	9.9	480	110	276.6	9.9	8.11	
14AB-A04_41	430	74.20	0.3657	0.0076	0.05189	0.00096	0.267	316.2	5.7	326.1	5.9	241	45	326.1	5.9	3.13	

Sample Name _Grain #	[U] ppm	U/Th	207/235	2σ error	206/238	2σ error	RHO	207/235 Age (Ma)	2σ error	206/238 Age (Ma)	2σ error	207/206 Age (Ma)	2σ error	Best age (Ma)	2σ error	% Discordance	Rim /Core
14AB-A04_42	96.4	1.02	0.8820	0.0250	0.10500	0.00250	0.349	642	13	643	14	614	60	643.0	14.0	0.16	
14AB-A04_43	177	4.27	0.7840	0.0160	0.09990	0.00220	0.692	589	9.2	613	13	530	36	613.0	13.0	4.07	
14AB-A04_44	267	3.17	0.2850	0.0100	0.03940	0.00130	0.495	254.1	8.2	248.8	8	331	84	248.8	8.0	2.09	
14AB-A04_45	549	18.44	0.9720	0.0470	0.09660	0.00150	0.063	688	24	594.2	9.1	990	110	DISC	DISC	13.63	
14AB-A04_46	222	1.85	0.3830	0.0100	0.05050	0.00110	0.417	328.5	7.4	317.3	6.6	401	57	317.3	6.6	3.41	
14AB-A04_47	142.9	5.67	0.6370	0.0140	0.07960	0.00130	0.501	500.8	9.1	493.4	7.6	529	42	493.4	7.6	1.48	
14AB-A04_48	1480	16.00	0.2750	0.0110	0.03420	0.00110	0.547	246.4	8.8	216.7	6.9	545	56	DISC	DISC	12.05	
14AB-A04_49	45.4	1.48	0.6710	0.0230	0.08830	0.00210	0.155	519	14	545	12	360	84	545.0	12.0	5.01	
14AB-A04_50	113.7	4.26	1.7530	0.0430	0.17590	0.00440	0.664	1029	16	1044	24	1024	45	1024.0	45.0	1.95	
14AB-A04_51	165	2.78	0.7670	0.0230	0.09530	0.00240	0.619	581	14	586	14	557	49	586.0	14.0	0.86	
14AB-A04_52	285	2.57	0.3709	0.0088	0.05079	0.00097	0.360	320.1	6.5	319.3	6	337	55	319.3	6.0	0.25	
14AB-A04_53	891	4.99	0.4490	0.0120	0.06080	0.00160	0.748	376	8.3	380.5	9.7	307	38	380.5	9.7	1.20	
14AB-A04_54	317	2.02	0.3810	0.0100	0.05052	0.00096	0.247	327.7	7.3	317.7	5.9	377	68	317.7	5.9	3.05	
14AB-A04_55	506	3.59	0.3350	0.0120	0.04430	0.00150	0.725	293	9.1	279.1	9.1	381	60	279.1	9.1	4.74	
14AB-A04_56	236	2.74	0.3776	0.0080	0.05013	0.00083	0.376	325.1	5.9	315.3	5.1	388	51	315.3	5.1	3.01	
14AB-A04_57	170.2	1.14	6.1000	0.1500	0.37480	0.00870	0.857	1989	21	2051	41	1905	23	1905.0	23.0	7.66	
14AB-A04_58	444	1.55	0.3964	0.0095	0.05360	0.00120	0.675	339.5	6.8	336.7	7.4	356	44	336.7	7.4	0.82	
14AB-A04_59	268	1.94	0.3661	0.0074	0.04926	0.00066	0.475	317.2	5.6	310	4.1	381	41	310.0	4.1	2.27	
14AB-A04_60	57.3	1.69	1.9710	0.0350	0.19110	0.00300	0.482	1104	12	1127	16	1076	35	1076.0	35.0	4.74	
14AB-A04_61	186	1.87	0.3536	0.0083	0.04865	0.00063	0.280	307.1	6.2	306.2	3.9	322	46	306.2	3.9	0.29	
14AB-A04_62	476	1.39	0.6970	0.0290	0.08230	0.00440	0.697	536	17	510	26	611	83	510.0	26.0	4.85	
14AB-A04_63	37.4	1.43	2.2150	0.0770	0.19970	0.00480	0.559	1187	25	1173	26	1236	59	1236.0	59.0	5.10	
14AB-A04_64	877	1.82	0.4689	0.0065	0.06490	0.00120	0.572	390.3	4.5	405.3	7.1	290	36	405.3	7.1	3.84	
14AB-A04_65	90.4	0.92	1.0090	0.0260	0.11850	0.00300	0.366	707	13	721	17	662	57	721.0	17.0	1.98	
14AB-A04_66	675	3.57	0.3270	0.0140	0.03570	0.00130	0.746	286	11	226	7.8	812	61	DISC	DISC	20.98	

Sample Name _Grain #	[U] ppm	U/Th	207/235	2σ error	206/238	2σ error	RHO	207/235 Age (Ma)	2σ error	206/238 Age (Ma)	2σ error	207/206 Age (Ma)	2σ error	Best age (Ma)	2σ error	% Discordance	Rim /Core
14AB-A04_67	12.44	8.43	0.4240	0.0300	0.05300	0.00180	0.107	354	22	332	11	410	150	332.0	11.0	6.21	
14AB-A04_68	154	3.24	0.3877	0.0098	0.05398	0.00080	0.272	332.2	7.2	338.8	4.9	260	60	338.8	4.9	1.99	
14AB-A04_69	103.3	1.72	0.6810	0.0150	0.08610	0.00150	0.141	526.5	9.2	532.1	8.8	526	57	532.1	8.8	1.06	
14AB-A04_70	418	3.73	0.4220	0.0100	0.05560	0.00120	0.626	359.2	7.1	348.7	7.5	372	43	348.7	7.5	2.92	
14AB-A04_71	279	1.85	18.5700	0.3100	0.63800	0.01200	0.791	3021	17	3178	46	2907	18	2907.0	18.0	9.32	
14AB-A04_72	282	1.60	0.6100	0.0110	0.07700	0.00140	0.669	484.6	7.2	477.9	8.1	479	32	477.9	8.1	1.38	
14AB-A04_73	165	1.11	0.3712	0.0088	0.05044	0.00077	0.499	320.1	6.5	317.2	4.7	344	47	317.2	4.7	0.91	
14AB-A04_74	396	2.12	0.3891	0.0061	0.05357	0.00095	0.391	334.1	4.6	336.4	5.8	301	44	336.4	5.8	0.69	
14AB-A04_75	548	239.00	0.3930	0.0150	0.05540	0.00170	0.575	336	11	347	10	275	89	347.0	10.0	3.27	
14AB-A04_76	917	17.90	0.3450	0.0140	0.04680	0.00200	0.888	300	10	295	12	347	46	295.0	12.0	1.67	
14AB-A04_77	149	1.95	0.4484	0.0099	0.06019	0.00093	0.248	375.7	6.9	377.4	5.5	368	54	377.4	5.5	0.45	
14AB-A04_78	255	2.06	0.5867	0.0088	0.07492	0.00097	0.356	468.5	5.6	465.7	5.8	483	40	465.7	5.8	0.60	
14AB-A04_79	225	2.95	4.1820	0.0560	0.32060	0.00460	0.685	1670	11	1792	22	1528	20	1528.0	20.0	17.28	
14AB-A04_80	974	4.37	0.2355	0.0075	0.02772	0.00068	0.578	214.5	6.2	176.3	4.3	687	61	DISC	DISC	17.81	
14AB-A04_81	138	2.51	0.7920	0.0160	0.09840	0.00200	0.356	592.6	9.5	605	12	566	41	605.0	12.0	2.09	
14AB-A04_82	741	20.88	14.8900	0.2200	0.61400	0.00950	0.551	2808	13	3084	38	2609	21	2609.0	21.0	18.21	
14AB-A04_83	1090	2.84	0.2370	0.0049	0.02721	0.00071	0.471	215.9	4	173.1	4.4	706	52	DISC	DISC	19.82	
14AB-A04_84	70.7	1.24	5.1300	0.1200	0.32830	0.00730	0.762	1838	20	1829	36	1840	28	1840.0	28.0	0.60	
14AB-A04_85	68.8	0.82	1.8500	0.0280	0.18080	0.00300	0.546	1063.7	9.8	1071	17	1056	29	1056.0	29.0	1.42	
14AB-A04_86	176	2.00	0.3930	0.0110	0.05340	0.00130	0.424	336.2	8.2	335.5	8	318	64	335.5	8.0	0.21	
14AB-A04_87	127.4	3.73	1.0070	0.0200	0.11830	0.00140	0.357	706	10	720.8	8.3	663	41	720.8	8.3	2.10	
14AB-A04_88	62.8	1.79	1.0710	0.0360	0.12190	0.00320	0.003	737	18	741	18	710	74	741.0	18.0	0.54	
14AB-A04_89	342	2.59	0.3668	0.0078	0.05127	0.00094	0.648	316.9	5.8	322.2	5.8	291	37	322.2	5.8	1.67	
14AB-A04_90	165	1.99	0.4490	0.0350	0.05970	0.00210	0.058	373	21	373	13	340	100	373.0	13.0	0.00	
14AB-A04_91	298	2.85	0.3148	0.0098	0.04280	0.00090	0.528	277.5	7.5	270.2	5.6	356	58	270.2	5.6	2.63	

Sample Name _Grain #	[U] ppm	U/Th	207/235	2σ error	206/238	2σ error	RHO	207/235 Age (Ma)	2σ error	206/238 Age (Ma)	2σ error	207/206 Age (Ma)	2σ error	Best age (Ma)	2σ error	% Discordance	Rim /Core
14AB-A04_92	282	2.22	0.3834	0.0062	0.05259	0.00083	0.440	329.4	4.6	330.4	5.1	322	41	330.4	5.1	0.30	
14AB-A04_93	222	3.17	0.3547	0.0091	0.05000	0.00094	0.174	308	6.8	314.5	5.8	282	60	314.5	5.8	2.11	
14AB-A04_94	608	164.00	0.4038	0.0061	0.05616	0.00096	0.527	344.2	4.4	352.2	5.9	315	35	352.2	5.9	2.32	
14AB-A04_95	260	1.73	0.3680	0.0120	0.05160	0.00130	0.577	317.5	8.5	324.1	7.8	263	54	324.1	7.8	2.08	
14AB-A04_96	524	2.40	0.3748	0.0051	0.05170	0.00070	0.538	323	3.8	324.9	4.3	330	31	324.9	4.3	0.59	
14AB-A04_97	361	1.62	0.3469	0.0049	0.04786	0.00065	0.492	302.2	3.7	301.4	4	334	31	301.4	4.0	0.26	
14AB-A04_98	444	3.32	0.3970	0.0110	0.05310	0.00130	0.876	338.9	8.2	333.2	8.2	413	39	333.2	8.2	1.68	
14AB-A04_99	266	6.60	0.7010	0.0290	0.08570	0.00270	0.699	542	16	530	16	638	61	530.0	16.0	2.21	Rim
14AB-A04_99	169.4	2.99	2.4450	0.0810	0.22140	0.00550	0.581	1255	24	1289	29	1212	59	1212.0	59.0	6.35	Core
14AB-A04_100	128	1.62	1.1070	0.0250	0.12920	0.00230	0.626	759	12	783	13	684	42	783.0	13.0	3.16	
14AB-A04_101	195	2.55	0.4024	0.0092	0.05530	0.00140	0.221	343.9	6.5	346.8	8.4	340	65	346.8	8.4	0.84	
14AB-A04_102	270	7.06	0.6820	0.0100	0.08510	0.00140	0.484	527.8	6.3	526.6	8.1	521	33	526.6	8.1	0.23	
14AB-A04_103	100.7	4.52	1.6980	0.0340	0.17600	0.00330	0.566	1009	13	1045	18	935	36	935.0	36.0	11.76	
14AB-A04_104	333	3.02	0.3770	0.0100	0.05170	0.00100	0.683	325.2	7.5	324.9	6.4	301	42	324.9	6.4	0.09	
14AB-A04_105	217	3.67	0.3479	0.0074	0.04625	0.00081	0.279	302.9	5.6	291.4	5	349	55	291.4	5.0	3.80	
14AB-A04_106	320.2	2.01	0.3506	0.0074	0.04754	0.00079	0.504	304.9	5.6	299.4	4.9	293	41	299.4	4.9	1.80	
14AB-A04_107	184.8	1.71	0.3656	0.0086	0.05033	0.00094	0.392	317	6.3	316.5	5.8	331	52	316.5	5.8	0.16	
14AB-A04_108	186	2.52	0.3749	0.0094	0.04930	0.00110	0.491	322.9	6.9	310	6.9	383	57	310.0	6.9	4.00	
14AB-A04_109	128.5	1.80	0.4250	0.0120	0.04970	0.00110	0.418	360.1	8.4	312.8	6.9	624	48	DISC	DISC	13.14	
14AB-A04_110	72.4	2.53	1.3310	0.0380	0.13610	0.00360	0.308	857	17	828	20	908	68	828.0	20.0	3.38	
14AB-A04_111	476	87.40	0.3750	0.0200	0.05080	0.00210	0.825	322	15	320	13	346	67	320.0	13.0	0.62	Rim
14AB-A04_111	264.8	5.40	0.7960	0.0160	0.09420	0.00190	0.537	593.9	9.2	582	12	630	39	582.0	12.0	2.00	Core
14AB-A04_112	56.3	0.54	6.1800	0.1000	0.36830	0.00650	0.473	2000	15	2020	30	1978	31	1978.0	31.0	2.12	
14AB-A04_113	635	23.60	0.7570	0.0130	0.09330	0.00170	0.710	571.7	7.3	576	10	541	29	576.0	10.0	0.75	

Sample Name _Grain #	[U] ppm	U/Th	207/235	2σ error	206/238	2σ error	RHO	207/235 Age (Ma)	2σ error	206/238 Age (Ma)	2σ error	207/206 Age (Ma)	2σ error	Best age (Ma)	2σ error	% Discordance	Rim /Core
14AB-A04_114	535	5.21	0.3307	0.0080	0.03620	0.00110	0.672	289.8	6.1	229	6.7	797	49	DISC	DISC	20.98	
14AB-A04_115	33	2.17	0.9650	0.0340	0.11700	0.00280	0.370	687	18	713	16	575	74	713.0	16.0	3.78	
14AB-A04_116	98.8	2.24	1.2980	0.0440	0.14000	0.00390	0.664	843	20	844	22	788	57	844.0	22.0	0.12	
14AB-A04_117	156	3.85	0.6080	0.0110	0.07660	0.00150	0.442	483.4	6.9	475.5	8.9	484	48	475.5	8.9	1.63	
14AB-A04_118	275	2.42	0.3827	0.0077	0.05230	0.00083	0.480	328.7	5.7	328.6	5.1	321	44	328.6	5.1	0.03	
14AB-A04_119	423	3.37	0.3410	0.0130	0.04160	0.00150	0.588	298.1	9.5	262.9	9.4	576	64	DISC	DISC	11.81	
14AB-A04_120	183.4	2.12	0.3800	0.0110	0.05150	0.00150	0.638	327.8	8.3	323.4	9.2	363	58	323.4	9.2	1.34	
14AB-A05_1	350	2.07	0.3744	0.0067	0.05008	0.00059	0.284	322.7	4.9	315	3.6	362	36	315.0	3.6	2.39	
14AB-A05_2	164.7	4.15	0.9440	0.0160	0.11200	0.00150	0.479	675.3	8.1	684.2	8.7	652	32	684.2	8.7	1.32	
14AB-A05_3	550.5	73.30	0.4321	0.0062	0.05775	0.00073	0.502	364.5	4.4	361.9	4.4	357	30	361.9	4.4	0.71	
14AB-A05_4	407.8	1.76	15.4700	0.2100	0.53230	0.00590	0.724	2844	13	2750	25	2898	16	2898.0	16.0	5.11	
14AB-A05_5	312	1.48	0.7850	0.0130	0.09550	0.00130	0.394	588.9	7.4	587.6	7.6	586	36	587.6	7.6	0.22	
14AB-A05_6	69.8	1.69	1.0640	0.0250	0.12360	0.00190	0.229	738	12	751	11	677	58	751.0	11.0	1.76	
14AB-A05_7	259.6	3.76	0.9440	0.0140	0.11170	0.00140	0.366	674.5	7.4	682.5	7.9	628	32	682.5	7.9	1.19	
14AB-A05_8	402	2.66	0.6200	0.0120	0.07630	0.00140	0.272	489.9	7.4	474.1	8.4	522	46	474.1	8.4	3.23	
14AB-A05_9	264	1.97	0.3898	0.0079	0.05233	0.00067	0.197	333.9	5.8	328.8	4.1	360	47	328.8	4.1	1.53	
14AB-A05_10	500	2.24	0.4220	0.0094	0.05581	0.00099	0.001	357.1	6.7	350.1	6	360	46	350.1	6.0	1.96	
14AB-A05_11	320	85.80	0.9370	0.0110	0.11170	0.00110	0.158	673	5.9	682.7	6.2	628	33	682.7	6.2	1.44	
14AB-A05_12	79.5	0.78	0.8560	0.0190	0.10220	0.00160	0.114	627	10	627	9.4	633	50	627.0	9.4	0.00	
14AB-A05_13	242	3.13	0.6440	0.0130	0.08219	0.00085	0.182	504.4	8	509.1	5.1	442	45	509.1	5.1	0.93	
14AB-A05_14	525	2.78	0.5030	0.0180	0.05190	0.00062	0.493	412	12	326.2	3.8	918	61	DISC	DISC	20.83	
14AB-A05_15	97	1.74	2.9820	0.0380	0.24700	0.00250	0.346	1404	10	1423	13	1372	27	1372.0	27.0	3.72	
14AB-A05_16	205	1.21	1.9820	0.0320	0.18740	0.00240	0.593	1109	11	1107	13	1108	27	1108.0	27.0	0.09	
14AB-A05_17	370	9.18	0.6382	0.0090	0.08099	0.00096	0.289	500.9	5.6	502	5.7	482	32	502.0	5.7	0.22	
14AB-A05_18	278	1.00	1.9720	0.0360	0.19370	0.00280	0.678	1105	12	1141	15	1033	28	1033.0	28.0	10.45	

Sample Name _Grain #	[U] ppm	U/Th	207/235	2σ error	206/238	2σ error	RHO	207/235 Age (Ma)	2σ error	206/238 Age (Ma)	2σ error	207/206 Age (Ma)	2σ error	Best age (Ma)	2σ error	% Discordance	Rim /Core
14AB-A05_19	417.1	46.70	0.8130	0.0190	0.09690	0.00220	0.606	603	11	598	13	596	42	598.0	13.0	0.83	
14AB-A05_20	208	0.79	1.8550	0.0250	0.18130	0.00210	0.413	1064.6	8.9	1074	11	1042	29	1042.0	29.0	3.07	
14AB-A05_21	14.08	0.61	2.7000	0.1300	0.21070	0.00900	0.674	1333	39	1230	48	1489	86	1489.0	86.0	17.39	
14AB-A05_22	189	1.67	0.9140	0.0210	0.10750	0.00220	0.034	661	11	658	13	636	62	658.0	13.0	0.45	
14AB-A05_23	848	4.15	0.3607	0.0048	0.04950	0.00044	0.173	312.6	3.6	311.4	2.7	303	36	311.4	2.7	0.38	
14AB-A05_24	345	2.34	0.3753	0.0073	0.05187	0.00079	0.327	323.4	5.4	325.9	4.9	305	47	325.9	4.9	0.77	
14AB-A05_25	499	2.56	0.3764	0.0052	0.05194	0.00057	0.166	324.2	3.8	326.4	3.5	318	36	326.4	3.5	0.68	
14AB-A05_26	17.47	0.10	1.3310	0.0930	0.12100	0.00370	0.201	848	39	736	21	1170	140	DISC	DISC	13.21	
14AB-A05_27	257	0.82	1.1840	0.0170	0.13400	0.00150	0.264	792.7	8	810.3	8.6	752	37	810.3	8.6	2.22	
14AB-A05_28	67.9	5.70	1.3090	0.0300	0.14470	0.00300	0.203	850	14	873	17	788	57	788.0	17.0	2.71	
14AB-A05_29	264	6.00	0.8950	0.0360	0.10780	0.00300	0.631	648	19	660	18	628	73	660.0	18.0	1.85	
14AB-A05_30	725	228.00	0.9390	0.0170	0.11140	0.00180	0.560	673.5	8.6	681	10	641	39	681.0	10.0	1.11	
14AB-A05_31	172	0.90	0.7210	0.0180	0.09160	0.00140	0.355	552	11	565.1	8.2	506	56	565.1	8.2	2.37	
14AB-A05_32	674	19.70	0.6128	0.0082	0.07988	0.00099	0.565	485.1	5.2	495.3	5.9	468	27	495.3	5.9	2.10	
14AB-A05_33	99	0.65	0.7060	0.0150	0.08940	0.00150	0.118	541.7	8.7	552.1	8.9	517	53	552.1	8.9	1.92	
14AB-A05_34	374	2.11	0.3990	0.0140	0.05111	0.00054	0.380	342	10	321.3	3.3	468	72	321.3	3.3	6.05	
14AB-A05_35	315	2.17	0.3820	0.0075	0.05240	0.00077	0.062	328.2	5.5	329.2	4.7	347	50	329.2	4.7	0.30	
14AB-A05_37	424	2.05	0.3950	0.0150	0.05188	0.00077	0.565	337	11	326	4.7	414	64	326.0	4.7	3.26	
14AB-A05_38	53.8	0.94	1.3730	0.0290	0.14470	0.00230	0.126	876	13	871	13	891	54	891.0	54.0	2.24	
14AB-A05_40	115.7	2.23	6.3990	0.0900	0.35620	0.00550	0.518	2031	12	1964	26	2103	22	2103.0	22.0	6.61	
14AB-A05_45	270	1.60	0.8550	0.0130	0.10500	0.00110	0.334	627.2	7.3	643.5	6.5	567	32	643.5	6.5	2.60	
14AB-A05_46	120.4	2.36	2.7170	0.0820	0.19120	0.00500	0.735	1331	23	1127	27	1674	39	DISC	DISC	32.68	
14AB-A05_47	364	11.19	5.7100	0.0800	0.34540	0.00560	0.687	1934	13	1912	27	1971	21	1971.0	21.0	2.99	
14AB-A05_48	236	1.81	0.4490	0.0130	0.05909	0.00091	0.383	375.9	8.8	370.1	5.5	435	60	370.1	5.5	1.54	
14AB-A05_49	86.1	2.48	1.5950	0.0460	0.16390	0.00390	0.528	967	18	978	21	935	75	935.0	75.0	4.60	

Sample Name _Grain #	[U] ppm	U/Th	207/235	2σ error	206/238	2σ error	RHO	207/235 Age (Ma)	2σ error	206/238 Age (Ma)	2σ error	207/206 Age (Ma)	2σ error	Best age (Ma)	2σ error	% Discordance	Rim /Core
14AB-A05_50	501	2.70	0.3423	0.0067	0.04797	0.00071	0.359	300.8	4.9	302	4.4	286	47	302.0	4.4	0.40	
14AB-A05_51	244	2.44	1.2660	0.0180	0.12240	0.00130	0.572	831.9	7.7	744.2	7.2	1069	30	DISC	DISC	10.54	
14AB-A05_52	81.2	0.70	20.6600	0.3000	0.59860	0.00930	0.575	3122	14	3023	38	3198	22	3198.0	22.0	5.47	
14AB-A05_53	198.4	2.85	1.5630	0.0220	0.15830	0.00220	0.291	955.2	8.9	947	12	980	34	980.0	34.0	3.37	
14AB-A05_54	154.8	1.58	0.6270	0.0220	0.07870	0.00220	0.740	493	14	488	13	533	58	488.0	13.0	1.01	
14AB-A05_55	1091	6.11	10.6300	0.1500	0.46040	0.00760	0.617	2491	13	2440	34	2552	21	2552.0	21.0	4.39	
14AB-A05_56	430.6	1.65	0.3205	0.0048	0.04299	0.00063	0.229	282.7	3.6	271.3	3.9	419	41	271.3	3.9	4.03	
14AB-A05_57	655	3.30	0.5380	0.0220	0.06960	0.00190	0.722	440	13	433	12	517	44	433.0	12.0	1.59	
14AB-A05_58	586	5.12	4.9900	0.1500	0.28370	0.00900	0.902	1815	25	1608	45	2086	23	2086.0	23.0	22.91	
14AB-A05_59	161.5	3.66	0.7730	0.0130	0.09310	0.00110	0.152	581.3	7.6	573.7	6.6	588	45	573.7	6.6	1.31	
14AB-A05_60	487	6.40	0.4527	0.0086	0.05875	0.00093	0.286	379.8	5.8	368	5.7	440	43	368.0	5.7	3.11	
14AB-A05_62	1054	1.55	0.8210	0.0160	0.08720	0.00160	0.643	608.3	8.7	539	9.2	881	29	DISC	DISC	11.39	
14AB-A05_63	334	2.16	0.3458	0.0067	0.04764	0.00068	0.456	301.4	5.1	300	4.2	316	44	300.0	4.2	0.46	
14AB-A05_64	472.5	9.80	0.5922	0.0097	0.07730	0.00110	0.267	472	6.1	480.2	6.6	476	41	480.2	6.6	1.74	
14AB-A05_65	130	2.45	0.3252	0.0097	0.04565	0.00088	0.038	286.3	7.6	287.7	5.4	297	71	287.7	5.4	0.49	
14AB-A05_66	447	8.98	0.8470	0.0150	0.10380	0.00130	0.448	622.3	8.2	636.7	7.7	586	36	636.7	7.7	2.31	
14AB-A05_67	347	1.74	4.5210	0.0630	0.30620	0.00470	0.760	1738	12	1725	22	1760	19	1760.0	19.0	1.99	
14AB-A05_68	291.5	2.21	0.8500	0.0110	0.10230	0.00096	0.327	624.3	6.1	627.8	5.6	614	31	627.8	5.6	0.56	
14AB-A05_70	126.9	0.54	0.9000	0.0170	0.10570	0.00130	0.299	651.2	9.1	647.7	7.3	681	43	647.7	7.3	0.54	
14AB-A05_71	204.2	2.48	0.7310	0.0140	0.09026	0.00096	0.214	558.3	7.9	557	5.7	549	39	557.0	5.7	0.23	
14AB-A05_72	163.9	2.25	0.8790	0.0210	0.10370	0.00140	0.068	639	11	635.8	8.1	652	55	635.8	8.1	0.50	
14AB-A05_73	227	1.02	5.3460	0.0480	0.33150	0.00300	0.405	1876.9	7.8	1846	15	1920	17	1920.0	17.0	3.85	
14AB-A05_74	232.3	2.38	0.3384	0.0072	0.04814	0.00079	0.137	295.7	5.5	303	4.8	237	55	303.0	4.8	2.47	
14AB-A05_75	209.7	0.98	4.9220	0.0530	0.31330	0.00280	0.453	1806.8	8.9	1757	14	1871	20	1871.0	20.0	6.09	
14AB-A05_76	342	2.31	0.3570	0.0077	0.04771	0.00069	0.141	309.6	5.7	300.4	4.2	393	54	300.4	4.2	2.97	

Sample Name _Grain #	[U] ppm	U/Th	207/235	2σ error	206/238	2σ error	RHO	207/235 Age (Ma)	2σ error	206/238 Age (Ma)	2σ error	207/206 Age (Ma)	2σ error	Best age (Ma)	2σ error	% Discordance	Rim /Core
14AB-A05_77	253	2.13	1.0070	0.0250	0.11460	0.00260	0.589	706	13	699	15	729	47	699.0	15.0	0.99	
14AB-A05_78	356	1.82	0.3368	0.0062	0.04661	0.00087	0.212	294.6	4.7	293.6	5.4	320	55	293.6	5.4	0.34	
14AB-A05_79	366	2.41	0.3574	0.0072	0.05049	0.00083	0.182	310	5.4	317.5	5.1	263	49	317.5	5.1	2.42	
14AB-A05_80	156	1.17	1.2520	0.0260	0.13260	0.00200	0.363	823	12	803	11	884	42	803.0	11.0	2.43	
14AB-A05_81	540	2.21	0.3457	0.0065	0.04822	0.00054	0.181	301.9	5	303.6	3.3	284	44	303.6	3.3	0.56	
14AB-A05_82	336	2.56	0.3518	0.0060	0.04842	0.00075	0.070	305.9	4.5	304.8	4.6	330	53	304.8	4.6	0.36	
14AB-A05_83	139.1	0.40	0.8320	0.0160	0.10050	0.00120	0.357	613.9	8.8	617.3	6.8	626	42	617.3	6.8	0.55	
14AB-A05_84	113	2.95	0.7370	0.0230	0.09250	0.00160	0.260	561	13	570.1	9.6	561	63	570.1	9.6	1.62	
14AB-A05_85	85.5	1.12	4.4300	0.1100	0.28220	0.00670	0.644	1717	20	1602	34	1910	38	1910.0	38.0	16.13	
14AB-A05_86	746	2.17	0.3634	0.0063	0.05041	0.00087	0.599	314.6	4.7	317	5.4	319	34	317.0	5.4	0.76	
14AB-A05_87	448	2.29	0.3473	0.0053	0.04792	0.00055	0.279	302.5	4	301.7	3.4	312	35	301.7	3.4	0.26	
14AB-A05_88	499	1.34	1.7990	0.0260	0.17640	0.00240	0.532	1044.5	9.4	1047	13	1061	23	1061.0	23.0	1.32	
14AB-A05_89	456	1.77	0.5749	0.0074	0.07632	0.00095	0.248	461.7	4.9	474.1	5.7	453	35	474.1	5.7	2.69	
14AB-A05_90	11.97	1.09	1.6650	0.0810	0.16750	0.00550	0.269	996	29	997	30	1007	99	1007.0	99.0	0.99	
14AB-A05_91	216.9	1.41	0.7700	0.0140	0.09460	0.00170	0.457	579.1	8.1	582.6	9.9	610	39	582.6	9.9	0.60	
14AB-A05_92	345	1.47	0.9340	0.0130	0.10650	0.00130	0.389	670	6.7	652.5	7.8	757	32	652.5	7.8	2.61	
14AB-A05_93	360	1.88	0.3464	0.0061	0.04744	0.00057	0.226	301.8	4.6	298.8	3.5	361	42	298.8	3.5	0.99	
14AB-A05_94	333	2.35	0.3570	0.0061	0.04870	0.00049	0.152	310.3	4.7	306.5	3	336	44	306.5	3.0	1.22	
14AB-A05_96	272	2.21	0.3545	0.0069	0.04830	0.00055	0.179	307.8	5.1	304.1	3.4	322	47	304.1	3.4	1.20	
14AB-A05_97	202	3.06	0.5610	0.0110	0.07330	0.00110	0.266	451.6	7.1	456.2	6.4	445	44	456.2	6.4	1.02	
14AB-A05_98	367	4.70	0.6330	0.0140	0.08060	0.00130	0.716	497.5	8.8	499.6	7.8	497	34	499.6	7.8	0.42	
14AB-A05_99	143.3	1.84	0.7590	0.0150	0.09340	0.00150	0.125	572.8	8.5	575.4	8.7	582	48	575.4	8.7	0.45	
14AB-A05_100	730	1.33	0.4163	0.0044	0.05681	0.00046	0.043	353.3	3.2	356.2	2.8	350	30	356.2	2.8	0.82	
14AB-A05_101	493	44.90	0.8240	0.0100	0.10023	0.00098	0.349	611	5.5	615.7	5.7	607	28	615.7	5.7	0.77	
14AB-A05_102	298	1.85	0.3454	0.0073	0.04863	0.00059	0.249	301.8	5.7	306.1	3.6	284	44	306.1	3.6	1.42	

Sample Name _Grain #	[U] ppm	U/Th	207/235	2σ error	206/238	2σ error	RHO	207/235 Age (Ma)	2σ error	206/238 Age (Ma)	2σ error	207/206 Age (Ma)	2σ error	Best age (Ma)	2σ error	% Discordance	Rim /Core
14AB-A05_103	353	1.86	0.3608	0.0064	0.04926	0.00059	0.071	312.6	4.8	309.9	3.6	346	45	309.9	3.6	0.86	
14AB-A05_104	294	1.79	0.3602	0.0072	0.04848	0.00059	0.266	312.1	5.4	305.2	3.6	365	47	305.2	3.6	2.21	
14AB-A05_105	400	1.99	0.3601	0.0070	0.04985	0.00060	0.395	312	5.2	313.6	3.7	295	42	313.6	3.7	0.51	
14AB-A05_106	521	2.33	0.3639	0.0059	0.04978	0.00054	0.380	315.5	4.3	313.2	3.3	331	33	313.2	3.3	0.73	
14AB-A05_107	237	1.00	0.8060	0.0150	0.09710	0.00150	0.278	599.7	8.5	597.1	8.9	605	54	597.1	8.9	0.43	
14AB-A05_109	178.5	1.92	0.3243	0.0085	0.04586	0.00076	0.128	285.8	6.7	289	4.7	248	69	289.0	4.7	1.12	
14AB-A05_110	137	2.70	10.9500	0.1200	0.46730	0.00640	0.575	2521	10	2475	27	2567	20	2567.0	20.0	3.58	
14AB-A05_111	32.2	0.60	0.8640	0.0300	0.10100	0.00240	0.373	630	17	620	14	674	75	620.0	14.0	1.59	
14AB-A05_112	575	0.91	0.7600	0.0150	0.08440	0.00130	0.327	573.7	8.5	522.1	7.6	791	31	522.1	7.6	8.99	
14AB-A05_113	37.9	1.07	0.7500	0.0450	0.08780	0.00260	0.122	556	20	542	15	620	110	542.0	15.0	2.52	
14AB-A05_114	90.3	0.60	0.5640	0.0150	0.07380	0.00110	0.125	454.4	9.8	458.9	6.6	395	64	458.9	6.6	0.99	
14AB-A05_115	333	3.37	5.8360	0.0450	0.35050	0.00330	0.683	1951.4	6.8	1937	16	1977	14	1977.0	14.0	2.02	
14AB-A05_117	921	16.80	0.8369	0.0099	0.10060	0.00120	0.583	617.1	5.5	617.6	7	619	24	617.6	7.0	0.08	
14AB-A05_118	370	2.01	0.3579	0.0064	0.04800	0.00066	0.303	310.4	4.8	302.2	4	376	46	302.2	4.0	2.64	
14AB-A05_119	509	7.21	1.0190	0.0190	0.11740	0.00250	0.606	712.5	9.8	715	14	702	38	715.0	14.0	0.35	
14AB-A05_120	442	2.07	0.3536	0.0054	0.04818	0.00062	0.275	307.3	4.1	303.3	3.8	318	39	303.3	3.8	1.30	
14AB-A05_121	155.3	1.58	6.5690	0.0830	0.35490	0.00570	0.728	2055	11	1958	27	2166	17	2166.0	17.0	9.60	
14AB-A06_1	287	2.51	0.3661	0.0084	0.04990	0.00110	0.584	316.5	6.2	313.9	6.8	370	50	313.9	6.8	0.82	
14AB-A06_2	164	2.71	0.3480	0.0100	0.04726	0.00096	0.500	302.9	7.7	298.6	5.7	348	52	298.6	5.7	1.42	
14AB-A06_3	339.8	18.60	0.6510	0.0450	0.07510	0.00280	0.820	507	27	467	17	671	91	467.0	17.0	7.89	
14AB-A06_4	399	2.33	0.3546	0.0068	0.04754	0.00089	0.510	308	5.1	299.4	5.5	368	41	299.4	5.5	2.79	
14AB-A06_5	324	2.24	0.3574	0.0069	0.04857	0.00069	0.328	310.1	5.2	305.7	4.3	326	44	305.7	4.3	1.42	
14AB-A06_6	867	1.36	6.6400	0.2500	0.29570	0.00970	0.959	2061	33	1667	49	2472	18	DISC	DISC	32.56	
14AB-A06_7	465	2.25	0.3932	0.0098	0.05290	0.00120	0.783	336.2	7.1	332.2	7.4	367	37	332.2	7.4	1.19	
14AB-A06_8	214	3.04	0.9150	0.0130	0.10910	0.00160	0.404	659.4	7.1	667.5	9.2	630	32	667.5	9.2	1.23	

Sample Name _Grain #	[U] ppm	U/Th	207/235	2σ error	206/238	2σ error	RHO	207/235 Age (Ma)	2σ error	206/238 Age (Ma)	2σ error	207/206 Age (Ma)	2σ error	Best age (Ma)	2σ error	% Discordance	Rim /Core
14AB-A06_9	357	2.01	11.2800	0.1300	0.43450	0.00570	0.778	2546	11	2329	26	2725	15	2725.0	15.0	14.53	
14AB-A06_10	219	3.20	0.3606	0.0090	0.04878	0.00080	0.269	312.3	6.7	307	4.9	335	59	307.0	4.9	1.70	
14AB-A06_11	397	2.43	0.3489	0.0078	0.04753	0.00079	0.645	303.6	5.8	299.3	4.9	332	39	299.3	4.9	1.42	
14AB-A06_12	92.7	1.31	0.3470	0.0170	0.04690	0.00120	0.083	302	12	295.4	7.3	360	110	295.4	7.3	2.19	
14AB-A06_13	640	1.82	0.3750	0.0074	0.04950	0.00069	0.504	323.1	5.5	311.4	4.3	430	35	311.4	4.3	3.62	
14AB-A06_14	384	2.26	0.3840	0.0100	0.05130	0.00130	0.737	329.6	7.4	322.4	8.1	394	43	322.4	8.1	2.18	
14AB-A06_15	333	2.62	0.3682	0.0087	0.05070	0.00110	0.637	318	6.4	318.5	7	298	46	318.5	7.0	0.16	
14AB-A06_16	689	77.00	0.4188	0.0090	0.05720	0.00120	0.459	355	6.4	358.8	7.6	373	53	358.8	7.6	1.07	Rim
14AB-A06_16	116.4	1.98	0.7190	0.0190	0.08990	0.00180	0.195	550	11	555	11	515	69	555.0	11.0	0.91	Core
14AB-A06_17	825	2.69	0.5100	0.0110	0.06910	0.00140	0.788	418.3	7.4	430.4	8.6	369	33	430.4	8.6	2.89	
14AB-A06_18	161.3	2.57	0.6500	0.0100	0.08000	0.00130	0.250	508.3	6.4	496.3	7.6	565	44	496.3	7.6	2.36	
14AB-A06_19	292	3.10	0.3631	0.0082	0.04916	0.00066	0.308	314.2	6.1	309.3	4	335	50	309.3	4.0	1.56	
14AB-A06_20	235.2	1.68	0.3397	0.0068	0.04672	0.00063	0.008	296.7	5.1	294.3	3.9	335	52	294.3	3.9	0.81	
14AB-A06_21	212	2.74	0.3580	0.0120	0.04790	0.00130	0.253	310.6	8.9	301.7	8.1	355	90	301.7	8.1	2.87	
14AB-A06_22	97.1	1.31	0.6550	0.0210	0.08230	0.00170	0.116	511	13	511	10	516	80	511.0	10.0	0.00	
14AB-A06_23	174.4	1.81	0.3638	0.0094	0.04751	0.00096	0.303	314.8	7	299.2	5.9	360	66	299.2	5.9	4.96	
14AB-A06_24	419	1.97	0.3741	0.0078	0.05010	0.00110	0.677	322.5	5.7	315.2	6.6	357	40	315.2	6.6	2.26	
14AB-A06_25	454	1.94	0.3678	0.0074	0.04929	0.00093	0.453	317.8	5.5	310.1	5.7	345	47	310.1	5.7	2.42	
14AB-A06_26	238.2	2.48	1.4830	0.0690	0.14030	0.00190	0.300	919	27	846	11	1080	81	846.0	11.0	7.94	
14AB-A06_27	807	22.80	0.7010	0.0240	0.09280	0.00380	0.604	539	14	572	23	427	66	572.0	23.0	6.12	Rim
14AB-A06_27	453	1.60	1.6280	0.0220	0.16360	0.00260	0.525	980.6	8.6	977	14	989	29	989.0	29.0	1.21	Core
14AB-A06_28	79.4	1.13	1.3790	0.0440	0.13380	0.00390	0.518	879	19	809	22	1080	53	809.0	22.0	7.96	Rim
14AB-A06_28	84.8	0.62	1.6710	0.0320	0.16560	0.00230	0.301	997	12	988	13	1012	42	1012.0	42.0	2.37	Core
14AB-A06_29	394.6	2.87	0.3481	0.0059	0.04813	0.00076	0.601	303.1	4.4	303	4.6	319	34	303.0	4.6	0.03	
14AB-A06_30	822	2.09	0.4493	0.0079	0.06203	0.00087	0.465	376.6	5.6	388	5.3	326	38	388.0	5.3	3.03	

Sample Name _Grain #	[U] ppm	U/Th	207/235	2σ error	206/238	2σ error	RHO	207/235 Age (Ma)	2σ error	206/238 Age (Ma)	2σ error	207/206 Age (Ma)	2σ error	Best age (Ma)	2σ error	% Discordance	Rim /Core
14AB-A06_31	215	2.13	0.3506	0.0073	0.04873	0.00085	0.260	305	5.5	306.7	5.3	283	51	306.7	5.3	0.56	
14AB-A06_32	262	3.28	0.3449	0.0085	0.04773	0.00087	0.604	300.7	6.4	300.5	5.3	301	47	300.5	5.3	0.07	
14AB-A06_33	76.7	1.65	0.8600	0.0230	0.09780	0.00260	0.170	629	13	601	15	705	70	601.0	15.0	4.45	
14AB-A06_34	383	22.80	1.6340	0.0210	0.16460	0.00220	0.595	983.1	7.9	982	12	981	25	981.0	25.0	0.10	
14AB-A06_35	376	1.61	0.3433	0.0075	0.04725	0.00063	0.079	299.4	5.6	297.6	3.9	320	56	297.6	3.9	0.60	
14AB-A06_36	252	2.19	0.3636	0.0082	0.04870	0.00100	0.377	314.6	6.1	307.2	6.3	370	57	307.2	6.3	2.35	
14AB-A06_37	391	2.55	0.3878	0.0088	0.04992	0.00091	0.282	333.5	6.6	314.9	5.8	478	56	314.9	5.8	5.58	
14AB-A06_38	440	2.53	0.3602	0.0083	0.04936	0.00065	0.313	312.1	6.2	310.6	4	325	53	310.6	4.0	0.48	
14AB-A06_39	602	1.97	0.3560	0.0087	0.04750	0.00110	0.497	308.9	6.5	298.9	6.8	335	52	298.9	6.8	3.24	
14AB-A06_40	1202	4.83	1.1370	0.0180	0.13000	0.00250	0.694	772.1	8.8	788	14	693	33	788.0	14.0	2.06	
14AB-A06_41	620	2.08	0.3600	0.0120	0.04811	0.00095	0.555	311.8	9.3	302.9	5.8	374	60	302.9	5.8	2.85	
14AB-A06_42	783	3.51	0.4050	0.0140	0.05380	0.00130	0.835	345	10	338	7.7	380	39	338.0	7.7	2.03	
14AB-A06_43	310	3.15	0.3721	0.0067	0.05051	0.00080	0.451	321.7	5.1	317.6	4.9	370	39	317.6	4.9	1.27	
14AB-A06_44	196	2.34	0.3558	0.0070	0.04897	0.00052	0.023	308.8	5.3	308.2	3.2	309	49	308.2	3.2	0.19	
14AB-A06_45	272.7	3.05	15.0600	0.3500	0.54900	0.01400	0.649	2815	22	2815	59	2817	32	2817.0	32.0	0.07	
14AB-A06_46	460	2.20	0.3902	0.0075	0.05310	0.00100	0.652	334.3	5.5	333.5	6.1	306	38	333.5	6.1	0.24	
14AB-A06_47	64.3	0.97	1.3370	0.0430	0.14320	0.00450	0.653	860	19	862	25	859	59	859.0	59.0	0.35	
14AB-A06_48	50.6	1.94	1.3730	0.0260	0.14690	0.00250	0.097	877	11	883	14	872	53	872.0	53.0	1.26	
14AB-A06_49	265	2.89	0.3586	0.0076	0.04977	0.00073	0.105	310.9	5.7	313.1	4.5	291	49	313.1	4.5	0.71	
14AB-A06_50	791	2.85	0.8720	0.0170	0.10300	0.00160	0.289	637.8	8.7	632.1	9.2	679	47	632.1	9.2	0.89	
14AB-A06_51	1200	5.16	1.2090	0.0780	0.05910	0.00180	0.651	797	36	370	11	2307	79	DISC	DISC	53.58	
14AB-A06_52	622	1.05	0.8380	0.0130	0.10230	0.00160	0.605	618.7	7.1	627.7	9.1	594	28	627.7	9.1	1.45	
14AB-A06_53	611	8.25	2.7880	0.0610	0.19900	0.00360	0.852	1359	16	1169	19	1663	20	1663.0	20.0	29.71	
14AB-A06_54	595	1.16	0.4153	0.0088	0.05630	0.00100	0.573	353.1	6.4	352.9	6.1	354	41	352.9	6.1	0.06	
14AB-A06_55	180.4	2.04	0.4282	0.0093	0.05710	0.00086	0.223	361.5	6.6	357.9	5.3	380	52	357.9	5.3	1.00	

Sample Name _Grain #	[U] ppm	U/Th	207/235	2σ error	206/238	2σ error	RHO	207/235 Age (Ma)	2σ error	206/238 Age (Ma)	2σ error	207/206 Age (Ma)	2σ error	Best age (Ma)	2σ error	% Discordance	Rim /Core
14AB-A06_57	379	1.90	0.3670	0.0069	0.04989	0.00078	0.480	317.8	5.2	314.4	4.7	322	40	314.4	4.7	1.07	
14AB-A06_58	378	2.81	0.3711	0.0096	0.05090	0.00120	0.739	321.1	7.2	320	7.6	310	38	320.0	7.6	0.34	
14AB-A06_59	154	2.40	0.3704	0.0083	0.05157	0.00092	0.414	319.7	6.2	324.1	5.7	305	53	324.1	5.7	1.38	
14AB-A06_60	312	2.42	0.3524	0.0066	0.04918	0.00072	0.466	306.4	5	309.5	4.4	274	46	309.5	4.4	1.01	
14AB-A06_61	141	2.55	0.3569	0.0072	0.04908	0.00062	0.122	309.7	5.4	308.9	3.8	291	55	308.9	3.8	0.26	
14AB-A06_62	151	2.60	12.9000	0.1600	0.52940	0.00680	0.697	2671	11	2738	29	2621	17	2621.0	17.0	4.46	
14AB-A06_63	1364	8.30	0.4006	0.0054	0.05248	0.00089	0.679	342	3.9	329.7	5.5	432	29	329.7	5.5	3.60	
14AB-A06_64	107.8	1.48	0.8650	0.0160	0.10370	0.00140	0.164	633.5	8.4	636	8	622	41	636.0	8.0	0.39	
14AB-A06_65	217	1.88	0.4033	0.0099	0.04907	0.00086	0.421	344.6	7.3	308.8	5.3	576	50	DISC	DISC	10.39	
14AB-A06_66	295	2.14	0.4314	0.0092	0.05800	0.00120	0.762	363.9	6.5	363.5	7.2	387	36	363.5	7.2	0.11	
14AB-A06_67	250	12.35	0.5770	0.0110	0.07300	0.00150	0.627	462.2	7.3	453.9	8.7	539	38	453.9	8.7	1.80	
14AB-A06_68	196.3	2.59	0.3610	0.0081	0.04748	0.00071	0.251	312.6	6	299	4.3	396	54	299.0	4.3	4.35	
14AB-A06_70	845	5.14	0.4862	0.0099	0.05890	0.00140	0.105	402.1	6.8	368.6	8.8	608	66	368.6	8.8	8.33	
14AB-A06_71	263	2.15	0.3746	0.0071	0.05052	0.00077	0.321	322.8	5.2	317.7	4.7	375	47	317.7	4.7	1.58	
14AB-A06_72	232	2.62	0.3494	0.0080	0.04822	0.00072	0.159	304	6	303.5	4.5	310	57	303.5	4.5	0.16	
14AB-A06_73	298	3.87	0.3805	0.0087	0.05089	0.00087	0.211	327.1	6.4	319.9	5.3	353	57	319.9	5.3	2.20	
14AB-A06_74	220	2.05	0.3801	0.0078	0.05222	0.00074	0.155	326.9	5.7	328.1	4.5	305	49	328.1	4.5	0.37	
14AB-A06_75	477	3.48	0.4210	0.0240	0.04800	0.00100	0.475	355	17	302.2	6.4	701	97	DISC	DISC	14.87	
14AB-A06_77	404	3.27	1.0540	0.0370	0.10910	0.00430	0.797	729	18	667	25	892	47	667.0	25.0	8.50	
14AB-A06_78	61	2.48	0.7890	0.0220	0.09400	0.00210	0.310	589	13	579	12	643	66	579.0	12.0	1.70	
14AB-A06_79	178	3.51	0.3740	0.0120	0.05040	0.00100	0.257	322.1	8.7	316.9	6.2	338	74	316.9	6.2	1.61	
14AB-A06_80	287	5.43	0.6049	0.0088	0.07690	0.00110	0.413	480.1	5.6	477.7	6.6	498	32	477.7	6.6	0.50	
14AB-A06_81	372	1.84	1.0170	0.0420	0.08800	0.00140	0.076	710	21	543.8	8.5	1269	88	DISC	DISC	23.41	
14AB-A06_82	197	1.91	0.3481	0.0075	0.04860	0.00083	0.348	303.9	5.5	305.9	5.1	311	51	305.9	5.1	0.66	
14AB-A06_83	847	3.47	0.7230	0.0150	0.06610	0.00100	0.525	551.8	8.6	412.3	6.2	1182	34	DISC	DISC	25.28	

Sample Name _Grain #	[U] ppm	U/Th	207/235	2σ error	206/238	2σ error	RHO	207/235 Age (Ma)	2σ error	206/238 Age (Ma)	2σ error	207/206 Age (Ma)	2σ error	Best age (Ma)	2σ error	% Discordance	Rim /Core
14AB-A06_84	238	2.55	0.3621	0.0076	0.04926	0.00064	0.390	313.6	5.6	310	3.9	340	46	310.0	3.9	1.15	
14AB-A06_85	592	1.14	0.4560	0.0170	0.05450	0.00130	0.040	380	12	342.1	7.8	553	77	342.1	7.8	9.97	
14AB-A06_86	163	2.27	0.3708	0.0076	0.05038	0.00084	0.150	319.9	5.6	316.8	5.2	343	52	316.8	5.2	0.97	
14AB-A06_87	620	1.20	1.4270	0.0240	0.14650	0.00250	0.759	899.8	9.9	881	14	949	21	949.0	21.0	7.17	
14AB-A06_88	270	1.72	0.3958	0.0095	0.05256	0.00097	0.271	339.2	6.7	330.2	5.9	376	59	330.2	5.9	2.65	
14AB-A06_89	247	3.07	0.3618	0.0082	0.04940	0.00130	0.481	313.3	6.1	310.8	7.7	309	54	310.8	7.7	0.80	
14AB-A06_90	204	2.09	0.3496	0.0065	0.04884	0.00073	0.148	304.2	4.9	307.4	4.5	299	52	307.4	4.5	1.05	
14AB-A06_91	139.6	3.47	11.7900	0.1900	0.47770	0.00790	0.728	2586	15	2516	34	2636	19	2636.0	19.0	4.55	
14AB-A06_92	358	3.80	0.3617	0.0077	0.04837	0.00074	0.372	313.3	5.7	304.5	4.5	398	44	304.5	4.5	2.81	
14AB-A06_93	191	3.64	2.7710	0.0420	0.23430	0.00320	0.614	1348	11	1356	17	1347	25	1347.0	25.0	0.67	
14AB-A06_94	270	2.35	0.3504	0.0080	0.04815	0.00088	0.474	304.8	6	303.1	5.4	295	47	303.1	5.4	0.56	
14AB-A06_95	298	6.85	0.5700	0.0100	0.07297	0.00096	0.471	457.8	6.5	454.9	6	452	35	454.9	6.0	0.63	
14AB-A06_96	533	3.56	0.3880	0.0100	0.05280	0.00170	0.801	332.3	7.6	331	10	341	50	331.0	10.0	0.39	
14AB-A06_97	164.1	1.69	0.3441	0.0095	0.04720	0.00091	0.322	299.8	7.2	297.3	5.6	329	62	297.3	5.6	0.83	
14AB-A06_98	608	2.40	0.4270	0.0081	0.05900	0.00110	0.691	360.8	5.8	369.7	6.4	321	36	369.7	6.4	2.47	
14AB-A06_99	34.7	0.60	0.8220	0.0310	0.10020	0.00210	0.154	611	18	615	13	561	86	615.0	13.0	0.65	
14AB-A06_100	220.6	2.03	0.3484	0.0070	0.04804	0.00065	0.248	303.3	5.2	302.4	4	301	50	302.4	4.0	0.30	
14AB-A06_101	383	1.96	0.3550	0.0078	0.04880	0.00100	0.527	308.3	5.8	307.1	6.2	303	47	307.1	6.2	0.39	
14AB-A06_102	421	12.60	0.4490	0.0150	0.05540	0.00100	0.448	376	11	347.6	6.4	533	65	347.6	6.4	7.55	
14AB-A06_103	492.3	3.85	0.3773	0.0066	0.05221	0.00077	0.502	324.8	4.9	328.1	4.7	315	35	328.1	4.7	1.02	
14AB-A06_104	268	1.85	0.3495	0.0091	0.04754	0.00096	0.521	304.1	6.9	299.4	5.9	348	51	299.4	5.9	1.55	
14AB-A06_105	573	2.66	0.3840	0.0100	0.05330	0.00100	0.739	329.6	7.3	334.8	6.3	309	40	334.8	6.3	1.58	
14AB-A06_106	156.6	2.68	0.5030	0.0120	0.06680	0.00120	0.424	413.5	8.1	416.9	7.1	394	47	416.9	7.1	0.82	
14AB-A06_107	219	9.31	0.5921	0.0095	0.07520	0.00140	0.227	471.9	6.1	467.4	8.2	482	51	467.4	8.2	0.95	

Sample Name _Grain #	[U] ppm	U/Th	207/235	2σ error	206/238	2σ error	RHO	207/235 Age (Ma)	2σ error	206/238 Age (Ma)	2σ error	207/206 Age (Ma)	2σ error	Best age (Ma)	2σ error	% Discordance	Rim /Core
14AB-A06_108	281	154.00	0.3480	0.0100	0.04753	0.00091	0.520	303.6	8	299.3	5.6	316	56	299.3	5.6	1.42	
14AB-A06_109	670	2.33	0.4487	0.0070	0.05810	0.00110	0.520	376.1	4.9	364.3	6.5	451	39	364.3	6.5	3.14	
14AB-A06_110	24.5	1.32	1.8540	0.0800	0.17310	0.00630	0.606	1064	28	1028	35	1123	59	1123.0	59.0	8.46	
14AB-A06_111	305	1.90	0.3401	0.0066	0.04725	0.00067	0.229	297.7	4.9	297.6	4.2	288	51	297.6	4.2	0.03	
14AB-A06_112	763	11.41	8.9100	0.2100	0.44400	0.01200	0.651	2325	22	2365	54	2296	35	2296.0	35.0	3.01	
14AB-A06_113	307	1.51	0.3686	0.0087	0.04915	0.00097	0.729	318.3	6.4	309.2	5.9	368	36	309.2	5.9	2.86	
14AB-A06_114	56.7	1.45	2.5700	0.3100	0.13320	0.00270	0.540	1254	90	806	16	2040	210	DISC	DISC	35.73	
14AB-A06_115	149.1	1.88	1.7080	0.0200	0.16980	0.00220	0.209	1011.2	7.5	1012	12	1022	31	1022.0	31.0	0.98	
14AB-A06_116	313	1.33	0.8380	0.0120	0.09960	0.00120	0.267	617.8	6.5	611.8	6.7	636	30	611.8	6.7	0.97	
14AB-A06_117	257	3.06	0.3636	0.0083	0.04946	0.00069	0.540	316.3	5.9	311.2	4.2	364	44	311.2	4.2	1.61	
14AB-A06_118	279	3.92	0.3374	0.0058	0.04681	0.00084	0.417	295	4.4	294.9	5.2	294	45	294.9	5.2	0.03	
14AB-A06_119	247	1.77	0.3536	0.0078	0.04883	0.00091	0.388	307.2	5.9	307.3	5.6	304	51	307.3	5.6	0.03	
14AB-A06_120	163	2.16	0.3587	0.0086	0.04956	0.00078	0.319	310.8	6.4	311.8	4.8	318	50	311.8	4.8	0.32	
14AB-A06_121	190.2	13.10	0.8180	0.0200	0.09800	0.00190	0.444	606	11	602	11	661	50	602.0	11.0	0.66	
15AB-118_1	717	1.86	0.3335	0.0075	0.04563	0.00058	0.531	291.9	5.7	287.6	3.6	311	43	287.6	3.6	1.47	
15AB-118_2	401.7	0.51	5.7900	0.1100	0.34030	0.00570	0.709	1947	16	1888	28	1991	24	1991.0	24.0	5.17	
15AB-118_3	428	0.79	1.8760	0.0420	0.17930	0.00370	0.475	1072	15	1063	20	1059	45	1059.0	45.0	0.38	
15AB-118_4	829	2.16	5.3270	0.0770	0.31820	0.00600	0.794	1874	12	1780	29	1956	19	1956.0	19.0	9.00	
15AB-118_5	296	2.81	1.1190	0.0330	0.12200	0.00290	0.610	762	16	742	16	821	43	742.0	16.0	2.62	
15AB-118_6	363	2.21	0.3589	0.0081	0.04730	0.00100	0.476	311	6.1	298	6.2	407	49	298.0	6.2	4.18	
15AB-118_7	692	2.24	0.3304	0.0057	0.04588	0.00053	0.337	289.7	4.3	289.1	3.2	301	36	289.1	3.2	0.21	
15AB-118_8	179	0.93	5.2620	0.0610	0.32980	0.00370	0.305	1862	9.8	1837	18	1889	24	1889.0	24.0	2.75	
15AB-118_9	886	14.37	0.9000	0.0140	0.10440	0.00110	0.469	651.4	7.4	640.3	6.6	675	32	640.3	6.6	1.70	
15AB-118_10	340	2.17	0.3401	0.0074	0.04788	0.00089	0.146	297	5.6	301.4	5.5	219	54	301.4	5.5	1.48	
15AB-118_11	1066	5.13	0.2604	0.0077	0.03393	0.00079	0.849	234.8	6.2	215.1	4.9	419	35	215.1	4.9	8.39	

Sample Name _Grain #	[U] ppm	U/Th	207/235	2σ error	206/238	2σ error	RHO	207/235 Age (Ma)	2σ error	206/238 Age (Ma)	2σ error	207/206 Age (Ma)	2σ error	Best age (Ma)	2σ error	% Discordance	Rim /Core
15AB-118_12	123.8	1.17	1.1440	0.0210	0.12180	0.00200	0.296	774	10	741	12	850	44	741.0	12.0	4.26	
15AB-118_13	424	1.91	0.3546	0.0076	0.04953	0.00071	0.206	308.7	5.5	311.6	4.3	305	54	311.6	4.3	0.94	
15AB-118_14	468	1.59	0.3351	0.0060	0.04648	0.00060	0.210	293.3	4.6	292.9	3.7	279	48	292.9	3.7	0.14	
15AB-118_15	467	2.25	0.3461	0.0056	0.04816	0.00077	0.495	301.7	4.2	303.8	4.6	305	36	303.8	4.6	0.70	
15AB-118_16	478	2.57	0.3659	0.0080	0.04930	0.00089	0.351	317.1	5.8	310.2	5.5	351	53	310.2	5.5	2.18	
15AB-118_17	374	1.65	0.3430	0.0061	0.04783	0.00055	0.288	299.3	4.6	301.2	3.4	289	45	301.2	3.4	0.63	
15AB-118_18	356	3.91	0.3029	0.0088	0.04193	0.00066	0.297	268.3	6.9	264.8	4.1	279	71	264.8	4.1	1.30	
15AB-118_19	723	4.04	1.1100	0.0300	0.11570	0.00340	0.754	760	14	706	19	911	41	706.0	19.0	7.11	
15AB-118_20	376	3.14	0.3311	0.0067	0.04616	0.00073	0.425	290.2	5.1	290.9	4.5	292	46	290.9	4.5	0.24	
15AB-118_21	348	2.47	0.3334	0.0082	0.04632	0.00059	0.226	292.7	6.1	291.9	3.6	289	58	291.9	3.6	0.27	
15AB-118_22	338	1.75	0.3710	0.0071	0.05028	0.00059	0.075	320.7	5.3	316.2	3.6	325	45	316.2	3.6	1.40	
15AB-118_23	78.4	1.43	6.9960	0.0840	0.38030	0.00430	0.488	2110	11	2077	20	2138	19	2138.0	19.0	2.85	
15AB-118_24	922	3.31	0.3478	0.0079	0.04709	0.00096	0.109	302.8	6	296.6	5.9	336	39	296.6	5.9	2.05	
15AB-118_25	1458	5.32	0.4193	0.0046	0.05817	0.00057	0.525	355.4	3.3	364.4	3.5	310	25	364.4	3.5	2.53	
15AB-118_26	495	2.11	0.3667	0.0081	0.04951	0.00060	0.452	316.9	6	311.5	3.7	355	44	311.5	3.7	1.70	
15AB-118_27	755	9.71	0.8100	0.0190	0.09100	0.00230	0.652	602	11	562	14	769	44	562.0	14.0	6.64	
15AB-118_28	331	2.27	0.3459	0.0090	0.04749	0.00087	0.392	302.1	6.9	299.1	5.4	308	57	299.1	5.4	0.99	
15AB-118_29	389	2.71	0.3648	0.0068	0.04931	0.00057	0.222	315.6	5	310.3	3.5	340	43	310.3	3.5	1.68	
15AB-118_30	373.8	2.12	4.4020	0.0670	0.26740	0.00420	0.494	1712	13	1527	22	1928	27	1928.0	27.0	20.80	
15AB-118_31	450	2.68	0.8060	0.0110	0.09800	0.00120	0.379	600.1	6.4	602.4	6.8	584	29	602.4	6.8	0.38	
15AB-118_32	478	2.01	0.3455	0.0091	0.04707	0.00078	0.404	301.1	6.8	296.5	4.8	335	55	296.5	4.8	1.53	
15AB-118_33	790	2.97	0.3550	0.0061	0.04942	0.00065	0.517	308.3	4.6	310.9	4	278	33	310.9	4.0	0.84	
15AB-118_34	767	72.00	0.4130	0.0250	0.05480	0.00180	0.718	351	18	344	11	396	93	344.0	11.0	1.99	Rim
15AB-118_34	96.6	0.80	11.2700	0.3100	0.45800	0.01000	0.782	2544	26	2431	46	2639	40	2639.0	40.0	7.88	Core
15AB-118_35	424	1.73	0.3591	0.0082	0.04905	0.00072	0.137	312.1	6	308.7	4.4	339	52	308.7	4.4	1.09	

Sample Name _Grain #	[U] ppm	U/Th	207/235	2σ error	206/238	2σ error	RHO	207/235 Age (Ma)	2σ error	206/238 Age (Ma)	2σ error	207/206 Age (Ma)	2σ error	Best age (Ma)	2σ error	% Discordance	Rim /Core
15AB-118_36	455	0.38	1.5130	0.0220	0.15140	0.00150	0.694	935.3	9	908.6	8.3	1007	25	1007.0	25.0	9.77	
15AB-118_37	689	7.80	0.5950	0.0120	0.07670	0.00110	0.480	473.7	7.3	476.2	6.3	462	36	476.2	6.3	0.53	
15AB-118_38	468	4.82	0.9720	0.0130	0.11410	0.00180	0.691	689.1	6.9	696	10	685	22	696.0	10.0	1.00	
15AB-118_39	483	1.65	0.7694	0.0098	0.09390	0.00110	0.348	579.2	5.6	578.5	6.3	573	28	578.5	6.3	0.12	
15AB-118_40	339.6	2.15	0.3480	0.0058	0.04748	0.00053	0.264	303	4.4	299	3.2	324	43	299.0	3.2	1.32	
15AB-118_41	305	2.59	0.3545	0.0079	0.04839	0.00073	0.411	307.7	5.9	304.6	4.5	324	47	304.6	4.5	1.01	
15AB-118_42	221	0.62	1.5830	0.0410	0.15660	0.00370	0.719	962	16	938	20	1033	36	1033.0	36.0	9.20	
15AB-118_43	284	2.31	0.3565	0.0065	0.04798	0.00057	0.116	309.4	4.9	302.1	3.5	339	49	302.1	3.5	2.36	
15AB-118_44	283	1.14	0.8560	0.0210	0.10260	0.00240	0.459	627	12	630	14	628	51	630.0	14.0	0.48	
15AB-118_45	797	4.13	1.4150	0.0260	0.14850	0.00300	0.852	897	11	892	17	899	22	899.0	22.0	0.78	
15AB-118_46	189.6	2.44	0.5380	0.0190	0.06400	0.00240	0.374	437	12	400	14	617	90	400.0	14.0	8.47	Rim
15AB-118_46	768	2.28	1.1100	0.0210	0.11720	0.00230	0.651	758	10	715	13	887	33	715.0	13.0	5.67	Core
15AB-118_47	720	4.21	0.2631	0.0070	0.03537	0.00078	0.652	236.9	5.7	224.1	4.8	374	43	224.1	4.8	5.40	
15AB-118_48	386	2.55	0.3930	0.0082	0.05236	0.00078	0.230	336.3	6	329	4.8	396	53	329.0	4.8	2.17	
15AB-118_49	258.1	2.30	10.5600	0.1800	0.44500	0.01000	0.815	2484	16	2378	44	2589	22	2589.0	22.0	8.15	
15AB-118_50	631	1.87	0.3418	0.0061	0.04773	0.00052	0.196	298.3	4.6	300.6	3.2	280	41	300.6	3.2	0.77	
15AB-118_51	490	2.61	0.3800	0.0078	0.05130	0.00084	0.473	326.8	5.7	322.5	5.2	368	43	322.5	5.2	1.32	
15AB-118_52	717	7.16	6.3240	0.0730	0.36770	0.00410	0.772	2021	10	2018	19	2021	19	2021.0	19.0	0.15	
15AB-118_53	173.3	1.95	1.8210	0.0310	0.17320	0.00220	0.452	1054	11	1030	12	1111	29	1111.0	29.0	7.29	
15AB-118_54	333	1.26	0.7510	0.0130	0.09219	0.00091	0.257	568.7	7.4	568.4	5.4	571	34	568.4	5.4	0.05	
15AB-118_55	127.2	1.61	6.1500	0.1200	0.35330	0.00710	0.718	1996	17	1949	34	2066	25	2066.0	25.0	5.66	
15AB-118_56	772	1.57	0.7823	0.0098	0.09531	0.00094	0.425	586.5	5.6	586.8	5.5	607	29	586.8	5.5	0.05	
15AB-118_57	381	2.49	0.3157	0.0090	0.04481	0.00095	0.533	278.3	7	282.5	5.9	244	57	282.5	5.9	1.51	
15AB-118_59	441	3.35	0.3490	0.0058	0.04736	0.00063	0.054	303.8	4.3	298.3	3.9	345	47	298.3	3.9	1.81	
15AB-118_60	396	2.00	0.3509	0.0059	0.04836	0.00054	0.268	305.2	4.5	304.4	3.3	304	46	304.4	3.3	0.26	

Sample Name _Grain #	[U] ppm	U/Th	207/235	2σ error	206/238	2σ error	RHO	207/235 Age (Ma)	2σ error	206/238 Age (Ma)	2σ error	207/206 Age (Ma)	2σ error	Best age (Ma)	2σ error	% Discordance	Rim /Core
15AB-118_61	174.2	0.93	7.3400	0.1800	0.29210	0.00770	0.501	2152	22	1652	38	2674	43	DISC	DISC	38.22	
15AB-118_62	325	3.21	0.5580	0.0110	0.07300	0.00140	0.227	449.6	7.5	454.1	8.4	403	55	454.1	8.4	1.00	
15AB-118_63	221	1.45	11.3300	0.3300	0.46300	0.01500	0.744	2551	28	2461	63	2623	33	2623.0	33.0	6.18	
15AB-118_64	143.2	2.13	1.3370	0.0280	0.13310	0.00240	0.294	863	12	806	14	1001	47	806.0	14.0	6.60	
15AB-118_65	289	4.37	0.3382	0.0080	0.04702	0.00079	0.235	295.5	6.1	296.2	4.8	290	63	296.2	4.8	0.24	
15AB-118_66	531	2.15	0.3681	0.0098	0.05068	0.00090	0.547	317.9	7.3	318.7	5.5	295	48	318.7	5.5	0.25	
15AB-118_67	463	4.05	0.9100	0.0160	0.11060	0.00180	0.671	656.8	8.3	676	11	613	31	676.0	11.0	2.92	
15AB-118_68	438	3.52	0.3619	0.0069	0.04867	0.00053	0.178	313.4	5.2	306.4	3.3	372	50	306.4	3.3	2.23	
15AB-118_69	425	1.99	0.3482	0.0062	0.04817	0.00068	0.276	303.8	4.6	303.2	4.2	257	39	303.2	4.2	0.20	
15AB-118_70	331.9	2.62	0.3613	0.0091	0.04759	0.00067	0.297	312.8	6.8	299.7	4.1	411	56	299.7	4.1	4.19	
15AB-118_71	673	1.88	0.3362	0.0058	0.04671	0.00072	0.471	294.9	4.2	294.3	4.4	279	39	294.3	4.4	0.20	
15AB-118_72	571	2.53	0.3673	0.0070	0.05080	0.00110	0.428	317.4	5.2	319.1	6.6	326	47	319.1	6.6	0.54	
15AB-118_73	301	2.30	0.3526	0.0087	0.04826	0.00073	0.231	306.3	6.5	303.8	4.5	326	59	303.8	4.5	0.82	
15AB-118_74	198	2.29	0.3590	0.0110	0.05036	0.00093	0.278	310.8	8.2	316.7	5.7	289	69	316.7	5.7	1.90	
15AB-118_75	102.3	2.35	0.7430	0.0200	0.08880	0.00150	0.251	563	12	548.5	8.9	625	63	548.5	8.9	2.58	
15AB-118_76	356	1.65	0.3228	0.0063	0.04439	0.00087	0.224	283.9	4.8	279.9	5.4	314	61	279.9	5.4	1.41	
15AB-118_77	608	3.32	0.3441	0.0066	0.04497	0.00093	0.608	300.1	5	283.5	5.8	408	41	283.5	5.8	5.53	
15AB-118_78	353	2.28	0.3860	0.0150	0.04715	0.00098	0.527	331	11	296.9	6	604	63	DISC	DISC	10.30	
15AB-118_79	299	2.52	0.8920	0.0270	0.10290	0.00300	0.447	647	14	631	18	691	57	631.0	18.0	2.47	Rim
15AB-118_79	129.3	1.02	1.5120	0.0350	0.15910	0.00220	0.247	934	14	952	12	878	48	878.0	48.0	8.43	Core
15AB-118_80	948	1.64	1.0650	0.0130	0.12070	0.00160	0.673	737.2	6.4	734.7	9	741	22	734.7	9.0	0.34	
15AB-118_81	73.5	2.19	1.6240	0.0350	0.16040	0.00360	0.192	978	14	958	20	1058	61	1058.0	61.0	9.45	
15AB-118_82	353	2.75	0.3598	0.0091	0.04906	0.00072	0.231	311.7	6.8	308.7	4.4	329	62	308.7	4.4	0.96	
15AB-118_83	697	2.87	0.3386	0.0045	0.04619	0.00065	0.303	296	3.4	291.1	4	350	39	291.1	4.0	1.66	
15AB-118_84	1790	4.50	0.2883	0.0074	0.03930	0.00110	0.831	257.7	5.9	248.7	6.6	330	35	248.7	6.6	3.49	

Sample Name _Grain #	[U] ppm	U/Th	207/235	2σ error	206/238	2σ error	RHO	207/235 Age (Ma)	2σ error	206/238 Age (Ma)	2σ error	207/206 Age (Ma)	2σ error	Best age (Ma)	2σ error	% Discordance	Rim /Core
15AB-118_85	229.4	1.13	1.7550	0.0310	0.17470	0.00260	0.525	1030	12	1038	14	1007	33	1007.0	33.0	3.08	
15AB-118_86	1316	2.78	0.3844	0.0081	0.05326	0.00099	0.697	330	6	334.5	6.1	316	33	334.5	6.1	1.36	
15AB-118_87	1735	4.49	0.4124	0.0048	0.05640	0.00048	0.627	350.5	3.5	353.7	2.9	331	21	353.7	2.9	0.91	
15AB-118_88	346	1.96	0.3519	0.0067	0.04854	0.00069	0.228	305.9	5	305.5	4.2	306	48	305.5	4.2	0.13	
15AB-118_89	422	0.87	0.8860	0.0110	0.10520	0.00120	0.312	643.7	6.1	644.5	7.1	666	29	644.5	7.1	0.12	
15AB-118_90	580	1.98	0.3512	0.0064	0.04890	0.00065	0.363	305.4	4.8	307.7	4	283	42	307.7	4.0	0.75	
15AB-118_91	272	2.69	0.3532	0.0078	0.05005	0.00073	0.062	306.8	5.9	314.8	4.5	250	59	314.8	4.5	2.61	
15AB-118_92	609	3.12	0.3344	0.0070	0.04001	0.00084	0.197	292.8	5.4	252.9	5.2	624	59	DISC	DISC	13.63	
15AB-118_93	210	1.48	0.3380	0.0110	0.04668	0.00084	0.122	296	8.2	294.1	5.2	266	78	294.1	5.2	0.64	
15AB-118_94	363	3.40	0.7400	0.0130	0.08840	0.00140	0.323	562	7.8	545.8	8.2	653	43	545.8	8.2	2.88	
15AB-118_95	847	25.10	1.0250	0.0130	0.11760	0.00160	0.558	717.6	6.4	716.5	9.5	728	25	716.5	9.5	0.15	
15AB-118_96	456	21.20	0.6380	0.0510	0.08080	0.00440	0.809	499	32	501	27	540	100	501.0	27.0	0.40	Rim
15AB-118_96	113.4	1.67	6.0500	0.1300	0.34660	0.00760	0.578	1987	20	1918	37	2072	33	2072.0	33.0	7.43	Core
15AB-118_97	71.7	1.06	1.5750	0.0430	0.15320	0.00430	0.330	958	17	918	24	1082	55	1082.0	55.0	15.16	
15AB-118_98	780	2.84	0.3777	0.0048	0.05189	0.00049	0.440	325.2	3.5	326.1	3	326	28	326.1	3.0	0.28	
15AB-118_99	266	2.32	0.3767	0.0083	0.05270	0.00100	0.297	324.3	6.1	330.8	6.3	262	58	330.8	6.3	2.00	
15AB-118_100	304	1.88	1.2910	0.0210	0.13950	0.00220	0.503	841	9.3	842	12	831	32	842.0	12.0	0.12	
15AB-118_101	459	2.13	0.3648	0.0071	0.05018	0.00079	0.365	315.6	5.3	315.6	4.9	309	45	315.6	4.9	0.00	
15AB-118_102	234	1.02	0.6030	0.0130	0.07760	0.00110	0.301	479.5	8.7	481.4	6.6	468	54	481.4	6.6	0.40	
15AB-118_103	171.4	1.29	0.7180	0.0150	0.09270	0.00150	0.289	549.1	9	571.4	8.8	470	49	571.4	8.8	4.06	
15AB-118_104	637	2.39	0.3463	0.0058	0.04754	0.00069	0.565	301.8	4.3	299.4	4.2	350	35	299.4	4.2	0.80	
15AB-118_105	538	1.22	1.8610	0.0190	0.18260	0.00170	0.487	1066.9	6.8	1081	9.1	1049	17	1049.0	17.0	3.05	
15AB-118_106	617	3.93	0.3733	0.0092	0.05138	0.00092	0.500	323	7	323	5.6	331	51	323.0	5.6	0.00	Rim
15AB-118_106	839	1.64	5.0300	0.1700	0.24310	0.00870	0.783	1823	29	1402	45	2357	38	DISC	DISC	40.52	Core
15AB-118_107	366	2.55	0.3303	0.0072	0.04333	0.00074	0.304	289.5	5.5	273.4	4.6	405	53	273.4	4.6	5.56	

Sample Name _Grain #	[U] ppm	U/Th	207/235	2σ error	206/238	2σ error	RHO	207/235 Age (Ma)	2σ error	206/238 Age (Ma)	2σ error	207/206 Age (Ma)	2σ error	Best age (Ma)	2σ error	% Discordance	Rim /Core
15AB-118_108	1840	66.00	0.8040	0.0140	0.09880	0.00190	0.554	599	7.9	607	11	563	36	607.0	11.0	1.34	Rim
15AB-118_108	164.7	1.62	4.2260	0.0980	0.27100	0.00730	0.780	1678	19	1545	37	1840	32	1840.0	32.0	16.03	Core
15AB-118_109	886	2.74	0.3691	0.0071	0.05002	0.00082	0.404	319.5	5.2	314.6	5	349	46	314.6	5.0	1.53	
15AB-118_110	312	1.53	1.7220	0.0230	0.17250	0.00230	0.508	1016.3	8.4	1026	13	983	28	983.0	28.0	4.37	
15AB-118_111	518	1.60	0.3584	0.0077	0.05023	0.00087	0.488	310.7	5.7	315.9	5.3	274	40	315.9	5.3	1.67	
15AB-118_112	330	0.72	0.7220	0.0140	0.08610	0.00120	0.415	552.2	8.2	532.2	7.2	656	40	532.2	7.2	3.62	
15AB-118_113	1080	3.40	0.3647	0.0097	0.04780	0.00110	0.797	315.4	7.2	300.9	6.7	441	35	300.9	6.7	4.60	
15AB-118_114	960	4.14	0.3800	0.0120	0.04870	0.00120	0.759	328	8.9	306.2	7.1	511	38	306.2	7.1	6.65	
15AB-118_115	635	1.83	0.3544	0.0058	0.04967	0.00051	0.251	307.8	4.3	312.5	3.2	281	41	312.5	3.2	1.53	
15AB-118_116	397	1.81	0.8420	0.0110	0.10080	0.00110	0.132	620.8	6.4	619.1	6.2	628	34	619.1	6.2	0.27	
15AB-118_117	499	3.03	0.3710	0.0120	0.05140	0.00120	0.236	321.8	8.7	323.2	7.3	273	74	323.2	7.3	0.44	
15AB-118_118	843	132.00	0.4771	0.0065	0.06456	0.00082	0.571	396.7	4.7	403.3	5	380	29	403.3	5.0	1.66	
15AB-118_119	458	2.00	0.3388	0.0059	0.04692	0.00059	0.550	296.1	4.5	295.6	3.7	297	37	295.6	3.7	0.17	
15AB-118_120	360	1.69	0.6660	0.0110	0.08460	0.00100	0.446	517.7	6.9	523.6	6.2	506	34	523.6	6.2	1.14	
15AB-118_121	595	3.13	1.6700	0.0400	0.16220	0.00370	0.719	999	16	968	21	1079	33	1079.0	33.0	10.29	
15AB-118_122	359	2.62	0.3616	0.0071	0.04979	0.00057	0.265	313.1	5.3	313.2	3.5	316	48	313.2	3.5	0.03	
15AB-352_1	301	2.17	0.3680	0.0093	0.05055	0.00096	0.123	317.7	6.9	318.6	6	329	61	318.6	6.0	0.28	
15AB-352_2	229.3	2.06	0.3520	0.0110	0.04900	0.00120	0.071	305.5	8.6	308.2	7.2	289	83	308.2	7.2	0.88	
15AB-352_3	205	2.01	0.3590	0.0130	0.04864	0.00091	0.097	313.1	9.3	306.1	5.6	351	84	306.1	5.6	2.24	
15AB-352_4	62.1	1.35	6.4800	0.1600	0.36470	0.00730	0.463	2041	22	2004	35	2079	42	2079.0	42.0	3.61	
15AB-352_5	176	2.52	0.3550	0.0140	0.04890	0.00110	0.052	311	10	307.4	7	268	88	307.4	7.0	1.16	
15AB-352_6	108.3	0.79	1.1490	0.0380	0.12870	0.00340	0.221	778	19	780	19	777	81	780.0	19.0	0.26	
15AB-352_7	466	59.00	0.4240	0.0310	0.05210	0.00220	0.678	358	22	327	13	540	130	327.0	13.0	8.66	Rim
15AB-352_7	203.1	0.71	4.9300	0.1200	0.28550	0.00640	0.742	1805	21	1619	32	2012	31	2012.0	31.0	19.53	Core
15AB-352_8	667	6.35	0.3635	0.0078	0.04889	0.00071	0.108	314.5	5.8	307.7	4.4	385	49	307.7	4.4	2.16	

Sample Name _Grain #	[U] ppm	U/Th	207/235	2σ error	206/238	2σ error	RHO	207/235 Age (Ma)	2σ error	206/238 Age (Ma)	2σ error	207/206 Age (Ma)	2σ error	Best age (Ma)	2σ error	% Discordance	Rim /Core
15AB-352_9	187	0.99	0.2730	0.0120	0.04020	0.00100	0.159	244.6	9.2	254.3	6.4	170	100	254.3	6.4	3.97	
15AB-352_10	390.7	2.20	0.3473	0.0083	0.04673	0.00082	0.233	303.1	6.1	294.4	5	369	61	294.4	5.0	2.87	
15AB-352_11	245	5.43	0.5490	0.0130	0.07090	0.00100	0.376	444.6	8.9	441.4	6.3	478	52	441.4	6.3	0.72	
15AB-352_12	157	1.39	0.8540	0.0350	0.09600	0.00210	0.138	624	19	591	13	758	87	591.0	13.0	5.29	
15AB-352_13	90.8	2.54	1.1260	0.0380	0.12250	0.00280	0.337	764	18	745	16	836	64	745.0	16.0	2.49	
15AB-352_14	159	2.29	0.3980	0.0160	0.04885	0.00094	0.059	340	12	307.4	5.8	530	100	307.4	5.8	9.59	
15AB-352_15	438	3.05	0.3020	0.0120	0.03920	0.00150	0.480	268.8	9.5	247.7	9	452	83	247.7	9.0	7.85	
15AB-352_16	241	2.31	0.3610	0.0140	0.04860	0.00180	0.365	312	11	306	11	313	90	306.0	11.0	1.92	
15AB-352_17	397	1.79	0.3500	0.0078	0.04804	0.00079	0.318	304.4	5.9	302.4	4.8	318	54	302.4	4.8	0.66	
15AB-352_18	189.9	2.45	3.3780	0.0700	0.21770	0.00480	0.387	1498	16	1269	26	1856	47	DISC	DISC	31.63	
15AB-352_19	443	3.38	0.3532	0.0092	0.04711	0.00093	0.545	309.7	7.5	296.7	5.8	400	56	296.7	5.8	4.20	
15AB-352_20	473	2.72	0.3580	0.0100	0.04530	0.00089	0.030	309.8	7.6	285.6	5.5	505	83	285.6	5.5	7.81	
15AB-352_21	970	311.00	0.3460	0.0150	0.04710	0.00170	0.522	301	11	297	10	368	77	297.0	10.0	1.33	Rim
15AB-352_21	257.3	7.99	0.6840	0.0300	0.08670	0.00260	0.041	528	18	536	15	560	120	536.0	15.0	1.52	Core
15AB-352_22	149.3	2.23	0.3600	0.0150	0.04710	0.00130	0.187	311	12	296.8	8.2	394	95	296.8	8.2	4.57	
15AB-352_23	272	1.95	0.3600	0.0110	0.04870	0.00120	0.315	312.2	8.1	306.3	7.3	339	81	306.3	7.3	1.89	
15AB-352_24	264	1.70	0.3430	0.0100	0.04769	0.00069	0.214	298.6	8	300.3	4.2	288	66	300.3	4.2	0.57	
15AB-352_25	394	2.42	0.3517	0.0092	0.04756	0.00096	0.280	306.4	6.8	299.4	5.9	363	57	299.4	5.9	2.28	
15AB-352_26	82.3	1.66	1.2420	0.0320	0.13710	0.00260	0.495	818	14	828	15	814	45	828.0	15.0	1.22	
15AB-352_27	581	2.26	0.3480	0.0083	0.04683	0.00071	0.103	303.6	6.4	295	4.4	374	58	295.0	4.4	2.83	
15AB-352_28	82.4	1.56	1.0590	0.0440	0.11440	0.00240	0.126	733	21	700	14	830	91	700.0	14.0	4.50	
15AB-352_29	242.2	2.07	0.3440	0.0110	0.04786	0.00081	0.206	299.8	8	301.3	5	314	70	301.3	5.0	0.50	
15AB-352_30	60.6	0.14	0.8760	0.0420	0.10950	0.00330	0.036	640	22	670	19	550	120	670.0	19.0	4.69	
15AB-352_31	216	2.69	0.3530	0.0140	0.04830	0.00160	0.463	307	11	304.1	9.9	302	86	304.1	9.9	0.94	
15AB-352_32	350	76.00	0.3150	0.0110	0.04630	0.00110	0.157	278.5	7.9	291.7	6.7	215	82	291.7	6.7	4.74	

Sample Name _Grain #	[U] ppm	U/Th	207/235	2σ error	206/238	2σ error	RHO	207/235 Age (Ma)	2σ error	206/238 Age (Ma)	2σ error	207/206 Age (Ma)	2σ error	Best age (Ma)	2σ error	% Discordance	Rim /Core
15AB-352_33	96	0.94	0.3170	0.0170	0.04280	0.00110	0.126	278	13	269.9	6.8	350	120	269.9	6.8	2.91	
15AB-352_34	402.9	2.09	0.8610	0.0170	0.10440	0.00170	0.366	631.6	8.9	640.3	9.9	616	42	640.3	9.9	1.38	
15AB-352_35	146.9	2.47	17.4000	0.4100	0.45500	0.01000	0.612	2956	23	2418	46	3381	38	3381.0	38.0	28.48	
15AB-352_36	230	1.68	0.3520	0.0130	0.04657	0.00099	0.073	306.6	9.9	293.4	6.1	402	93	293.4	6.1	4.31	
15AB-352_37	441	3.54	6.6100	0.1400	0.35490	0.00870	0.677	2059	18	1956	41	2165	34	2165.0	34.0	9.65	
15AB-352_38	145	1.62	0.3670	0.0180	0.04990	0.00110	0.211	318	13	313.6	7	330	100	313.6	7.0	1.38	
15AB-352_39	50.4	0.70	5.2440	0.0950	0.32920	0.00700	0.196	1858	16	1833	34	1886	42	1886.0	42.0	2.81	
15AB-352_40	106.9	1.29	5.6260	0.0870	0.35090	0.00580	0.545	1922	13	1942	27	1924	28	1924.0	28.0	0.94	
15AB-352_42	437	5.46	0.9040	0.0150	0.10590	0.00130	0.151	654.2	8	648.8	7.7	682	40	648.8	7.7	0.83	
15AB-352_43	356	1.13	0.6270	0.0200	0.07210	0.00210	0.503	494	13	449	13	683	70	449.0	13.0	9.11	
15AB-352_44	980	5.08	0.3220	0.0110	0.04180	0.00150	0.689	282.9	8.8	263.8	9	429	63	263.8	9.0	6.75	
15AB-352_45	306	0.80	8.0000	0.1100	0.36910	0.00650	0.608	2233	12	2024	30	2442	22	2442.0	22.0	17.12	
15AB-352_46	326	3.05	0.3700	0.0110	0.04980	0.00160	0.422	319	8.2	313.2	9.9	341	78	313.2	9.9	1.82	
15AB-352_47	155	1.43	1.3000	0.0640	0.12360	0.00570	0.427	857	28	751	33	1110	100	DISC	DISC	12.37	Rim
15AB-352_47	66.5	0.96	1.4960	0.0560	0.15680	0.00550	0.497	926	23	938	30	925	74	925.0	74.0	1.41	Core
15AB-352_48	240	2.96	0.3670	0.0120	0.04776	0.00087	0.087	317.8	9.3	300.7	5.3	464	79	300.7	5.3	5.38	
15AB-352_49	143.5	2.47	0.3370	0.0150	0.04850	0.00160	0.364	294	11	305.2	9.9	237	98	305.2	9.9	3.81	
15AB-352_50	504	3.32	0.3462	0.0093	0.04840	0.00120	0.440	301.4	7	305.8	6.9	305	57	305.8	6.9	1.46	
15AB-352_51	178	2.39	0.8130	0.0230	0.09840	0.00270	0.334	603	13	605	16	626	67	605.0	16.0	0.33	
15AB-352_52	49	0.81	0.9830	0.0800	0.10320	0.00360	0.373	682	39	639	20	840	160	639.0	20.0	6.30	
15AB-352_53	201	2.02	0.3361	0.0091	0.04793	0.00099	0.082	293.8	6.9	301.7	6.1	237	81	301.7	6.1	2.69	
15AB-352_54	513	1.60	0.3498	0.0086	0.04906	0.00069	0.264	305	6.4	308.8	4.2	332	51	308.8	4.2	1.25	
15AB-352_56	359	7.90	0.5420	0.0200	0.06390	0.00220	0.330	439	13	399	13	640	100	399.0	13.0	9.11	Rim
15AB-352_56	297	1.61	0.7640	0.0270	0.09080	0.00230	0.242	576	16	560	14	669	76	560.0	14.0	2.78	Core
15AB-352_57	366	2.27	0.3555	0.0094	0.04839	0.00077	0.036	308.4	7	304.6	4.7	359	71	304.6	4.7	1.23	

Sample Name _Grain #	[U] ppm	U/Th	207/235	2σ error	206/238	2σ error	RHO	207/235 Age (Ma)	2σ error	206/238 Age (Ma)	2σ error	207/206 Age (Ma)	2σ error	Best age (Ma)	2σ error	% Discordance	Rim /Core
15AB-352_58	176.9	2.34	0.3470	0.0120	0.04780	0.00120	0.330	301.9	9	300.8	7.2	333	80	300.8	7.2	0.36	
15AB-352_59	303	1.67	0.3399	0.0098	0.04804	0.00095	0.101	296.6	7.5	302.4	5.8	265	75	302.4	5.8	1.96	
15AB-352_60	232	1.19	11.6500	0.1700	0.48950	0.00890	0.546	2576	13	2568	39	2617	29	2617.0	29.0	1.87	
15AB-352_61	320	2.90	0.3463	0.0098	0.04838	0.00080	0.184	301.4	7.4	304.5	4.9	279	67	304.5	4.9	1.03	
15AB-352_62	69.6	1.89	0.7560	0.0520	0.08720	0.00250	0.354	567	30	539	15	670	120	539.0	15.0	4.94	
15AB-352_63	286.7	2.34	0.3310	0.0120	0.04770	0.00120	0.264	291.2	9.1	300.2	7.4	221	82	300.2	7.4	3.09	
15AB-352_64	328	1.97	0.3640	0.0110	0.04752	0.00091	0.160	314.8	8.1	299.2	5.6	403	75	299.2	5.6	4.96	
15AB-352_65	149.5	1.92	0.3530	0.0130	0.04790	0.00110	0.055	306.5	9.6	301.5	6.5	367	96	301.5	6.5	1.63	
15AB-352_66	67.4	0.68	9.7700	0.2600	0.43700	0.01200	0.494	2412	24	2335	53	2485	46	2485.0	46.0	6.04	
15AB-352_67	73.3	1.72	0.7910	0.0470	0.10280	0.00280	0.232	597	25	630	16	440	120	630.0	16.0	5.53	
15AB-352_69	92	1.20	0.7570	0.0250	0.09800	0.00210	0.068	574	15	603	12	444	88	603.0	12.0	5.05	
15AB-352_70	222	2.53	0.3390	0.0140	0.04510	0.00170	0.317	296	11	284	11	400	100	284.0	11.0	4.05	
15AB-352_71	275	2.05	0.3600	0.0110	0.04728	0.00093	0.189	312.9	8.2	297.8	5.7	410	68	297.8	5.7	4.83	
15AB-352_72	12.01	3.84	1.1450	0.0930	0.12370	0.00760	0.068	764	44	751	44	760	220	751.0	44.0	1.70	
15AB-352_73	902	3.63	0.8160	0.0140	0.09610	0.00190	0.541	605.1	8.1	591	11	669	41	591.0	11.0	2.33	
15AB-352_74	79.2	1.09	0.9600	0.0470	0.10930	0.00340	0.295	680	24	668	20	670	110	668.0	20.0	1.76	
15AB-352_75	169	2.22	0.3410	0.0130	0.04740	0.00130	0.089	297	9.5	298.5	8	290	100	298.5	8.0	0.51	
15AB-352_76	612	2.67	0.3361	0.0075	0.04503	0.00079	0.475	294	5.7	283.9	4.9	385	47	283.9	4.9	3.44	
15AB-352_77	584	9.76	0.5680	0.0120	0.07260	0.00120	0.149	456.2	7.5	451.7	6.9	488	56	451.7	6.9	0.99	
15AB-352_78	418	3.34	0.3940	0.0130	0.04750	0.00081	0.385	337.6	9.4	299.1	5	646	67	DISC	DISC	11.40	
15AB-352_79	612	74.00	0.3560	0.0170	0.04860	0.00140	0.624	308	12	306	8.6	387	76	306.0	8.6	0.65	
15AB-352_80	246	3.77	0.3640	0.0110	0.04900	0.00150	0.177	315.5	7.8	307.9	9.5	337	87	307.9	9.5	2.41	
15AB-352_81	477	2.56	0.3568	0.0082	0.04677	0.00071	0.214	309.5	6.1	294.6	4.3	420	54	294.6	4.3	4.81	
15AB-352_82	144	61.00	0.8850	0.0730	0.09960	0.00700	0.636	641	40	612	41	840	150	612.0	41.0	4.52	Rim

Sample Name _Grain #	[U] ppm	U/Th	207/235	2σ error	206/238	2σ error	RHO	207/235 Age (Ma)	2σ error	206/238 Age (Ma)	2σ error	207/206 Age (Ma)	2σ error	Best age (Ma)	2σ error	% Discordance	Rim /Core
15AB-352_82	85.9	1.76	5.3400	0.1000	0.33280	0.00630	0.464	1880	18	1851	30	1917	37	1917.0	37.0	3.44	Core
15AB-352_83	382	4.14	0.4560	0.0330	0.04440	0.00130	0.205	383	24	279.9	7.8	1020	140	DISC	DISC	26.92	
15AB-352_84	250	2.16	0.3760	0.0150	0.04842	0.00095	0.365	327	12	304.8	5.8	494	82	304.8	5.8	6.79	
15AB-352_85	9.03	1.98	4.2700	0.2900	0.26400	0.01400	0.323	1685	55	1505	73	1920	120	1920.0	120.0	21.61	
15AB-352_86	320	2.10	0.3383	0.0082	0.04643	0.00092	0.115	295.5	6.2	292.5	5.7	335	63	292.5	5.7	1.02	
15AB-352_87	397	3.07	0.8340	0.0150	0.09890	0.00150	0.369	615.4	8.3	607.9	8.8	653	39	607.9	8.8	1.22	
15AB-352_88	456	7.11	0.3433	0.0079	0.04733	0.00066	0.113	299.4	5.9	298.1	4.1	293	60	298.1	4.1	0.43	
15AB-352_89	468	36.20	0.3219	0.0082	0.04452	0.00095	0.361	283.7	6.2	280.7	5.8	346	61	280.7	5.8	1.06	
15AB-352_90	407	5.20	6.3000	0.1200	0.36170	0.00650	0.671	2017	16	1989	31	2044	25	2044.0	25.0	2.69	
15AB-352_91	198	0.90	0.5360	0.0140	0.06910	0.00180	0.257	436.2	9.3	431	11	470	72	431.0	11.0	1.19	
15AB-352_92	435	8.14	0.6190	0.0170	0.07410	0.00150	0.403	490	11	460.7	9.1	629	59	460.7	9.1	5.98	
15AB-352_93	670	1.82	0.3447	0.0075	0.04717	0.00069	0.280	300.4	5.7	297.1	4.3	335	52	297.1	4.3	1.10	
15AB-352_94	424	1.95	1.0540	0.0360	0.10920	0.00190	0.337	731	18	668	11	948	67	668.0	11.0	8.62	
15AB-352_95	210.2	44.60	1.1520	0.0340	0.12390	0.00370	0.507	778	17	752	21	857	64	752.0	21.0	3.34	
15AB-352_96	202.7	1.94	0.3387	0.0092	0.04720	0.00086	0.260	295.7	7	297.3	5.3	285	66	297.3	5.3	0.54	
15AB-352_97	234	1.37	5.9110	0.0990	0.35050	0.00740	0.759	1961	14	1935	35	1990	24	1990.0	24.0	2.76	
15AB-352_98	980	4.44	0.2630	0.0120	0.03180	0.00140	0.617	236.5	9.3	201.4	8.9	600	92	DISC	DISC	14.84	
15AB-352_99	256.8	2.57	0.3630	0.0110	0.04800	0.00100	0.342	314	8.4	301.9	6.4	397	73	301.9	6.4	3.85	
15AB-352_100	199	1.64	0.9790	0.0290	0.11550	0.00290	0.481	693	14	704	17	650	62	704.0	17.0	1.59	
15AB-352_101	68.5	1.32	3.3410	0.0850	0.26830	0.00490	0.357	1491	20	1531	25	1454	54	1454.0	54.0	5.30	
15AB-352_102	367	2.51	9.6900	0.1600	0.44820	0.00840	0.634	2404	15	2391	36	2432	25	2432.0	25.0	1.69	
15AB-352_103	17.1	0.73	0.4660	0.0440	0.05810	0.00370	0.071	395	32	364	22	540	220	364.0	22.0	7.85	
15AB-352_104	400	4.11	1.4200	0.1400	0.09760	0.00990	0.790	899	55	598	58	1730	100	DISC	DISC	33.48	Rim
15AB-352_104	50.4	1.02	6.6500	0.2200	0.35700	0.01300	0.478	2061	30	1965	62	2159	64	2159.0	64.0	8.99	Core
15AB-352_105	147.8	0.89	1.0290	0.0220	0.12000	0.00250	0.200	720	11	730	14	692	60	730.0	14.0	1.39	

Sample Name _Grain #	[U] ppm	U/Th	207/235	2σ error	206/238	2σ error	RHO	207/235 Age (Ma)	2σ error	206/238 Age (Ma)	2σ error	207/206 Age (Ma)	2σ error	Best age (Ma)	2σ error	% Discordance	Rim /Core
15AB-352_106	236	2.13	0.3520	0.0110	0.04774	0.00099	0.216	306.7	8.4	300.6	6.1	346	77	300.6	6.1	1.99	
15AB-352_107	262	1.86	0.7510	0.0360	0.08870	0.00360	0.219	571	20	547	21	611	79	547.0	21.0	4.20	
15AB-352_108	186.7	2.36	0.3480	0.0170	0.04500	0.00200	0.265	302	13	284	12	400	110	284.0	12.0	5.96	
15AB-352_109	118	1.09	29.1300	0.4800	0.68500	0.01400	0.599	3457	16	3364	55	3519	22	3519.0	22.0	4.40	
15AB-352_110	128.7	1.26	1.2440	0.0300	0.13530	0.00240	0.114	819	14	818	14	813	62	818.0	14.0	0.12	
15AB-352_111	397	1.63	1.6130	0.0460	0.15860	0.00200	0.399	974	18	949	11	1043	53	1043.0	53.0	9.01	
15AB-352_112	196	2.13	0.3450	0.0130	0.04880	0.00110	0.194	301.8	9.5	306.8	6.7	261	82	306.8	6.7	1.66	
15AB-352_113	323	2.47	0.8210	0.0250	0.09280	0.00210	0.007	611	13	572	13	797	70	572.0	13.0	6.38	
15AB-352_114	174.5	1.10	6.0110	0.0630	0.36570	0.00470	0.329	1978	9.2	2009	22	1954	25	1954.0	25.0	2.81	
15AB-352_115	130.6	1.54	1.7370	0.0410	0.16780	0.00290	0.448	1020	15	1000	16	1062	41	1062.0	41.0	5.84	
15AB-352_116	411	3.17	0.3890	0.0180	0.05130	0.00270	0.328	333	13	322	17	360	110	322.0	17.0	3.30	
15AB-352_117	357	2.50	0.3530	0.0100	0.04800	0.00120	0.425	307.5	7.9	302.4	7.1	322	64	302.4	7.1	1.66	
15AB-352_118	166	0.56	4.2100	0.1000	0.27680	0.00720	0.445	1675	20	1575	37	1815	56	1815.0	56.0	13.22	
15AB-352_119	138.4	2.14	7.0100	0.3200	0.12050	0.00410	0.613	2108	40	733	24	3982	48	DISC	DISC	65.23	
15AB-352_120	625	2.89	0.3756	0.0077	0.04805	0.00080	0.368	323.5	5.7	302.5	4.9	472	46	302.5	4.9	6.49	
15AB-352_121	66.3	1.74	0.8750	0.0370	0.09860	0.00250	0.251	640	20	606	15	754	94	606.0	15.0	5.31	
15AB-352_122	239	30.30	0.5880	0.0310	0.07580	0.00220	0.023	468	20	471	13	430	130	471.0	13.0	0.64	Rim
15AB-352_122	140.2	8.74	14.4500	0.5800	0.48900	0.01800	0.593	2778	38	2565	76	2986	59	2986.0	59.0	14.10	Core
15AB-352_123	72.5	4.40	0.4710	0.0240	0.05950	0.00220	0.292	390	17	373	14	480	120	373.0	14.0	4.36	
15AB-352_124	835	290.00	0.3343	0.0097	0.04690	0.00130	0.340	292.6	7.4	295.7	7.8	261	72	295.7	7.8	1.06	Rim
15AB-352_124	509	4.80	0.6110	0.0200	0.07410	0.00240	0.397	483	12	461	14	588	83	461.0	14.0	4.55	Core
15AB-352_125	85.4	0.85	0.7430	0.0350	0.09010	0.00240	0.345	561	20	556	14	592	95	556.0	14.0	0.89	
15AB-352_126	148.5	1.65	1.0740	0.0420	0.12320	0.00280	0.411	743	19	749	16	689	80	749.0	16.0	0.81	
15AB-352_127	456	2.58	0.3900	0.0120	0.05070	0.00110	0.308	333.6	8.9	319.7	7	419	69	319.7	7.0	4.17	
15AB-352_128	109	1.52	1.6900	0.0510	0.17270	0.00350	0.409	1003	20	1027	19	952	58	952.0	58.0	7.88	

Sample Name _Grain #	[U] ppm	U/Th	207/235	2σ error	206/238	2σ error	RHO	207/235 Age (Ma)	2σ error	206/238 Age (Ma)	2σ error	207/206 Age (Ma)	2σ error	Best age (Ma)	2σ error	% Discordance	Rim /Core
15AB-352_129	176	1.82	0.3480	0.0120	0.04670	0.00100	0.055	303.5	8.7	294.4	6.2	325	85	294.4	6.2	3.00	
15AB-352_130	730	3.30	0.3850	0.0130	0.04807	0.00088	0.213	331	9.5	302.6	5.4	498	92	302.6	5.4	8.58	
14AB-G07_1	500	7.57	1.7430	0.0340	0.17250	0.00370	0.655	1023	12	1026	20	1017	32	1017.0	32.0	0.88	
14AB-G07_2	177	2.48	0.3545	0.0085	0.04809	0.00078	0.032	308.6	6.5	302.7	4.8	320	68	302.7	4.8	1.91	
14AB-G07_3	80.3	2.20	0.8590	0.0240	0.10220	0.00200	0.365	630	13	627	11	601	60	627.0	11.0	0.48	
14AB-G07_4	150	0.99	1.5790	0.0580	0.15890	0.00590	0.844	959	23	955	32	956	44	956.0	44.0	0.10	
14AB-G07_5	2120	7.33	0.3460	0.0120	0.04620	0.00170	0.859	301.3	9.3	291	11	406	39	291.0	11.0	3.42	
14AB-G07_6	154	1.32	1.2180	0.0270	0.13250	0.00260	0.520	807	13	802	15	796	44	802.0	15.0	0.62	
14AB-G07_7	90	1.66	0.7070	0.0260	0.08310	0.00190	0.293	541	16	515	11	655	81	515.0	11.0	4.81	
14AB-G07_8	412	1.82	0.3555	0.0065	0.04912	0.00078	0.328	308.6	4.9	309.6	4.9	310	43	309.6	4.9	0.32	
14AB-G07_9	1546	3.27	0.6540	0.0100	0.07480	0.00120	0.747	511	6.3	465.3	7	734	26	465.3	7.0	8.94	Rim
14AB-G07_9	156	2.29	1.2450	0.0330	0.13170	0.00290	0.180	820	15	797	17	869	69	797.0	17.0	2.80	Core
14AB-G07_10	150	8.40	0.4590	0.0150	0.06140	0.00150	0.434	383	11	384.2	9.3	374	67	384.2	9.3	0.31	
14AB-G07_11	149.1	1.21	0.8340	0.0170	0.10030	0.00160	0.262	616.4	9.6	616.2	9.5	625	53	616.2	9.5	0.03	
14AB-G07_12	96.1	1.86	0.6860	0.0200	0.08870	0.00190	0.260	531	12	548	11	500	71	548.0	11.0	3.20	
14AB-G07_13	100.6	1.63	1.5270	0.0320	0.15980	0.00200	0.071	940	13	955	11	924	49	924.0	49.0	3.35	
14AB-G07_14	83.7	1.73	0.9450	0.0180	0.11050	0.00200	0.063	676	9.3	675	12	662	60	675.0	12.0	0.15	
14AB-G07_15	194	1.15	1.1090	0.0270	0.12400	0.00260	0.556	758	13	753	15	746	41	753.0	15.0	0.66	
14AB-G07_16	183	3.11	1.1960	0.0300	0.13150	0.00170	0.555	797	14	796.2	9.4	810	48	796.2	9.4	0.10	
14AB-G07_17	422	1.64	0.3739	0.0081	0.04799	0.00064	0.009	322.2	6	302.2	3.9	456	55	302.2	3.9	6.21	
14AB-G07_18	62.4	1.18	13.0400	0.2100	0.51180	0.00980	0.635	2681	15	2662	42	2710	23	2710.0	23.0	1.77	
14AB-G07_19	569	1.97	0.3494	0.0063	0.04791	0.00070	0.092	304	4.7	301.6	4.3	326	48	301.6	4.3	0.79	
14AB-G07_20	55.2	1.19	1.5820	0.0990	0.14530	0.00300	0.568	945	32	874	17	1126	86	1126.0	86.0	22.38	
14AB-G07_21	315	4.76	1.4330	0.0310	0.14720	0.00290	0.538	902	13	885	16	952	43	952.0	43.0	7.04	
14AB-G07_22	196	1.70	0.4290	0.0098	0.05759	0.00088	0.204	362.9	7.1	360.9	5.4	412	53	360.9	5.4	0.55	

Sample Name _Grain #	[U] ppm	U/Th	207/235	2σ error	206/238	2σ error	RHO	207/235 Age (Ma)	2σ error	206/238 Age (Ma)	2σ error	207/206 Age (Ma)	2σ error	Best age (Ma)	2σ error	% Discordance	Rim /Core
14AB-G07_23	100.2	0.90	0.8050	0.0210	0.09690	0.00140	0.055	599	11	596.2	8.4	662	62	596.2	8.4	0.47	
14AB-G07_24	479	1.32	0.7050	0.0150	0.08650	0.00140	0.506	542.1	8.5	534.8	8.5	558	42	534.8	8.5	1.35	
14AB-G07_25	427	2.41	0.3418	0.0072	0.04900	0.00069	0.324	299.7	5.4	308.4	4.2	260	47	308.4	4.2	2.90	
14AB-G07_26	287.6	3.84	4.5580	0.0580	0.31320	0.00440	0.646	1742	11	1756	22	1736	20	1736.0	20.0	1.15	
14AB-G07_27	115.8	1.19	0.3430	0.0110	0.04769	0.00089	0.064	300.2	8.6	300.3	5.5	315	87	300.3	5.5	0.03	
14AB-G07_28	112.4	1.06	1.4410	0.0280	0.14670	0.00200	0.089	907	12	883	11	1003	42	1003.0	42.0	11.96	
14AB-G07_29	117	0.83	0.8460	0.0200	0.10340	0.00180	0.093	622	11	634	10	627	64	634.0	10.0	1.93	
14AB-G07_30	327	9.30	0.7480	0.0110	0.09380	0.00150	0.317	567.4	6.6	577.7	8.7	559	39	577.7	8.7	1.82	
14AB-G07_31	828	12.11	0.9590	0.0280	0.10650	0.00200	0.642	682	14	652	12	811	41	652.0	12.0	4.40	
14AB-G07_32	107	1.59	0.6160	0.0260	0.07570	0.00170	0.348	485	16	470	10	542	93	470.0	10.0	3.09	
14AB-G07_33	43	1.39	1.8490	0.0530	0.18110	0.00390	0.261	1062	19	1072	21	1067	57	1067.0	57.0	0.47	
14AB-G07_34	167	2.84	1.9880	0.0270	0.18810	0.00270	0.326	1110.7	9.3	1113	15	1121	30	1121.0	30.0	0.71	
14AB-G07_35	119	1.25	0.6010	0.0160	0.07610	0.00180	0.108	477	10	473	11	508	75	473.0	11.0	0.84	
14AB-G07_36	338	0.95	0.8200	0.0140	0.10120	0.00160	0.656	607.5	7.8	621.6	9.2	600	33	621.6	9.2	2.32	
14AB-G07_37	95.2	1.15	1.7020	0.0360	0.17050	0.00260	0.235	1008	14	1015	14	1023	47	1023.0	47.0	0.78	
14AB-G07_38	139.7	1.82	0.8900	0.0180	0.10560	0.00180	0.251	645.5	9.9	647	10	671	50	647.0	10.0	0.23	
14AB-G07_39	7.55	0.40	1.8900	0.1300	0.19260	0.00920	0.276	1081	45	1141	51	1000	150	1000.0	150.0	14.10	
14AB-G07_40	64.4	0.50	0.7910	0.0220	0.09770	0.00260	0.232	591	12	601	15	591	71	601.0	15.0	1.69	
14AB-G07_41	20.1	2.75	1.2510	0.0690	0.14030	0.00530	0.154	832	32	845	30	790	130	845.0	30.0	1.56	
14AB-G07_42	143	0.72	5.7870	0.0750	0.34740	0.00430	0.449	1944	11	1921	21	1970	26	1970.0	26.0	2.49	
14AB-G07_43	87.4	0.72	3.8510	0.0640	0.28300	0.00470	0.549	1604	14	1606	23	1618	29	1618.0	29.0	0.74	
14AB-G07_44	127.9	1.94	11.2300	0.1700	0.45960	0.00680	0.691	2541	14	2437	30	2632	18	2632.0	18.0	7.41	
14AB-G07_45	288	1.49	0.9400	0.0170	0.11020	0.00160	0.493	672.3	8.9	674.9	9.7	682	38	674.9	9.7	0.39	
14AB-G07_46	223.5	3.05	0.3670	0.0100	0.05006	0.00082	0.173	317.2	7.7	314.9	5	361	66	314.9	5.0	0.73	
14AB-G07_47	130.1	0.53	0.8670	0.0240	0.10340	0.00190	0.189	633	13	634	11	628	61	634.0	11.0	0.16	

Sample Name _Grain #	[U] ppm	U/Th	207/235	2σ error	206/238	2σ error	RHO	207/235 Age (Ma)	2σ error	206/238 Age (Ma)	2σ error	207/206 Age (Ma)	2σ error	Best age (Ma)	2σ error	% Discordance	Rim /Core
14AB-G07_48	91.6	9.59	0.8790	0.0230	0.10920	0.00210	0.425	641	12	668	12	571	51	668.0	12.0	4.21	
14AB-G07_49	159	0.52	0.8150	0.0200	0.09900	0.00170	0.127	605	11	608	10	612	57	608.0	10.0	0.50	
14AB-G07_50	230	2.31	0.8700	0.0140	0.10440	0.00180	0.346	635.2	7.7	641	10	613	38	641.0	10.0	0.91	
14AB-G07_51	293	1.94	0.3738	0.0085	0.05195	0.00081	0.074	322.1	6.3	326.5	4.9	279	53	326.5	4.9	1.37	
14AB-G07_52	287	1.87	0.7090	0.0150	0.08780	0.00150	0.608	545	8.5	542.2	9	536	44	542.2	9.0	0.51	
14AB-G07_53	103.1	1.24	0.7900	0.0170	0.09770	0.00180	0.325	590.5	9.5	601	10	578	47	601.0	10.0	1.78	
14AB-G07_54	158.7	1.37	0.8650	0.0180	0.10230	0.00230	0.613	632	9.6	627	14	625	41	627.0	14.0	0.79	
14AB-G07_55	147	1.10	0.8810	0.0250	0.10170	0.00190	0.300	640	13	624	11	691	62	624.0	11.0	2.50	
14AB-G07_56	156.1	2.84	0.8980	0.0190	0.10800	0.00150	0.289	650	10	661.1	8.7	615	53	661.1	8.7	1.71	
14AB-G07_57	28.3	1.05	0.8580	0.0360	0.10050	0.00250	0.063	628	20	617	15	630	100	617.0	15.0	1.75	
14AB-G07_58	78.2	2.72	1.0680	0.0390	0.11850	0.00360	0.154	740	21	721	21	797	91	721.0	21.0	2.57	
14AB-G07_59	428	18.70	0.9700	0.0110	0.11460	0.00100	0.445	687.9	5.7	699.2	6.1	658	24	699.2	6.1	1.64	
14AB-G07_60	339	2.60	1.8930	0.0180	0.18530	0.00200	0.269	1078.2	6.4	1095	11	1038	23	1038.0	23.0	5.49	
14AB-G07_61	52.01	0.66	0.7730	0.0230	0.09670	0.00210	0.147	580	13	595	12	492	73	595.0	12.0	2.59	
14AB-G07_62	572	1.69	0.3538	0.0064	0.04814	0.00076	0.485	307.3	4.8	303	4.7	320	37	303.0	4.7	1.40	
14AB-G07_63	111	1.53	1.5960	0.0320	0.16400	0.00250	0.295	967	12	978	14	937	42	937.0	42.0	4.38	
14AB-G07_64	142	0.49	0.8250	0.0150	0.09950	0.00160	0.300	610	8.4	611.1	9.1	572	47	611.1	9.1	0.18	
14AB-G07_65	124	1.90	12.7000	0.1200	0.51020	0.00530	0.581	2659.5	8.2	2657	23	2644	14	2644.0	14.0	0.49	
14AB-G07_66	133.6	1.92	1.6330	0.0410	0.16420	0.00310	0.624	987	16	980	17	1005	44	1005.0	44.0	2.49	
14AB-G07_67	1033	3.77	0.3601	0.0052	0.04982	0.00048	0.326	312.2	3.9	313.4	3	294	33	313.4	3.0	0.38	
14AB-G07_68	378	1.98	0.8090	0.0120	0.09750	0.00110	0.378	601.2	6.9	599.9	6.5	584	30	599.9	6.5	0.22	
14AB-G07_69	328	6.53	0.6570	0.0180	0.08360	0.00200	0.411	513	11	518	12	482	63	518.0	12.0	0.97	
14AB-G07_70	167	0.60	5.7430	0.0620	0.36230	0.00550	0.349	1937.3	9.4	1992	26	1853	26	1853.0	26.0	7.50	
14AB-G07_71	151	2.36	3.5200	0.1300	0.23790	0.00680	0.829	1526	28	1374	35	1751	35	1751.0	35.0	21.53	
14AB-G07_72	153.2	1.80	2.3080	0.0960	0.18230	0.00600	0.818	1211	29	1079	33	1434	44	1434.0	44.0	24.76	

Sample Name _Grain #	[U] ppm	U/Th	207/235	2σ error	206/238	2σ error	RHO	207/235 Age (Ma)	2σ error	206/238 Age (Ma)	2σ error	207/206 Age (Ma)	2σ error	Best age (Ma)	2σ error	% Discordance	Rim /Core
14AB-G07_73	152.8	1.73	0.9520	0.0180	0.11200	0.00160	0.170	678.4	9.4	684.3	9.5	682	47	684.3	9.5	0.87	
14AB-G07_74	328	1.32	11.5600	0.1200	0.48800	0.00490	0.609	2568.5	9.9	2567	21	2559	15	2559.0	15.0	0.31	
14AB-G07_75	54	1.45	1.2480	0.0420	0.13630	0.00320	0.269	828	19	824	18	805	79	824.0	18.0	0.48	
14AB-G07_76	900	0.85	3.5000	0.1500	0.21820	0.00940	0.974	1526	33	1275	51	1893	17	DISC	DISC	32.65	
14AB-G07_77	70.1	1.45	0.7500	0.0260	0.09090	0.00260	0.082	567	15	560	15	623	95	560.0	15.0	1.23	
14AB-G07_78	49	1.42	0.8980	0.0370	0.10590	0.00220	0.003	652	20	649	13	630	100	649.0	13.0	0.46	
14AB-G07_79	122	0.95	0.8830	0.0280	0.10440	0.00160	0.060	641	15	639.9	9.2	645	77	639.9	9.2	0.17	
14AB-G07_80	145	2.13	0.9160	0.0180	0.10900	0.00170	0.342	659.8	9.6	666.9	9.8	643	45	666.9	9.8	1.08	
14AB-G07_81	397	4.15	0.3577	0.0079	0.04848	0.00077	0.277	311	6	305.2	4.7	337	53	305.2	4.7	1.86	
14AB-G07_82	222.1	3.10	0.3930	0.0140	0.04939	0.00095	0.419	336	10	310.7	5.8	504	76	310.7	5.8	7.53	
14AB-G07_83	19.38	0.76	0.6790	0.0440	0.07210	0.00280	0.144	533	27	449	17	880	150	DISC	DISC	15.76	
14AB-G07_84	479	1.86	0.3498	0.0063	0.04758	0.00050	0.246	304.4	4.8	299.6	3.1	340	42	299.6	3.1	1.58	
14AB-G07_85	63.2	1.29	3.9100	0.1100	0.25400	0.00560	0.541	1628	23	1459	29	1842	46	1842.0	46.0	20.79	
14AB-G07_86	262	2.31	0.3787	0.0085	0.05161	0.00075	0.274	325.7	6.3	324.3	4.6	287	52	324.3	4.6	0.43	
14AB-G07_87	312	2.21	12.3000	0.3000	0.50200	0.01400	0.806	2627	23	2627	57	2621	30	2621.0	30.0	0.23	
14AB-G07_88	637	0.43	0.8900	0.0250	0.09920	0.00190	0.798	646	13	609	11	774	31	609.0	11.0	5.73	
14AB-G07_89	415	2.35	1.1380	0.0190	0.12370	0.00230	0.601	771.2	9.3	752	13	838	37	752.0	13.0	2.49	
14AB-G07_90	492	13.70	1.1410	0.0370	0.12510	0.00260	0.894	771	17	760	15	858	35	760.0	15.0	1.43	
14AB-G07_91	280	2.25	0.3515	0.0075	0.04851	0.00068	0.244	305.5	5.6	305.3	4.2	318	49	305.3	4.2	0.07	
14AB-G07_92	300	1.80	0.4006	0.0085	0.05420	0.00110	0.449	341.8	6.2	340.3	6.6	369	48	340.3	6.6	0.44	
14AB-G07_93	86.3	1.32	0.9710	0.0220	0.11000	0.00220	0.299	690	12	672	13	742	56	672.0	13.0	2.61	
14AB-G07_94	269.1	5.32	10.0630	0.0990	0.44880	0.00600	0.546	2440	9.1	2389	27	2483	18	2483.0	18.0	3.79	
14AB-G07_95	66.4	0.98	1.8070	0.0420	0.18050	0.00250	0.049	1048	15	1069	14	993	55	993.0	55.0	7.65	
14AB-G07_96	1021	1.72	0.3225	0.0093	0.04200	0.00130	0.760	284.3	7	265.2	7.7	422	46	265.2	7.7	6.72	
14AB-G07_97	23.54	1.31	1.6650	0.0700	0.16480	0.00410	0.219	995	26	986	22	970	96	970.0	96.0	1.65	

Sample Name _Grain #	[U] ppm	U/Th	207/235	2σ error	206/238	2σ error	RHO	207/235 Age (Ma)	2σ error	206/238 Age (Ma)	2σ error	207/206 Age (Ma)	2σ error	Best age (Ma)	2σ error	% Discordance	Rim /Core
14AB-G07_98	406	1.82	0.3498	0.0070	0.04938	0.00067	0.412	304.4	5.3	310.7	4.1	273	42	310.7	4.1	2.07	
14AB-G07_99	108.6	1.18	12.1700	0.1600	0.51480	0.00670	0.503	2616	12	2676	28	2592	21	2592.0	21.0	3.24	
14AB-G07_100	491	0.67	11.7900	0.1300	0.48100	0.00610	0.765	2589	10	2531	26	2652	14	2652.0	14.0	4.56	
14AB-G07_101	449	3.27	0.7550	0.0120	0.09470	0.00130	0.405	570.8	6.8	583.5	7.7	545	34	583.5	7.7	2.22	
14AB-G07_102	63.2	1.01	1.6290	0.0390	0.16010	0.00410	0.413	984	14	957	23	1055	57	1055.0	57.0	9.29	
14AB-G07_103	533	48.10	1.1700	0.0500	0.12710	0.00570	0.656	784	24	770	33	841	84	770.0	33.0	1.79	
14AB-G07_104	251	3.05	1.7620	0.0230	0.17300	0.00180	0.483	1033.1	8.7	1028.5	9.8	1051	25	1051.0	25.0	2.14	
14AB-G07_105	196.8	3.34	0.8850	0.0200	0.10680	0.00230	0.646	648	11	654	13	648	41	654.0	13.0	0.93	
14AB-G07_106	557	2.19	0.3399	0.0053	0.04771	0.00047	0.141	297	4	300.4	2.9	283	40	300.4	2.9	1.14	
14AB-G07_107	378	2.17	0.3626	0.0078	0.04909	0.00070	0.252	313.8	5.8	308.9	4.3	360	49	308.9	4.3	1.56	
14AB-G07_108	277	1.57	0.3357	0.0063	0.04736	0.00073	0.122	293.7	4.8	298.2	4.5	268	50	298.2	4.5	1.53	
14AB-G07_109	63.9	1.73	0.8460	0.0270	0.10170	0.00190	0.167	625	15	624	11	678	75	624.0	11.0	0.16	
14AB-G07_110	234	1.54	1.3970	0.0200	0.14640	0.00180	0.454	888.4	8	881	10	902	30	902.0	30.0	2.33	
14AB-G07_111	108.8	1.44	0.7530	0.0220	0.09230	0.00200	0.299	571	13	569	12	613	64	569.0	12.0	0.35	
14AB-G07_112	116.1	1.33	1.0290	0.0230	0.12150	0.00190	0.332	719	11	739	11	644	50	739.0	11.0	2.78	
14AB-G07_113	240	2.50	1.0410	0.0190	0.11890	0.00130	0.159	723.4	9.6	724	7.8	736	39	724.0	7.8	0.08	
14AB-G07_114	159.2	5.61	0.8830	0.0210	0.10150	0.00140	0.297	642	11	622.8	8.1	718	52	622.8	8.1	2.99	
14AB-G07_115	324	2.66	0.3545	0.0070	0.04801	0.00069	0.454	308.5	5.4	302.3	4.2	351	44	302.3	4.2	2.01	
14AB-G07_116	118	0.69	0.7590	0.0180	0.09380	0.00160	0.192	574	11	578	9.7	557	56	578.0	9.7	0.70	
14AB-G07_117	70.6	1.90	0.8700	0.0330	0.10220	0.00210	0.034	633	18	627	12	655	88	627.0	12.0	0.95	
14AB-G07_118	452	2.68	0.3519	0.0064	0.04829	0.00057	0.149	306	4.8	304	3.5	324	45	304.0	3.5	0.65	
14AB-G07_119	208	38.40	0.8920	0.0160	0.10800	0.00170	0.418	648	8.5	662.1	9.6	618	34	662.1	9.6	2.18	
14AB-G07_120	89.6	0.89	0.8090	0.0280	0.10090	0.00200	0.234	602	15	620	12	536	76	620.0	12.0	2.99	
14AB-G07_121	430	16.90	0.5785	0.0096	0.07434	0.00090	0.298	463.2	6.2	462.2	5.4	476	40	462.2	5.4	0.22	
3_Gerbe_1	526	2.09	0.3433	0.0048	0.04820	0.00059	0.440	299.5	3.6	303.4	3.6	283	32	303.4	3.6	1.30	

Sample Name _Grain #	[U] ppm	U/Th	207/235	2σ error	206/238	2σ error	RHO	207/235 Age (Ma)	2σ error	206/238 Age (Ma)	2σ error	207/206 Age (Ma)	2σ error	Best age (Ma)	2σ error	% Discordance	Rim /Core
3_Gerbe_2	816	2.77	0.3585	0.0052	0.04913	0.00087	0.619	310.9	3.9	309.1	5.3	335	32	309.1	5.3	0.58	
3_Gerbe_3	299	0.87	0.7883	0.0091	0.09510	0.00110	0.251	589.9	5.2	586.1	6.2	608	28	586.1	6.2	0.64	
3_Gerbe_4	323	2.51	0.5971	0.0096	0.07637	0.00096	0.434	475	6.1	474.4	5.8	485	31	474.4	5.8	0.13	
3_Gerbe_5	272	0.80	0.8497	0.0077	0.10022	0.00090	0.521	624.3	4.2	615.7	5.3	649	19	615.7	5.3	1.38	
3_Gerbe_6	251.2	2.11	1.7130	0.0150	0.16740	0.00170	0.775	1013.4	5.4	997.7	9.6	1045	17	1045.0	17.0	4.53	
3_Gerbe_7	89	2.02	0.8930	0.0150	0.10390	0.00150	0.359	647.2	8.1	638	8.7	648	40	638.0	8.7	1.42	
3_Gerbe_8	317	16.80	0.9550	0.0170	0.11140	0.00190	0.582	679.8	8.9	680	11	686	29	680.0	11.0	0.03	
3_Gerbe_9	548	9.29	0.6350	0.0140	0.08180	0.00160	0.760	498.6	9.1	506.6	9.8	489	35	506.6	9.8	1.60	
3_Gerbe_10	193	2.34	1.9470	0.0290	0.18490	0.00390	0.410	1097	10	1094	21	1116	40	1116.0	40.0	1.97	
3_Gerbe_11	595	1.84	1.0240	0.0250	0.11600	0.00200	0.646	716	13	708	12	736	33	708.0	12.0	1.12	
3_Gerbe_12	203	2.45	0.8950	0.0160	0.10480	0.00150	0.192	648.3	8.7	642.6	8.8	670	40	642.6	8.8	0.88	
3_Gerbe_13	108.7	1.79	0.8990	0.0150	0.10310	0.00150	0.242	650.8	8	632.3	8.8	716	39	632.3	8.8	2.84	
3_Gerbe_14	215.1	1.27	1.7790	0.0190	0.17360	0.00180	0.276	1038.4	6.6	1032	9.8	1042	24	1042.0	24.0	0.96	
3_Gerbe_15	634	2.11	0.5030	0.0110	0.06440	0.00140	0.477	413.5	7.7	403.6	8.2	470	38	403.6	8.2	2.39	
3_Gerbe_16	375	1.57	0.4910	0.0130	0.05760	0.00140	0.460	405.1	9	360.9	8.3	643	66	DISC	DISC	10.91	
3_Gerbe_17	1155	1.03	1.1320	0.0220	0.11340	0.00260	0.707	768	10	692	15	1008	30	692.0	15.0	9.90	
3_Gerbe_18	333	3.48	0.5881	0.0071	0.07479	0.00079	0.273	470	4.6	464.9	4.8	475	33	464.9	4.8	1.09	
3_Gerbe_19	1171	5.55	0.3410	0.0047	0.04676	0.00070	0.591	298.3	3.5	294.6	4.3	316	30	294.6	4.3	1.24	
3_Gerbe_20	40.8	23.20	14.8400	0.2300	0.52620	0.00890	0.742	2807	15	2725	38	2859	21	2859.0	21.0	4.69	
3_Gerbe_21	188.5	1.45	0.9080	0.0120	0.10760	0.00160	0.541	655.5	6.7	658.9	9.2	643	30	658.9	9.2	0.52	
3_Gerbe_22	841	30.10	0.7960	0.0250	0.09040	0.00280	0.608	594	14	558	17	704	52	558.0	17.0	6.06	Rim
3_Gerbe_22	336	2.09	1.1910	0.0250	0.12370	0.00230	0.630	796	12	752	13	920	36	752.0	13.0	5.53	Core
3_Gerbe_23	258	2.46	7.1130	0.0740	0.38570	0.00370	0.699	2125.2	9.3	2106	17	2152	15	2152.0	15.0	2.14	
3_Gerbe_26	470	2.22	0.3628	0.0046	0.05013	0.00057	0.392	314.2	3.4	315.3	3.5	310	27	315.3	3.5	0.35	
3_Gerbe_27	144.2	1.56	5.0970	0.0630	0.31740	0.00430	0.522	1835	10	1776	21	1910	22	1910.0	22.0	7.02	

Sample Name _Grain #	[U] ppm	U/Th	207/235	2σ error	206/238	2σ error	RHO	207/235 Age (Ma)	2σ error	206/238 Age (Ma)	2σ error	207/206 Age (Ma)	2σ error	Best age (Ma)	2σ error	% Discordance	Rim /Core
3_Gerbe_29	72.7	1.64	15.8100	0.1500	0.53850	0.00580	0.684	2866.3	9.2	2777	24	2926	14	2926.0	14.0	5.09	
3_Gerbe_30	260	3.61	0.6319	0.0090	0.07980	0.00110	0.540	497	5.6	494.8	6.5	482	28	494.8	6.5	0.44	
3_Gerbe_31	333	3.93	0.5626	0.0081	0.07220	0.00110	0.649	453	5.3	449.5	6.6	467	30	449.5	6.6	0.77	
3_Gerbe_32	231	3.33	0.3637	0.0063	0.04928	0.00055	0.369	314.7	4.7	310.1	3.4	369	41	310.1	3.4	1.46	
3_Gerbe_33	250	3.20	0.5547	0.0092	0.07247	0.00092	0.317	447.8	6	451	5.5	444	36	451.0	5.5	0.71	
3_Gerbe_34	219	0.38	0.8420	0.0120	0.10080	0.00130	0.501	619.7	6.7	619.1	7.7	621	29	619.1	7.7	0.10	
3_Gerbe_35	405	1.83	0.3554	0.0042	0.04973	0.00038	0.226	308.7	3.2	312.8	2.4	276	30	312.8	2.4	1.33	
3_Gerbe_36	579	3.38	0.9890	0.0120	0.11370	0.00170	0.577	697.7	6.3	694.1	9.7	717	24	694.1	9.7	0.52	
3_Gerbe_37	55	0.95	0.8790	0.0190	0.10450	0.00130	0.044	640	10	640.9	7.3	634	55	640.9	7.3	0.14	
3_Gerbe_38	706	2.09	0.7500	0.0130	0.09070	0.00200	0.577	570.4	7.8	560	12	590	40	560.0	12.0	1.82	
3_Gerbe_39	461	1.40	0.7180	0.0130	0.08720	0.00130	0.627	549	7.6	538.8	7.6	590	33	538.8	7.6	1.86	
3_Gerbe_40	456	2.11	0.3824	0.0065	0.05131	0.00089	0.565	328.6	4.8	322.5	5.4	358	38	322.5	5.4	1.86	
3_Gerbe_41	379	4.85	0.7649	0.0090	0.09248	0.00085	0.362	576.6	5.2	570.2	5	590	23	570.2	5.0	1.11	
3_Gerbe_43	186.6	2.34	0.7130	0.0130	0.08830	0.00150	0.563	546	7.8	545.5	9	568	37	545.5	9.0	0.09	
3_Gerbe_44	341	2.21	1.4380	0.0180	0.14870	0.00150	0.613	906.4	7.5	893.6	8.3	932	21	932.0	21.0	4.12	
3_Gerbe_45	419	2.21	4.8250	0.0640	0.29750	0.00460	0.831	1789	11	1679	23	1922	18	1922.0	18.0	12.64	
3_Gerbe_46	272.5	4.49	0.4755	0.0093	0.06080	0.00110	0.715	394.7	6.4	380.3	6.5	456	34	380.3	6.5	3.65	
3_Gerbe_47	575	43.40	0.4805	0.0095	0.06139	0.00098	0.759	398.2	6.5	384	5.9	465	30	384.0	5.9	3.57	
3_Gerbe_48	488	0.95	1.0900	0.1700	0.09530	0.00180	0.470	729	76	587	11	1170	260	DISC	DISC	19.48	
3_Gerbe_49	277.7	1.84	1.5660	0.0330	0.15700	0.00330	0.627	955	13	939	18	978	39	978.0	39.0	3.99	
3_Gerbe_50	213.4	2.50	0.8220	0.0150	0.09750	0.00160	0.498	608.4	8.3	599.9	9.6	645	32	599.9	9.6	1.40	
3_Gerbe_51	820	1.47	0.3049	0.0041	0.04144	0.00056	0.656	270.2	3.2	261.7	3.5	358	26	261.7	3.5	3.15	
3_Gerbe_52	1459	3.01	0.3200	0.0034	0.04310	0.00032	0.397	281.8	2.6	272	2	356	24	272.0	2.0	3.48	
3_Gerbe_53	315	4.65	0.5603	0.0095	0.07115	0.00086	0.619	451.4	6.2	443.1	5.2	498	30	443.1	5.2	1.84	

Sample Name _Grain #	[U] ppm	U/Th	207/235	2σ error	206/238	2σ error	RHO	207/235 Age (Ma)	2σ error	206/238 Age (Ma)	2σ error	207/206 Age (Ma)	2σ error	Best age (Ma)	2σ error	% Discordance	Rim /Core
3_Gerbe_54	836	1.94	0.3402	0.0043	0.04579	0.00046	0.477	297.2	3.3	288.6	2.8	357	29	288.6	2.8	2.89	
3_Gerbe_55	668	20.60	1.0030	0.0250	0.11330	0.00230	0.895	704	13	691	13	750	23	691.0	13.0	1.85	
3_Gerbe_56	2830	14.86	0.2390	0.0120	0.02941	0.00095	0.416	216.8	9.5	186.8	5.9	546	83	DISC	DISC	13.84	
3_Gerbe_57	418.6	2.19	0.3423	0.0057	0.04685	0.00080	0.503	298.8	4.3	295.1	4.9	365	38	295.1	4.9	1.24	
3_Gerbe_58	718	2.19	1.6520	0.0250	0.16120	0.00240	0.694	989.5	9.6	963	13	1047	20	1047.0	20.0	8.02	
3_Gerbe_60	667	13.50	0.9450	0.0120	0.10980	0.00130	0.496	675.4	6.5	671.8	7.5	713	27	671.8	7.5	0.53	
3_Gerbe_61	299	0.92	1.0400	0.0110	0.11650	0.00130	0.482	723.5	5.7	710.1	7.6	754	22	710.1	7.6	1.85	
3_Gerbe_62	277	1.08	1.0510	0.0180	0.12020	0.00180	0.219	728.6	8.9	731	10	720	28	731.0	10.0	0.33	
3_Gerbe_63	545	1.51	0.6006	0.0080	0.07577	0.00082	0.411	477.4	5	470.8	4.9	518	27	470.8	4.9	1.38	
3_Gerbe_64	334	1.89	0.8010	0.0160	0.09350	0.00260	0.773	597	9.2	578	15	665	37	578.0	15.0	3.18	
3_Gerbe_65	436	1.45	1.2790	0.0140	0.13840	0.00110	0.726	836.3	6.1	835.6	6.5	841	16	835.6	6.5	0.08	
3_Gerbe_68	68.9	1.50	10.8800	0.1400	0.45410	0.00560	0.733	2512	12	2413	25	2589	14	2589.0	14.0	6.80	
3_Gerbe_69	166.4	2.38	1.1030	0.0200	0.12340	0.00170	0.456	754.2	9.5	750	10	763	33	750.0	10.0	0.56	
3_Gerbe_70	545	8.41	0.5799	0.0064	0.07462	0.00072	0.536	464.2	4.1	463.9	4.3	464	21	463.9	4.3	0.06	
3_Gerbe_71	382	4.87	12.1800	0.2000	0.48280	0.00790	0.810	2619	15	2538	34	2677	17	2677.0	17.0	5.19	
3_Gerbe_72	175	1.06	10.8700	0.2900	0.44800	0.01400	0.915	2509	25	2396	60	2600	20	2600.0	20.0	7.85	
3_Gerbe_73	238	6.02	0.5870	0.0160	0.07500	0.00170	0.443	469.5	9.7	466	10	456	54	466.0	10.0	0.75	
3_Gerbe_74	920	6.37	8.2500	0.3800	0.39630	0.00750	0.662	2252	41	2151	35	2346	60	2346.0	60.0	8.31	
3_Gerbe_75	286	2.47	1.5110	0.0220	0.15190	0.00180	0.753	934.5	8.9	911	10	965	20	965.0	20.0	5.60	
3_Gerbe_76	41.79	0.62	6.0670	0.0870	0.34480	0.00520	0.361	1986	13	1909	25	2076	24	2076.0	24.0	8.04	
3_Gerbe_78	469	24.10	9.7600	0.1400	0.40880	0.00530	0.745	2412	13	2209	24	2595	16	2595.0	16.0	14.87	
3_Gerbe_79	236	0.91	1.4210	0.0280	0.14950	0.00240	0.626	897	12	901	13	875	30	875.0	30.0	2.97	
3_Gerbe_80	2193	15.70	1.3000	0.0270	0.12310	0.00180	0.914	845	12	748	11	1101	16	DISC	DISC	11.48	Rim
3_Gerbe_80	354	3.55	6.0260	0.0360	0.35150	0.00260	0.458	1979.6	5.2	1942	13	2024	15	2024.0	15.0	4.05	Core
3_Gerbe_81	43.9	1.30	0.8030	0.0200	0.09550	0.00200	0.103	599	12	588	12	631	70	588.0	12.0	1.84	

Sample Name _Grain #	[U] ppm	U/Th	207/235	2σ error	206/238	2σ error	RHO	207/235 Age (Ma)	2σ error	206/238 Age (Ma)	2σ error	207/206 Age (Ma)	2σ error	Best age (Ma)	2σ error	% Discordance	Rim /Core
3_Gerbe_82	86.9	0.69	1.0720	0.0170	0.12170	0.00150	0.436	741.6	8.8	740.3	8.8	712	30	740.3	8.8	0.18	
3_Gerbe_83	125.2	0.86	1.7040	0.0220	0.16790	0.00170	0.400	1011.5	7.9	1000.6	9.2	1015	25	1015.0	25.0	1.42	
3_Gerbe_84	158	2.16	0.6910	0.0390	0.06350	0.00180	0.065	529	22	397	11	1140	110	DISC	DISC	24.95	
3_Gerbe_85	145.6	0.83	0.8650	0.0180	0.09490	0.00130	0.278	632	9.4	584.2	7.5	799	42	584.2	7.5	7.56	
3_Gerbe_86	220	1.95	1.1660	0.0220	0.12840	0.00180	0.669	784	10	778	10	786	31	778.0	10.0	0.77	
3_Gerbe_87	327	4.48	1.1080	0.0290	0.12450	0.00390	0.643	756	14	759	21	740	50	759.0	21.0	0.40	
3_Gerbe_88	578	2.20	0.3397	0.0064	0.04643	0.00079	0.561	296.7	4.8	292.5	4.8	303	36	292.5	4.8	1.42	
3_Gerbe_89	414	0.96	0.6579	0.0063	0.08250	0.00067	0.430	513.2	3.9	511	4	521	20	511.0	4.0	0.43	
3_Gerbe_90	429	7.74	0.5790	0.0100	0.07430	0.00150	0.645	463.5	6.7	462.1	8.9	475	33	462.1	8.9	0.30	
3_Gerbe_91	194	1.55	1.8100	0.0180	0.17700	0.00160	0.197	1049.5	6.7	1050.2	8.6	1046	22	1046.0	22.0	0.40	
3_Gerbe_92	390	1.69	0.6170	0.0100	0.07712	0.00080	0.579	487.4	6.5	478.9	4.8	536	32	478.9	4.8	1.74	
3_Gerbe_93	370	12.80	0.9010	0.0110	0.10730	0.00130	0.473	652	5.8	657.2	7.6	631	27	657.2	7.6	0.80	
3_Gerbe_94	222	1.04	8.5170	0.0910	0.37250	0.00450	0.749	2288.3	9.9	2041	21	2514	13	2514.0	13.0	18.81	
3_Gerbe_95	110.5	1.16	11.3000	0.1500	0.45980	0.00530	0.619	2548	13	2438	23	2620	23	2620.0	23.0	6.95	
3_Gerbe_96	410	4.35	1.6310	0.0200	0.16210	0.00200	0.703	981.8	7.7	970	11	1010	20	1010.0	20.0	3.96	
3_Gerbe_97	181	1.12	1.4660	0.0190	0.14690	0.00190	0.462	918	7.6	884	11	996	25	996.0	25.0	11.24	
3_Gerbe_98	894	2.00	0.9720	0.0160	0.11240	0.00190	0.786	688.7	8.1	687	11	695	27	687.0	11.0	0.25	
3_Gerbe_99	122	1.53	0.8680	0.0200	0.10260	0.00160	0.671	634	11	629.8	9.3	640	38	629.8	9.3	0.66	
3_Gerbe_100	171	4.57	0.8830	0.0120	0.10230	0.00110	0.388	642.1	6.3	627.7	6.3	697	27	627.7	6.3	2.24	
3_Gerbe_101	319	2.34	0.3692	0.0077	0.04907	0.00041	0.315	318.7	5.7	308.8	2.5	368	45	308.8	2.5	3.11	
3_Gerbe_102	1070	2.98	0.3566	0.0056	0.04880	0.00093	0.789	309.5	4.2	307.1	5.7	354	25	307.1	5.7	0.78	
3_Gerbe_103	527	2.03	0.6520	0.0140	0.07300	0.00140	0.656	509.4	8.5	453.9	8.4	787	32	DISC	DISC	10.90	
3_Gerbe_104	477	2.25	0.3608	0.0042	0.05011	0.00047	0.361	312.7	3.1	315.2	2.9	297	26	315.2	2.9	0.80	
3_Gerbe_105	263	3.08	1.3710	0.0240	0.14320	0.00250	0.669	876	10	865	14	904	29	904.0	29.0	4.31	
3_Gerbe_106	400	7.03	0.9460	0.0230	0.10770	0.00200	0.468	675	12	659	11	713	45	659.0	11.0	2.37	

Sample Name _Grain #	[U] ppm	U/Th	207/235	2σ error	206/238	2σ error	RHO	207/235 Age (Ma)	2σ error	206/238 Age (Ma)	2σ error	207/206 Age (Ma)	2σ error	Best age (Ma)	2σ error	% Discordance	Rim /Core
3_Gerbe_107	244	2.25	10.0300	0.1200	0.41110	0.00430	0.746	2438	11	2219	20	2629	13	2629.0	13.0	15.60	
3_Gerbe_109	128.3	0.69	1.6350	0.0380	0.16190	0.00480	0.768	985	15	967	27	1019	44	1019.0	44.0	5.10	
3_Gerbe_110	406	1.36	0.8453	0.0097	0.10090	0.00120	0.729	621.8	5.3	619.5	7.1	637	20	619.5	7.1	0.37	
3_Gerbe_111	228	1.54	3.1800	0.0500	0.24010	0.00390	0.723	1454	13	1387	20	1546	24	1546.0	24.0	10.28	
3_Gerbe_113	142	0.98	0.9830	0.0270	0.10900	0.00270	0.497	694	14	667	15	763	54	667.0	15.0	3.89	
3_Gerbe_114	100.5	1.07	0.9940	0.0190	0.11340	0.00190	0.229	702.9	9.3	692	11	738	47	692.0	11.0	1.55	
3_Gerbe_115	152.6	0.70	0.8150	0.0200	0.09580	0.00150	0.368	604	11	589.6	8.8	675	49	589.6	8.8	2.38	
3_Gerbe_116	238	7.67	1.6790	0.0160	0.16730	0.00130	0.262	1000.3	6	997.1	7.3	1019	21	1019.0	21.0	2.15	
3_Gerbe_117	297.9	5.16	9.4400	0.1700	0.37970	0.00750	0.783	2380	17	2079	34	2651	20	2651.0	20.0	21.58	
3_Gerbe_118	463	2.79	0.9340	0.0140	0.10490	0.00130	0.599	669.2	7.1	643.1	7.6	745	26	643.1	7.6	3.90	
3_Gerbe_119	264	1.70	0.8220	0.0140	0.09820	0.00130	0.630	610	8.2	604	7.4	616	30	604.0	7.4	0.98	
3_Gerbe_120	952	1.50	2.9690	0.0400	0.23980	0.00310	0.857	1399	10	1385	16	1436	13	1436.0	13.0	3.55	
2_Arro_1	576	2.43	0.3598	0.0050	0.04916	0.00060	0.553	311.9	3.7	309.3	3.7	325	27	309.3	3.7	0.83	
2_Arro_2	67.6	0.86	1.5830	0.0320	0.16050	0.00240	0.488	962	13	959	14	960	37	960.0	37.0	0.10	
2_Arro_3	566	0.79	0.8814	0.0088	0.10350	0.00120	0.695	641.6	4.7	634.8	6.9	656	18	634.8	6.9	1.06	
2_Arro_4	174	2.11	0.3280	0.0086	0.04379	0.00064	0.244	287.7	6.5	276.2	4	369	62	276.2	4.0	4.00	
2_Arro_5	509	1.61	0.4040	0.0140	0.04772	0.00063	0.180	344	10	300.5	3.9	667	77	DISC	DISC	12.65	
2_Arro_6	5.84	0.69	2.2210	0.0810	0.20050	0.00660	0.004	1188	26	1176	35	1217	86	1217.0	86.0	3.37	
2_Arro_7	165.8	1.74	10.8000	0.1600	0.44790	0.00730	0.890	2505	14	2385	32	2599	11	2599.0	11.0	8.23	
2_Arro_8	138.7	0.93	0.7850	0.0120	0.09640	0.00150	0.403	587.8	6.8	593.5	8.9	571	36	593.5	8.9	0.97	
2_Arro_9	103.5	1.01	0.5710	0.0290	0.07040	0.00340	0.310	458	19	439	20	590	130	439.0	20.0	4.15	
2_Arro_10	243.5	1.58	0.3525	0.0059	0.04839	0.00061	0.423	306.4	4.4	304.6	3.8	316	37	304.6	3.8	0.59	
2_Arro_11	262.8	1.23	0.3477	0.0064	0.04890	0.00057	0.414	302.8	4.8	307.8	3.5	262	40	307.8	3.5	1.65	
2_Arro_12	118	48.50	0.5920	0.0110	0.07580	0.00100	0.320	471.7	7.3	470.7	6.1	461	44	470.7	6.1	0.21	
2_Arro_13	337	12.00	0.5962	0.0092	0.07690	0.00120	0.635	475.5	6	477.4	7.2	459	31	477.4	7.2	0.40	Rim

Sample Name _Grain #	[U] ppm	U/Th	207/235	2σ error	206/238	2σ error	RHO	207/235 Age (Ma)	2σ error	206/238 Age (Ma)	2σ error	207/206 Age (Ma)	2σ error	Best age (Ma)	2σ error	% Discordance	Rim /Core
2_Arro_13	641	5.52	0.7550	0.0240	0.09230	0.00220	0.614	571	14	569	13	594	57	569.0	13.0	0.35	Core
2_Arro_14	177.6	1.46	0.3660	0.0140	0.04860	0.00110	0.148	316	10	305.7	6.9	359	79	305.7	6.9	3.26	
2_Arro_15	216.1	6.25	0.6080	0.0140	0.07510	0.00130	0.405	482.2	9.1	467	7.5	541	50	467.0	7.5	3.15	
2_Arro_16	224	1.60	4.5830	0.0420	0.30420	0.00300	0.682	1746.6	7.7	1712	15	1797	13	1797.0	13.0	4.73	
2_Arro_17	398	2.19	0.3636	0.0066	0.04981	0.00062	0.460	314.7	4.9	313.3	3.8	336	37	313.3	3.8	0.44	
2_Arro_18	213.3	0.66	0.8290	0.0110	0.09810	0.00110	0.133	612.6	6.4	603.4	6.7	634	31	603.4	6.7	1.50	
2_Arro_19	79.7	0.86	0.8640	0.0150	0.10170	0.00140	0.307	631.6	8.2	624.1	7.9	649	43	624.1	7.9	1.19	
2_Arro_20	43.4	0.54	0.5850	0.0180	0.07230	0.00140	0.185	467	12	450.1	8.4	538	71	450.1	8.4	3.62	
2_Arro_21	509	0.69	11.2000	0.1200	0.46090	0.00600	0.769	2538.8	9.7	2446	27	2612	14	2612.0	14.0	6.36	
2_Arro_22	370	1.61	0.3620	0.0082	0.04916	0.00097	0.396	314.4	5.9	309.3	6	346	51	309.3	6.0	1.62	
2_Arro_23	617	148.00	0.3530	0.0140	0.04880	0.00130	0.706	307	11	307.3	8.2	321	94	307.3	8.2	0.10	Rim
2_Arro_23	239	1.25	0.8490	0.0160	0.10220	0.00170	0.510	623.7	9.1	627	10	593	37	627.0	10.0	0.53	Core
2_Arro_24	226	2.35	1.0480	0.0480	0.11130	0.00360	0.014	727	24	680	21	890	120	680.0	21.0	6.46	
2_Arro_25	57.4	1.01	4.6400	0.0490	0.30650	0.00330	0.467	1758	8.8	1725	16	1787	19	1787.0	19.0	3.47	
2_Arro_26	39.8	0.51	6.3600	0.1100	0.35560	0.00630	0.765	2033	14	1964	31	2084	19	2084.0	19.0	5.76	
2_Arro_27	274	2.04	0.3587	0.0071	0.04901	0.00070	0.345	312.5	5.3	308.4	4.3	324	39	308.4	4.3	1.31	
2_Arro_28	139	1.27	1.6430	0.0170	0.16500	0.00150	0.391	986.4	6.6	984.6	8	976	23	976.0	23.0	0.88	
2_Arro_29	104	1.78	1.7420	0.0190	0.17210	0.00220	0.499	1024	7	1024	12	1056	24	1056.0	24.0	3.03	
2_Arro_30	229	1.52	0.3518	0.0062	0.04932	0.00079	0.437	305.9	4.7	310.3	4.9	280	43	310.3	4.9	1.44	
2_Arro_31	639	190.00	0.3660	0.0160	0.05040	0.00200	0.818	316	12	317	12	285	64	317.0	12.0	0.32	Rim
2_Arro_31	157	1.78	0.6740	0.0190	0.08400	0.00220	0.366	523	12	520	13	536	78	520.0	13.0	0.57	Core
2_Arro_32	68	1.02	0.8180	0.0150	0.09750	0.00120	0.201	606.4	8.5	599.8	7.2	659	40	599.8	7.2	1.09	
2_Arro_33	249	3.15	0.3491	0.0064	0.04773	0.00080	0.463	303.8	4.8	300.5	4.9	332	39	300.5	4.9	1.09	
2_Arro_34	252.3	5.80	0.3770	0.0150	0.04990	0.00130	0.095	325	11	313.8	8	382	83	313.8	8.0	3.45	Rim
2_Arro_34	85.2	1.96	0.5490	0.0280	0.06810	0.00210	0.029	444	18	424	13	540	130	424.0	13.0	4.50	Core

Sample Name _Grain #	[U] ppm	U/Th	207/235	2σ error	206/238	2σ error	RHO	207/235 Age (Ma)	2σ error	206/238 Age (Ma)	2σ error	207/206 Age (Ma)	2σ error	Best age (Ma)	2σ error	% Discordance	Rim /Core
2_Arro_35	267	2.18	0.3617	0.0050	0.04946	0.00061	0.266	313.3	3.7	311.2	3.7	329	37	311.2	3.7	0.67	
2_Arro_36	279	2.18	0.3597	0.0076	0.04852	0.00097	0.397	311.7	5.6	305.4	6	377	47	305.4	6.0	2.02	
2_Arro_37	266	5.45	0.3553	0.0058	0.04930	0.00052	0.262	308.5	4.4	310.2	3.2	281	38	310.2	3.2	0.55	
2_Arro_38	435	2.48	0.9280	0.0130	0.10840	0.00110	0.314	666.4	6.7	663.6	6.3	674	30	663.6	6.3	0.42	
2_Arro_39	181	1.87	0.3668	0.0077	0.04966	0.00064	0.197	316.9	5.7	312.4	3.9	358	45	312.4	3.9	1.42	
2_Arro_40	195.1	2.51	0.3660	0.0080	0.04857	0.00055	0.218	316.4	5.9	305.7	3.4	404	53	305.7	3.4	3.38	
2_Arro_41	151.1	1.73	0.3651	0.0074	0.05016	0.00065	0.310	315.8	5.5	315.5	4	292	45	315.5	4.0	0.09	
2_Arro_42	99.6	0.56	2.3700	0.0280	0.21050	0.00230	0.453	1232.8	8.5	1231	12	1234	23	1234.0	23.0	0.24	
2_Arro_43	357	1.98	0.3467	0.0074	0.04723	0.00071	0.365	302	5.6	297.5	4.4	351	49	297.5	4.4	1.49	
2_Arro_44	415	102.90	0.3538	0.0098	0.04786	0.00063	0.444	307.4	7.3	301.4	3.9	335	56	301.4	3.9	1.95	Rim
2_Arro_44	596	2.20	1.1770	0.0280	0.12930	0.00270	0.771	789	13	784	15	788	20	784.0	15.0	0.63	Core
2_Arro_45	303	1.41	0.3641	0.0065	0.04984	0.00054	0.379	315.6	4.7	313.5	3.3	324	38	313.5	3.3	0.67	
2_Arro_46	138.2	1.86	0.3573	0.0063	0.04974	0.00065	0.271	310	4.7	312.9	4	290	41	312.9	4.0	0.94	
2_Arro_47	213	1.83	0.3703	0.0081	0.04996	0.00093	0.440	319.7	6	314.2	5.7	369	45	314.2	5.7	1.72	
2_Arro_48	30.5	1.11	2.5610	0.0530	0.21700	0.00350	0.425	1290	15	1266	19	1341	38	1341.0	38.0	5.59	
2_Arro_49	196	8.20	0.6015	0.0091	0.07720	0.00100	0.542	477.9	5.8	479.5	6.3	454	32	479.5	6.3	0.33	
2_Arro_50	564	3.44	0.3680	0.0072	0.05012	0.00092	0.586	318	5.4	315.3	5.7	330	41	315.3	5.7	0.85	
2_Arro_51	364	1.47	0.3671	0.0066	0.05029	0.00059	0.299	317.2	4.9	316.8	3.7	303	42	316.8	3.7	0.13	
2_Arro_52	135	1.75	0.3581	0.0078	0.04908	0.00055	0.231	310.5	5.8	308.9	3.4	304	51	308.9	3.4	0.52	
2_Arro_53	145	1.48	0.3508	0.0068	0.04901	0.00056	0.031	305.1	5.1	308.4	3.4	266	52	308.4	3.4	1.08	
2_Arro_54	400	1.43	0.3736	0.0094	0.05042	0.00079	0.647	322.1	6.9	317.1	4.9	357	43	317.1	4.9	1.55	
2_Arro_55	254.1	1.47	0.3457	0.0055	0.04777	0.00075	0.318	301.3	4.1	300.8	4.6	278	42	300.8	4.6	0.17	
2_Arro_56	324	1.10	0.3425	0.0049	0.04700	0.00048	0.389	299	3.7	296.1	3	289	30	296.1	3.0	0.97	
2_Arro_57	144.1	1.76	0.3599	0.0065	0.04943	0.00055	0.342	311.9	4.9	311	3.4	304	41	311.0	3.4	0.29	
2_Arro_58	253	1.58	0.3705	0.0061	0.05027	0.00075	0.407	319.9	4.5	316.2	4.6	335	37	316.2	4.6	1.16	

Sample Name _Grain #	[U] ppm	U/Th	207/235	2σ error	206/238	2σ error	RHO	207/235 Age (Ma)	2σ error	206/238 Age (Ma)	2σ error	207/206 Age (Ma)	2σ error	Best age (Ma)	2σ error	% Discordance	Rim /Core
2_Arro_59	452	1.83	0.3480	0.0100	0.04720	0.00110	0.398	304.7	8.1	297.4	6.8	318	46	297.4	6.8	2.40	
2_Arro_60	498	2.30	0.3542	0.0059	0.04895	0.00083	0.143	307.8	4.4	308	5.1	285	44	308.0	5.1	0.06	
2_Arro_61	89.9	1.79	1.5430	0.0280	0.15470	0.00220	0.383	947	11	927	12	987	34	987.0	34.0	6.08	
2_Arro_62	23.8	0.51	12.9400	0.2100	0.50840	0.00920	0.294	2674	15	2649	39	2682	31	2682.0	31.0	1.23	
2_Arro_63	180	0.74	5.1730	0.0450	0.32170	0.00380	0.518	1847.8	7.3	1798	19	1901	20	1901.0	20.0	5.42	
2_Arro_64	165.5	1.75	0.3687	0.0079	0.04976	0.00085	0.161	318.4	5.9	313	5.2	353	56	313.0	5.2	1.70	
2_Arro_65	269	1.42	0.3405	0.0074	0.04717	0.00061	0.378	298	5.4	297.1	3.8	288	41	297.1	3.8	0.30	
2_Arro_66	40.3	0.41	1.4080	0.0370	0.14630	0.00240	0.497	893	15	880	13	934	47	934.0	47.0	5.78	
2_Arro_67	306	1.31	0.3630	0.0046	0.05038	0.00066	0.302	314.3	3.4	316.8	4	311	34	316.8	4.0	0.80	
2_Arro_68	350	0.81	7.2700	0.1500	0.39180	0.00890	0.831	2143	19	2131	41	2170	24	2170.0	24.0	1.80	
2_Arro_69	71.8	2.32	1.2970	0.0290	0.13820	0.00270	0.653	843	13	834	15	876	36	834.0	15.0	1.07	
2_Arro_70	532	1.49	0.3893	0.0097	0.05100	0.00110	0.446	333.6	7	320.4	6.7	422	42	320.4	6.7	3.96	
2_Arro_71	373.6	1.19	0.4017	0.0055	0.05347	0.00070	0.412	342.7	4	335.7	4.3	378	34	335.7	4.3	2.04	
2_Arro_72	478	1.70	0.3713	0.0072	0.04994	0.00084	0.561	320.4	5.3	314.1	5.1	335	42	314.1	5.1	1.97	
2_Arro_73	73.8	0.51	10.3800	0.1300	0.45130	0.00660	0.714	2468	12	2400	29	2513	17	2513.0	17.0	4.50	
2_Arro_74	111.5	7.69	0.3653	0.0096	0.04931	0.00061	0.207	314.5	6.8	310.2	3.8	329	62	310.2	3.8	1.37	
2_Arro_75	69.8	2.64	0.8760	0.0200	0.10540	0.00170	0.476	638	11	645.6	9.6	610	45	645.6	9.6	1.19	
2_Arro_76	226.8	1.21	0.3547	0.0053	0.04918	0.00052	0.230	308.1	4	309.5	3.2	277	34	309.5	3.2	0.45	
2_Arro_77	264	9.10	0.5160	0.0140	0.06720	0.00140	0.336	422.5	9.4	419.4	8.5	428	71	419.4	8.5	0.73	
2_Arro_78	315	1.21	0.3420	0.0100	0.04630	0.00110	0.287	298.7	8	291.4	6.7	353	62	291.4	6.7	2.44	
2_Arro_79	198.8	1.48	0.3507	0.0066	0.04779	0.00071	0.421	305.8	5.1	300.9	4.4	300	37	300.9	4.4	1.60	
2_Arro_80	135.1	0.96	1.6100	0.0360	0.16150	0.00250	0.242	973	14	965	14	992	49	992.0	49.0	2.72	
2_Arro_81	29.4	1.71	1.5150	0.0450	0.15230	0.00390	0.237	935	18	913	22	991	74	991.0	74.0	7.87	
2_Arro_82	307	3.84	0.6810	0.0150	0.08430	0.00170	0.644	529.3	8.4	521.9	9.9	557	46	521.9	9.9	1.40	
2_Arro_83	296	0.91	0.3542	0.0085	0.04766	0.00074	0.263	307.7	6.3	300.1	4.5	399	58	300.1	4.5	2.47	

Sample Name _Grain #	[U] ppm	U/Th	207/235	2σ error	206/238	2σ error	RHO	207/235 Age (Ma)	2σ error	206/238 Age (Ma)	2σ error	207/206 Age (Ma)	2σ error	Best age (Ma)	2σ error	% Discordance	Rim /Core
2_Arro_84	129	1.08	0.7790	0.0180	0.09270	0.00140	0.470	587	11	571.2	8.5	619	46	571.2	8.5	2.69	
2_Arro_85	522	1.62	0.3551	0.0050	0.04852	0.00049	0.404	308.5	3.8	305.4	3	319	30	305.4	3.0	1.00	
2_Arro_86	165.4	1.35	0.3756	0.0080	0.05001	0.00067	0.193	323.5	5.9	314.6	4.1	368	52	314.6	4.1	2.75	
2_Arro_87	181	1.94	0.3286	0.0062	0.04557	0.00069	0.199	288.2	4.7	287.3	4.2	301	45	287.3	4.2	0.31	
2_Arro_88	205	1.64	0.3581	0.0079	0.04865	0.00060	0.575	311.3	6	306.2	3.7	322	39	306.2	3.7	1.64	
2_Arro_89	52.8	0.82	1.8110	0.0270	0.17740	0.00230	0.180	1048.8	9.7	1053	13	1047	37	1047.0	37.0	0.57	
2_Arro_90	296	1.80	0.3683	0.0068	0.05067	0.00071	0.556	318.1	5	318.6	4.4	289	34	318.6	4.4	0.16	
2_Arro_92	192.6	1.63	0.3628	0.0057	0.04939	0.00065	0.354	314.1	4.2	310.7	4	322	41	310.7	4.0	1.08	
2_Arro_93	195.4	0.88	0.7940	0.0120	0.09670	0.00120	0.407	593.4	7.1	594.7	7.2	580	38	594.7	7.2	0.22	
2_Arro_95	249	1.31	0.3596	0.0062	0.04944	0.00067	0.347	312.3	4.6	311	4.1	316	40	311.0	4.1	0.42	
2_Arro_96	357	5.49	0.4370	0.0190	0.05870	0.00210	0.719	368	14	368	13	426	68	368.0	13.0	0.00	Rim
2_Arro_96	270.3	1.94	0.5700	0.0150	0.07450	0.00120	0.546	459.8	9	463.4	7.5	445	44	463.4	7.5	0.78	Core
2_Arro_97	150	2.02	0.3680	0.0087	0.04895	0.00083	0.232	319	6.7	308	5.1	380	52	308.0	5.1	3.45	
2_Arro_98	280	2.06	1.7460	0.0260	0.17150	0.00310	0.698	1026.7	9.8	1020	17	1054	28	1054.0	28.0	3.23	
2_Arro_99	177.6	2.11	0.8890	0.0130	0.10578	0.00092	0.194	646.3	6.9	648.1	5.4	620	34	648.1	5.4	0.28	
2_Arro_100	61	0.24	1.6580	0.0280	0.16830	0.00200	0.280	991	11	1002	11	978	36	978.0	36.0	2.45	
2_Arro_101	536	51.00	0.9720	0.0300	0.11350	0.00400	0.768	689	16	693	23	699	45	693.0	23.0	0.58	Rim
2_Arro_101	155.7	1.26	1.5310	0.0260	0.15440	0.00300	0.669	942	11	925	17	978	27	978.0	27.0	5.42	Core
2_Arro_102	248	4.93	0.9570	0.0110	0.11230	0.00130	0.450	681.7	5.9	686.2	7.7	657	29	686.2	7.7	0.66	
2_Arro_103	150	1.59	0.8780	0.0150	0.10440	0.00210	0.676	639.5	8.3	640	12	663	35	640.0	12.0	0.08	
2_Arro_104	48.7	0.79	1.6810	0.0330	0.16740	0.00240	0.197	1000	13	998	13	1006	46	1006.0	46.0	0.80	
2_Arro_105	324	2.96	0.7850	0.0100	0.09640	0.00120	0.216	588.1	5.7	593	6.9	575	34	593.0	6.9	0.83	
2_Arro_106	73.2	0.63	2.2880	0.0480	0.20230	0.00350	0.551	1208	15	1188	19	1233	38	1233.0	38.0	3.65	
2_Arro_107	263	1.52	0.3408	0.0049	0.04709	0.00048	0.113	297.6	3.7	296.6	2.9	315	40	296.6	2.9	0.34	
2_Arro_108	258.1	1.31	0.3590	0.0064	0.04890	0.00056	0.207	311.3	4.8	307.7	3.4	339	40	307.7	3.4	1.16	

Sample Name _Grain #	[U] ppm	U/Th	207/235	2σ error	206/238	2σ error	RHO	207/235 Age (Ma)	2σ error	206/238 Age (Ma)	2σ error	207/206 Age (Ma)	2σ error	Best age (Ma)	2σ error	% Discordance	Rim /Core
2_Arro_109	183	1.25	0.3590	0.0087	0.04939	0.00058	0.340	311.1	6.5	310.8	3.6	295	51	310.8	3.6	0.10	
2_Arro_110	119	1.53	0.9900	0.0180	0.11310	0.00170	0.629	698.1	9.3	692	10	694	32	692.0	10.0	0.87	
2_Arro_111	173.5	5.42	0.8040	0.0100	0.09750	0.00110	0.528	599.3	6	599.6	6.5	582	26	599.6	6.5	0.05	
2_Arro_112	62.6	1.07	11.4900	0.1500	0.47970	0.00660	0.707	2564	12	2525	29	2607	19	2607.0	19.0	3.15	
2_Arro_113	148	1.11	3.3520	0.0340	0.25900	0.00320	0.511	1492.7	7.9	1484	17	1498	21	1498.0	21.0	0.93	
2_Arro_114	169	0.82	1.2850	0.0200	0.13930	0.00160	0.472	839.4	9	840.6	8.9	811	29	840.6	8.9	0.14	
2_Arro_115	208	1.49	0.3544	0.0065	0.04912	0.00057	0.465	307.8	4.8	309.1	3.5	287	36	309.1	3.5	0.42	
2_Arro_116	276.6	2.73	1.2200	0.1100	0.05600	0.00170	0.679	811	50	351	10	2380	140	DISC	DISC	56.72	
2_Arro_117	156	1.34	0.3599	0.0081	0.04951	0.00078	0.215	311.7	6.1	311.5	4.8	305	56	311.5	4.8	0.06	
2_Arro_118	665	14.00	0.6280	0.0170	0.08020	0.00220	0.535	494	10	497	13	479	63	497.0	13.0	0.61	Rim
2_Arro_118	291	1.03	1.3930	0.0180	0.14600	0.00170	0.540	885.9	7.5	878.6	9.5	885	22	885.0	22.0	0.72	Core
2_Arro_119	121.8	1.04	1.2680	0.0180	0.13780	0.00140	0.509	831.7	7.9	832.1	7.9	832	27	832.1	7.9	0.05	
2_Arro_120	345	102.00	0.3558	0.0065	0.04940	0.00180	0.506	309.1	4.9	311	11	322	63	311.0	11.0	0.61	Rim
2_Arro_120	125.3	2.46	0.8050	0.0140	0.09820	0.00210	0.256	599.1	8.1	604	12	599	45	604.0	12.0	0.82	Core
1Fosado_1	326	1.67	0.3529	0.0064	0.04746	0.00066	0.464	307.4	5	298.9	4	361	41	298.9	4.0	2.77	
1Fosado_2	146	2.34	0.3880	0.0110	0.05248	0.00095	0.490	332.3	7.9	329.7	5.8	314	56	329.7	5.8	0.78	
1Fosado_3	215	1.61	0.3770	0.0066	0.05149	0.00076	0.374	325.2	5	323.6	4.6	314	45	323.6	4.6	0.49	
1Fosado_4	168.7	1.30	0.3501	0.0075	0.04734	0.00051	0.387	304.6	5.6	298.2	3.1	354	47	298.2	3.1	2.10	
1Fosado_5	102.9	0.23	0.9100	0.0320	0.10400	0.00260	0.391	655	17	637	15	743	76	637.0	15.0	2.75	
1Fosado_6	48.8	1.57	1.0990	0.0460	0.12070	0.00350	0.567	748	22	734	20	766	66	734.0	20.0	1.87	
1Fosado_8	85.1	1.25	1.2750	0.0190	0.13720	0.00180	0.433	835.1	8.1	829	10	849	31	829.0	10.0	0.73	
1Fosado_9	19.59	2.08	14.6800	0.4200	0.54600	0.01500	0.702	2793	28	2807	63	2792	41	2792.0	41.0	0.54	
1Fosado_10	324	1.55	0.3778	0.0060	0.05116	0.00058	0.446	325.9	4.3	321.6	3.5	341	36	321.6	3.5	1.32	
1Fosado_11	743	5.30	0.9730	0.0150	0.11220	0.00210	0.831	689.7	7.9	685	12	694	22	685.0	12.0	0.68	
1Fosado_12	245	0.89	0.9070	0.0110	0.10580	0.00100	0.604	656.7	6	648.4	6	681	24	648.4	6.0	1.26	

Sample Name _Grain #	[U] ppm	U/Th	207/235	2σ error	206/238	2σ error	RHO	207/235 Age (Ma)	2σ error	206/238 Age (Ma)	2σ error	207/206 Age (Ma)	2σ error	Best age (Ma)	2σ error	% Discordance	Rim /Core
1Fosado_13	326	3.23	0.8520	0.0140	0.10140	0.00240	0.527	628	8.1	622	14	635	46	622.0	14.0	0.96	
1Fosado_14	149	0.68	0.9170	0.0190	0.10850	0.00170	0.489	659.9	9.8	664	10	627	38	664.0	10.0	0.62	
1Fosado_15	159	1.95	0.9170	0.0190	0.10630	0.00160	0.533	660	10	651	9.2	670	43	651.0	9.2	1.36	Rim
1Fosado_15	98.2	0.59	1.4720	0.0450	0.14960	0.00280	0.069	918	19	899	16	966	79	966.0	79.0	6.94	Core
1Fosado_16	489	22.50	0.9240	0.0100	0.10850	0.00100	0.494	664.3	5.5	663.8	5.8	657	24	663.8	5.8	0.08	
1Fosado_18	428	1.25	0.3366	0.0053	0.04639	0.00062	0.479	294.5	4	292.3	3.8	339	33	292.3	3.8	0.75	
1Fosado_19	265	0.91	0.8661	0.0096	0.10325	0.00099	0.459	633.2	5.2	633.4	5.8	633	25	633.4	5.8	0.03	
1Fosado_20	93.6	1.14	0.9840	0.0160	0.11320	0.00130	0.267	695	8.4	691.2	7.4	716	34	691.2	7.4	0.55	
1Fosado_21	240	1.55	1.0310	0.0180	0.11830	0.00160	0.513	718.9	8.8	721	9.2	720	34	721.0	9.2	0.29	
1Fosado_22	170	0.72	2.0730	0.0470	0.19600	0.00430	0.640	1142	16	1153	23	1140	39	1140.0	39.0	1.14	
1Fosado_23	278	1.50	0.3706	0.0063	0.05015	0.00062	0.413	320.5	4.5	315.4	3.8	370	36	315.4	3.8	1.59	
1Fosado_24	229	1.93	0.3710	0.0072	0.05031	0.00077	0.431	320.2	5.4	316.4	4.7	348	45	316.4	4.7	1.19	
1Fosado_25	97.8	1.51	0.9010	0.0150	0.10570	0.00140	0.331	651.5	8.1	647.6	8.3	685	40	647.6	8.3	0.60	
1Fosado_26	47.2	2.43	15.2100	0.2700	0.53420	0.00910	0.729	2827	17	2758	38	2853	21	2853.0	21.0	3.33	
1Fosado_27	99.4	0.71	1.1240	0.0220	0.12560	0.00160	0.007	764	10	762.5	9.4	771	44	762.5	9.4	0.20	
1Fosado_28	187	1.32	0.3262	0.0064	0.04490	0.00067	0.417	286.4	4.9	283.1	4.2	292	45	283.1	4.2	1.15	
1Fosado_29	279	1.21	0.3392	0.0050	0.04668	0.00050	0.315	296.4	3.8	294.1	3.1	313	33	294.1	3.1	0.78	
1Fosado_30	363	1.06	0.3621	0.0060	0.04889	0.00059	0.339	313.6	4.5	307.7	3.6	348	37	307.7	3.6	1.88	
1Fosado_31	220	1.27	0.9700	0.0150	0.10990	0.00150	0.504	690.3	7.7	671.8	8.9	732	33	671.8	8.9	2.68	
1Fosado_33	425	1.55	0.3256	0.0058	0.04432	0.00050	0.546	286	4.4	279.6	3.1	326	37	279.6	3.1	2.24	
1Fosado_34	253	2.32	1.6200	0.0160	0.16310	0.00200	0.455	977.6	6.4	974	11	984	24	984.0	24.0	1.02	
1Fosado_35	391	7.43	0.9254	0.0095	0.10610	0.00110	0.443	665	5	650.3	6.3	707	23	650.3	6.3	2.21	
1Fosado_36	237	3.33	1.5710	0.0260	0.15960	0.00280	0.636	960	11	954	16	958	31	958.0	31.0	0.42	
1Fosado_37	154.6	1.45	1.0060	0.0160	0.11220	0.00130	0.392	707.3	8.1	685.4	7.3	770	34	685.4	7.3	3.10	

Sample Name _Grain #	[U] ppm	U/Th	207/235	2σ error	206/238	2σ error	RHO	207/235 Age (Ma)	2σ error	206/238 Age (Ma)	2σ error	207/206 Age (Ma)	2σ error	Best age (Ma)	2σ error	% Discordance	Rim /Core
1Fosado_38	956	1.49	1.2630	0.0120	0.13610	0.00130	0.738	829.6	5.3	822.5	7.6	846	15	822.5	7.6	0.86	
1Fosado_39	150	2.71	1.7310	0.0270	0.16970	0.00210	0.470	1019	10	1012	12	1047	28	1047.0	28.0	3.34	
1Fosado_40	163	0.61	1.5570	0.0190	0.15720	0.00150	0.429	952.7	7.6	942.3	8.8	968	25	968.0	25.0	2.65	
1Fosado_41	257	4.66	12.6400	0.1400	0.51310	0.00630	0.770	2653	11	2669	27	2641	13	2641.0	13.0	1.06	
1Fosado_42	159	1.18	0.3456	0.0078	0.04778	0.00057	0.022	301	5.9	300.9	3.5	300	54	300.9	3.5	0.03	
1Fosado_43	162.6	1.44	0.3571	0.0077	0.04928	0.00067	0.051	309.8	5.8	310.1	4.1	308	55	310.1	4.1	0.10	
1Fosado_44	174	1.50	0.3543	0.0065	0.04766	0.00073	0.252	307.7	4.9	300.1	4.5	371	45	300.1	4.5	2.47	
1Fosado_45	299	0.49	5.8420	0.0420	0.34970	0.00300	0.599	1952.5	6.2	1933	14	1968	12	1968.0	12.0	1.78	
1Fosado_46	152.2	1.85	0.3421	0.0081	0.04688	0.00064	0.268	298.5	6.1	295.3	3.9	300	54	295.3	3.9	1.07	
1Fosado_47	217	3.40	0.9210	0.0160	0.10810	0.00160	0.592	662.1	8.7	661.8	9.3	655	34	661.8	9.3	0.05	
1Fosado_48	396	1.21	0.3350	0.0063	0.04629	0.00063	0.677	293.2	4.8	291.7	3.9	317	31	291.7	3.9	0.51	
1Fosado_49	45.6	0.41	1.5570	0.0410	0.15970	0.00360	0.004	952	16	955	20	957	65	957.0	65.0	0.21	
1Fosado_52	382	2.62	0.3342	0.0064	0.04513	0.00063	0.378	292.6	4.9	284.5	3.9	347	43	284.5	3.9	2.77	
1Fosado_53	260	1.35	0.3301	0.0068	0.04581	0.00089	0.487	290.8	5.2	288.7	5.5	296	43	288.7	5.5	0.72	
1Fosado_54	200	1.34	0.5940	0.0110	0.07490	0.00110	0.510	473.9	6.8	465.6	6.8	530	35	465.6	6.8	1.75	
1Fosado_55	89.8	0.79	0.8410	0.0160	0.09980	0.00180	0.270	619.4	8.7	615	11	674	49	615.0	11.0	0.71	
1Fosado_56	113.8	0.51	0.7990	0.0160	0.09400	0.00160	0.354	595.8	9.1	579.2	9.4	640	49	579.2	9.4	2.79	
1Fosado_57	909	0.85	0.8570	0.0120	0.10150	0.00190	0.692	628.5	6.8	623	11	650	35	623.0	11.0	0.88	
1Fosado_58	174	0.79	6.2240	0.0530	0.35360	0.00400	0.648	2007.4	7.4	1951	19	2064	16	2064.0	16.0	5.47	
1Fosado_59	396	1.40	0.3570	0.0120	0.04770	0.00100	0.479	311.4	8	300.3	6.4	395	56	300.3	6.4	3.56	
1Fosado_60	319	2.97	6.1910	0.0790	0.34920	0.00290	0.676	2002	11	1931	14	2081	16	2081.0	16.0	7.21	
1Fosado_61	2530	8.35	0.3450	0.0120	0.04500	0.00160	0.488	300.5	8.6	284	10	431	78	284.0	10.0	5.49	Rim
1Fosado_61	260	1.38	0.8210	0.0290	0.09850	0.00240	0.126	608	16	605	14	600	62	605.0	14.0	0.49	Core
1Fosado_62	290	3.74	1.4440	0.0290	0.14940	0.00340	0.644	906	12	898	19	886	38	886.0	38.0	1.35	
1Fosado_63	45.2	0.55	1.4930	0.0390	0.14720	0.00230	0.112	929	15	885	13	1032	55	1032.0	55.0	14.24	

Sample Name _Grain #	[U] ppm	U/Th	207/235	2σ error	206/238	2σ error	RHO	207/235 Age (Ma)	2σ error	206/238 Age (Ma)	2σ error	207/206 Age (Ma)	2σ error	Best age (Ma)	2σ error	% Discordance	Rim /Core
1Fosado_64	154.9	1.39	0.3179	0.0059	0.04375	0.00061	0.231	280.1	4.6	276	3.8	313	51	276.0	3.8	1.46	
1Fosado_65	460	1.24	0.3152	0.0045	0.04390	0.00046	0.174	278.1	3.5	276.9	2.8	271	37	276.9	2.8	0.43	
1Fosado_66	262	1.19	0.9800	0.0130	0.11160	0.00120	0.474	693	6.6	681.7	7.2	717	26	681.7	7.2	1.63	
1Fosado_67	71.4	2.11	6.7900	0.1300	0.37560	0.00810	0.583	2083	17	2055	38	2116	36	2116.0	36.0	2.88	
1Fosado_68	61.3	0.89	0.7630	0.0200	0.09410	0.00130	0.225	574	11	579.8	7.6	544	59	579.8	7.6	1.01	
1Fosado_69	329	1.04	0.3572	0.0064	0.04916	0.00097	0.367	309.9	4.8	309.3	6	328	48	309.3	6.0	0.19	
1Fosado_70	73.2	1.40	1.1010	0.0170	0.12480	0.00180	0.378	753.2	8.2	758	10	749	42	758.0	10.0	0.64	
1Fosado_71	40.4	1.03	0.7360	0.0210	0.08880	0.00150	0.178	559	13	548.1	8.9	570	60	548.1	8.9	1.95	
1Fosado_72	277	1.36	0.3534	0.0094	0.04843	0.00077	0.081	306.8	7	304.9	4.7	305	51	304.9	4.7	0.62	
1Fosado_73	187.1	1.29	0.3660	0.0100	0.04868	0.00075	0.330	316.4	7.4	306.4	4.6	409	58	306.4	4.6	3.16	
1Fosado_74	222	1.02	0.3671	0.0072	0.04717	0.00077	0.436	317.2	5.4	297.1	4.7	448	47	297.1	4.7	6.34	
1Fosado_75	425	45.80	0.8850	0.0230	0.10420	0.00240	0.590	643	13	639	14	654	37	639.0	14.0	0.62	
1Fosado_76	755	9.40	0.9480	0.0200	0.10900	0.00260	0.761	678	11	669	16	705	34	669.0	16.0	1.33	
1Fosado_77	99.8	1.07	6.0750	0.0730	0.34600	0.00400	0.756	1986	11	1915	19	2073	15	2073.0	15.0	7.62	
1Fosado_78	237	1.07	0.3417	0.0068	0.04636	0.00057	0.342	299.1	4.9	292.1	3.5	344	45	292.1	3.5	2.34	
1Fosado_79	55.6	0.74	6.2360	0.0930	0.36390	0.00490	0.317	2008	13	2002	23	2007	23	2007.0	23.0	0.25	
1Fosado_80	45.1	1.24	1.5970	0.0320	0.15610	0.00230	0.019	968	12	935	13	1030	48	1030.0	48.0	9.22	
1Fosado_82	262	1.48	0.3621	0.0085	0.04986	0.00096	0.401	313.4	6.4	314.4	5.7	300	55	314.4	5.7	0.32	
1Fosado_83	141.8	0.37	0.8250	0.0130	0.09870	0.00120	0.377	610.2	7.3	606.7	7.3	630	35	606.7	7.3	0.57	
1Fosado_84	148	3.14	1.3760	0.0260	0.14680	0.00210	0.286	878	11	883	12	868	35	868.0	35.0	1.73	
1Fosado_85	264	0.72	1.8570	0.0300	0.17800	0.00230	0.636	1065	11	1056	13	1081	25	1081.0	25.0	2.31	
1Fosado_86	423.9	3.07	1.4290	0.0310	0.14670	0.00230	0.068	901	13	882	13	934	56	934.0	56.0	5.57	
1Fosado_87	123	10.27	1.0860	0.0170	0.12230	0.00130	0.364	746.1	8.3	744	7.2	753	33	744.0	7.2	0.28	
1Fosado_88	225	2.90	0.5953	0.0099	0.07590	0.00110	0.362	473.8	6.3	471.3	6.6	477	39	471.3	6.6	0.53	
1Fosado_89	184.8	1.49	0.3435	0.0065	0.04729	0.00064	0.220	299.6	4.9	297.8	3.9	303	46	297.8	3.9	0.60	

Sample Name _Grain #	[U] ppm	U/Th	207/235	2σ error	206/238	2σ error	RHO	207/235 Age (Ma)	2σ error	206/238 Age (Ma)	2σ error	207/206 Age (Ma)	2σ error	Best age (Ma)	2σ error	% Discordance	Rim /Core
1Fosado_90	180	1.49	0.3451	0.0068	0.04706	0.00052	0.173	301.4	5	296.4	3.2	328	46	296.4	3.2	1.66	
1Fosado_91	248	1.15	1.7540	0.0240	0.17190	0.00220	0.521	1028	8.9	1022	12	1040	25	1040.0	25.0	1.73	
1Fosado_92	65.7	1.19	0.8200	0.0150	0.09630	0.00140	0.134	607.6	8.4	592.9	8.2	642	46	592.9	8.2	2.42	
1Fosado_93	537	1.42	0.3469	0.0048	0.04838	0.00060	0.310	302.3	3.6	304.5	3.7	301	38	304.5	3.7	0.73	
1Fosado_94	404	2.28	1.7810	0.0210	0.17370	0.00230	0.657	1038	7.6	1032	13	1049	19	1049.0	19.0	1.62	
1Fosado_95	277	1.28	1.5320	0.0240	0.15580	0.00190	0.414	943.6	9.9	933	10	970	29	970.0	29.0	3.81	
1Fosado_96	368	1.98	0.3418	0.0058	0.04715	0.00092	0.377	298.4	4.4	297	5.7	298	46	297.0	5.7	0.47	
1Fosado_98	435	0.98	0.3508	0.0053	0.04811	0.00040	0.243	305.1	4	302.9	2.5	319	33	302.9	2.5	0.72	
1Fosado_99	71.3	1.59	0.7120	0.0160	0.08700	0.00120	0.019	545.2	9.5	537.4	7.1	564	57	537.4	7.1	1.43	
1Fosado_100	425	1.39	0.3434	0.0055	0.04648	0.00065	0.486	299.6	4.2	292.8	4	381	32	292.8	4.0	2.27	
1Fosado_101	67.5	0.40	6.1840	0.0690	0.36210	0.00450	0.437	2002.7	9.4	1991	21	2017	20	2017.0	20.0	1.29	
1Fosado_102	479	2.10	0.3627	0.0049	0.04944	0.00060	0.339	314.1	3.7	311.1	3.7	342	31	311.1	3.7	0.96	
1Fosado_103	451	3.18	0.3582	0.0055	0.04937	0.00053	0.272	311.2	4.2	310.7	3.3	316	37	310.7	3.3	0.16	
1Fosado_104	410	1.30	0.3525	0.0070	0.04794	0.00054	0.196	306.4	5.2	301.8	3.3	350	47	301.8	3.3	1.50	
1Fosado_105	369	1.51	0.3561	0.0065	0.04884	0.00066	0.462	309.1	4.9	307.4	4.1	327	38	307.4	4.1	0.55	
1Fosado_106	199	1.66	0.3482	0.0070	0.04703	0.00071	0.365	303.8	5.2	296.2	4.4	343	44	296.2	4.4	2.50	
1Fosado_107	473	3.50	0.3365	0.0057	0.04671	0.00059	0.478	295.4	4.3	294.3	3.6	298	32	294.3	3.6	0.37	
1Fosado_108	133.4	0.97	0.8080	0.0150	0.09630	0.00180	0.544	600.6	8.3	592	11	640	42	592.0	11.0	1.43	
1Fosado_109	715	89.20	0.8850	0.0190	0.10440	0.00260	0.728	643	10	640	15	657	31	640.0	15.0	0.47	Rim
1Fosado_109	87	0.65	1.2810	0.0370	0.13840	0.00400	0.622	839	17	835	23	854	57	835.0	23.0	0.48	Core
1Fosado_110	42.2	2.56	1.2100	0.0270	0.13080	0.00180	0.146	804	13	792	10	831	59	792.0	10.0	1.49	
1Fosado_111	178.6	1.39	0.3460	0.0100	0.04750	0.00100	0.536	301.1	7.8	298.9	6.4	342	59	298.9	6.4	0.73	
1Fosado_112	330	1.63	0.3839	0.0058	0.05150	0.00060	0.455	329.7	4.3	323.7	3.6	375	33	323.7	3.6	1.82	
1Fosado_113	192	1.94	0.3507	0.0072	0.04827	0.00061	0.533	305.8	5.6	303.9	3.8	327	40	303.9	3.8	0.62	
1Fosado_114	251	1.45	0.3652	0.0062	0.04917	0.00052	0.211	315.9	4.6	309.4	3.2	364	39	309.4	3.2	2.06	

Sample Name _Grain #	[U] ppm	U/Th	207/235	2σ error	206/238	2σ error	RHO	207/235 Age (Ma)	2σ error	206/238 Age (Ma)	2σ error	207/206 Age (Ma)	2σ error	Best age (Ma)	2σ error	% Discordance	Rim /Core
1Fosado_115	293	1.51	0.5790	0.0130	0.07400	0.00170	0.443	463.7	8.4	460	10	495	56	460.0	10.0	0.80	Rim
1Fosado_115	214.1	1.10	0.7490	0.0160	0.09080	0.00120	0.417	567.1	9.5	560.4	7.1	611	38	560.4	7.1	1.18	Core
1Fosado_116	46.2	1.29	0.9080	0.0180	0.10410	0.00170	0.256	655.1	9.8	639.4	9.9	699	51	639.4	9.9	2.40	
1Fosado_117	460	2.11	0.9700	0.0100	0.11350	0.00110	0.519	688.4	5.3	693.1	6.2	672	22	693.1	6.2	0.68	
1Fosado_118	244	0.91	0.3459	0.0076	0.04814	0.00067	0.425	301.3	5.7	303.1	4.1	281	49	303.1	4.1	0.60	
1Fosado_119	692	2.05	0.3348	0.0043	0.04596	0.00051	0.513	293.1	3.3	289.7	3.1	326	29	289.7	3.1	1.16	
1Fosado_120	383	2.52	0.8240	0.0120	0.09850	0.00150	0.644	609.7	6.6	605.5	8.8	653	27	605.5	8.8	0.69	
14AB-F01_1	460	1.67	0.8370	0.0210	0.10000	0.00230	0.690	617	11	614	14	610	41	614.0	14.0	0.49	Rim
14AB-F01_1	616	1.56	0.4080	0.0250	0.04814	0.00094	0.494	346	18	303.1	5.8	640	120	DISC	DISC	12.40	Core
14AB-F01_2	331	1.68	0.3586	0.0068	0.04918	0.00057	0.192	312.3	5.1	309.5	3.5	317	47	309.5	3.5	0.90	
14AB-F01_3	214.6	1.92	0.3740	0.0092	0.04981	0.00071	0.265	322.2	6.8	313.3	4.4	363	56	313.3	4.4	2.76	
14AB-F01_4	609	1.49	0.7570	0.0100	0.09120	0.00094	0.404	573.3	5.7	562.6	5.5	599	28	562.6	5.5	1.87	
14AB-F01_5	366	16.00	0.6080	0.0200	0.07460	0.00120	0.382	482	12	463.7	7.1	536	68	463.7	7.1	3.80	Rim
14AB-F01_5	444	162.00	0.4010	0.0460	0.04640	0.00120	0.347	328	20	292.6	7.3	510	130	DISC	DISC	10.79	Core
14AB-F01_29	583	218.00	0.3545	0.0095	0.04851	0.00088	0.368	307.8	7.1	305.3	5.4	355	56	305.3	5.4	0.81	
14AB-F01_30	107.5	1.26	0.7710	0.0170	0.09480	0.00130	0.315	582.3	9.9	583.5	7.6	601	50	583.5	7.6	0.21	
14AB-F01_31	197.8	2.19	0.3350	0.0070	0.04797	0.00079	0.152	293.8	5.2	302	4.9	245	55	302.0	4.9	2.79	
14AB-F01_32	345	2.03	0.3740	0.0110	0.04980	0.00067	0.225	322.2	7.8	313.3	4.1	403	63	313.3	4.1	2.76	
14AB-F01_33	444	2.21	0.8160	0.0120	0.09900	0.00150	0.644	607.4	6.9	608.7	8.8	607	28	608.7	8.8	0.21	
14AB-F01_35	494	2.02	6.7100	0.1800	0.35370	0.00460	0.588	2069	25	1952	22	2212	37	2212.0	37.0	11.75	
14AB-F01_36	353	4.33	0.3442	0.0094	0.04638	0.00071	0.141	299.9	7	292.2	4.4	349	53	292.2	4.4	2.57	
14AB-F01_37	174	2.35	0.4020	0.0150	0.05130	0.00110	0.180	342	11	322.3	6.8	468	92	322.3	6.8	5.76	
14AB-F01_38	234.3	1.23	1.1720	0.0150	0.13050	0.00130	0.296	787.8	7.1	790.6	7.5	804	27	790.6	7.5	0.36	
14AB-F01_39	195	1.66	0.3616	0.0083	0.04853	0.00065	0.343	313.8	6.1	305.5	4	372	49	305.5	4.0	2.64	
14AB-F01_40	330	1.74	0.3820	0.0150	0.04904	0.00063	0.129	328	10	308.6	3.9	390	62	308.6	3.9	5.91	

Sample Name _Grain #	[U] ppm	U/Th	207/235	2σ error	206/238	2σ error	RHO	207/235 Age (Ma)	2σ error	206/238 Age (Ma)	2σ error	207/206 Age (Ma)	2σ error	Best age (Ma)	2σ error	% Discordance	Rim /Core
14AB-F01_41	265.5	7.31	0.5870	0.0120	0.07460	0.00120	0.423	468.3	7.3	463.5	7.4	478	45	463.5	7.4	1.02	
14AB-F01_42	167.2	2.05	1.0750	0.0130	0.12440	0.00110	0.248	740.8	6.1	756	6.2	718	26	756.0	6.2	2.05	
14AB-F01_43	211	3.84	2.8320	0.0340	0.22820	0.00200	0.323	1364.7	9.1	1325	11	1417	23	1417.0	23.0	6.49	
14AB-F01_44	387	3.14	0.3573	0.0079	0.04894	0.00062	0.449	309.9	5.9	308	3.8	341	46	308.0	3.8	0.61	
14AB-F01_45	121	1.08	1.5420	0.0310	0.15650	0.00270	0.385	946	12	937	15	973	32	973.0	32.0	3.70	
14AB-F01_46	336	2.13	0.3127	0.0058	0.04323	0.00058	0.233	276.1	4.5	272.8	3.6	321	41	272.8	3.6	1.20	
14AB-F01_47	235.6	18.00	0.8430	0.0160	0.09970	0.00120	0.274	620.1	8.5	612.5	6.9	645	40	612.5	6.9	1.23	
14AB-F01_48	200	1.65	5.7460	0.0820	0.34770	0.00540	0.709	1937	12	1923	26	1974	20	1974.0	20.0	2.58	
14AB-F01_49	225	0.78	0.8400	0.0140	0.09490	0.00120	0.318	618.9	7.6	584.4	7.2	740	37	584.4	7.2	5.57	
14AB-F01_50	129.8	1.91	0.3563	0.0095	0.04952	0.00084	0.229	309.8	6.9	311.5	5.2	274	65	311.5	5.2	0.55	
14AB-F01_51	323	2.54	0.3558	0.0072	0.04858	0.00064	0.262	308.8	5.4	305.8	3.9	325	47	305.8	3.9	0.97	
14AB-F01_52	171.5	1.52	6.8300	0.2300	0.38200	0.01100	0.933	2084	31	2084	49	2098	21	2098.0	21.0	0.67	
14AB-F01_53	269.1	0.48	0.6660	0.0110	0.07470	0.00100	0.622	518.1	7	464.2	6.1	768	30	DISC	DISC	10.40	
14AB-F01_54	215	1.80	0.3610	0.0100	0.04792	0.00081	0.440	313.3	7.7	301.7	5	373	52	301.7	5.0	3.70	
14AB-F01_55	48.6	0.27	0.8240	0.0350	0.09580	0.00190	0.070	603	18	590	11	630	100	590.0	11.0	2.16	
14AB-F01_56	252	3.29	0.9230	0.0440	0.10740	0.00270	0.528	662	23	657	15	644	81	657.0	15.0	0.76	
14AB-F01_57	794	2.17	0.4318	0.0050	0.05648	0.00053	0.380	364.3	3.6	354.1	3.2	392	27	354.1	3.2	2.80	
14AB-F01_58	198	0.91	0.9970	0.0240	0.10890	0.00120	0.022	701	12	666.2	6.7	778	52	666.2	6.7	4.96	
14AB-F01_59	443	3.14	0.8920	0.0100	0.10430	0.00100	0.260	647.1	5.4	639.2	5.9	674	25	639.2	5.9	1.22	
14AB-F01_61	190.9	1.95	1.7540	0.0250	0.17330	0.00210	0.364	1027.9	9.3	1030	12	1000	29	1000.0	29.0	3.00	
14AB-F01_62	123.8	0.69	10.9300	0.1100	0.47500	0.00530	0.330	2516.8	9.4	2505	23	2515	19	2515.0	19.0	0.40	
14AB-F01_63	151.8	2.87	1.5410	0.0270	0.15630	0.00230	0.172	946	11	936	13	927	38	927.0	38.0	0.97	
14AB-F01_64	487	1.06	1.3390	0.0160	0.14000	0.00110	0.199	862.5	6.8	844.6	6	886	24	844.6	6.0	2.08	
14AB-F01_65	1093	17.91	0.9782	0.0094	0.11570	0.00120	0.698	692.4	4.8	705.7	6.7	623	16	705.7	6.7	1.92	
14AB-F01_66	549.3	1.92	4.1570	0.0720	0.25990	0.00280	0.725	1668	13	1489	14	1867	20	1867.0	20.0	20.25	

Sample Name _Grain #	[U] ppm	U/Th	207/235	2σ error	206/238	2σ error	RHO	207/235 Age (Ma)	2σ error	206/238 Age (Ma)	2σ error	207/206 Age (Ma)	2σ error	Best age (Ma)	2σ error	% Discordance	Rim /Core
14AB-F01_67	197	1.50	1.7090	0.0260	0.17050	0.00180	0.528	1012.3	9.5	1014.6	9.9	979	26	979.0	26.0	3.64	
14AB-F01_68	264	3.17	0.3814	0.0060	0.05170	0.00064	0.137	327.8	4.4	324.9	3.9	320	45	324.9	3.9	0.88	
14AB-F01_69	350	1.82	0.3461	0.0059	0.04878	0.00071	0.029	301.6	4.4	307	4.3	256	51	307.0	4.3	1.79	
14AB-F01_70	258	1.54	0.3223	0.0085	0.04548	0.00061	0.119	283.3	6.5	286.7	3.8	236	64	286.7	3.8	1.20	
14AB-F01_71	232	1.85	0.9610	0.0140	0.10860	0.00140	0.197	684.3	7.3	664.3	8.1	758	37	664.3	8.1	2.92	
14AB-F01_72	35.1	0.93	0.8560	0.0380	0.09690	0.00190	0.178	624	21	596	11	695	96	596.0	11.0	4.49	
14AB-F01_73	346	2.32	0.3726	0.0069	0.05141	0.00089	0.432	322.8	5.1	323.1	5.5	326	39	323.1	5.5	0.09	
14AB-F01_74	372	1.69	0.3325	0.0069	0.04567	0.00073	0.098	291.3	5.3	287.8	4.5	320	56	287.8	4.5	1.20	
14AB-F01_75	296	1.91	1.4670	0.0600	0.14960	0.00490	0.942	912	25	898	27	956	27	956.0	27.0	6.07	
14AB-F01_76	213.6	2.31	0.8750	0.0160	0.10770	0.00190	0.316	639.6	9.1	659	11	584	45	659.0	11.0	3.03	
14AB-F01_77	843	2.27	0.3845	0.0064	0.05279	0.00076	0.637	330.1	4.7	331.6	4.6	332	29	331.6	4.6	0.45	
14AB-F01_78	194	0.80	1.5180	0.0240	0.15130	0.00200	0.502	938.5	9.8	908	11	998	31	998.0	31.0	9.02	
14AB-F01_79	155	1.08	1.7040	0.0260	0.16730	0.00240	0.321	1009.4	9.7	997	13	1061	35	1061.0	35.0	6.03	
14AB-F01_80	309	112.00	0.3560	0.0110	0.04980	0.00110	0.240	308.6	7.9	313.2	6.7	273	82	313.2	6.7	1.49	Rim
14AB-F01_80	796	0.35	0.7500	0.0150	0.09290	0.00160	0.699	568.1	8.6	572.4	9.2	594	28	572.4	9.2	0.76	Core
14AB-F01_81	260	1.66	1.5540	0.0420	0.15820	0.00400	0.714	952	17	946	22	1004	38	1004.0	38.0	5.78	
14AB-F01_82	202	0.96	1.0340	0.0340	0.11730	0.00140	0.045	714	12	715.1	8.1	726	47	715.1	8.1	0.15	
14AB-F01_84	113.8	1.07	10.2000	0.2000	0.42210	0.00920	0.772	2452	18	2269	42	2618	23	2618.0	23.0	13.33	
14AB-F01_85	168	1.71	1.7420	0.0280	0.17520	0.00240	0.428	1023	11	1041	13	1011	33	1011.0	33.0	2.97	
14AB-F01_86	1193	2.65	0.2748	0.0093	0.03705	0.00082	0.792	246	7.4	234.5	5.1	374	38	234.5	5.1	4.67	
14AB-F01_87	153.8	2.05	0.3790	0.0140	0.05100	0.00091	0.227	326	10	320.7	5.6	340	86	320.7	5.6	1.63	
14AB-F01_89	365	3.35	0.8030	0.0140	0.09210	0.00150	0.523	598.2	7.9	567.8	9	727	34	567.8	9.0	5.08	
14AB-F01_90	87.6	2.01	1.6350	0.0360	0.15770	0.00220	0.363	983	14	944	12	1044	45	1044.0	45.0	9.58	
14AB-F01_91	327	2.25	0.7270	0.0120	0.08907	0.00093	0.463	554.5	7.1	550	5.5	566	32	550.0	5.5	0.81	
14AB-F01_92	169	0.92	0.9420	0.0180	0.11180	0.00150	0.217	673.1	9.4	683	8.5	635	41	683.0	8.5	1.47	

Sample Name _Grain #	[U] ppm	U/Th	207/235	2σ error	206/238	2σ error	RHO	207/235 Age (Ma)	2σ error	206/238 Age (Ma)	2σ error	207/206 Age (Ma)	2σ error	Best age (Ma)	2σ error	% Discordance	Rim /Core
14AB-F01_93	170.2	1.06	1.2560	0.0180	0.13800	0.00140	0.449	825.6	8.1	833.3	7.8	808	28	833.3	7.8	0.93	
14AB-F01_94	427	1.70	0.3357	0.0065	0.04626	0.00058	0.314	293.7	4.9	291.5	3.6	301	41	291.5	3.6	0.75	
14AB-F01_95	254	3.25	0.5270	0.0310	0.04731	0.00082	0.301	427	20	297.9	5.1	1140	100	DISC	DISC	30.23	
14AB-F01_96	447	9.30	0.4570	0.0085	0.06086	0.00093	0.578	381.9	6	380.8	5.7	381	33	380.8	5.7	0.29	
14AB-F01_97	89.4	2.23	6.4590	0.0730	0.37190	0.00380	0.490	2039.4	9.9	2038	18	2042	20	2042.0	20.0	0.20	
14AB-F01_98	151.9	1.84	0.3550	0.0110	0.04744	0.00088	0.273	309.4	8.2	298.8	5.4	389	67	298.8	5.4	3.43	
14AB-F01_99	466	74.00	0.3740	0.0160	0.04870	0.00120	0.661	322	12	306.4	7.6	409	86	306.4	7.6	4.84	Rim
14AB-F01_99	465	1.18	0.7540	0.0180	0.09210	0.00190	0.595	570	11	568	11	583	44	568.0	11.0	0.35	Core
14AB-F01_100	185	2.18	0.3600	0.0073	0.04960	0.00065	0.037	312	5.5	312	4	313	53	312.0	4.0	0.00	
14AB-F01_101	430	14.30	0.9670	0.0460	0.11260	0.00390	0.823	685	24	688	23	691	54	688.0	23.0	0.44	
14AB-F01_102	462.8	1.99	0.3317	0.0072	0.04525	0.00061	0.241	290.6	5.4	285.3	3.8	334	48	285.3	3.8	1.82	
14AB-F01_103	59	34.80	0.9570	0.0730	0.10520	0.00340	0.162	679	38	645	20	770	180	645.0	20.0	5.01	Rim
14AB-F01_103	119	0.82	2.9570	0.0740	0.22210	0.00480	0.751	1398	20	1293	25	1573	30	1573.0	30.0	17.80	Core
14AB-F01_104	232	1.80	0.3623	0.0088	0.04961	0.00058	0.202	313.5	6.5	312.1	3.5	349	52	312.1	3.5	0.45	
14AB-F01_105	272	6.04	0.5540	0.0120	0.07090	0.00110	0.492	447.4	7.7	441.7	6.4	490	38	441.7	6.4	1.27	
14AB-F01_106	303.6	1.11	0.8870	0.0130	0.10459	0.00090	0.014	644.3	7.1	641.2	5.2	673	31	641.2	5.2	0.48	
14AB-F01_107	406	3.48	1.3630	0.0270	0.11690	0.00190	0.666	873	11	712	11	1316	26	DISC	DISC	18.44	
14AB-F01_108	23.64	0.68	5.2000	0.1600	0.32650	0.00740	0.377	1849	27	1826	37	1878	54	1878.0	54.0	2.77	
14AB-F01_109	386	6.76	0.5759	0.0072	0.07518	0.00075	0.520	462.2	4.5	467.2	4.5	442	25	467.2	4.5	1.08	
14AB-F01_110	431	3.36	0.6100	0.0110	0.07717	0.00098	0.196	483.2	6.7	479.2	5.9	503	40	479.2	5.9	0.83	
14AB-F01_111	547	2.50	5.2620	0.0640	0.33110	0.00350	0.805	1864	11	1843	17	1864	14	1864.0	14.0	1.13	
14AB-F01_112	510	1.23	0.8960	0.0130	0.10700	0.00160	0.533	649.3	7	655.3	9.1	643	29	655.3	9.1	0.92	
14AB-F01_113	484	2.02	0.3543	0.0066	0.04749	0.00074	0.326	307.8	4.9	299.1	4.6	343	46	299.1	4.6	2.83	
14AB-F01_114	1020	3.61	0.4890	0.0210	0.04020	0.00150	0.692	404	14	253.9	9.2	1390	140	DISC	DISC	37.15	
14AB-F01_115	336	2.08	0.3446	0.0062	0.04649	0.00056	0.187	300.5	4.7	292.9	3.4	352	46	292.9	3.4	2.53	

Sample Name _Grain #	[U] ppm	U/Th	207/235	2σ error	206/238	2σ error	RHO	207/235 Age (Ma)	2σ error	206/238 Age (Ma)	2σ error	207/206 Age (Ma)	2σ error	Best age (Ma)	2σ error	% Discordance	Rim /Core
14AB-F01_117	234	3.87	0.5980	0.0140	0.07750	0.00100	0.176	475.6	9.1	481	6.3	451	57	481.0	6.3	1.14	
14AB-F01_118	232	3.41	1.2300	0.0210	0.13620	0.00170	0.502	815	9.8	822.8	9.6	776	26	822.8	9.6	0.96	
14AB-F01_119	262	2.27	0.3806	0.0069	0.05050	0.00076	0.163	327.2	5.1	317.6	4.7	409	48	317.6	4.7	2.93	
14AB-F01_120	335	0.89	0.8900	0.0120	0.10490	0.00120	0.293	646	6.3	643	6.9	658	32	643.0	6.9	0.46	
14AB-F01_121	580	3.09	0.3336	0.0062	0.04595	0.00060	0.379	292.1	4.7	289.6	3.7	322	45	289.6	3.7	0.86	
14AB-F01_122	265	1.11	1.1730	0.0250	0.12540	0.00190	0.545	787	12	761	11	858	39	761.0	11.0	3.30	
14AB-F01_123	812	2.06	0.3497	0.0048	0.04829	0.00067	0.570	304.9	3.7	304	4.1	325	25	304.0	4.1	0.30	

APPENDIX A: DETRITAL ZIRCON (U-TH)/HE THERMOCHRONOLOGY RESULTS

Sample-Grain#	(U-Th)/He Age (Ma)	2σ error	U	Th	147Sm	[U]e	Th/U	He	mass	Ft	ESR	U-Pb Age (Ma)	U-Pb 2σ error
12-Escanilla-1	66.5119	5.32096	321.565	59.6404	0.517449	335.297	0.185469	95.3653	7.76	0.789402	55.06	310.7	3.4
12-Escanilla-101	109.988	8.79904	118.208	44.1429	0.364282	128.371	0.373436	59.7858	6.61	0.778475	52.88	2079	18
12-Escanilla-110	104.0502	8.324015	36.14597	83.94643	6.255205	55.50171	2.322428	24.94545	8.58	0.788622	58.35	429.4	9.3
12-Escanilla-114	62.2818	4.98255	76.8646	34.6949	0.733068	84.855	0.451377	21.3378	3.65	0.744603	45.59	531.6	7.4
12-Escanilla-120	64.45449	5.156359	104.5547	30.11058	2.370472	111.498	0.287989	30.72577	7.08	0.788857	55.44	556.4	8
12-Escanilla-15	138.9909	11.11927	228.4384	71.23892	3.832975	244.8568	0.311852	148.5935	9.32	0.801008	59.12	315.1	4.1
12-Escanilla-19	76.1179	6.08944	70.9905	57.5359	0.471654	84.2376	0.810473	25.5673	3.97	0.733466	44.1	1021	59
12-Escanilla-23	47.20084	3.776067	197.4124	49.28252	2.769462	208.7711	0.249642	41.88339	6.06	0.785405	54.38	475	8.4
12-Escanilla-24	75.5791	6.04633	111.958	41.7218	0.999922	121.567	0.372657	40.62	12.62	0.81457	64.17	637	13
12-Escanilla-38	54.1216	4.32973	210.813	103.441	0.407429	234.627	0.490679	53.3359	5.91	0.774771	52.27	376.8	5.6
12-Escanilla-44	46.92794	3.754236	264.9531	127.7839	2.617729	294.3821	0.482289	58.17676	6.01	0.777191	52.8	334.7	4.3
12-Escanilla-45	85.4411	6.83529	295.439	195.672	1.13573	340.488	0.66231	117.225	4.48	0.741243	45.33	346.7	3.3
12-Escanilla-47	51.3474	4.10779	104.51	82.4398	0.395709	123.489	0.788825	27.5999	9.47	0.80174	60.71	1915	16
12-Escanilla-49	86.66862	6.93349	162.2421	58.5791	2.237582	175.7382	0.36106	66.21136	7.97	0.800429	59.19	308.1	4.1
12-Escanilla-5	45.38	3.6304	47.6319	42.6091	0.662738	57.4439	0.894549	10.8293	5.25	0.765196	50.84	1022	43
12-Escanilla-58	68.3251	5.46601	99.6213	18.0298	0.287339	103.773	0.180983	30.8338	8.38	0.802629	59.01	627	11
12-Escanilla-59	64.5345	5.16276	36.766	22.6658	0.435457	41.9859	0.616487	11.1056	4.3	0.755084	48.02	503	12
12-Escanilla-65	49.69296	3.975436	587.9971	95.88215	4.355125	610.0909	0.163066	134.2083	11.11	0.818196	64.52	316.5	4.5
12-Escanilla-69	193.879	15.5103	260.475	93.5923	0.684064	282.023	0.359314	218.936	3.52	0.732334	43.04	330.5	4.3
12-Escanilla-7	52.31691	4.185352	72.90922	42.95757	2.634685	82.81123	0.589193	18.43487	6.37	0.784473	55.04	651.3	6.9
12-Escanilla-82	48.1638	3.85311	163.474	41.9698	0.5567	173.138	0.256737	35.5774	6.25	0.788301	55.06	502.7	5.4
12-Escanilla-84	52.5178	4.20142	13.2062	8.05973	0.357222	15.0634	0.610298	3.4594	8.99	0.806041	61.83	643.7	6.9
12-Escanilla-89	60.8597	4.86878	150.701	58.8124	0.781932	164.243	0.39026	46.5009	24.78	0.857789	84.92	663	12
10-Sobrarbe-1	64.16272	5.133018	205.0933	50.52027	1.886585	216.7325	0.246328	62.20549	13.3538	0.825421	67.6517	307	5.5

Sample-Grain#	(U-Th)/He Age (Ma)	2σ error	U	Th	147Sm	[U]e	Th/U	He	mass	Ft	ESR	U-Pb Age (Ma)	U-Pb 2σ error
10-Sobrarbe-105	72.06796	5.765437	344.7772	82.73289	5.807253	363.8513	0.23996	111.2778	6.87776	0.782822	53.5424	307.9	3.9
10-Sobrarbe-106	91.19389	7.295511	547.2641	122.2961	13.61402	575.4847	0.223468	226.3752	7.76524	0.794571	56.7723	307.8	4.2
10-Sobrarbe-107	57.53285	4.602628	292.3391	59.37502	2.844151	306.0214	0.203103	77.18541	9.958	0.809631	61.4927	301.8	5.2
10-Sobrarbe-109	72.04387	5.76351	394.9573	82.60007	8.044167	414.012	0.209137	124.9517	5.6674	0.772957	50.9084	307.4	3.7
10-Sobrarbe-11	57.01474	4.561179	371.3522	55.67823	5.652761	384.1976	0.149934	96.92165	10.75	0.817392	63.87	307.1	3.7
10-Sobrarbe-115	115.6262	9.250097	356.0907	80.19067	4.211692	374.5716	0.225197	182.7048	5.52124	0.77584	51.684	311.6	3.2
10-Sobrarbe-119	62.41321	4.993057	370.6053	87.16448	6.899766	390.705	0.235195	108.2921	11.1914	0.819621	65.29	303.1	2.6
10-Sobrarbe-14	95.16483	7.613187	242.3091	76.70801	26.68164	260.1007	0.316571	105.1072	7.23	0.78147	53.56	306.1	8.5
10-Sobrarbe-15	59.17846	4.734276	165.9616	48.41073	3.494855	177.1232	0.291698	46.13323	9.87	0.812258	62.72	306	13
10-Sobrarbe-18	52.54727	4.203782	230.6109	84.56979	11.34852	250.1356	0.366721	51.31222	2.94268	0.720762	41.0479	308	3.5
10-Sobrarbe-2	56.43526	4.514821	354.9619	84.99855	15.44146	374.6058	0.239458	84.28614	3.39	0.736397	43.34	316.4	3.8
10-Sobrarbe-25	70.50635	5.640508	212.1078	54.49643	2.57716	224.6658	0.256928	69.54011	9.32	0.809707	61.87	295.1	5
10-Sobrarbe-26	58.72043	4.697635	432.9505	80.18661	11.9184	451.4691	0.18521	114.9177	8.38	0.800562	58.4	290.2	4.3
10-Sobrarbe-4	100.8061	8.064485	397.5469	112.3309	5.288368	423.4319	0.28256	178.0858	5.16379	0.767959	49.999	311	4.2
10-Sobrarbe-47	97.74696	7.819757	344.127	69.54138	2.497874	360.1479	0.202081	147.9304	5.43	0.773965	51.18	455.7	2.8
10-Sobrarbe-57	68.45242	5.476193	318.7484	70.16674	7.715594	334.9393	0.220132	98.16216	7.33	0.790031	55.53	302.3	2.6
10-Sobrarbe-6	128.8812	10.3105	221.9919	65.37994	3.784628	237.0613	0.294515	130.0545	6.07	0.781767	53.57	312.6	3.9
10-Sobrarbe-61	104.5716	8.365728	229.5537	66.00281	5.057222	244.7729	0.287527	111.1685	8.31501	0.798939	58.3731	297	3.2
10-Sobrarbe-66	48.1114	3.848912	146.0481	48.93413	2.486222	157.3252	0.335055	33.23145	9.24	0.81073	62.51	597	4.7
10-Sobrarbe-69	58.28973	4.663178	345.6727	95.22723	2.945105	367.6088	0.275484	88.57058	4.80209	0.763185	48.88	316.6	3.6
10-Sobrarbe-88	59.57025	4.76562	394.7168	66.57061	4.220588	410.0624	0.168654	107.6555	10.2133	0.813933	62.8298	318.8	6.3
10-Sobrarbe-89	65.45731	5.236585	468.4821	87.98992	7.763128	488.7762	0.187819	130.0893	3.92313	0.750793	45.9181	314.6	2.9
10-Sobrarbe-9	49.85988	3.988791	307.3251	84.85277	8.605191	326.9012	0.276101	66.9993	4.74	0.759375	47.99	309.1	4.7
10-Sobrarbe-97	45.74211	3.659369	336.589	81.95621	3.875036	355.4747	0.24349	71.23866	9.142	0.809625	61.6846	305.6	4.7
7_Guaso-107	209.1096	16.72877	159.6442	34.93904	2.51637	167.6998	0.218856	147.3053	4.56	0.767331	49.56	1056	22

Sample-Grain#	(U-Th)/He Age (Ma)	2σ error	U	Th	147Sm	[U]e	Th/U	He	mass	Ft	ESR	U-Pb Age (Ma)	U-Pb 2σ error
7_Guaso-111	86.53772	6.923018	485.4158	97.70885	8.366117	507.9502	0.201289	182.092	4.75	0.763643	48.76	319.3	5.1
7_Guaso-37	44.6804	3.574432	769.1565	221.6247	5.638294	820.2027	0.28814	147.9196	4.26	0.74596	45.3	307.3	4.6
7_Guaso-43	68.84985	5.507988	73.44791	29.3064	2.033502	80.20441	0.399009	23.64921	6.67	0.78944	55.86	307.9	3.1
7_Guaso-44	33.99522	2.719618	81.75414	37.56591	1.067873	90.40715	0.459498	13.38337	8.79	0.804389	60.73	1430	16
7_Guaso-49	202.1101	16.16881	293.585	35.84676	13.38307	301.9039	0.1221	253.2921	3.99	0.759062	47.31	624.2	8.4
7_Guaso-5	72.56667	5.805334	96.18681	63.14425	2.988691	110.7376	0.656475	31.79668	3.49	0.728507	42.94	2070	18
7_Guaso-56	50.81479	4.065183	898.1597	326.203	22.88527	973.366	0.36319	199.7108	4.04	0.74554	45.41	299.5	3.8
7_Guaso-69	259.4657	20.75725	102.5669	65.12242	3.310666	117.5747	0.634926	118.0981	2.52	0.704573	39.09	422.6	5
7-Guaso-104	66.88967	5.351174	106.0561	100.1462	7.700795	129.1483	0.944275	32.82522	2.86	0.698944	38.73	433.9	5.3
7-Guaso-105	76.37987	6.110389	226.0947	67.58924	7.632483	241.6918	0.298942	72.68476	3.28	0.726096	41.7	295.5	4.7
7-Guaso-115	338.7074	27.09659	264.5228	70.19667	7.505492	280.7196	0.265371	363.4987	2.4	0.693079	36.68	418.2	4.6
7-Guaso-120	223.3878	17.87103	54.76986	16.47717	2.039853	58.57311	0.300844	50.32909	2.45	0.702599	38.04	485.4	7.5
7-Guaso-27	70.64921	5.651937	96.52481	88.78282	2.572791	116.9755	0.919793	31.68187	2.72	0.705148	39.57	78.1	3.1
7-Guaso-51	47.17645	3.774116	397.1877	130.6216	3.862269	427.2761	0.328866	75.93707	2.33	0.696081	37.26	313.2	3.9
7-Guaso-54	303.1949	24.25559	100.7125	40.52932	2.203428	110.0534	0.402426	135.1628	3.63	0.734965	43.6	1084	42
7-Guaso-58	398.4215	31.87372	65.19419	42.49369	3.224284	74.99236	0.651802	110.0613	1.55	0.665189	34.02	1070	21
7-Guaso-6	46.75734	3.740587	172.4283	159.7493	2.97082	209.2175	0.926468	39.52028	4.04	0.744015	46.29	45.11	0.87
7-Guaso-61	50.23781	4.019025	112.4758	38.69355	2.120604	121.3937	0.344017	24.29842	3.3	0.735833	43.57	644.6	6.8
7-Guaso-66	52.63379	4.210703	262.4738	100.4559	9.712665	285.6473	0.382728	63.99955	7.56	0.785634	54.78	313	3
7-Guaso-7	61.49163	4.91933	122.0859	39.70532	1.779343	131.235	0.325224	34.02934	5.62	0.77811	52.64	645	11
7-Guaso-72	49.83377	3.986701	55.55642	50.93367	1.868449	67.29069	0.916792	13.30488	3.21	0.730608	43.81	617.1	5.3
7-Guaso-84	80.04077	6.403262	126.1999	152.711	3.774008	161.3728	1.210072	51.87005	5.57	0.737217	45.35	76.4	2
7-Guaso-97	65.30148	5.224118	348.1099	41.33012	2.209382	357.6351	0.118727	109.7361	34.61	0.867408	89.07	59.69	0.92
7-Guaso-98	293.6407	23.49126	79.82771	57.33134	4.596807	93.04837	0.718188	100.3412	1.74	0.66737	34.37	1029	33
14AB-M02-100	47.78466	3.822773	239.0695	48.96515	3.90168	250.3608	0.204816	44.46254	2.05	0.68722	35.71	491	6.3

Sample-Grain#	(U-Th)/He Age (Ma)	2σ error	U	Th	147Sm	[U]e	Th/U	He	mass	Ft	ESR	U-Pb Age (Ma)	U-Pb 2σ error
14AB-M02-104	90.16983	7.213586	190.6137	53.59954	13.68347	203.0208	0.281195	74.86501	4.11	0.753294	46.83	322.2	3.8
14AB-M02-106	44.0275	3.5222	260.3327	99.76496	7.846014	283.3378	0.383221	51.58944	4.61	0.763797	49.32	318.6	4.6
14AB-M02-108	56.78353	4.542683	408.7737	312.5159	7.105734	480.7504	0.764521	99.68597	1.83	0.672835	35.07	619.2	7.8
14AB-M02-109	80.30416	6.424333	190.4165	71.72116	2.697659	206.9402	0.376654	70.69688	6.43	0.783707	54.31	315.6	4.1
14AB-M02-11	248.8434	19.90747	146.0737	33.13489	2.868661	153.7157	0.226837	157.8902	4	0.752008	46.36	829	15
14AB-M02-111	109.749	8.77995	504.02	163.107	25.4405	541.695	0.323613	238.568	3.31	0.738154	43.96	1106	23
14AB-M02-12	74.75998	5.980798	428.3264	104.338	11.51433	452.4025	0.243595	145.5674	7.61	0.793691	56.66	313.2	3.7
14AB-M02-121	57.81961	4.625568	152.9301	55.25557	3.313529	165.6665	0.361313	38.10818	3.32	0.734303	43.33	601.6	3.8
14AB-M02-17	87.7069	7.01655	285.276	73.5957	2.54058	302.23	0.257981	114.46	8.01	0.795488	57.28	327.3	4.4
14AB-M02-20	54.07146	4.325717	489.3848	80.8953	8.391668	508.0489	0.1653	115.5728	5.62	0.777454	51.77	292.9	5.3
14AB-M02-22	268.031	21.4425	299.465	41.7876	11.2683	309.141	0.139541	341.351	4.25	0.749694	45.59	476.3	6.4
14AB-M02-23	59.42279	4.753823	254.6869	49.87775	2.849194	266.183	0.195839	68.28325	7.73	0.797233	57.39	320.9	4.8
14AB-M02-34	52.48238	4.19859	781.2053	114.7791	10.09834	807.6779	0.146926	174.6574	4.77	0.761669	48.08	330.4	5.1
14AB-M02-4	54.15142	4.332113	102.2264	58.59835	1.773981	115.7246	0.573221	23.07675	1.69	0.679247	35.54	641	17
14AB-M02-51	53.3202	4.265616	224.6189	76.97265	1.074316	242.3433	0.342681	53.97837	5.63768	0.77123	50.9834	321.5	4.1
14AB-M02-52	61.92315	4.953852	281.2865	95.47851	3.741747	303.2844	0.339435	73.09975	3.15	0.718397	40.64	313.4	2.7
14AB-M02-66	94.1959	7.53567	210.495	54.1565	3.78663	222.981	0.257282	88.7423	5.56	0.778089	52.29	322.5	3.5
14AB-M02-77	241.987	19.359	115.184	64.0386	6.28492	129.957	0.555966	129.789	3.91	0.751352	47.09	2103	20
14AB-M02-78	217.104	17.3683	96.7037	79.8814	11.5944	115.15	0.826042	106.838	6.4	0.778143	53.87	613.5	6.3
14AB-M02-80	68.7368	5.49895	290.506	46.6598	3.62624	301.265	0.160616	93.998	14.38	0.837647	72.66	315.8	3.4
14AB-M02-83	52.40653	4.192522	118.435	65.56085	4.271215	133.5484	0.55356	27.05186	2.81	0.712954	40.26	457.4	6.4
14AB-M02-88	158.5362	12.6829	16.69788	13.87745	1.47461	19.89984	0.83109	13.37466	6.11	0.775107	53.19	691	17
14AB-M02-90	130.174	10.4139	100.136	35.3309	2.56698	108.282	0.352828	63.1484	11.77	0.822045	66.88	556	10
14AB-M02-93	52.76627	4.221301	121.8966	38.12989	3.907414	130.6936	0.312805	28.22575	4.61	0.755805	47.39	476.9	4.9
14AB-A05-1	79.2952	6.34361	394.48	86.9685	1.48801	414.508	0.220464	133.674	3.78	0.750123	45.91	315	3.6

Sample-Grain#	(U-Th)/He Age (Ma)	2σ error	U	Th	147Sm	[U]e	Th/U	He	mass	Ft	ESR	U-Pb Age (Ma)	U-Pb 2σ error
14AB-A05-102	49.94822	3.995857	282.5582	62.56183	4.444223	296.9822	0.221412	59.8845	3.54	0.746106	45.12	306.1	3.6
14AB-A05-114	193.5742	15.48594	63.1168	36.43907	11.23697	71.56126	0.577328	55.54417	3.48	0.732386	43.51	458.9	6.6
14AB-A05-120	32.03973	2.563178	760.6536	346.0641	3.191766	840.3335	0.454956	99.69656	1.97	0.684368	36.02	303.3	3.8
14AB-A05-2	274.2774	21.94219	60.47093	18.07311	0.561702	64.63416	0.298873	72.61134	3.73	0.744787	45.12	684.2	8.7
14AB-A05-20	56.05855	4.484684	104.7969	73.8563	2.437421	121.8108	0.704757	23.71823	1.23	0.640291	31.39	1042	29
14AB-A05-25	132.9433	10.63546	296.3915	76.18479	2.931907	313.9439	0.257041	165.3624	2.86	0.72807	41.96	326.4	3.5
14AB-A05-29	93.6356	7.49084	160.361	27.608	0.1903	166.717	0.172162	60.9188	2.81	0.719447	40.2	660	18
14AB-A05-32	63.93592	5.114874	432.8387	11.48409	1.976741	435.4922	0.026532	102.542	1.59	0.681095	34.32	495.3	5.9
14AB-A05-49	83.48136	6.678509	52.51831	17.52619	1.684286	56.56126	0.333716	17.53212	1.78	0.684493	35.75	935	75
14AB-A05-50	73.02835	5.842268	252.8917	43.57925	1.329779	262.9303	0.172324	78.65295	3.94	0.756031	46.9	302	4.4
14AB-A05-57	71.48224	5.718579	230.182	169.2197	2.32859	269.148	0.735156	73.55959	2.25	0.703866	39.13	433	12
14AB-A05-58	60.07753	4.806203	213.4367	36.932	2.459778	221.9508	0.173035	50.53152	2.13	0.70028	37.39	2086	23
14AB-A05-66	55.25343	4.420274	178.7424	60.07874	4.836753	192.5967	0.336119	37.66266	1.3	0.653692	32.16	636.7	7.7
14AB-A05-68	230.5324	18.44259	215.4753	86.64564	22.04676	235.5314	0.402114	197.6264	1.5	0.664676	33.5	313.4	9.2
14AB-A05-72	167.559	13.4047	64.1733	39.3894	0.567075	73.2436	0.613797	48.0382	2.83	0.71659	40.93	635.8	8.1
14AB-A05-8	220.878	17.6703	210.712	116.437	2.01977	237.526	0.552586	188.326	1.59	0.655831	32.76	474.1	8.4
14AB-A05-80	87.40498	6.992398	54.13384	40.76277	5.098036	63.54292	0.753	22.14607	3.73	0.732973	43.98	803	11
14AB-A05-83	57.3724	4.58979	96.5183	138.842	1.50432	128.487	1.4385	30.4762	4.81	0.759252	50.09	617.3	6.8
14AB-A05-88	94.30219	7.544175	349.5647	213.679	6.54018	398.7863	0.611272	127.2491	1.07	0.622825	29.6	1061	23
14AB-A05-93	101.5838	8.126706	149.9039	55.97509	2.246338	162.8006	0.373406	63.84263	2.67	0.710572	39.41	298.8	3.5
14AB-A05-94	116.342	9.30736	324.944	83.0582	1.50955	344.072	0.255607	153.948	2.66	0.707689	38.71	306.5	3
14AB-A05-96	85.62072	6.849658	257.0063	58.97786	4.592301	270.6059	0.22948	97.0883	5.67	0.772334	50.87	304.1	3.4
4Ainsa-1	69.06215	5.524972	561.6693	120.5094	46.43088	589.6427	0.214556	166.8849	4.9	0.75623	47.12	293.6	4.2
4Ainsa-10	237.3146	18.98516	171.668	58.75223	6.579393	185.2257	0.342243	185.4518	5.23	0.768625	50.41	287.6	3.3
4Ainsa-107	95.65447	7.652358	290.2932	97.77686	5.948909	312.8311	0.336821	122.9555	4.42	0.756449	47.6	301.6	3.8

Sample-Grain#	(U-Th)/He Age (Ma)	2σ error	U	Th	147Sm	[U]e	Th/U	He	mass	Ft	ESR	U-Pb Age (Ma)	U-Pb 2σ error
4Ainsa-11	126.9298	10.15439	326.4512	103.6789	5.462878	350.3454	0.317594	194.4624	8.62	0.802938	59.77	299	3.4
4Ainsa-12	110.5246	8.841966	218.6843	50.74674	2.185006	230.3772	0.232055	114.018	11.57	0.823421	66.77	281.2	4.1
4Ainsa-15	86.08595	6.886876	267.7359	81.74686	7.354396	286.5908	0.305326	106.1972	7.69	0.792854	56.69	297.9	3.5
4Ainsa-18	127.6612	10.2129	333.6049	83.46224	6.578357	352.8509	0.250183	193.5761	6.36	0.789397	55.38	294.5	3.3
4Ainsa-20	101.7091	8.136727	162.6495	54.84557	1.621128	175.2831	0.337201	79.80027	11.59	0.823209	67.36	542.5	6.1
4Ainsa-25	45.55253	3.644202	36.09838	11.42156	1.344763	38.73435	0.316401	7.856973	11.64	0.822433	66.87	621	11
4Ainsa-3	59.22779	4.738224	154.3302	50.43679	3.114167	165.9563	0.326811	39.78471	4.02	0.747103	45.66	299.8	3.3
4Ainsa-31	102.9505	8.236041	182.6574	52.68571	2.009124	194.7957	0.28844	87.67469	8.55	0.804299	60.11	292.2	3.6
4Ainsa-32	79.30296	6.344236	241.413	54.00864	4.884334	253.8703	0.223719	89.94569	12.01	0.823526	66.89	285.1	3.1
4Ainsa-36	54.3166	4.34533	367.663	170.094	9.04061	406.863	0.462637	87.0139	3.42	0.726511	42.23	638.6	5.6
4Ainsa-47	101.866	8.149283	95.09604	31.03678	2.025721	102.2508	0.326373	44.39102	6.18	0.784094	54.19	298.6	5.7
4Ainsa-49	87.1144	6.96915	246.091	60.9572	3.16829	260.139	0.247702	104.302	18.7	0.847625	77.88	299.6	3.3
4Ainsa-5	255.9405	20.47524	45.90335	33.88139	3.021765	53.71796	0.738103	59.6711	6.91	0.788233	56.43	646.5	7.5
4Ainsa-52	144.029	11.5224	168.579	51.401	2.95955	180.426	0.304908	123.642	33.54	0.871729	93.63	281.7	3.2
4Ainsa-55	161.7705	12.94164	184.1441	53.04873	2.848245	196.3702	0.288083	139.8533	8.52	0.806303	60.67	279.5	3.6
4Ainsa-64	99.9989	7.999912	261.4361	82.82443	3.69616	280.5208	0.316806	114.8324	4.1	0.753504	46.89	313.9	6.8
4Ainsa-76	88.66373	7.093099	340.8499	67.10082	6.290182	356.328	0.196863	141.2879	12.68	0.823875	66.89	283.9	4.4
4Ainsa-78	52.773	4.22184	104.813	43.5818	10.1796	114.897	0.415805	26.246	7.57	0.798539	58.78	695.3	6.4
4Ainsa-80	197.9249	15.83399	318.7459	97.35815	18.97826	341.2526	0.305441	278.1284	3.98	0.752683	46.77	2027.6	8
4Ainsa-89	62.35562	4.98845	806.7947	192.745	28.52048	851.3073	0.238902	220.2608	5.07	0.765986	49.39	295.3	3.4
4Ainsa-9	202.6755	16.21404	147.1463	23.6343	3.721302	152.6056	0.160618	131.2416	5.33	0.77554	51.28	2349	16
4Ainsa-98	42.3352	3.386816	48.21366	13.97738	1.413134	51.43832	0.289905	9.475615	8.12	0.804056	60	726	11
15AB-118-10	71.23129	5.698503	367.7672	88.4953	6.532605	388.1714	0.240629	120.6251	8.64804	0.804683	60.0063	301.4	5.5
15AB-118-101	121.6151	9.729209	215.4908	73.49015	3.770088	232.4271	0.341036	116.8138	4.60094	0.759384	48.2578	315.6	4.9
15AB-118-116	259.2838	20.7427	232.3941	121.6633	5.198964	260.427	0.523521	258.0676	2	0.696004	37.65	619.1	6.2

Sample-Grain#	(U-Th)/He Age (Ma)	2σ error	U	Th	147Sm	[U]e	Th/U	He	mass	Ft	ESR	U-Pb Age (Ma)	U-Pb 2σ error
15AB-118-118	71.08529	5.686823	416.0697	33.18163	1.694791	423.7166	0.07975	118.9897	3.27	0.729784	41.51	403.3	5
15AB-118-12	59.89693	4.791754	100.2494	49.16342	4.748337	111.5906	0.490411	26.77462	3.50661	0.738667	44.4796	741	12
15AB-118-120	223.1722	17.85378	119.1223	48.50291	3.038945	130.3029	0.407169	118.4153	3.65	0.742898	45.02	523.6	6.2
15AB-118-121	180.5073	14.44059	218.775	66.8641	3.03111	234.1823	0.30563	166.1228	2.74356	0.719731	40.7136	1079	33
15AB-118-18	58.24805	4.659844	369.804	94.52987	4.091887	391.5852	0.255622	96.36916	5.77	0.780114	52.95	264.8	4.1
15AB-118-24	131.1337	10.4907	331.0203	65.55516	4.422622	346.1332	0.19804	199.1976	9.12719	0.80601	60.2432	296.6	5.9
15AB-118-3	239.409	19.15272	176.6728	104.3078	6.472369	200.7168	0.590401	189.05	2.68	0.716863	40.93	1059	45
15AB-118-37	210.5663	16.8453	118.2191	16.93218	1.114117	122.1224	0.143227	106.7243	4.35212	0.758453	47.3252	476.2	6.3
15AB-118-40	80.16099	6.412879	175.3752	44.11696	4.092535	185.5514	0.251558	58.40508	2.88	0.724171	41.33	299	3.2
15AB-118-41	63.27694	5.062155	247.179	69.28677	3.846108	263.148	0.28031	68.50269	4.51	0.759308	48.03	304.6	4.5
15AB-118-44	54.88205	4.390564	108.0921	46.11119	2.077909	118.7173	0.426592	26.73763	4.67	0.757225	48.08	630	14
15AB-118-49	168.6179	13.48943	80.86687	45.64553	1.204483	91.38049	0.564453	60.74694	2.8749	0.72178	41.6685	2589	22
15AB-118-51	30.78407	2.462725	1112.672	186.26	9.026595	1155.594	0.167399	138.8656	2.77	0.722698	40.81	322.5	5.2
15AB-118-52	212.97	17.0376	303.3312	77.01443	6.074565	321.0903	0.253895	273.992	2.97	0.732128	42.7	2021	19
15AB-118-56	71.84308	5.747446	275.4349	146.0746	4.014954	309.0813	0.530342	85.86259	2.5898	0.712505	40.113	586.8	5.5
15AB-118-62	54.29158	4.343327	61.82987	26.53083	8.179289	67.97816	0.429094	15.73224	7.33676	0.786217	55.1424	454.1	8.4
15AB-118-68	161.7578	12.94062	238.2767	55.26064	3.654027	251.016	0.231918	180.941	10.09	0.816235	64.11	306.4	3.3
15AB-118-74	125.5752	10.04601	460.4008	126.9038	8.306186	489.6556	0.275638	250.5719	3.85	0.74895	45.83	316.7	5.7
15AB-118-8	263.6412	21.0913	81.79296	84.48422	3.215469	101.2573	1.032903	114.1809	6.47644	0.776053	53.7172	1889	24
15AB-118-85	268.2896	21.46317	75.07854	48.58186	2.227441	86.27322	0.64708	93.69765	3.42201	0.735742	44.2687	1007	33
15AB-118-9	195.9276	15.6742	154.6186	19.33559	1.76236	159.0784	0.125053	133.8722	5.9	0.785443	53.78	640.3	6.6
15AB-118-95	190.4991	15.23993	373.7657	30.58708	3.596344	380.8249	0.081835	298.3148	4.05	0.752882	45.83	716.5	9.5
14AB-G07-1	61.3784	4.910272	120.1392	45.67313	7.083457	130.6886	0.380169	36.85509	18.887	0.84712	78.5262	1017	32
14AB-G07-10	278.3851	22.27081	107.1532	5.253512	0.461474	108.3648	0.049028	135.0347	8.7481	0.812788	61.7074	384.2	9.3
14AB-G07-109	211.568	16.9254	51.7865	10.7689	0.871962	54.2698	0.207949	50.4832	8.03349	0.802472	59.1372	624	11

Sample-Grain#	(U-Th)/He Age (Ma)	2σ error	U	Th	147Sm	[U]e	Th/U	He	mass	Ft	ESR	U-Pb Age (Ma)	U-Pb 2σ error
14AB-G07-11	38.75262	3.100209	80.9174	64.70763	10.81762	95.86718	0.799675	15.09527	4.02632	0.748879	47.093	616.2	9.5
14AB-G07-112	62.66064	5.012851	286.4662	108.8104	2.071449	311.5247	0.379837	70.29913	1.46153	0.664713	33.4538	739	11
14AB-G07-113	82.76757	6.621406	187.1021	57.28036	2.911976	200.3026	0.306145	59.56284	1.38635	0.662599	33.0493	724	7.8
14AB-G07-116	77.53316	6.202652	73.73215	82.60165	1.156451	92.75283	1.120293	27.41173	2.61791	0.700289	39.1241	578	9.7
14AB-G07-12	53.8182	4.305456	103.1546	37.78752	1.873406	111.8627	0.366319	25.93528	7.24	0.795102	57.46	548	11
14AB-G07-18	60.6924	4.855392	44.97328	20.46525	2.21703	49.69547	0.455054	12.57551	5.01076	0.768809	50.7452	2710	23
14AB-G07-2	69.54183	5.563346	233.4542	86.54948	137.2455	254.0641	0.370734	72.11567	4.11318	0.751411	46.6606	302.7	4.8
14AB-G07-22	76.9148	6.153184	110.0028	47.72862	2.674009	121.0033	0.433885	39.71819	6.80258	0.786089	55.1217	360.9	5.4
14AB-G07-23	57.7814	4.62252	91.7791	95.8929	18.0029	113.944	1.04482	28.9173	9.66357	0.807309	63.1317	596.2	8.4
14AB-G07-3	66.92412	5.35393	60.77433	30.87378	1.969365	67.89132	0.508007	19.565	7.18133	0.793377	57.4411	627	11
14AB-G07-33	99.86799	7.989439	28.71247	20.99603	2.784596	33.55967	0.731251	13.13696	3.26349	0.720097	41.6922	1067	57
14AB-G07-36	301.7688	24.1415	63.07058	38.26652	2.849509	71.89378	0.606725	93.42722	5.86	0.779937	53.92	621.6	9.2
14AB-G07-48	105.2171	8.417368	59.31213	8.849716	1.050351	61.35459	0.149206	26.37659	3.97	0.752494	46.04	668	12
14AB-G07-49	63.83642	5.106914	127.1648	66.11874	1.707561	142.3939	0.519945	37.87699	5.32192	0.768007	50.7279	608	10
14AB-G07-5	53.4662	4.277296	594.3718	84.61752	4.3134	613.8724	0.142365	145.0159	10.43	0.816508	63.72	291	11
14AB-G07-50	72.1859	5.77488	235.79	116.187	2.11704	262.547	0.492756	77.1476	3.97132	0.750037	46.7065	641	10
14AB-G07-58	56.56868	4.525495	70.83019	29.9635	2.234507	77.73896	0.423033	18.62167	6.07	0.781163	53.83	721	21
14AB-G07-66	67.90636	5.432508	113.2917	53.76197	1.146608	125.6734	0.474545	31.24384	1.76009	0.675134	34.8719	1005	44
14AB-G07-68	72.4623	5.79699	259.924	95.6408	3.67144	281.959	0.367956	81.3344	3.24561	0.734034	43.3197	599.9	6.5
14AB-G07-8	78.40089	6.272071	363.3945	125.3985	6.976211	392.2961	0.345075	124.4739	4.3506	0.745972	45.4938	309.6	4.9
14AB-G07-90	69.3327	5.546616	143.2572	16.01262	0.60559	146.9463	0.111775	37.83208	1.6661	0.686109	35.2886	760	15
14AB-G07-99	49.8224	3.985792	136.738	39.82246	0.686036	145.9086	0.291232	26.32476	1.47073	0.66924	33.77	2592	21
2-Arro-102	92.8425	7.4274	239.336	78.8124	1.63859	257.486	0.329297	86.8475	1.63293	0.66949	33.8907	686.2	7.7
2-Arro-107	115.2455	9.219636	178.9132	76.80517	3.298681	196.6102	0.429287	93.72121	4.59411	0.760063	48.6689	296.6	2.9
2-Arro-109	97.04069	7.763255	472.6548	96.0759	6.247434	494.8027	0.203269	195.9081	4.04661	0.751648	46.1505	310.8	3.6

Sample-Grain#	(U-Th)/He Age (Ma)	2σ error	U	Th	147Sm	[U]e	Th/U	He	mass	Ft	ESR	U-Pb Age (Ma)	U-Pb 2σ error
2-Arro-111	62.82747	5.026197	94.88414	16.79299	1.833439	98.75906	0.176984	25.39105	3.85443	0.755776	46.8996	599.6	6.5
2-Arro-115	129.2938	10.3435	259.3799	70.72184	3.316374	275.6766	0.272657	134.7187	2.1309	0.694943	36.9518	309.1	3.5
2-Arro-120	62.17247	4.973798	135.5776	14.00873	1.578707	138.8103	0.103326	34.56659	3.19681	0.740189	43.5278	604	12
2-Arro-15	212.3934	16.99148	210.9898	27.3802	4.614629	217.3158	0.12977	182.3275	2.62648	0.722351	40.5532	467	7.5
2-Arro-2	56.6409	4.53127	115.989	28.5858	0.241993	122.571	0.246453	26.4646	2.20975	0.70426	38.1819	960	37
2-Arro-23	73.2383	5.85907	230.637	67.4403	0.747051	246.166	0.292408	76.7284	7.17	0.784796	54.28	627	10
2-Arro-28	174.19	13.9352	155.245	76.5254	0.802424	172.865	0.492932	112.284	1.99997	0.683084	35.8982	976	23
2-Arro-31	205.5727	16.44581	330.9067	60.6086	0.918136	344.8634	0.183159	302.1973	6.59679	0.778835	52.2619	520	13
2-Arro-38	69.47005	5.557604	302.2168	66.12078	5.195546	317.4637	0.218786	92.2624	5.25613	0.772002	50.7167	663.6	6.3
2-Arro-40	91.5709	7.32567	300.698	92.3669	4.33496	321.982	0.307175	124.402	6.31901	0.77698	52.2834	305.7	3.4
2-Arro-43	108.064	8.6451	317.28	103.145	8.42601	341.066	0.325091	152.962	5.76777	0.763354	49.0875	297.5	4.4
2-Arro-48	99.66058	7.972846	30.22442	21.2528	4.158451	35.13761	0.703166	14.36845	5.0467	0.7536	47.9035	1341	38
2-Arro-49	219.256	17.5405	235.521	26.8574	1.67978	241.712	0.114034	223.901	6.71	0.771441	50.14	479.5	6.3
2-Arro-53	96.49409	7.719528	434.7353	97.56131	7.585919	457.2318	0.224415	175.6168	4.00099	0.733345	42.7574	308.4	3.4
2-Arro-54	77.2499	6.18	466.879	105.023	7.89909	491.095	0.224947	154.146	4.18228	0.749493	45.7966	317.1	4.9
2-Arro-71	164.3819	13.15056	381.3059	202.0982	2.361943	427.8407	0.530016	298.7637	6.21622	0.777428	53.0817	335.7	4.3
2-Arro-79	88.9419	7.11535	95.5209	33.5103	2.03585	103.245	0.350816	41.8824	15.8805	0.839417	74.4316	300.9	4.4
2-Arro-85	78.0262	6.242096	651.0886	125.3895	10.90064	680.0078	0.192584	222.3112	6.5751	0.772841	50.8112	305.4	3
2-Arro-89	72.6038	5.8083	131.836	73.1306	1.04315	148.676	0.554709	37.7521	1.28191	0.644621	31.6099	1047	37
2-Arro-9	190.3399	15.22719	68.2262	91.27285	5.866055	89.26654	1.337798	69.56413	3.9361	0.746133	47.2255	439	20
2-Arro-93	126.5094	10.12075	227.6006	79.04281	3.246931	245.8125	0.347287	119.1803	2.48763	0.704433	38.4845	594.7	7.2
2-Arro-97	149.3195	11.94556	449.3719	102.9213	4.913319	473.089	0.229034	288.0143	4.27134	0.748264	45.5666	308	5.1
1-Fosado-101	55.66853	4.453482	84.73837	84.18687	5.263141	104.1445	0.993492	23.71373	4.4183	0.752538	48.1518	311.1	3.7
1-Fosado-102	76.82632	6.146106	619.4423	165.903	14.63372	657.7063	0.267826	223.5883	10.8417	0.815643	63.9474	310.7	3.3
1-Fosado-103	94.84138	7.58731	183.0228	41.21638	1.881958	192.5202	0.225198	81.50591	11.2798	0.821883	66.1208	640	15

Sample-Grain#	(U-Th)/He Age (Ma)	2σ error	U	Th	147Sm	[U]e	Th/U	He	mass	Ft	ESR	U-Pb Age (Ma)	U-Pb 2σ error
1-Fosado-109	139.5512	11.1641	152.2745	113.866	6.508807	178.519	0.747768	108.4553	8.88213	0.797116	59.1902	460	10
1-Fosado-115	58.26836	4.661469	107.4986	49.75428	3.009724	118.967	0.462837	30.71081	11.4332	0.816862	65.1863	663.8	5.8
1-Fosado-16	61.53864	4.923091	177.3236	48.79789	2.403132	188.5689	0.275191	49.56197	6.72718	0.788285	55.1765	633.4	5.8
1-Fosado-19	67.93114	5.434491	293.8278	217.3898	8.951901	343.9156	0.739855	90.58643	2.71087	0.713865	40.7007	762.5	9.4
1-Fosado-2	100.1879	8.015033	235.4527	51.02357	2.924093	247.2129	0.216704	112.2175	14.02	0.833794	71.27	329.7	5.8
1-Fosado-20	60.58159	4.846527	89.56834	40.05645	3.508721	98.80688	0.447217	25.61027	7.48	0.788893	55.93	691.2	7.4
1-Fosado-22	38.12814	3.050251	140.9693	43.76834	2.596054	151.0578	0.310481	22.74664	3.23	0.730129	42.49	1140	39
1-Fosado-27	167.6879	13.41503	71.92312	54.56221	5.041471	84.50854	0.758619	58.09831	4.61257	0.749632	47.1767	984	24
1-Fosado-34	91.78439	7.342751	177.3277	37.57134	4.93903	186.0013	0.211875	73.10537	6.3506	0.788849	55.0699	295.3	3.9
1-Fosado-35	48.48653	3.878922	281.1504	59.57501	3.208644	294.8806	0.211897	62.85161	9.82	0.812328	62.43	650.3	6.3
1-Fosado-40	74.15215	5.932172	97.44392	62.17367	4.602695	111.7793	0.638046	37.48279	14.19	0.831989	71.94	968	25
1-Fosado-42	44.45936	3.556749	224.9674	82.41591	2.821157	243.9537	0.366346	48.6414	13.41	0.828174	69.4	300.9	3.5
1-Fosado-44	90.56388	7.245111	156.3627	55.03369	2.585091	169.0443	0.351962	69.84634	17.9	0.839574	74.61	300.1	4.5
1-Fosado-46	81.53264	6.522611	379.1721	88.9118	6.923152	399.6742	0.234489	140.1041	7.46737	0.79253	56.2209	957	65
1-Fosado-49	71.10883	5.688707	154.3901	60.68965	1.985102	168.3708	0.393093	54.37509	15.8006	0.836844	73.3826	2116	36
1-Fosado-54	97.98821	7.839057	122.0493	32.96537	2.822433	129.6521	0.270099	51.83158	4.83	0.751258	46.4	465.6	6.8
1-Fosado-67	60.03001	4.802401	136.4566	32.46376	1.655374	143.938	0.237905	35.03791	3.65884	0.748834	45.7116	2007	23
1-Fosado-8	56.88042	4.550434	57.17965	27.23331	1.026533	63.45389	0.476276	15.54526	7.86839	0.79427	57.6139	829	10
1-Fosado-88	59.24165	4.739332	186.7675	63.25483	4.200925	201.3498	0.338682	47.39405	3.60742	0.733379	43.1207	471.3	6.6
1-Fosado-89	78.26694	6.261355	255.9154	94.91834	5.372374	277.7924	0.370897	92.24065	5.83835	0.781689	53.725	297.8	3.9
1-Fosado-9	51.66061	4.132849	143.3725	34.01379	3.039825	151.2176	0.237241	32.04996	4.83	0.758015	47.6	2792	41
1-Fosado-94	56.73182	4.538545	293.9596	121.3058	2.417878	321.8962	0.412661	72.1314	3.3406	0.728926	42.5373	1049	19

References

Allen, P.A., 2008, From landscapes into geological history: Nature, v. 451, no. 7176, p. 274–276.

Allen, P.A., Armitage, J.J., Carter, A., Duller, R.A., Michael, N.A., Sinclair, H.D., Whitchurch, A.L., and Whittaker, A.C., 2013, The Qs problem: sediment volumetric balance of proximal foreland basin systems: Sedimentology, v. 60, no. 1, p. 102–130.

Armitage, J.J., Allen, P.A., Burgess, P.M., Hampson, G.J., Whittaker, A.C., Duller, R.A., and Michael, N.A., 2015, Sediment Transport Model For the Eocene Escanilla Sediment-Routing System: Implications For the Uniqueness of Sequence Stratigraphic Architectures: Journal of Sedimentary Research, v. 85, no. 12, p. 1510-1524

Beamud, E., 2013, Paleomagnetism and thermochronology in tertiary syntectonic sediments of the south-central Pyrenees: chronostratigraphy, kinematic and exhumation constraints [PhD Thesis]: Universitat de Barcelona, 274 p.

Beamud, E., Muñoz, J.A., Fitzgerald, P.G., Baldwin, S.L., Garcés, M., Cabrera, L., and Metcalf, J.R., 2011, Magnetostratigraphy and detrital apatite fission track thermochronology in syntectonic conglomerates: constraints on the exhumation of the South-Central Pyrenees: Basin Research, v. 23, no. 3, p. 309–331.

Beaumont, C., Muñoz, J.A., Hamilton, J., and Fullsack, P., 2000, Factors controlling the Alpine evolution of the central Pyrenees inferred from a comparison of observations and geodynamical models: Journal of Geophysical Research: Solid Earth, v. 105, no. B4, p. 8121–8145.

Bentham, P., and Burbank, D.W., 1996, Chronology of Eocene foreland basin evolution along the western oblique margin of the South-Central Pyrenees: Tertiary Basins of Spain. The Stratigraphic Record of Crustal Kinematics. World and Regional Geology, v. 6, p. 144–152.

Bentham, P.A., Burbank, D.W., and Puigdefabregas, C., 1992, Temporal and spatial controls on the alluvial architecture of an axial drainage system: late Eocene Escanilla Formation, southern Pyrenean foreland basin, Spain: Basin Research, v. 4, no. 3-4, p. 335–352.

Bosch, G.V., Teixell, A., Jolivet, M., Labaume, P., Stockli, D., Domenech, M., and Monie, P., 2016, Timing of Eocene–Miocene thrust activity in the Western Axial

Zone and Chaînons Béarnais (west-central Pyrenees) revealed by multi-method thermochronology: Comptes Rendus Géoscience, v. 348, no. 3, p. 246–256.

Bosworth, W., Guiraud, R., and Kessler, L.G., 1999, Late Cretaceous (ca. 84 Ma) compressive deformation of the stable platform of northeast Africa (Egypt): Far-field stress effects of the "Santonian event" and origin of the Syrian arc deformation belt: Geology, v. 27, no. 7, p. 633–636.

Caja, M.A., Marfil, R., Garcia, D., Remacha, E., Morad, S., Mansurbeg, H., Amorosi, A., Martínez-Calvo, C., and Lahoz-Beltrá, R., 2010, Provenance of siliciclastic and hybrid turbiditic arenites of the Eocene Hecho Group, Spanish Pyrenees: implications for the tectonic evolution of a foreland basin: Basin Research, v. 22, no. 2, p. 157–180.

Campbell, I.H., Reiners, P.W., Allen, C.M., Nicolescu, S., and Upadhyay, R., 2005, He–Pb double dating of detrital zircons from the Ganges and Indus Rivers: implication for quantifying sediment recycling and provenance studies: Earth and Planetary Science Letters, v. 237, no. 3, p. 402–432.

Cantalejo, B., and Pickering, K.T., 2014, Climate forcing of fine-grained deep-marine systems in an active tectonic setting: Middle Eocene, Ainsa Basin, Spanish Pyrenees: Palaeogeography, Palaeoclimatology, Palaeoecology, v. 410, p. 351–371.

Carrapa, B., 2010, Resolving tectonic problems by dating detrital minerals: Geology, v. 38, no. 2, p. 191–192.

Carrapa, B., DeCelles, P.G., Reiners, P.W., Gehrels, G.E., and Sudo, M., 2009, Apatite triple dating and white mica 40Ar/39Ar thermochronology of syntectonic detritus in the Central Andes: A multiphase tectonothermal history: Geology, v. 37, no. 5, p. 407–410.

Castelltort, S., and Van Den Driessche, J., 2003, How plausible are high-frequency sediment supply-driven cycles in the stratigraphic record? Sedimentary Geology, v. 157, no. 1, p. 3–13.

Choukroune, P., 1992, Tectonic evolution of the Pyrenees: Annual Review of Earth and Planetary Sciences, v. 20, p. 143.

Choukroune, P., 1989, The ECORS Pyrenean deep seismic profile reflection data and the overall structure of an orogenic belt: Tectonics, v. 8, no. 1, p. 23–39.

Costa, E., Garcés, M., López-Blanco, M., Beamud, E., Gómez-Paccard, M., and

Larrasoaña, J.C., 2010, Closing and continentalization of the South Pyrenean foreland basin (NE Spain): magnetochronological constraints: Basin Research, v. 22, no. 6, p. 904–917.

Dahlen, F.A., Suppe, J., and Davis, D., 1984, Mechanics of fold-and-thrust belts and accretionary wedges: Cohesive Coulomb theory: Journal of Geophysical Research: Solid Earth, v. 89, no. B12, p. 10087–10101.

Davis, D., Suppe, J., and Dahlen, F.A., 1983, Mechanics of fold-and-thrust belts and accretionary wedges: Journal of Geophysical Research: Solid Earth, v. 88, no. B2, p. 1153–1172.

DeCelles, P.G., and Giles, K.A., 1996, Foreland basin systems: Basin research, v. 8, no. 2, p. 105–123.

Delvolvé, J.-J., Vachard, D., and Souquet, P., 1998, Stratigraphic record of thrust propagation, Carboniferous foreland basin, Pyrenees, with emphasis on Pays-de-Sault (France/Spain): Geologische Rundschau, v. 87, no. 3, p. 363–372.

Denèle, Y., Laumonier, B., Paquette, J.-L., Olivier, P., Gleizes, G., and Barbey, P., 2014, Timing of granite emplacement, crustal flow and gneiss dome formation in the Variscan segment of the Pyrenees: Geological Society, London, Special Publications, v. 405, no. 1, p. 265–287.

Dewey, J.F., Pitman, W.C., Ryan, W.B., and Bonnin, J., 1973, Plate tectonics and the evolution of the Alpine system: Geological society of America bulletin, v. 84, no. 10, p. 3137–3180.

Dickinson, W.R., 1988, Provenance and sediment dispersal in relation to paleotectonics and paleogeography of sedimentary basins, *in* New perspectives in basin analysis, Springer, p. 3–25.

Dreyer, T., Corregidor, J., Arbues, P., and Puigdefabregas, C., 1999, Architecture of the tectonically influenced Sobrarbe deltaic complex in the Ainsa Basin, northern Spain: Sedimentary Geology, v. 127, no. 3, p. 127–169.

Erdos, Z., Beek, P., and Huismans, R.S., 2014, Evaluating balanced section restoration with thermochronology data: A case study from the Central Pyrenees: Tectonics, v. 33, no. 5, p. 617–634.

Farley, K.A., 2002, (U-Th)/He dating: Techniques, calibrations, and applications: Reviews in Mineralogy and Geochemistry, v. 47, no. 1, p. 819–844.

Fedo, C.M., Sircombe, K.N., and Rainbird, R.H., 2003, Detrital zircon analysis of the sedimentary record: Reviews in Mineralogy and Geochemistry, v. 53, no. 1, p. 277–303.

Filleaudeau, P.-Y., Mouthereau, F., and Pik, R., 2012, Thermo-tectonic evolution of the south-central Pyrenees from rifting to orogeny: insights from detrital zircon U/Pb and (U-Th)/He thermochronometry: Basin Research, v. 24, no. 4, p. 401–417.

Fitzgerald, P.G., Muñoz, J.A., Coney, P.J., and Baldwin, S.L., 1999, Asymmetric exhumation across the Pyrenean orogen: implications for the tectonic evolution of a collisional orogen: Earth and Planetary Science Letters, v. 173, no. 3, p. 157–170.

Flemings, P.B., and Jordan, T.E., 1990, Stratigraphic modeling of foreland basins: Interpreting thrust deformation and lithosphere rheology: Geology, v. 18, no. 5, p. 430–434.

Fontana, D., Zuffa, G.G., and Garzanti, E., 1989, The interaction of eustacy and tectonism from provenance studies of the Eocene Hecho Group Turbidite Complex (South-Central Pyrenees, Spain): Basin Research, v. 2, no. 4, p. 223–237.

Ford, M., Hemmer, L., Vacherat, A., Gallagher, K., and Christophoul, F., 2016, Retro-wedge foreland basin evolution along the ECORS line, eastern Pyrenees, France: Journal of the Geological Society, v. 173, no. 3, p. 419–437.

Fosdick, J.C., Grove, M., Graham, S.A., Hourigan, J.K., Lovera, O., and Romans, B.W., 2015, Detrital thermochronologic record of burial heating and sediment recycling in the Magallanes foreland basin, Patagonian Andes: Basin Research, v. 27, no. 4, p. 546–572.

Garver, J.I., Brandon, M.T., Roden-Tice, M., and Kamp, P.J., 1999, Exhumation history of orogenic highlands determined by detrital fission-track thermochronology: Geological Society, London, Special Publications, v. 154, no. 1, p. 283–304.

Gehrels, G., 2014, Detrital zircon U-Pb geochronology applied to tectonics: Annual Review of Earth and Planetary Sciences, v. 42, p. 127–149.

Guenthner, W.R., Reiners, P.W., Ketcham, R.A., Nasdala, L., and Giester, G., 2013, Helium diffusion in natural zircon: Radiation damage, anisotropy, and the interpretation of zircon (U-Th)/He thermochronology: American Journal of Science, v. 313, no. 3, p. 145–198, doi: 10.2475/03.2013.01.

Gupta, K.D, 2008, Tectono-stratigraphic evolution of deep-marine clastic systems in the Eocene Ainsa and Jaca basins, Spanish Pyrenees: petrographic and geochemical constraints [PhD Thesis]: University College London, 205 p.

Gupta, K.D., and Pickering, K.T., 2008, Petrography and temporal changes in petrofacies of deep-marine Ainsa–Jaca basin sandstone systems, Early and Middle Eocene, Spanish Pyrenees: Sedimentology, v. 55, no. 4, p. 1083–1114.

Hart, N.R, 2015, Temporal constraints on progressive rifting of a hyper-extended continental margin using bedrock and detrital zircon (U-Th)/(Pb-He) dating, Mauléon Basin, western Pyrenees [Master's Thesis]: University of Texas at Austin, 430 p.

Hart, N.R., Stockli, D.F., and Hayman, N.W., 2016, Provenance evolution during progressive rifting and hyperextension using bedrock and detrital zircon U-Pb geochronology, Mauléon Basin, western Pyrenees: Geosphere, v. 12, no. 4, p. 1166–1186.

Hogan, P.J., and Burbank, D.W., 1996, E14 Evolution of the Jaca piggyback basin and emergence of the External Sierra, southern Pyrenees: Tertiary Basins of Spain: the Stratigraphic Record of Crustal Kinematics, v. 6, p. 153.

Honegger, L., 2015, Sedimentary record of climate signals from soure-to-sink: a field and stable isotope study of the early-middle Eocene fluvial to deep-marine successions in the South Pyrenean foreland basin, Tremp-Graus-Ainsa (Spain) [Master's thesis]: Université de Genève

Huyghe, D., Mouthereau, F., Castelltort, S., Filleaudeau, P.-Y., and Emmanuel, L., 2009, Paleogene propagation of the southern Pyrenean thrust wedge revealed by finite strain analysis in frontal thrust sheets: Implications for mountain building: Earth and Planetary Science Letters, v. 288, no. 3, p. 421–433.

Jackson, S.E., Pearson, N.J., Griffin, W.L., and Belousova, E.A., 2004, The application of laser ablation-inductively coupled plasma-mass spectrometry to in situ U–Pb zircon geochronology: Chemical Geology, v. 211, no. 1, p. 47–69.

Johnsson, M.J., Stallard, R.F., and Lundberg, N., 1991, Controls on the composition of fluvial sands from a tropical weathering environment: Sands of the Orinoco River drainage basin, Venezuela and Colombia: Geological Society of America Bulletin, v. 103, no. 12, p. 1622–1647.

Julivert, M., and Durán, H., 1990, The Hercynian structure of the Catalonian Coastel Ranges (NE Spain): Acta geológica hispánica, v. 25, no. 1, p. 13–21.

Kominz, M.A., Browning, J.V., Miller, K.G., Sugarman, P.J., Mizintseva, S., and Scotese, C.R., 2008, Late Cretaceous to Miocene sea-level estimates from the New Jersey and Delaware coastal plain coreholes: An error analysis: Basin Research, v. 20, no. 2, p. 211–226.

Labaume, P., Mutti, E., and Seguret, M., 1987, Megaturbidites: a depositional model from the Eocene of the SW-Pyrenean foreland basin, Spain: Geo-Marine Letters, v. 7, no. 2, p. 91–101.

Lunsen, H.A., 1970, Geology of the Ara-Cinca region, Spanish Pyrenees, province of Huesca:(with special reference to compartmentation of the Flysch basin):.

Malusà, M.G., Resentini, A., and Garzanti, E., 2016, Hydraulic sorting and mineral fertility bias in detrital geochronology: Gondwana Research, v. 31, p. 1–19.

Mansurbeg, H., Caja, M.A., Marfil, R., Morad, S., Remacha, E., Garcia, D., Martin-Crespo, T., El-Ghali, M.A.K., and Nystuen, J.P., 2009, Diagenetic evolution and porosity destruction of turbiditic hybrid arenites and siliciclastic sandstones of foreland basins: evidence from the Eocene Hecho Group, Pyrenees, Spain: Journal of Sedimentary Research, v. 79, no. 9, p. 711–735.

Margalef, A., Castiñeiras, P., Casas, J.M., Navidad, M., Liesa, M., Linnemann, U., Hofmann, M., and Gärtner, A., 2016, Detrital zircons from the Ordovician rocks of the Pyrenees: Geochronological constraints and provenance: Tectonophysics,.

Marsh, J.H., and Stockli, D.F., 2015, Zircon U–Pb and trace element zoning characteristics in an anatectic granulite domain: Insights from LASS-ICP-MS depth profiling: Lithos, v. 239, p. 170–185.

Martínez, F.J., Dietsch, C., Aleinikoff, J., Cirés, J., Arboleya, M.L., Reche, J., and Gómez-Gras, D., 2016, Provenance, age, and tectonic evolution of Variscan flysch, southeastern France and northeastern Spain, based on zircon geochronology: Geological Society of America Bulletin, v. 128, no. 5-6, p. 842–859.

Matte, P., 1986, Tectonics and plate tectonics model for the Variscan belt of Europe: Tectonophysics, v. 126, no. 2, p. 329–374.

Metcalf, J.R., Fitzgerald, P.G., Baldwin, S.L., and Muñoz, J.-A., 2009, Thermochronology of a convergent orogen: Constraints on the timing of thrust faulting and subsequent exhumation of the Maladeta Pluton in the Central Pyrenean Axial Zone: Earth and Planetary Science Letters, v. 287, no. 3, p. 488–503.

Mey, P.H.W., Nagtegaal, P.J.C., Roberti, K.J., and Hartevelt, J.J.A., 1968, Lithostratigraphic subdivision of post-Hercynian deposits in the south-central Pyrenees, Spain: Leidse Geologische Mededelingen, v. 41, no. 1, p. 221–228.

Michael, N.A., Whittaker, A.C., Carter, A., and Allen, P.A., 2014, Volumetric budget and grain-size fractionation of a geological sediment routing system: Eocene Escanilla Formation, south-central Pyrenees: Geological Society of America Bulletin, v. 126, no. 3-4, p. 585–599.

Mochales, T., Barnolas, A., Pueyo, E.L., Serra-Kiel, J., Casas, A.M., Samsó, J.M., Ramajo, J., and Sanjuán, J., 2012a, Chronostratigraphy of the Boltaña anticline and the Ainsa Basin (southern Pyrenees): Geological Society of America Bulletin, v. 124, no. 7-8, p. 1229–1250.

Mochales, T., Casas, A.M., Pueyo, E.L., and Barnolas, A., 2012b, Rotational velocity for oblique structures (Boltaña anticline, Southern Pyrenees): Journal of Structural Geology, v. 35, p. 2–16.

Mochales, T., Pueyo, E.L., Casas, A.M., and Barnolas, A., 2016, Restoring paleomagnetic data in complex superposed folding settings: The Boltaña anticline (Southern Pyrenees): Tectonophysics, v. 671, p. 281–298.

Morris, R.G., Sinclair, H.D., and Yelland, A.J., 1998, Exhumation of the Pyrenean orogen: implications for sediment discharge: Basin Research, v. 10, no. 1, p. 69–85.

Mouthereau, F., Filleaudeau, P.-Y., Vacherat, A., Pik, R., Lacombe, O., Fellin, M.G., Castelltort, S., Christophoul, F., and Masini, E., 2014, Placing limits to shortening evolution in the Pyrenees: Role of margin architecture and implications for the Iberia/Europe convergence: Tectonics, v. 33, no. 12, p. 2283–2314.

Muñoz, J.A., 1992, Evolution of a continental collision belt: ECORS-Pyrenees crustal balanced cross-section, *in* Thrust tectonics, Springer, p. 235–246.

Muñoz, J.-A., Beamud, E., Fernández, O., Arbués, P., Dinarès-Turell, J., and Poblet, J., 2013, The Ainsa Fold and thrust oblique zone of the central Pyrenees: Kinematics of a curved contractional system from paleomagnetic and structural data: Tectonics, v. 32, no. 5, p. 1142–1175.

Mutti, E., 1977, Distinctive thin-bedded turbidite facies and related depositional environments in the Eocene Hecho Group (South-central Pyrenees, Spain): Sedimentology, v. 24, no. 1, p. 107–131.

Mutti, E., Remacha, E., Sgavetti, M., Rosell, J., Valloni, R., and Zamorano, M., 1985,

Stratigraphy and facies characteristics of the Eocene Hecho Group turbidite systems, south-central Pyrenees, *in* Excursion Guidebook of the 6th European Regional Meeting, International Association of Sedimentologists, Lleida, Spain, p. 519–576.

Nijman, W., 1990, Thrust sheet rotation?—The South Pyrenean Tertiary basin configuration reconsidered: Geodinamica Acta, v. 4, no. 1, p. 17–42.

Parsons, A.J., Michael, N.A., Whittaker, A.C., Duller, R.A., and Allen, P.A., 2012, Grain-size trends reveal the late orogenic tectonic and erosional history of the south–central Pyrenees, Spain: Journal of the Geological Society, v. 169, no. 2, p. 111–114.

Paton, C., Hellstrom, J., Paul, B., Woodhead, J., and Hergt, J., 2011, Iolite: Freeware for the visualisation and processing of mass spectrometric data: Journal of Analytical Atomic Spectrometry, v. 26, no. 12, p. 2508–2518.

Payros, A., Tosquella, J., Bernaola, G., Dinarès-Turell, J., Orue-Etxebarria, X., and Pujalte, V., 2009, Filling the North European Early/Middle Eocene (Ypresian/Lutetian) boundary gap: insights from the Pyrenean continental to deep-marine record: Palaeogeography, Palaeoclimatology, Palaeoecology, v. 280, no. 3, p. 313–332.

Petrus, J.A., and Kamber, B.S., 2012, VizualAge: A Novel Approach to Laser Ablation ICP-MS U-Pb Geochronology Data Reduction: Geostandards and Geoanalytical Research, v. 36, no. 3, p. 247–270.

Pickering, K.T., and Bayliss, N.J., 2009, Deconvolving tectono-climatic signals in deep-marine siliciclastics, Eocene Ainsa Basin, Spanish Pyrenees: Seesaw tectonics versus eustasy: Geology, v. 37, no. 3, p. 203–206.

Puigdefàbregas, C., Muñoz, J.A., and Vergés, J., 1992, Thrusting and foreland basin evolution in the southern Pyrenees, *in* Thrust tectonics, Springer, p. 247–254.

Puigdefàbregas, C., and Souquet, P., 1986, Tecto-sedimentary cycles and depositional sequences of the Mesozoic and Tertiary from the Pyrenees: Tectonophysics, v. 129, no. 1, p. 173–203.

Puigdefàbregas, C., 2016, Geologic Map of the Ainsa Basin. (in preparation)

Rahl, J.M., Ehlers, T.A., and van der Pluijm, B.A., 2007, Quantifying transient erosion of orogens with detrital thermochronology from syntectonic basin deposits: Earth and Planetary Science Letters, v. 256, no. 1, p. 147–161.

Rahl, J.M., Haines, S.H., and Van der Pluijm, B.A., 2011, Links between orogenic wedge

deformation and erosional exhumation: Evidence from illite age analysis of fault rock and detrital thermochronology of syn-tectonic conglomerates in the Spanish Pyrenees: Earth and Planetary Science Letters, v. 307, no. 1, p. 180–190.

Rahl, J.M., Reiners, P.W., Campbell, I.H., Nicolescu, S., and Allen, C.M., 2003, Combined single-grain (U-Th)/He and U/Pb dating of detrital zircons from the Navajo Sandstone, Utah: Geology, v. 31, no. 9, p. 761–764.

Reiners, P.W., Farley, K.A., and Hickes, H.J., 2002, He diffusion and (U–Th)/He thermochronometry of zircon: initial results from Fish Canyon Tuff and Gold Butte: Tectonophysics, v. 349, no. 1, p. 297–308.

Reiners, P.W., 2005, Zircon (U-Th)/He thermochronometry: Reviews in Mineralogy and Geochemistry, v. 58, no. 1, p. 151–179.

Remacha, E., and Fernández, L.P., 2003, High-resolution correlation patterns in the turbidite systems of the Hecho Group (South-Central Pyrenees, Spain): Marine and Petroleum Geology, v. 20, no. 6, p. 711–726.

Roigé, M., Gómez-Gras, D., Remacha, E., Daza, R., and Boya, S., 2016, Tectonic control on sediment sources in the Jaca basin (Middle and Upper Eocene of the South-Central Pyrenees): Comptes Rendus Geoscience, v. 348, no. 3, p. 236–245.

Romans, B.W., Castelltort, S., Covault, J.A., Fildani, A., and Walsh, J.P., 2016, Environmental signal propagation in sedimentary systems across timescales: Earth-Science Reviews, v. 153, p. 7–29.

Rosenbaum, G., Lister, G.S., and Duboz, C., 2002, Relative motions of Africa, Iberia and Europe during Alpine orogeny: Tectonophysics, v. 359, no. 1, p. 117–129.

Rushlow, C.R., Barnes, J.B., Ehlers, T.A., and Vergés, J., 2013, Exhumation of the southern Pyrenean fold-thrust belt (Spain) from orogenic growth to decay: Tectonics, v. 32, no. 4, p. 843–860.

Saylor, J.E., Stockli, D.F., Horton, B.K., Nie, J., and Mora, A., 2012, Discriminating rapid exhumation from syndepositional volcanism using detrital zircon double dating: Implications for the tectonic history of the Eastern Cordillera, Colombia: Geological Society of America Bulletin, v. 124, no. 5-6, p. 762–779.

Scotchman, J.I., Bown, P., Pickering, K.T., BouDagher-Fadel, M., Bayliss, N.J., and Robinson, S.A., 2015a, A new age model for the middle Eocene deep-marine Ainsa Basin, Spanish Pyrenees: Earth-Science Reviews, v. 144, p. 10–22.

Scotchman, J.I., Pickering, K.T., Sutcliffe, C., Dakin, N., and Armstrong, E., 2015b, Milankovitch cyclicity within the middle Eocene deep-marine Guaso system,

Ainsa Basin, Spanish Pyrenees: Earth-Science Reviews, v. 144, p. 107–121.

Séguret, M., Labaume, P., and Madariaga, R., 1984, Eocene seismicity in the Pyrenees from megaturbidites of the South Pyrenean Basin (Spain): Marine Geology, v. 55, no. 1, p. 117–131.

Shanmugam, G., 1997, The Bouma sequence and the turbidite mind set: Earth-Science Reviews, v. 42, no. 4, p. 201–229.

Sinclair, H.D., Gibson, M., Naylor, M., and Morris, R.G., 2005, Asymmetric growth of the Pyrenees revealed through measurement and modeling of orogenic fluxes: American Journal of Science, v. 305, no. 5, p. 369–406.

Sláma, J., Košler, J., Condon, D.J., Crowley, J.L., Gerdes, A., Hanchar, J.M., Horstwood, M.S., Morris, G.A., Nasdala, L., Norberg, N., and others, 2008, Plešovice zircon—a new natural reference material for U–Pb and Hf isotopic microanalysis: Chemical Geology, v. 249, no. 1, p. 1–35.

Solé, J., Pi, T., and Enrique, P., 2003, New geochronological data on the Late Cretaceous alkaline magmatism of the northeast Iberian Peninsula: Cretaceous Research, v. 24, no. 2, p. 135–140.

Sømme, T.O., Helland-Hansen, W., Martinsen, O.J., and Thurmond, J.B., 2009, Relationships between morphological and sedimentological parameters in source-to-sink systems: a basis for predicting semi-quantitative characteristics in subsurface systems: Basin Research, v. 21, no. 4, p. 361–387.

Teixell, A., 1998, Crustal structure and orogenic material budget in the west central Pyrenees: Tectonics, v. 17, no. 3, p. 395–406.

Teixell, A., Labaume, P., and Lagabrielle, Y., 2016, The crustal evolution of the west-central Pyrenees revisited: inferences from a new kinematic scenario: Comptes Rendus Geoscience, v. 348, no. 3, p. 257–267.

Vacherat, A., Mouthereau, F., Pik, R., Bernet, M., Gautheron, C., Masini, E., Le Pourhiet, L., Tibari, B., and Lahfid, A., 2014, Thermal imprint of rift-related processes in orogens as recorded in the Pyrenees: Earth and Planetary Science Letters, v. 408, p. 296–306.

Vergés, J., Fernàndez, M., and Martínez, A., 2002, The Pyrenean orogen: pre-, syn-, and post-collisional evolution: Journal of the Virtual Explorer, v. 8, p. 57–76.

Vergés, J., and Muñoz, J.A., 1990, Thrust sequences in the southern central Pyrenees: Bulletin de la Société géologique de France, v. 8, no. 6, p. 265–271.

Vermeesch, P., 2004, How many grains are needed for a provenance study? Earth and Planetary Science Letters, v. 224, no. 3, p. 441–451.

Vermeesch, P., 2012, On the visualisation of detrital age distributions: Chemical Geology, v. 312, p. 190–194.

Vissers, R.L.M., and Meijer, P.T., 2012, Mesozoic rotation of Iberia: Subduction in the Pyrenees? Earth-Science Reviews, v. 110, no. 1, p. 93–110.

Whipple, K.X., 2009, The influence of climate on the tectonic evolution of mountain belts: Nature Geoscience, v. 2, no. 2, p. 97–104.

Whitchurch, A.L., Carter, A., Sinclair, H.D., Duller, R.A., Whittaker, A.C., and Allen, P.A., 2011, Sediment routing system evolution within a diachronously uplifting orogen: Insights from detrital zircon thermochronological analyses from the South-Central Pyrenees: American Journal of Science, v. 311, no. 5, p. 442–482.

Wiedenbeck, M., Alle, P., Corfu, F., Griffin, W.L., Meier, M., Oberli, F., Quadt, A. von, Roddick, J.C., and Spiegel, W., 1995, Three natural zircon standards for U-Th-Pb, Lu-Hf, trace element and REE analyses: Geostandards newsletter, v. 19, no. 1, p. 1–23.

Wolfe, M.R., and Stockli, D.F., 2010, Zircon (U–Th)/He thermochronometry in the KTB drill hole, Germany, and its implications for bulk He diffusion kinetics in zircon: Earth and Planetary Science Letters, v. 295, no. 1, p. 69–82.

Zachos, J.C., Dickens, G.R., and Zeebe, R.E., 2008, An early Cenozoic perspective on greenhouse warming and carbon-cycle dynamics: Nature, v. 451, no. 7176, p. 279–283.

Ziegler, P.A., and Stampfli, G.M., 2001, Late Palaeozoic-Early Mesozoic plate boundary reorganization: collapse of the Variscan orogen and opening of Neotethys: Natura Bresciana, v. 25, p. 17–34.

Vita

Kelly Thomson was born and raised in Juneau, Alaska. After graduating from Juneau Douglas High School he attended the University of Alaska Anchorage where he graduated with honors in 2013 with a Bachelor's of Science degree in Geological Sciences and a minor in Mathematics. During his undergraduate education Kelly worked as a geotechnician in the Alaska Range for Kiska Metals on a mineral exploration project. He attended summer field camp with the University of Oregon during 2012, in eastern Oregon and southwestern Montana. He worked for the University of Alaska as a teaching assistant and wellfield manager, as well as volunteered with the USGS investigating the petrography of plutonic rocks in the western Alaska Range. Upon graduating Kelly took a position as a junior geologist for Alaska Earth Science and worked on a mineral exploration project in the interior of Alaska. In fall 2013 Kelly volunteered at Denali National Park and worked with Dr. Denny Capps on landslide susceptibility within the park. Kelly began his graduate studies in the fall of 2014 under the supervision of Dr. Daniel Stockli. After graduating with a Master's Degree in August 2016, he will begin research and coursework for pursuing a PhD at the University of Texas at Austin under the supervision of Dr. Daniel Stockli and Dr. Jake Covault.

Permanent email address: kellydthomson@gmail.com

This thesis was typed by Kelly David Thomson